

## **FUNCTIONS OF PLATELET MMRN1 IN ADHESION TO COLLAGEN**

THE ROLE OF MULTIMERIN 1 (MMRN1) IN PLATELET ADHESION AND  
CHARACTERIZATION OF ITS INTERACTIONS WITH FIBRILLAR COLLAGENS

By: Alexander Leatherdale, BA Honors

A thesis submitted to the School of Graduate Studies in partial fulfilment of the  
requirements for the degree Doctor of Philosophy in Health Science

McMaster University © Copyright by Alexander Leatherdale March 2020

McMaster University DOCTORATE OF PHILOSOPHY (2020)  
Hamilton, Ontario (Health Science)

TITLE: The role of multimerin 1 (MMRN1) in platelet adhesion and characterization of its interactions with fibrillar collagens

AUTHOR: Alexander Leatherdale, BA Honors

SUPERVISOR: Dr. Catherine P.M. Hayward

NUMBER OF PAGES: xvi, 216

## ABSTRACT

Multimerin 1 (human: MMRN1, mouse: *Mmrn1*) is a large homopolymeric glycoprotein that is synthesized and stored by platelets and endothelial cells until activation-induced release. MMRN1 is able to support platelet adhesion through mechanisms involving von Willebrand factor (VWF) and glycoprotein (GP)Ib $\alpha$ , and  $\beta_3$  integrins on activated platelets, and it enhances platelet adhesion to fibrillar collagen, potentially by binding to putative MMRN1-specific GPAGPOGPX (where O is hydroxyproline and X is valine or glutamine) motifs in fibrillar collagens. Using mice with and without selective *Mmrn1* deficiency, the goals of this thesis were: 1) further characterize the ability of *Mmrn1* to enhance platelet adhesion to collagen, 2) explore the role of fluid shear stress in the ability of *Mmrn1* to enhance platelet adhesion, and 3) test the specificity of the GPAGPOGPX motif for *Mmrn1* and the ability of GPAGPOGPX to support or enhance platelet adhesion. *Mmrn1*-deficient (*Mmrn1*<sup>-/-</sup>) mouse platelets showed impaired aggregate formation on fibrillar collagen surfaces under high (1500 s<sup>-1</sup>) and low (300 s<sup>-1</sup>) shear flow compared to wild-type (*Mmrn1*<sup>+/+</sup>) mouse platelets, which was due to reduced initial adhesion and a slower rate of platelet accumulation onto collagen surfaces. Similarly, *Mmrn1*<sup>-/-</sup> platelets formed smaller aggregates on immobilized recombinant (r)Vwf surfaces compared to wild-type platelets, and *Mmrn1*<sup>-/-</sup> platelets had impaired adhesion and aggregate formation on immobilized murine fibrinogen, but not fibrin, when platelets were pre-activated to release *Mmrn1*. Type I fibrillar collagen was found to contain a variant of the GPAGPOGPX motif

(GPAGPOGPI), and GPAGPOGPX motifs supported adhesion of wild-type, but not *Mmrn1*<sup>-/-</sup>, platelets. When presented with the VWF-binding GPRGQOGVMGFO motif and the integrin  $\alpha_2\beta_1$ -binding GFOGER motif present in fibrillar collagens, the GPAGPOGPX motifs synergistically enhanced platelet adhesion. These findings expand upon the known adhesive functions of platelet multimerin 1 and update knowledge of the motifs that support platelet adhesion to fibrillar collagens.

## ACKNOWLEDGMENTS

I would foremost like to thank my supervisor Dr. Catherine Hayward for her guidance, support, and mentorship throughout this experience, and for providing me with the opportunity to pursue this project. I thank my supervisory committee members Dr. Peter Gross and Dr. Bill Sheffield for their insight and guidance throughout, which contributed greatly to the shape and direction of this thesis. Additionally, Dr. Gross provided access to facilities, laboratory space, microscopy equipment, and hands-on instruction with microscopy. Special thanks are warranted for Dr. Subia Tasneem and Dr. D'Andra Parker for making this thesis possible: without their efforts in generating the mouse model and the fundamental work of characterizing various aspects of its phenotype, this project could not have happened. Dr. Parker also closely mentored me during our overlapping time at McMaster and trained me in many of the techniques used in this thesis. I owe part of this thesis to our collaborator Dr. Richard Farndale, who provided our laboratory with the collagen peptides used in a large portion of this work, and provided thoughtful feedback on experimental results throughout. I also thank Dr. Dominique Bihan and Dr. Arkadiusz Bonna for synthesizing all of the collagen peptides used in this thesis.

I thank the following people for their contributions to this thesis: Dr. Bradley Doble assisted in the generation of the mouse model used herein; Dr. Waliul Khan provided the dissection microscope used for mouse blood collection; Dr. Alison Fox-

Robichaud provided access to an inverted epifluorescent microscope used in some experiments, and Peter Grin provided technical assistance and training with its use; Karen Moffat provided access to the Special Coagulation Laboratory aggregometry equipment, and Steve Carlino provided technical advice and training with its use; Dr. Ishac Nazi provided access to the flow cytometer, and Nikola Ivetic provided technical assistance and training in flow cytometry, as well as assistance in optimizing flow protocols for mouse platelets; Jane Moore and Jim Smith provided access to equipment used in some experiments; Dr. Janaki Iyer provided technical advice for some experimental procedures; Rumi Clare provided materials and advice related to fluorescence microscopy and flow cytometry; and the staff at the Central Animal Facility oversaw the care and medical treatment of our mice.

I am grateful for the friendships I have made during my time at McMaster, and thank the following people for their support and friendship: Matthew Badin, Felix Boivin, Justin Brunet, Emily Anne Hicks, Angela Huynh, Nikola Ivetic, and Ivan Ristovski. Lastly, I thank my father Richard Leatherdale, my mother Ann Leatherdale, and my brother James Leatherdale for always believing in me.

## TABLE OF CONTENTS

TITLE PAGE .....	i
DESCRIPTIVE NOTE .....	ii
ABSTRACT .....	iii
ACKNOWLEDGMENTS .....	v
TABLE OF CONTENTS .....	vii
LIST OF FIGURES .....	x
LIST OF TABLES .....	xiii
LIST OF ABBREVIATIONS AND SYMBOLS .....	xiv
CHAPTER 1: INTRODUCTION	
1.1 Thesis objectives .....	1
1.1.1 Multimerin 1 structure, synthesis, and storage .....	2
1.1.2 Multimerin 1 adhesive and procoagulant functions .....	4
1.1.3 Multimerin 1-deficient mice .....	6
1.1.4 Multimerin 1 deficiency states in humans .....	8
1.2 Hemostasis and thrombosis .....	9
1.2.1 Blood coagulation and fibrinolysis .....	10
1.2.2 Platelets .....	14
1.3 Platelet adhesion .....	16
1.3.1 Platelet adhesive proteins .....	21
1.3.1.1 Fibrinogen and fibrin .....	25
1.3.1.2 Fibronectin .....	30
1.3.1.3 Von Willebrand factor .....	35
1.3.1.4 Thrombospondin-1 .....	39
1.3.1.5 Vitronectin .....	43
1.3.2 Platelet adhesive receptors .....	45
1.3.2.1 Alpha-IIb beta-3 .....	46
1.3.2.2 Alpha-2 beta-1 .....	49
1.3.2.3 Glycoprotein VI .....	52
1.3.2.4 Glycoprotein Ib/IX/V .....	54
1.4 The collagen family .....	55
1.4.1 Fibrillar collagen structure, synthesis, and assembly .....	57
1.4.2 Non-fibrillar collagens IV, VI, and VIII .....	60
1.4.3 Collagens in hemostasis and thrombosis .....	62
1.4.3.1 VWF recognition motifs in fibrillar collagens .....	66
1.4.3.2 Alpha-2 beta-1 recognition motifs in fibrillar collagens .....	68
1.4.3.3 GPVI recognition motifs in fibrillar collagens .....	69
1.4.4 Fibrillar collagen-related disease states .....	70
1.5 Unanswered questions regarding MMRN1 adhesive functions .....	72
1.5.1 Hypothesis .....	77
1.5.2 Experimental aims .....	78

## CHAPTER 2: MATERIALS AND METHODS

2.1 Materials .....	80
2.1.1 Reagents and supplies .....	80
2.1.2 Antibody sources .....	81
2.1.3 Purified proteins.....	82
2.1.3.1 Recombinant human multimerin 1.....	82
2.1.3.2 Triple-helical collagen mimetic peptides.....	83
2.1.3.3 Other protein sources .....	85
2.2 Methods.....	86
2.2.1 Helsinki Declaration on human research .....	86
2.2.2 Animal handling.....	86
2.2.3 Generation of multimerin 1-deficient mice.....	87
2.2.4 Genotyping of experimental mice.....	88
2.2.5 Mouse blood collection.....	88
2.2.6 Assays of platelet adhesion under shear .....	89
2.2.7 Quantification of platelet adhesion and aggregate size.....	91
2.2.8 Assays of collagen-induced platelet aggregation in whole blood.....	92
2.2.9 Assays of shear-induced platelet aggregation.....	93
2.2.10 Protein binding assays.....	95
2.2.11 <i>In silico</i> analyses of collagen amino acid sequences .....	96
2.2.12 Assays of static platelet adhesion using human or mouse platelets.....	96
2.2.13 Assays of platelet adhesion under high shear using collagen peptides.....	99
2.3 Statistical analyses .....	100

## CHAPTER 3: RESULTS

3.1 Multimerin 1-deficient mice .....	101
3.2 Aggregate formation of wild-type and <i>Mmrn1</i> <sup>-/-</sup> mouse platelets on Horm collagen and Vwf under high shear flow (1500 s <sup>-1</sup> ).....	102
3.3 Adhesion of wild-type and <i>Mmrn1</i> <sup>-/-</sup> mouse platelets to fibrinogen, fibrin, and fibronectin .....	110
3.4 Effect of integrin alpha-IIb beta-3 on static adhesion of activated wild-type and <i>Mmrn1</i> <sup>-/-</sup> mouse platelets.....	121
3.5 Collagen-induced aggregation of wild-type and <i>Mmrn1</i> <sup>-/-</sup> platelets in whole blood .....	123
3.6 Shear-induced aggregation of wild-type and <i>Mmrn1</i> <sup>-/-</sup> mouse platelets .....	124
3.7 <i>In silico</i> analysis of collagen amino acid sequences and MMRN1 binding to variant sequences of GPAGPOGPX .....	128
3.8 Static adhesion of activated wild-type and <i>Mmrn1</i> <sup>-/-</sup> mouse platelets to GPAGPOGPX, GFOGER, and full-length fibrillar collagen .....	131
3.9 Adhesion of wild-type and <i>Mmrn1</i> <sup>-/-</sup> mouse platelets to triple-helical collagen peptides under high shear flow (1500 s <sup>-1</sup> ).....	133
3.10 Static adhesion of human platelets to triple-helical collagen peptides .....	136

CHAPTER 4: DICUSSION	
4.1 Summary of thesis work and key observations.....	139
4.2 Proposed role of Mmrn1 in platelet adhesion to collagen .....	141
4.2.1 Potential roles of Mmrn1 in primary platelet adhesion and platelet tethering onto fibrillar collagen.....	141
4.2.2 Potential roles of Mmrn1 in supporting platelet aggregate formation onto fibrillar collagen.....	148
4.3 Updated model of recognition motifs in fibrillar collagens involved in platelet adhesion or activation .....	159
4.4 Strengths and limitations of this thesis .....	167
4.5 Conclusions and future directions.....	171
4.5.1 Possible effect of MMRN1 on VWF multimer size .....	174
4.5.2 Generation and testing of additional mouse models .....	175
4.5.3 Impact of triple-helical conformation and collagen mutations in MMRN1 binding to GPAGPOGPX sequences .....	176
REFERENCES .....	179

## LIST OF FIGURES

<b>Figure 1: Structure of a native MMRN1 homotrimer</b> .....	2
<b>Figure 2: Overview of platelet adhesion following injury to the vessel wall under high shear flow</b> .....	17
<b>Figure 3: Distribution of select proteins within plasma, platelets <math>\alpha</math>-granules, and the vessel wall that are known to support platelet adhesion and/or aggregation</b> .....	22
<b>Figure 4: Estimated abundance of major receptors on resting human and mouse platelets</b> .....	46
<b>Figure 5: Structure of Collagen Toolkit III peptides</b> .....	65
<b>Figure 6: Recognition motifs in types I and III fibrillar collagens for <math>\alpha_2\beta_1</math>, GPVI, and VWF</b> .....	66
<b>Figure 7: Electrophoretic mobility of P1-P2 fragments from <i>Mmrn1</i><sup>+/+</sup>, <i>Mmrn1</i><sup>+/-</sup>, and <i>Mmrn1</i><sup>-/-</sup> mice</b> .....	102
<b>Figure 8: Aggregate size of wild-type versus <i>Mmrn1</i><sup>-/-</sup> mouse platelets adherent to Horm collagen under high shear flow (1500 s<sup>-1</sup>)</b> .....	104
<b>Figure 9: Aggregate size of wild-type versus <i>Mmrn1</i><sup>-/-</sup> mouse platelets adherent to recombinant (r)Vwf under high shear flow (1500 s<sup>-1</sup>)</b> .....	105
<b>Figure 10: Real-time adhesion of wild-type versus <i>Mmrn1</i><sup>-/-</sup> mouse platelets to Horm collagen under high shear flow (1500 s<sup>-1</sup>)</b> .....	107
<b>Figure 11: Adhesion of wild-type versus <i>Mmrn1</i><sup>-/-</sup> mouse platelets to Horm collagen under low shear flow (300 s<sup>-1</sup>)</b> .....	109
<b>Figure 12: rhMMRN1 binding to human FG, fibrin, or FN</b> .....	111
<b>Figure 13: Static adhesion of wild-type versus <i>Mmrn1</i><sup>-/-</sup> CRP-activated mouse platelets to murine Fg, fibrin, and Fn</b> .....	111
<b>Figure 14: Wild-type versus <i>Mmrn1</i><sup>-/-</sup> mouse platelet adhesion to immobilized murine fibrinogen under low shear flow (300 s<sup>-1</sup>)</b> .....	113

<b>Figure 15: Wild-type versus <i>Mmrn1</i><sup>-/-</sup> mouse platelet aggregate size and feature count captured onto immobilized murine fibrinogen under low shear flow (300 s<sup>-1</sup>)</b> .....	114
<b>Figure 16: Wild-type versus <i>Mmrn1</i><sup>-/-</sup> mouse platelet adhesion to immobilized murine fibrin under low shear flow (300 s<sup>-1</sup>)</b> .....	116
<b>Figure 17: Wild-type versus <i>Mmrn1</i><sup>-/-</sup> mouse platelet aggregate size and feature count captured onto immobilized murine fibrin under low shear flow (300 s<sup>-1</sup>)</b> .....	117
<b>Figure 18: Wild-type versus <i>Mmrn1</i><sup>-/-</sup> mouse platelet adhesion to immobilized murine fibronectin under low shear flow (300 s<sup>-1</sup>)</b> .....	119
<b>Figure 19: Wild-type versus <i>Mmrn1</i><sup>-/-</sup> mouse platelet aggregate size and feature count captured onto immobilized murine fibronectin under low shear flow (300 s<sup>-1</sup>)</b> .....	120
<b>Figure 20: Effect of anti-mouse <math>\beta_3</math> blocking antibody 9D2 on static adhesion of wild-type versus <i>Mmrn1</i><sup>-/-</sup> CRP-activated mouse platelets</b> .....	122
<b>Figure 21: Effect of 9D2 concentration on static adhesion of wild-type versus <i>Mmrn1</i><sup>-/-</sup> CRP-activated mouse platelets to immobilized rhMMRN1</b> .....	123
<b>Figure 22: Aggregation responses of wild-type versus <i>Mmrn1</i><sup>-/-</sup> mouse platelets tested in whole blood to Horm collagen</b> .....	124
<b>Figure 23: Representative scatterplots showing the effects of shear on wild-type versus <i>Mmrn1</i><sup>-/-</sup> mouse platelets detected by flow cytometry</b> .....	125
<b>Figure 24: Aggregation of wild-type versus <i>Mmrn1</i><sup>-/-</sup> mouse platelets in whole blood in response to variable shear rates</b> .....	126
<b>Figure 25: rhMMRN1 binding to homotrimeric triple-helical peptides derived from GPAGPOGPX-like motifs in the alpha-chains of type I collagen</b> .....	130
<b>Figure 26: Static adhesion of wild-type versus <i>Mmrn1</i><sup>-/-</sup> CRP-activated mouse platelets to triple-helical collagen mimetic peptides or Horm collagen</b> .....	132
<b>Figure 27: Static adhesion of CRP-activated mouse platelets to <math>\alpha_2\beta_1</math>-binding peptide GFOGER</b> .....	133
<b>Figure 28: Adhesion of washed, CRP-activated mouse platelets to triple-helical collagen mimetic peptides under high shear flow (1500 s<sup>-1</sup>)</b> .....	135

<b>Figure 29: Synergistic effects of triple-helical peptide combinations on static adhesion of CRP-activated human platelets.....</b>	<b>137</b>
<b>Figure 30: Effect of CRP activation on static adhesion of human platelets .....</b>	<b>138</b>
<b>Figure 31: Potential mechanisms through which MMRN1/Mmrn1 enhances primary platelet adhesion to fibrillar collagen under high shear flow .....</b>	<b>143</b>
<b>Figure 32: Potential mechanisms through which MMRN1/Mmrn1 enhances aggregate formation onto fibrillar collagens .....</b>	<b>150</b>
<b>Figure 33: Updated model of recognition motifs on fibrillar collagens that support platelet adhesion .....</b>	<b>160</b>

## LIST OF TABLES

<b>Table 1: Phenotypic traits of transgenic and knockout mice for select proteins involved in platelet adhesion, hemostasis, and thrombosis .....</b>	<b>24</b>
<b>Table 2: Tissue distribution, estimated abundance, and functions of major fibrillar and non-fibrillar collagens present in the vessel wall .....</b>	<b>57</b>
<b>Table 3: Triple-helical collagen mimetic peptides used in this thesis .....</b>	<b>85</b>
<b>Table 4: Conservation of GPAGPOGPX sequences in types I, II, and III fibrillar collagens .....</b>	<b>129</b>
<b>Table 5: Comparison of inhibition of static adhesion of ADP-activated human platelets to MMRN1, FG, and FN with inhibition of static adhesion of CRP-activated mouse platelets to MMRN1, murine Fg, and murine Fn.....</b>	<b>155</b>

## LIST OF ABBREVIATIONS AND SYMBOLS

-/-	Homozygous null
+/-	Heterozygous null
+/+	Wild-type
$\alpha$	Alpha
$\alpha_1$ (I)	Type I collagen alpha-1 chain
$\alpha_2$ (I)	Type I collagen alpha-2 chain
$\alpha_1$ (II)	Type II collagen alpha-1 chain
$\alpha_1$ (III)	Type III collagen alpha-1 chain
$\beta$	Beta
$\gamma$	Gamma (denotes shear rate)
$\lambda$	Lamda
$\tau$	Tau (denotes shear stress)
$\mu$	Mu (denotes viscosity or unit prefix “micro”)
aa	Amino acid
ACD	Acid citrate dextrose
ADAMTS	A disintegrin-like and metalloprotease with thrombospondin type I repeats
ADP	Adenosine Diphosphate
APC	Activated protein C
ANOVA	Analysis of variance
BMP	Bone morphogenetic protein
BSA	Bovine serum albumin
BSS	Bernard-Soulier syndrome
C-terminal	Carboxyl-terminal
cDNA	Complimentary deoxyribonucleic acid
CD	Cluster of differentiation
COL	Collagen
CRP	Collagen-related peptide
Da	Dalton
DNA	Deoxyribonucleic acid
dyn	Dynes (unit of force)
ECMR	Extracellular matrix receptor
ECM	Extracellular matrix
ED	Extra domain
EDS	Ehlers-Danlos syndrome
EDTA	Ethylenediaminetetraacetic acid
ELISA	Enzyme-linked immunosorbent assay
EMILIN	Elastin microfibril interface-located protein
EMI	Elastin microfibril interface domain
FcR	Crystalizing fragment (Fc) receptor
FG	Fibrinogen (human)
Fg	Fibrinogen (mouse)

FN	Fibronectin (human)
Fn	Fibronectin (mouse)
Fmoc	Fluorenylmethyloxycarbonyl
F	Coagulation factor
GFP	Gel-filtered platelets
GP	Glycoprotein
GPS	Gray platelet syndrome
GT	Glanzmann thrombasthenia
HEK	Human embryonic kidney
IAP	Integrin-associated protein
Ig	Immunoglobulin
ITAM	Immunoreceptor tyrosine-based activation motif
k	Prefix “kilo”
LTA	Light transmission aggregometry
m	meter(s) or denotes the prefix “milli”
M	Molar
MA	Maximal aggregation
MIDAS	Metal ion-dependent adhesion site
MMRN1	Multimerin 1 (human)
Mmrn1	Multimerin 1 (mouse)
N-terminal	Amino-terminal
n	prefix “nano”
NO	Nitrous oxide
OI	Osteogenesis imperfecta
OCS	Open canalicular system
OD	Optical density
PAR	Protease-activated receptor
PCR	Polymerase chain reaction
PE	Phosphatidylethanolamine
PFA	Paraformaldehyde
PGI <sub>2</sub>	Prostacyclin
PPP	Platelet-poor plasma
PRP	Platelet-rich plasma
PS	Phosphatidylserine
QPD	Quebec platelet disorder
RBC	Red blood cell
RGD	Arginine-glycine-aspartic acid tripeptide
R	Recombinant
rh	Recombinant human
s	Second(s)
SD	Standard deviation
SDS-PAGE	Sodium dodecyl sulfate polyacrylamide gel electrophoresis
SEM	Standard error of the mean
SNCA	$\alpha$ -synuclein (human)

SncA	$\alpha$ -synuclein (mouse)
SPD	Storage pool deficiency
TF	Tissue factor
TKO	Triple knockout
TTP	Thrombotic thrombocytopenic purpura
TRAP	Thrombin receptor-activating peptide
TSP-1	Thrombospondin-1 (human)
Tsp-1	Thrombospondin-1 (mouse)
TSR	Thrombospondin type repeat
TxA2	Thromboxane A2
U	Unit
ULVWF	Ultra-large von Willebrand factor
VLA	Very late antigen
VN	Vitronectin (human)
Vn	Vitronectin (mouse)
VTE	Venous thromboembolism
VWD	Von Willebrand disease
VWF	Von Willebrand factor (human)
Vwf	Von Willebrand factor (mouse)
WPB	Weibel-Palade body
X	Placeholder designation for an amino acid residue

## CHAPTER 1: INTRODUCTION

### 1.1 THESIS OBJECTIVES

The objectives of this thesis were to further characterize the role of multimerin 1 (human: MMRN1, mouse: *Mmrn1*) in platelet adhesion, specifically through: 1) its interactions with fibrillar collagens, 2) identifying additional potential binding partners for MMRN1, and 3) testing the effects of fluid shear stress on MMRN1 adhesive functions. Previous studies have demonstrated that MMRN1 is capable of supporting platelet adhesion under a range of shear conditions,<sup>1,2</sup> contributes to platelet adhesion onto fibrillar collagens,<sup>2-4</sup> modulates thrombin generation and platelet factor V storage,<sup>5-7</sup> and contributes to thrombus formation *in vivo*.<sup>3,4</sup> The structure and known functions of MMRN1 will be discussed in the following subsections. Next, background on hemostasis and thrombosis, platelet adhesion, and major adhesive proteins and platelet receptors involved in platelet adhesion will be presented. Lastly, in light of this information, currently unanswered questions regarding MMRN1 adhesive functions will be presented and discussed, which form the rationale for the work included in this thesis.

### 1.1.1 Multimerin 1 structure, synthesis, and storage

Multimerin 1 is a member of the EMILIN/Multimerin family, which consists of four homotrimeric proteins encoded by separate genes that share an N-terminal elastin microfibril interface (EMI) domain, a central region predicted to contain coiled-coil structures, and a C-terminal globular C1q-like domain (*Figure 1*).<sup>8-10</sup> MMRN1 is unique from other EMILINs, which are synthesized by a variety of cell types and constitutively secreted into the elastic fiber system of connective tissues.<sup>9</sup> MMRN1 is synthesized by megakaryocytes and endothelial cells, and is packaged and stored within granules until activation-induced secretion.<sup>10-13</sup> MMRN1 is not detectable in plasma,<sup>14-16</sup> but studies of cultured endothelial cells *in vitro* show that secreted MMRN1 is incorporated into extracellular matrix (ECM) fibers,<sup>17</sup> suggesting MMRN1 may also be a component of the normal endothelial basement membrane.

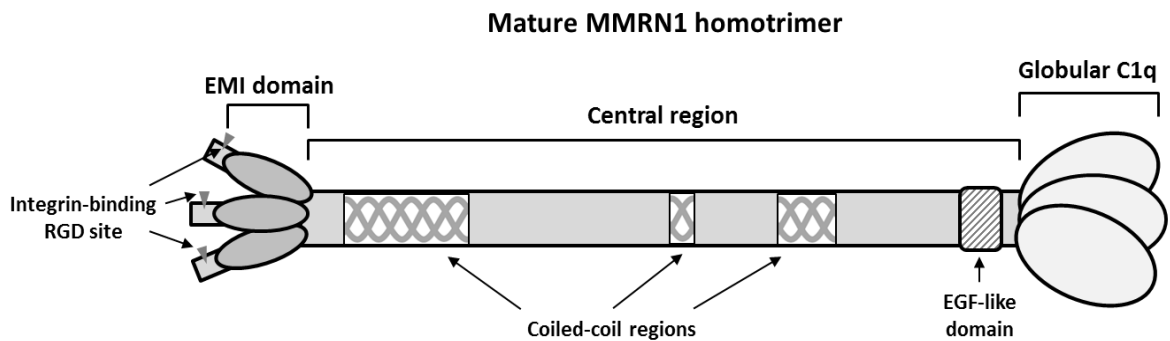


**Figure 1: Structure of a native MMRN1 homotrimer.** The EMI domain contains multiple free Cys residues that are likely involved in multimerization, whereas the gC1q domain is the potential locus of trimerization, similar to other gC1q-containing EMILINs.<sup>9</sup> Human MMRN1 and mouse Mmrn1 share the same domains and organization, except that Mmrn1 lacks the N-terminal RGD site. While *MMRN1*

synthesizes a prepolypeptide that is 1228-aa long, the *Mmrn1* gene product is 1210-aa, and MMRN1 and *Mmrn1* share 67% amino acid similarity.<sup>18</sup>

MMRN1 is synthesized as a 1228-aa polypeptide, denoted as proMMRN1, that consists of a 19-aa N-terminal signal peptide and the 1209-aa proMMRN1 polypeptide.<sup>10</sup> The signal peptide is cleaved to produce proMMRN1, which undergoes extensive N-linked glycosylation and minimal O-linked glycosylation.<sup>11</sup> Together, N- and O-linked carbohydrates account for approximately one third of the molecular mass of the MMRN1 subunit.<sup>16</sup> proMMRN1 polypeptides form homotrimers through inter-chain disulfide linkages and subsequently form larger multimers that undergo further proteolytic processing to remove the propolypeptide domain.<sup>19</sup> MMRN1 multimers can range from a single 450 kDa homotrimer to millions of Da in size.<sup>14,15</sup> There are two distinct MMRN1 subunits stored within human platelets, denoted as p-155 and p-170 based on their size in kDa.<sup>16</sup> p-155 makes up the majority of human platelet MMRN1, whereas p-170 is a larger MMRN1 subunit present in small quantities within platelets, and it is cleaved from proMMRN1 closer to the N-terminus than p-155,<sup>11</sup> although the biological significance of the differences in p-155 and p-170 is presently unknown. MMRN1 subunits produced by endothelial cells are slightly larger, which likely reflects differences in proteolytic processing of synthesized polypeptides between endothelial cells and megakaryocytes/platelets.<sup>12</sup> Human MMRN1 and mouse *Mmrn1* share 67% similarity, and a key difference is that *Mmrn1* lacks the N-terminal integrin-binding RGD site.<sup>18</sup>

Within human platelet  $\alpha$ -granules, MMRN1 is stored complexed to coagulation factor V (FV).<sup>7</sup> Approximately 25% of platelet FV is covalently bound to MMRN1 via disulfide linkage to the B-domain of FV, whereas the remaining FV in platelets is non-covalently bound to MMRN1.<sup>20</sup> Although the significance of these two types of FV-MMRN1 complexes is unclear, both forms can be converted to activated FV (FVa).<sup>20</sup> Following platelet activation, released MMRN1 binds to the external platelet membrane, and it is also found within the open canalicular system (OCS),<sup>1,11</sup> with the largest multimers remaining bound to the platelet surface and smaller multimers are released into the local milieu.<sup>14</sup> MMRN1 in endothelial cells is primarily stored in dense-core granules that are morphologically distinct from Weibel-Palade bodies (WPBs) that contain VWF and P-selectin, although small amounts of MMRN1 are present in WPBs.<sup>17</sup> It is interesting to consider that differential packaging and storage of MMRN1 versus VWF by endothelial cells could be of biologic importance. Following activation-induced secretion, endothelial cell MMRN1 stays on the external cell membrane, without detectable secretion into culture media.<sup>17</sup>

### 1.1.2 Multimerin 1 adhesive and procoagulant functions

MMRN1 is a ligand for VWF,<sup>21</sup> collagens I-III and VI,<sup>2,22</sup> FV,<sup>5,23</sup> phosphatidylserine (PS),<sup>23</sup> and  $\alpha_{IIb}\beta_3$  and  $\alpha_v\beta_3$  on activated platelets.<sup>1</sup> MMRN1 binds to VWF through a two-site, two-step interaction with the VWF A1 and A3 domains, and VWF is required for platelets to adhere to MMRN1 under high shear flow ( $1500 \text{ s}^{-1}$ ).<sup>2,21</sup>

Similarly, GPIb $\alpha$  is required for platelets to adhere to MMRN1, but MMRN1 has no detectable binding to GPIb $\alpha$ ,<sup>2</sup> which suggests that VWF-GPIb $\alpha$  interactions and VWF-MMRN1 binding mediate platelet adhesion to MMRN1 under high shear flow.

Exogenous MMRN1 enhances platelet adhesion to fibrillar collagen under high shear flow through a mechanism that requires VWF,<sup>2</sup> and *Mmrn1*-deficient (*Mmrn1*<sup>-/-</sup>) mice have impaired platelet adhesion to collagen under high shear.<sup>3,4</sup> Under stasis and low shear flow ( $\leq 150$  s<sup>-1</sup>), platelets adhere to MMRN1 through mechanisms involving  $\alpha_{IIb}\beta_3$  and  $\alpha_v\beta_3$ , with less reliance on VWF-GPIb $\alpha$  binding.<sup>1,2</sup> Resting platelets do not adhere to MMRN1 under stasis or flow,<sup>1,2</sup> which suggests that the high-affinity conformation or receptor clustering of  $\beta_3$  integrins triggered by platelet activation are required for MMRN1 binding.

MMRN1 is able to modulate thrombin generation through its interactions with FV, activated FV(a), and PS on the surface of activated platelets.<sup>5</sup> Within the platelet cytosol, FV undergoes variable proteolytic cleavage of its B-domain, which results in a variety of partially active forms of FV within platelets,<sup>24</sup> meaning that once released, FV that was complexed to MMRN1 within platelet  $\alpha$ -granules is capable of binding to the external platelet membrane and promoting coagulation.<sup>7,25</sup> Diseases that result in MMRN1 deficiency or impair MMRN1-FV binding are associated with impaired platelet FV storage.<sup>6,26,27</sup> MMRN1 is hypothesized to affect thrombin generation: MMRN1 binds to FV with high affinity and FVa shows less stable binding to MMRN1 than FV, which is posited to facilitate FVa delivery onto the platelet surface.<sup>7,23</sup> MMRN1 also competitively

binds to the C1 and C2 domains of FV/FVa,<sup>25</sup> so that while FV or FVa are bound to MMRN1, FVa is prevented from binding to PS on the platelet surface to form the prothrombinase complex. In this regard, MMRN1 may regulate the rate of prothrombinase formation through its interactions with FVa.

### 1.1.3 Multimerin 1-deficient mice

Two different mouse models of *Mmrn1* deficiency have been studied to date. C57BL/6J mice with a spontaneous tandem deletion of the adjacent genes *Mmrn1* and *Snca* (which encodes  $\alpha$ -synuclein) were first studied in the absence of a model for selective *Mmrn1* deficiency.<sup>28</sup> Double-deficient (*Mmrn1*<sup>-/-</sup>/*Snca*<sup>-/-</sup>) mice, which have a complete deletion of the *Mmrn1* gene, have normal bleeding times, but show impaired platelet-rich thrombus formation *in vivo* in FeCl<sub>3</sub>-treated mesenteric arterioles and impaired platelet adhesion to Horn collagen *in vitro* that are corrected by adding back recombinant human (rh)MMRN1.<sup>3</sup> *Mmrn1*<sup>-/-</sup>/*Snca*<sup>-/-</sup> platelets also show enhanced  $\alpha$ -granule release in response to thrombin compared to the wild-type, which is postulated to result from loss of  $\alpha$ -synuclein.<sup>29</sup> Due to enhanced  $\alpha$ -granule release shown by *Mmrn1*<sup>-/-</sup>/*Snca*<sup>-/-</sup> mice, the phenotype of *Mmrn1*<sup>-/-</sup>/*Snca*<sup>-/-</sup> is hypothesized to be less severe than mice with selective *Mmrn1* deficiency.<sup>3,4</sup>

Selective *Mmrn1*-deficient (*Mmrn1*<sup>-/-</sup>) mice were subsequently generated using the knockout-first allele strategy.<sup>30</sup> Adult mice heterozygous for the *Mmrn1* knockout-

first allele were purchased from the European Mutant Mouse Archive and used to generate mice with selective *Mmrn1* deficiency. Generation of selective *Mmrn1*<sup>-/-</sup> mice was performed as a collaborative effort between the laboratories of Dr. Catherine Hayward and Dr. Bradley Doble. In this model, exon 3 of *Mmrn1* was excised by Cre-Lox recombination, causing a frameshift mutation that is predicted to result in an aberrant transcript susceptible to nonsense-mediated decay.<sup>30,31</sup> *Mmrn1*<sup>-/-</sup> mice are viable and fertile without any overt developmental abnormalities, spontaneous bleeding, or reduced survival, and have no detectable platelet *Mmrn1*.<sup>4</sup> Dr. D'Andra Parker characterized some phenotypic aspects of selective *Mmrn1*-deficient mice as part of her doctoral thesis work under the supervision of Dr. Catherine Hayward, which includes analyses of: complete blood cell counts; Western blotting for *Mmrn1* in platelet lysates; plasma and platelet Vwf levels; expression of GpIb $\alpha$ ,  $\beta_1$  integrin, and  $\beta_3$  integrins on resting platelets; P-selectin and activated  $\alpha_{IIb}\beta_3$  expression on thrombin-activated platelets; bleeding time and blood loss; light transmission aggregometry (LTA) responses; and high shear platelet adhesion assays to Horm collagen and recombinant (r)Vwf.<sup>4</sup> Additionally, analyses of thrombus formation *in vivo* were performed by Dr. Yiming Wang in the laboratory of Dr. Heyu Ni as part of collaborative studies between the laboratories of Dr. Ni and Dr. Hayward.

*Mmrn1*<sup>-/-</sup> and wild-type mice have similar blood cell counts, plasma and platelet Vwf levels, and resting platelet expression of GpIb $\alpha$ ,  $\beta_1$  integrin, and  $\beta_3$  integrins. Notably, P-selectin expression of thrombin-activated platelets is similar between *Mmrn1*<sup>-/-</sup>

and wild-type mice. LTA responses are similar between *Mmrn1*<sup>-/-</sup> and wild-type platelets using murine TRAP (500 µM; tested in PRP), thrombin (0.5 and 1.0 U/ml; tested in GFP), ADP (10 and 20 µM; tested in PRP), and Horm collagen (5 and 10 µg/ml; tested in PRP), but gel-filtered *Mmrn1*<sup>-/-</sup> platelets show a significant defect in maximal aggregation responses (20-30% reduction) to Horm collagen compared to wild-type platelets. Additionally, *Mmrn1*<sup>-/-</sup> platelets show impaired adhesion to Horm collagen under high shear flow, but similar adhesion to rVwf compared to the wild-type. Lastly, *Mmrn1*<sup>-/-</sup> mice have normal bleeding times and wound blood loss, but impaired platelet adhesion, thrombus formation, and vessel occlusion *in vivo* in FeCl<sub>3</sub>-treated mesenteric arterioles. Platelet aggregates formed by *Mmrn1*<sup>-/-</sup> mice also show a tendency to break apart from the apex of the developing thrombi, contributing to the delay in time until the first thrombus greater than 20 µm and time until vessel occlusion. Notably, most other knockout or transgenic mouse models tested using the FeCl<sub>3</sub>-induced vessel injury model show defects in one or two parameters (*Table 1*), whereas platelet adhesion and occlusive thrombus formation are abnormal in *Mmrn1*<sup>-/-</sup> mice from start to finish. These findings suggest that *Mmrn1* has a supportive role in platelet adhesion, thrombus formation, and thrombus stability.

#### 1.1.4 Multimerin 1 deficiency states in humans

To date, no selective qualitative or quantitative defect in MMRN1 has been described in humans, but some disease states are associated with platelet MMRN1

deficiency: Quebec platelet disorder (QPD), gray platelet syndrome (GPS), and  $\alpha\delta$ -storage pool deficiency (SPD). QPD is an autosomal dominant disorder that results in delayed mucocutaneous bleeding due to a fibrinolytic defect.<sup>32</sup> QPD is caused by a duplication mutation that includes *PLAU*, which results in overexpression of *PLAU* by megakaryocytes and intra-platelet activation of the fibrinolytic cascade, leading to  $\alpha$ -granule protein degradation, with loss of MMRN1 and FV.<sup>6</sup> GPS is characterized by a reduction or absence of platelet  $\alpha$ -granules due to impaired retention of  $\alpha$ -granule proteins caused by mutations affecting *NBEAL2*,<sup>33–35</sup> *GFI1B*,<sup>36</sup> or *GATA1*,<sup>37</sup> or acquired through unknown mechanisms.<sup>38</sup> Lastly,  $\alpha\delta$ -SPD is associated with reduced numbers of both  $\alpha$ - and dense granules in platelets, causing a deficiency of their contents, which has been attributed in some cases to mutations in *GFI1B* or *IKZF5*.<sup>39,40</sup>

## 1.2 HEMOSTASIS AND THROMBOSIS

Hemostasis is the process through which animals with a closed circulatory system prevent blood loss from damaged or ruptured vessels. Hemostasis is regulated by the interaction of numerous cell types, proteins, and enzymes, and culminates in the formation of a hemostatic plug composed of platelets, erythrocytes, and plasma proteins within and around a polymeric fibrin meshwork.<sup>41</sup> The fibrin meshwork acts as a provisional scaffold to cease blood loss while allowing for the attachment and penetration of cells for remodeling of the damaged area. Impairments in hemostasis due to defects or deficiencies in any of the cells, receptors, plasma or granule proteins, and coagulation

factors involved in hemostatic plug formation lead to unchecked blood loss, which can result in spontaneous and/or severe hemorrhage if untreated.

The formation of a hemostatic plug normally does not occlude the injured portion of the blood vessel and blood continues to circulate following plug formation.

Thrombosis is the pathological formation of a platelet-rich clot, or thrombus, within a vessel that can partially or entirely occlude a blood vessel. Thrombi have the potential to occlude vessels or dislodge from the vessel wall and occlude smaller vessels downstream. Depending on the site of thrombus deposition, vessel occlusion can result in, among other conditions, myocardial infarction, ischaemic stroke, or venous thromboembolism (VTE), which are leading causes of morbidity and mortality in North America.<sup>42–44</sup> The following sections describe the biological basis of hemostatic plug formation and thrombosis, the role of platelets in these processes, and the clearance of platelet-rich fibrin meshworks via fibrinolysis.

### 1.2.1 Blood coagulation and fibrinolysis

The development of a polymeric fibrin clot involves the interaction of numerous enzymes and non-enzymatic cofactors that culminate in the cleavage of soluble fibrinogen (FG) to fibrin by thrombin, which changes blood from a liquid to a gel.<sup>41</sup> This process is referred to as blood coagulation, and polymeric fibrin is a major constituent of coagulated blood.<sup>45</sup> Blood coagulation can occur via two pathways: extrinsic and

intrinsic,<sup>46,47</sup> which converge at the activation of coagulation factor X (FX). Activated FX, FX(a), cleaves circulating prothrombin, the zymogen precursor of thrombin, to thrombin.

The extrinsic pathway of blood coagulation involves the initiation of coagulation by a protein normally “extrinsic” to blood. Tissue factor (TF) is a membrane-associated lipoprotein that is present in most cells, including platelets, endothelial cells, and monocytes.<sup>48</sup> TF is constitutively expressed on the membrane of fibroblasts and smooth muscle cells in the deeper layers of the vessel wall,<sup>49–52</sup> and can be expressed on the surface of platelets,<sup>53–55</sup> endothelial cells,<sup>56–58</sup> or monocytes in response to activation.<sup>51,59</sup> When TF is exposed to flowing blood, either by exposure of flowing blood to TF-bearing cells in the vessel wall or following activation of blood cells,<sup>60</sup> it binds to coagulation factor VII (FVII),<sup>61</sup> and induces conformational change of FVII to an active form FVII(a). The TF-FVIIa complex binds to coagulation factors IX (FIX) and (FX), subsequently activating them to FIXa and FXa.<sup>62</sup> FIXa generates additional FXa, and FXa produces small amounts of thrombin during what is referred to as the “initiation” phase of coagulation.<sup>41,63</sup>

The intrinsic pathway is defined by all of the components necessary for coagulation being present in blood. It is initiated following exposure of blood to negatively charged surfaces (e.g. extracellular DNA, RNA, or polyphosphate – the latter is released from platelet dense granules),<sup>64</sup> which triggers autodigestion of factor XII

(FXII) to its active form FXII(a).<sup>65</sup> FXIIa cleaves factor XI (FXI) to its active form FXI(a),<sup>66,67</sup> and FXIa triggers a cascade of enzymatic reactions that also leads to FXa and thrombin generation.<sup>41</sup> The intrinsic pathway is not independent of the extrinsic pathway. For example, following the initiation phase, thrombin proteolytically activates components of the intrinsic pathway: FVIII, FIX, and FXI, and thrombin can initiate the intrinsic pathway independent of FXIIa by cleavage of FXI.<sup>68</sup> The intrinsic pathway can also be initiated by autoactivation of FXI in contact with a negatively charged surface,<sup>69</sup> such as platelet polyphosphate.<sup>70</sup> The extrinsic pathway is considered to be the major initiation pathway of coagulation *in vivo*,<sup>71-73</sup> whereas the intrinsic pathway has been linked to thrombus growth and inflammation.<sup>63</sup>

The trace amounts of thrombin generated during the initiation phase cleave and activate circulating plasma FV to FVa and factor VIII (FVIII) to activated FVIII(a).<sup>41</sup> FVa and FVIIIa are non-enzymatic cofactors that greatly increase the generation of FXa by FIXa and thrombin by FXa, respectively.<sup>74-76</sup> It is possible that the partially activated FVa released from platelets provides the initial FVa for thrombin generation.<sup>77,78</sup> Formation of the FIXa/FVIIIa and FXa/FVa complexes results in a burst of thrombin generation, which is referred to as the “amplification phase”.<sup>63</sup> The large quantities of thrombin cleave circulating plasma FG and FG released from platelet granules to fibrin monomers, which spontaneously aggregate into fibrils.<sup>79,80</sup> Thrombin also converts factor XIII (FXIII) to its active form FXIII(a),<sup>81</sup> and in the presence of fibrin (as a cofactor), FXIIIa laterally crosslinks and stabilizes fibrin fibrils.<sup>82</sup>

The generation of thrombin is tightly regulated to prevent inappropriate activation of coagulation and fibrin formation in flowing blood.<sup>68</sup> Thrombin generation is self-limiting, in that it cleaves and activates protein C, a major physiologic inhibitor of thrombin generation.<sup>83</sup> Activated protein C (APC) cleaves FVa and FVIIIa, which attenuates thrombin generation.<sup>83</sup> Additionally, heparin sulfate-containing proteoglycans in the vessel wall bind and activate antithrombin,<sup>84</sup> which binds and inactivates thrombin,<sup>85</sup> among other coagulation factors, and accounts for roughly 75% of physiologic thrombin inhibition.<sup>86</sup> The dissolution of fibrin clots, which is the final stage of hemostasis, is mediated by plasmin.<sup>87</sup> Plasmin circulates as its zymogen precursor, plasminogen, in plasma and becomes activated by tissue plasminogen activator (tPA) or urokinase plasminogen activator (uPA).<sup>88,89</sup>

Most coagulation reactions occur on biological surfaces.<sup>90-94</sup> For instance, the prothrombinase complex is composed of FXa and FVa bound to PS or PE that are exposed on the surface of activated platelets,<sup>95</sup> and binding to membrane lipids stabilizes FXa-FVa interactions.<sup>96</sup> More specifically, platelets are vital to blood coagulation and the formation of a fibrin-rich hemostatic plug because they: 1) provide a surface for coagulation reactions at the site of injury, 2) contain many procoagulant molecules that they release locally to support coagulation, and 3) localize coagulation reactions to the site of injury.<sup>97</sup> This is partly evidenced by the bleeding diatheses exhibited by patients with various forms of thrombocytopenia,<sup>98-100</sup> and, conversely, the effects of anti-platelet

drugs, which can significantly reduce the risk of thrombosis and thrombosis-related mortality.<sup>101–105</sup>

### 1.1.2 Platelets

Platelets are small, anucleate cells that circulate in flowing blood at a concentration of approximately 150 to 450 x 10<sup>6</sup> cells/ml in humans.<sup>106</sup> Human platelets circulate in a resting state in a discoid shape of approximately 1 to 2 µm in diameter.<sup>107</sup> Mouse platelets are more numerous and smaller; they circulate at concentrations ranging from 400 to 1600 x 10<sup>6</sup> cells/ml.<sup>108</sup> Platelets are unique to mammals: fish, birds, and reptiles possess analogous cells called thrombocytes that carry out similar functions.<sup>109</sup>

Platelets are formed by polyploid megakaryocytes (MKs) in bone marrow.<sup>110</sup> The current view of platelet formation is that MKs form proplatelet extensions composed of a thin cytoplasmic process dotted with platelet-sized blebs.<sup>111–113</sup> These proplatelet extensions protrude into the vascular sinuses of blood vessels in bone marrow,<sup>114,115</sup> where they fragment into platelets and enter circulation.<sup>116,117</sup> Recently, the lung microcirculation has also been identified as a major site of platelet production.<sup>118</sup> Platelets are constitutively formed and released into circulation at a rate of approximately 100 billion per day in humans,<sup>119</sup> where they circulate for up to 10 days in humans and about 5 days in mice.<sup>120,121</sup> Circulating platelets gradually decrease in size, undergo membrane changes, and have reduced hemostatic efficiency,<sup>122,123</sup> meaning that at any moment, a

mosaic population of platelets of different size and adhesive potential circulate within flowing blood.

Platelets contain a variety of organelles and many proteins, including proteins endocytosed from plasma and proteins that are endogenously synthesized by MKs, such as MMRN1.<sup>7,11,13</sup> Platelets are anucleate but are capable of some protein synthesis, since they contain mRNAs and ribosomes derived from MKs.<sup>124</sup> A defining feature of platelets is the presence of numerous  $\alpha$ -granules and dense granules.<sup>125,126</sup> Alpha-granules are the site where most secreted proteins are stored in platelets and they are the most numerous organelle in platelets,<sup>127,128</sup> numbering from roughly 40 to over 100 per platelet, and account for roughly 10% of platelet volume.<sup>129</sup> Platelets release their  $\alpha$ -granule contents following activation, and the platelet secretome ranges in estimates from around 300 to over 700 proteins,<sup>130,131</sup> which includes soluble plasma proteins (e.g. FG, fibronectin [FN], vitronectin [VN], thrombospondin-1 [TSP-1], VWF, and MMRN1) and membrane-bound proteins (e.g. integrin  $\alpha_{IIb}\beta_3$ , GPVI, GPIb-IX-V, and CD36). Within dense granules, platelets store ADP and polyphosphate, which modulate platelet activation and coagulation, respectively.<sup>132,133</sup> In addition to storing and releasing procoagulant and pro-adhesive molecules, platelets store and release a variety of pro-inflammatory molecules, chemotactic factors, and growth factors. Accordingly, emerging roles of platelets in inflammation,<sup>134-136</sup> immunity,<sup>137-139</sup> angiogenesis,<sup>140-142</sup> and cancer have been reported,<sup>142-145</sup> but are outside the scope of this thesis.

In laminar flow, platelets are pushed to the vessel wall by circulating erythrocytes, which allows platelets to constantly survey the integrity of the vessel wall surface for sites of damage.<sup>146</sup> The endothelial cells lining blood vessels and capillaries maintain circulating platelets in a resting state by constitutive release of nitrous oxide (NO) and prostacyclin (PGI<sub>2</sub>),<sup>147,148</sup> expression of CD39,<sup>149</sup> and an extensive glycocalyx.<sup>150–152</sup> Once platelets encounter an area of vessel wall injury or endothelial cell activation, or leave the circulation through a severed vessel, they rapidly adhere and become activated. In wounds, this process is referred to as primary hemostasis.<sup>97,153</sup>

### 1.3 PLATELET ADHESION

Platelet adhesion is a critical initial step in hemostasis because localization of platelets at the site of vessel injury is absolutely required for platelets to fulfil their hemostatic functions.<sup>97,144,154–156</sup> Similarly, thrombus formation can be initiated by platelet adhesion.<sup>146</sup> Understanding the mechanisms of platelet adhesion is crucial to the development of treatment and prevention strategies in hemostatic and thrombotic disorders. This section will focus primarily on platelet adhesion in the hemostatic response to injury, although the mechanisms involved in platelet tethering and recruitment of additional circulating platelets onto a growing platelet aggregate are mostly conserved between hemostasis and thrombosis.<sup>157,158</sup> *Figure 2* outlines the general steps involved in platelet adhesion, from exposure of collagens in the vessel wall to formation of a stable, platelet-rich hemostatic plug. In recent years, a preliminary phase

referred to as the “protein wave” of hemostasis has been reported,<sup>155,159–161</sup> in which circulating plasma proteins that support platelet adhesion (e.g. FG, FN, and VWF) bind to the exposed extracellular matrix following vessel injury. These interactions result in an exposed vessel wall that is “hyper-adhesive”, in that it contains numerous sites for additional pro-adhesive plasma proteins and circulating platelets to attach, and provides a provisional protein scaffold from which a polymeric fibrin meshwork can later be deposited.

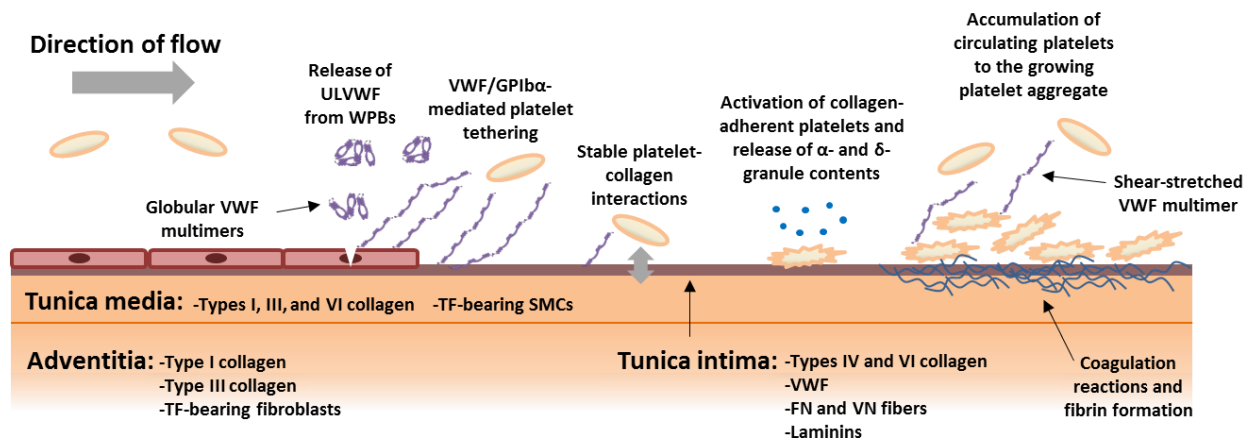


**Figure 2: Overview of platelet adhesion following injury to the vessel wall under high shear flow.** 1) Vessel injury exposes the subendothelium and deeper layers of the vessel wall to flowing blood, and ruptures or activates nearby endothelial cells lining the site of injury releasing ultra-large (UL)VWF and MMRN1. 2) Circulating plasma proteins, such as FG, FN, VWF, and VN bind to extracellular matrix components (e.g. collagens and laminins). Additionally, FN, VN, and VWF are constitutively present within the vessel wall. Together, these interactions prime the exposed vessel wall to support platelet adhesion. 3) Collagen- or EC-bound VWF multimers extend under shear into the vessel lumen, which transiently bind to GPIb $\alpha$  on circulating platelets. VWF/GPIb $\alpha$  binding decreases the velocity of platelets, allowing them to slowly translocate along the exposed vessel wall. 4) Platelets bind to exposed fibrillar collagens via integrin  $\alpha_2\beta_1$  and GPVI and become activated. 5) Platelet activation triggers the generation and release of soluble agonists (ADP and TxA<sub>2</sub>), procoagulant molecules (FV and polyphosphate), and pro-adhesive molecules (i.e. VWF, FG, FN, VN, TSP-1, and MMRN1). Integrins  $\alpha_2\beta_1$  and  $\alpha_{IIb}\beta_3$  shift to a high-affinity conformation on activated

platelets, which enables ligation of additional proteins or motifs and stabilizes adhesion. 6) Additional platelets are recruited onto the activated platelet monolayer by VWF multimers bound to activated  $\alpha_{IIb}\beta_3$  and become activated by the high local concentration of soluble agonists. Simultaneously, coagulation reactions occur on the surface of collagen- and thrombin-activated platelets at the interface of the vessel wall, resulting in fibrin meshwork formation.

Shear stress and shear rate affect the dynamics of platelet adhesion.<sup>156,162,163</sup> Wall shear stress ( $\tau_w$ , referred to hereafter as “shear stress”) refers to the force applied to the vessel wall as blood flows across the vessel wall through the lumen at a constant rate, taking into consideration the viscosity ( $\mu$ ) of the fluid, and is measured by units of force per area ( $\text{dyn}/\text{cm}^2$ ). Wall shear rate ( $\gamma_w$ , referred to hereafter as “shear rate”) refers to the rate of shearing deformation experienced by the vessel wall as blood flows across, expressed as reciprocal seconds ( $\text{s}^{-1}$ ), which is a function of the size of the vessel lumen and the velocity of flowing blood. Given that vessel diameter and velocity both affect the shear rate experienced by the vessel wall, arteries and veins of different sizes and capillaries experience different shear rates. In humans, normal shear rates range from 20 to  $200 \text{ s}^{-1}$  in veins, 300 to  $800 \text{ s}^{-1}$  in medium and large arteries, and 500 to  $5000 \text{ s}^{-1}$  in small arteries.<sup>159,164</sup> Under pathological conditions, stenotic vessels can experience shear rates in excess of  $40,000 \text{ s}^{-1}$ .<sup>165</sup> An important consideration is that shear rates are not constant or uniform *in vivo*: blood flow through the heart into downstream vessels is pulsatile, meaning that the shear rate increases and decreases as blood is pushed through vessels by muscular contractions of the heart.<sup>166</sup> Additionally, shear rate changes based on vascular tone, which is locally controlled by smooth muscle contraction or dilation of the tunica media.<sup>167</sup> Shear gradients and microenvironments have also been observed in areas

where the vessel lumen is constricted or obstructed,<sup>158,168,169</sup> or where vessels bend and branch.<sup>170</sup> Murray's law posits that the circulatory system branches in such a way that minimizes the energy cost of pumping blood through a vessel.<sup>171</sup> It is shown that this tendency toward energy minimization affects shear rates; vessel bifurcations result in areas of low shear stress or high oscillatory shear (i.e., reversal of shear stress that occurs during pulsatile flow).<sup>172</sup> Additionally, vessel injury stimulates the localized release of vasoconstrictive molecules from endothelial cells, which increases the shear rate at and around the site of injury as the lumen decreases in diameter.<sup>173</sup> Therefore, it is important to note that fluid shear rates are complex and dynamic, and its categorization into high and low shear is an abstraction that is useful for descriptive and experimental purposes. Blood is a Non-Newtonian colloid,<sup>156</sup> but exhibits the properties of a Newtonian fluid, in that its shear stress and shear rate are linearly correlated. For this reason, it is treated as a Newtonian fluid in these calculations.

Under shear rates  $>500 \text{ s}^{-1}$ , platelet receptors  $\alpha_2\beta_1$ ,  $\alpha_{IIb}\beta_3$ , and GPVI are increasingly insufficient to support significant platelet adhesion to the exposed vessel wall.<sup>174,175</sup> VWF binding to the vessel wall and its shear-induced unfolding into long strings is required for platelet adhesion under high shear flow (ranging from  $\sim 500$  to  $>20,000 \text{ s}^{-1}$ ).<sup>174,176,177</sup> The first point of contact between circulating platelets and the exposed subendothelium is generally considered to be immobilized VWF multimers extending into the lumen of the blood vessel,<sup>178–181</sup> which requires VWF to be bound to various proteins in the ECM. VWF multimers transiently bind to GPIIb $\alpha$  on platelets,

which decreases the velocity of circulating platelets and allows them to slowly translocate along the exposed vessel wall.<sup>174,178</sup> Platelet translocation facilitates activation via platelet GPVI binding to fibrillar collagens in the vessel wall and stable adhesion to collagens and other matrix constituents by platelet integrins  $\alpha_2\beta_1$  and  $\alpha_{IIb}\beta_3$ , respectively.<sup>174,175</sup> Under low ( $<500\text{ s}^{-1}$ ) shear flow, ligation of ECM components by platelet receptors  $\alpha_2\beta_1$ ,  $\alpha_{IIb}\beta_3$ , and GPVI are sufficient to support stable adhesion at the site of injury.<sup>174,175,182,183</sup>

Following the initial deposition of platelets onto the exposed vessel wall, additional platelets begin aggregating onto the stably adherent monolayer of activated platelets. Primary adherent platelets are activated through multiple mechanisms. First, ligation of GPIIb $\alpha$  by VWF stimulates intracellular  $\text{Ca}^{2+}$  mobilization and activation of integrin  $\alpha_{IIb}\beta_3$ ,<sup>184–186</sup> and ligation of either  $\alpha_2\beta_1$  or  $\alpha_{IIb}\beta_3$  similarly trigger outside-in signalling in platelets that results in shape change and intracellular  $\text{Ca}^{2+}$  mobilization.<sup>187–189</sup> Fibrillar collagen is a potent agonist of platelet activation, and collagen binding to GPVI is a key initiator of platelet activation.<sup>190</sup> Additionally, platelets are further activated by trace amounts of thrombin generated by TF/FVIIa-activated FX at the site of injury. Full platelet activation by either collagen or thrombin triggers intracellular shape change, synthesis of thromboxane  $\text{A}_2$  ( $\text{TxA}_2$ ), and the localized release of  $\alpha$ -granule contents, which include pro-adhesive proteins (e.g. VWF, FG, FN, TSP-1, VN, and MMRN1) and soluble platelet agonists (e.g. ADP and  $\text{TxA}_2$ ).<sup>191–196</sup> Plasma and platelet VWF multimers stably bind to activated  $\alpha_{IIb}\beta_3$  on the activated platelet surface, where they extend into the lumen to tether additional circulating platelets.<sup>156,197–199</sup> Captured

platelets become activated by the high local concentration of agonists and stably adhere to a growing network of platelets and adhesive glycoproteins.<sup>146,156,181,200</sup> This process of additional platelet recruitment continues until the site of injury is fully covered in a platelet aggregate.<sup>156,181,200</sup> Simultaneous to platelet adhesion, coagulation reactions take place on the surface of activated platelets, which results in a high local concentration of thrombin and the formation of a polymeric fibrin meshwork.<sup>201</sup> The process of fibrin clot formation occurring alongside platelet adhesion and activation is referred to as “secondary hemostasis”.<sup>41</sup> In addition to the self-limiting regulatory mechanisms of coagulation, platelet adhesion is tightly regulated in order to prevent the aggregation stage from continuing unchecked and occluding the vessel at the site of injury.<sup>160,202</sup> In particular, roles in the regulation of the extent of platelet aggregate formation at sites of injury have been reported for plasma FN, TSP-1, and VN, which are discussed in sections 1.2.1.3, 1.2.1.4, and 1.2.1.5, respectively.

### 1.3.1 Platelet adhesive proteins

The following sections focus on the roles of specific plasma, extracellular matrix, and/or platelet/endothelial cell granule proteins in supporting platelet adhesion and platelet aggregation (*Figure 3*). There are some striking structural and functional similarities between many of the adhesive glycoproteins circulating in plasma and stored within platelet and endothelial cell granules. FG, FN, TSP-1, VN, VWF, and MMRN1 are multi-domain glycoproteins, which enables these proteins to interact with a variety of

ligands. FN, VN, TSP-1, VWF, and MMRN1 can self-associate to create large homopolymers, and FG can also self-associate after thrombin-mediated conversion of FG to fibrin, which has the potential to greatly increase the avidity of binding interactions.

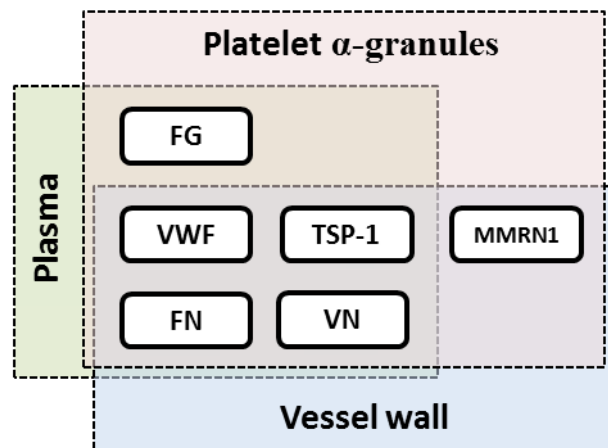


**Figure 3: Distribution of select proteins within plasma, platelets  $\alpha$ -granules, and the vessel wall that are known to support platelet adhesion and/or aggregation.**

FG, FN, TSP-1, and VN are also able to bind to one another. It has been postulated that adhesive plasma proteins, in particular FN, TSP-1, and VN, facilitate the formation of large macromolecular complexes at sites of injury that enhance platelet adhesion and aggregation.<sup>203–206</sup> Accordingly, a supporting, but non-essential role in platelet adhesion and thrombus formation has been reported for FN, TSP-1, and VN. Given their similarities to MMRN1, it is possible that MMRN1 similarly assists in the formation of large, macromolecular complexes at sites of injury or a developing thrombus to enhance platelet adhesion and stabilize platelet-platelet or platelet-matrix interactions. Mice with Fn-,<sup>207,208</sup> Tsp-1-,<sup>209</sup> or Vn-deficiency<sup>210</sup> do not experience abnormal bleeding,

but some parameters of platelet adhesion and *in vivo* thrombus formation are impaired in these animals (*Table 1*), which is similar to observations of *Mmrn1*<sup>-/-</sup> mice.<sup>203,208,211,212</sup> Additionally, Fg-, Vwf-, or combined Fg/Vwf-deficient mice are still able to aggregate *in vitro*<sup>213</sup> and form thrombi *in vivo* in response to experimentally-induced vessel injury,<sup>211</sup> which suggests other proteins, such as Fn, Tsp-1, Vn, and/or Mmrn1, support these processes in the absence of Fg and Vwf. Lastly, another functional similarity between FN, TSP-1, and VN is that they are demonstrated to play a dual role in platelet adhesion and platelet aggregation,<sup>203–205</sup> switching between supporting or inhibiting platelet aggregation based on their conformation or the presence of other plasma proteins.

<b>Ferric chloride mesenteric vessel injury model</b>					
<b>Model</b>	<b>Background</b>	<b>Bleeding following tail transection</b>	<b>Plt. Adhesion</b>	<b>Thrombus growth</b>	<b>Vessel occlusion</b>
<i><math>\alpha_2</math></i> <sup>-/-</sup>	C57BL/6J <sup>183,214,215</sup>	Normal <sup>214</sup> ; Severe <sup>183*</sup>	Normal <sup>215</sup>	Delayed; frequent emboli <sup>215</sup>	Delayed; frequent emboli <sup>215</sup>
<i>GpVI</i> <sup>-/-</sup>	C57BL/6J <sup>216-218</sup> ; BalbC <sup>183</sup>	Slight <sup>216</sup> ; Moderate <sup>183</sup> ; Normal <sup>218</sup>	-	Delayed <sup>217†</sup>	Delayed <sup>217†</sup>
<i>GpIb<math>\alpha</math></i> <sup>-/-</sup>	C57BL/6J <sup>219,220</sup>	Severe <sup>219</sup>	Abolished <sup>220‡</sup>	Abolished <sup>220‡</sup>	Abolished <sup>220‡</sup>
<i><math>\beta_3</math></i> <sup>-/-</sup>	C57BL/6J <sup>221</sup>	Severe <sup>221</sup>	-	-	-
<i>Vwf</i> <sup>-/-</sup>	C57BL/6J <sup>211,212,222,223</sup>	Severe <sup>222,223</sup>	Impaired <sup>211,212,222,223</sup>	Delayed <sup>211,222</sup>	Delayed/ absent <sup>211,222</sup>
<i>Tsp-1</i> <sup>-/-</sup>	C57BL/6J <sup>209,212,224</sup> ; Swiss <sup>225</sup>	Normal <sup>209</sup>	Normal <sup>212</sup>	Delayed <sup>212</sup>	Delayed <sup>212</sup>
<b>Global</b> <i>Fn</i> <sup>-/-</sup>	C57BL/6J <sup>226</sup>	-	-	-	-
<b>Cdtl.</b> <i>pFn</i> <sup>-/-</sup>	C57BL/6J <sup>207,208</sup>	Normal <sup>207</sup>	Normal <sup>208</sup>	Delayed <sup>208</sup>	Delayed <sup>208</sup>
<i>Fg</i> <sup>-/-</sup>	129/CF-1 <sup>227</sup> ; C57BL/6J <sup>211,227</sup>	Severe <sup>227¶</sup>	Normal <sup>211</sup>	Normal <sup>211</sup>	Embolize and occlude downstream <sup>211</sup>
<i>Vn</i> <sup>-/-</sup>	C57BL/6J <sup>203,228,229</sup>	Normal <sup>228</sup>	Normal <sup>203</sup>	Normal <sup>203</sup>	Delayed; frequent emboli <sup>203</sup>
<i>Mmrn1</i> <sup>-/-</sup>	C57BL/6J <sup>4</sup>	Normal <sup>4</sup>	Impaired <sup>4</sup>	Delayed <sup>4</sup>	Delayed/absent <sup>4</sup>

**Table 1: Phenotypic traits of transgenic and knockout mice for proteins involved in platelet adhesion, hemostasis, and thrombosis.** Distal tip tail amputations used in bleeding studies vary from 1 to 6 mm from the end of the tail. Studies report similar concentrations and application of FeCl<sub>3</sub>, and shear rate in mesenteric arterioles is estimated to be approximately 1400 s<sup>-1</sup>.<sup>222</sup> \*Tested using  $\alpha_2$ -deficient mice of a mixed C57BL/6J and BalbC background compared to C57BL/6J or BalbC wild-type controls.

†Studies were performed using FcR $\gamma$ -deficient mice, which have no detectable surface expression of GpVI. ‡Studies were performed using GpIb $\alpha$  functional knockout mice, which are transgenic mice that express a chimeric form of GpIb $\alpha$  that does not bind Vwf. These mice do not have giant platelets characteristic of *GpIb $\alpha$*  knockout mice or Bernard-Soulier syndrome. ¶Bleeding time for these animals was measured by amputation of the 5th digit. "-" indicates data not available or data that has not been reported.

### 1.3.1.1 Fibrinogen and fibrin

Fibrinogen (FG) is a large dimeric glycoprotein composed of three pairs of polypeptide chains: A $\alpha$ , B $\beta$ , and  $\gamma$ , which have a total mass of approximately 340-kDa.<sup>230</sup> The designation of polypeptide chains as a Latin and a Greek character is due to the thrombin-mediated cleavage of FG to fibrin.<sup>231</sup> Cleavage of FG by thrombin releases fibrinopeptides A and B leaving two  $\alpha\beta\gamma$  fibrin monomers.<sup>230</sup> The A $\alpha$ B $\beta$  $\gamma$  FG dimer is approximately 45 nm in length and held together at a central nodule by inter-chain disulfide bonds.<sup>232</sup> The majority of FG is synthesized by hepatocytes in humans,<sup>233</sup> where it is constitutively secreted into circulation at a very high concentration ranging from 2 to 4 g/l in plasma in humans.<sup>234</sup> In adult C57BL/6J mice, Fg circulates in plasma at concentrations ranging from 1.6 to 2.4 g/l.<sup>235–237</sup> Plasma FG is also uptaken into MKs and platelets and stored within  $\alpha$ -granules through a mechanism involving FG binding to  $\alpha_{IIb}\beta_3$ .<sup>238</sup>

FG is a ligand for FN,<sup>239,240</sup> TSP-1,<sup>241,242</sup> fibrin,<sup>243</sup> and  $\alpha_V\beta_3$ ,<sup>244</sup> but its interaction with  $\alpha_{IIb}\beta_3$  has been the most studied, leading to  $\alpha_{IIb}\beta_3$  being referred to as the “fibrinogen receptor”.<sup>245</sup> FG binds to  $\alpha_{IIb}\beta_3$  on activated platelets with a  $K_D$  of approximately 100

nM,<sup>246</sup> which is almost 100-fold less than the concentration of FG in plasma. These data suggest that the FG-binding site on  $\alpha_{IIb}\beta_3$  is likely immediately occupied by FG following platelet activation. FG binding to  $\alpha_{IIb}\beta_3$  is critical for platelet aggregation under low shear stress.<sup>247</sup> FG binding to  $\alpha_{IIb}\beta_3$  involves the KQAGDV sequence in the FG  $\gamma$ -chain and its dimeric structure allows FG to crosslink platelets by each FG  $\gamma$ -chain engaging a single copy of  $\alpha_{IIb}\beta_3$  on adjacent platelets.<sup>248</sup> The human FG dimer contains two pairs of integrin-binding RGD sequences (residues A $\alpha$  95-97 and A $\alpha$  572-574), however, these RGD motifs are not required for FG-mediated platelet aggregation.<sup>249,250</sup> RGDS peptides are able to inhibit  $\alpha_{IIb}\beta_3$  binding to FG *in vitro* presumably because they can compete with the FG  $\gamma$ -chain KQAGDV motif for ligation of  $\alpha_{IIb}\beta_3$ .<sup>251</sup> These motifs are shown to be necessary for clot retraction, suggesting they may be essential for the interaction of  $\alpha_{IIb}\beta_3$  with fibrin.<sup>252–255</sup>

FG is critically important to hemostasis. FG levels are a major predictor of blood loss and death following hemorrhage from surgery or severe trauma,<sup>256–260</sup> and FG concentrate is a commonly used intervention to prevent post-surgical or trauma-induced severe bleeding.<sup>261,262</sup> Human patients with congenital or acquired afibrinogenemia suffer from spontaneous bleeding and severe bleeding after minor trauma.<sup>263</sup> Conversely, elevated FG levels (4.0 to 4.9 g/l) are associated with a greater risk of thrombosis.<sup>264</sup> Mice with fibrinogen deficiency ( $Fg^{-/-}$ ) are viable and fertile, but have reduced survival due to spontaneous intraabdominal hemorrhage (*Table 1*).<sup>211,227</sup> Whole blood from  $Fg^{-/-}$  mice fails to clot either spontaneously or in response to thrombin, and  $Fg^{-/-}$  mice experience

severe bleeding in response to injury.<sup>227</sup> PRP from  $Fg^{-/-}$  mice also fails to aggregate in response to ADP.<sup>227</sup> In response to  $FeCl_3$  treatment of mesenteric arterioles,  $Fg^{-/-}$  mice show normal platelet adhesion and thrombus development, but their thrombi are unstable and embolize downstream of the initiation of thrombus growth.<sup>211</sup>

Immobilized FG is capable of supporting platelet adhesion through a mechanism that requires  $\alpha_{IIb}\beta_3$  under shear rates up to  $1000\text{ s}^{-1}$ .<sup>174</sup> Platelets immediately arrest onto FG surfaces under shear rates of approximately  $600$  to  $900\text{ s}^{-1}$ , with platelets typically adhering as a monolayer.<sup>265</sup> Maximal adhesion to FG is reported for shear rates between  $50$  and  $250\text{ s}^{-1}$ .<sup>174,265</sup> Platelet adhesion to FG has been observed under shear rates up to  $2000\text{ s}^{-1}$ , but very few platelets adhere to FG-coated surfaces under these conditions.<sup>174,265</sup> Additionally, platelet  $\alpha_{IIb}\beta_3$  binding to immobilized FG is very stable: real-time analyses of platelet adhesion to FG report it is 90% irreversible.<sup>174</sup> It is postulated that the slow rate of bond formation between FG and  $\alpha_{IIb}\beta_3$  is insufficient to support platelet adhesion under high shear rates, and that platelet  $GpIb\alpha$  binding to immobilized VWF potentiates stable platelet adhesion under high shear by reducing the velocity of flowing platelets, which enables immobilized FG to bind activated  $\alpha_{IIb}\beta_3$  on circulating platelets.<sup>181</sup>

Platelet adhesion to immobilized FG and fibrin are shown to be roughly identical,<sup>174</sup> but some differences in the mechanisms of platelet adhesion to FG versus fibrin have been described. Monoclonal anti- $\alpha_{IIb}\beta_3$  antibodies or the snake venom halysin, which blocks FG binding to  $\alpha_{IIb}\beta_3$ , block platelet adhesion to both immobilized FG and fibrin, whereas RGD peptides are only effective to partially inhibit platelet adhesion to

FG and do not inhibit adhesion to fibrin.<sup>266</sup> Similar to the effect of RGDS peptides on platelet aggregation, it is postulated that RGDS peptides compete for ligation of  $\alpha_{IIb}\beta_3$  with the KQAGDV motif in circulating FG, rather than inhibiting RGD-dependent binding of FG to  $\alpha_{IIb}\beta_3$ . In regard to platelet adhesion to fibrin, differences in ultrastructure between immobilized FG and three-dimensional fibrin meshworks likely play a significant role.

Following cleavage of FG to fibrin by thrombin, fibrin monomers rapidly self-associate into larger polymers. Fibrin polymerization is initiated by cleavage of fibrinopeptides A and B by thrombin,<sup>81</sup> which exposes fibrin-binding sites in the  $\alpha\beta\gamma$  fibrin monomer, allowing monomers to self-associate. Fibrin monomers bind one another in a half-staggered manner, adding additional monomers longitudinally to form large two-stranded oligomers.<sup>267,268</sup> Once oligomers reach 0.5  $\mu\text{m}$  in length, they are considered protofibrils,<sup>79,80</sup> which are capable of associating laterally into fibrin fibers. Fibers begin branching to produce a three-dimensional network of fibrin fibers,<sup>269,270</sup> although the mechanisms of fibrin branching are not well-understood. The biological requirements of fibrin networks are that they must be rigid enough to stop bleeding, but simultaneously allow the penetration of cells for wound healing and tissue remodelling.

Fibrin binds numerous other proteins, including activated coagulation factor XIII (FXIIIa),<sup>81</sup> FN,<sup>239</sup> FG,<sup>243</sup> VWF,<sup>271</sup>  $\beta_3$  integrins on activated platelets,<sup>272</sup>  $\alpha_V\beta_3$  and ICAM-1 on activated endothelial cells,<sup>273</sup> and  $\alpha_M\beta_2$  on activated leukocytes.<sup>274</sup> Collectively, these

interactions enable platelets and leukocytes to stably adhere to growing fibrin meshworks, which is essential for hemostasis as well as wound healing by attracting leukocytes to areas of vessel injury. FXIIIa stabilizes fibrin networks by catalyzing the formation of covalent lysine bonds between fibrin molecules and crosslinking other proteins to the fibrin network, such as FN, FG, and VWF.<sup>271</sup> FN affects fibrin fiber density and diameter in clots following crosslinkage to fibrin by FXIIIa, and is postulated to contribute to wound healing.<sup>275</sup> FG binding to fibrin monomers is hypothesized to be a regulatory mechanism that inhibits polymerization of small amounts of fibrin generated in flowing blood.<sup>243</sup> Additionally, a “platelet-trapping” phenomenon has been described, in which polymeric fibrin meshworks mechanically trap circulating platelets.<sup>276</sup> This process requires thrombin to produce fibrin and activate platelets, but not  $\alpha_{IIb}\beta_3$ . Thrombin can bind GPIb, PAR-1, or PAR-4 to activate platelets, which facilitates release of platelet FV, FV-mediated amplification of thrombin generation, and substantial fibrin generation. In the presence of lotrafiban, which blocks FG and VWF binding to  $\alpha_{IIb}\beta_3$ , platelets are able to aggregate, and this aggregation is dependent on fibrin polymerization by thrombin.<sup>276</sup>

Recently, fibrin has been shown to bind GPVI on human and mouse platelets, and fibrin binding to GPVI is capable of inducing outside-in signalling resulting in tyrosine phosphorylation.<sup>277,278</sup> A low level of FcR  $\gamma$ -chain phosphorylation has also been shown following platelet GPVI binding to immobilized FG, compared to other agonists such as collagen.<sup>279</sup> Although platelet activation is not required for platelets to adhere to FG,<sup>265</sup> GPVI activation by FG is involved in subsequent platelet spreading on immobilized FG.

GPVI-deficient platelets fail to generate extensive lamellipodial sheets on immobilized FG.<sup>279</sup> Platelet activation has long been known to be required for platelet spreading on FG,<sup>195,280</sup> and, interestingly, ligation of activated  $\alpha_{IIb}\beta_3$  has been reported to trigger outside-in signalling similar to ligation of GPVI, inducing  $Ca^{2+}$  mobilization in platelets.<sup>188,189</sup> FG binding to  $\alpha_{IIb}\beta_3$  similarly triggers  $Ca^{2+}$  mobilization through outside-in signalling.<sup>281,282</sup> Although fibrin binds to  $\alpha_{IIb}\beta_3$ , it is not yet known if fibrin similarly induces outside-in signalling via  $\alpha_{IIb}\beta_3$ .

#### *1.3.1.2 Fibronectin*

Fibronectin (human: FN; mouse: Fn) is a homodimeric glycoprotein composed of two 230- to 250-kDa subunits that are connected by a pair of disulfide bonds near their C-termini.<sup>275,283–285</sup> Each subunit is composed of repeating modules: 12 type I, 2 type II, 15 type III modules, two additional type III modules referred to as extra domains (ED)-A and ED-B, and a variable region. The FN monomer is encoded by a single gene and alternative splicing of *FN* pre-mRNA results in up to 20 FN variants in humans, which vary in abundance depending on tissue and cell type. FN isoforms are divided into two categories: 1) the soluble, inactive form in plasma (pFN) that does not contain ED-A or ED-B, and 2) the insoluble cellular form (cFN) that contains at least one ED.<sup>160</sup> cFN is a more heterogeneous group of isoforms with cell type-specific splicing of *FN* pre-mRNA, which are synthesized and deposited locally into extracellular matrices.<sup>286,287</sup> Plasma FN is synthesized exclusively by hepatocytes in humans and mice and constitutively released

into circulation.<sup>288</sup> pFN circulates in a compact, inactive conformation<sup>289</sup> at a concentration of roughly 100 to 300  $\mu\text{g/ml}$  in humans and 580  $\mu\text{g/ml}$  in mice,<sup>290</sup> and also accounts for up to 50% of FN content in some murine tissues.<sup>291</sup> pFN is endocytosed and packaged into platelet  $\alpha$ -granules through a mechanism involving  $\alpha_{\text{IIb}}\beta_3$  and accounts for roughly 80% of Fn content in mouse platelets.<sup>207</sup> The latter portion of platelet Fn is made up of cFn, which is likely of megakaryocyte origin.<sup>207</sup>

The active form of FN is in a fibrillar conformation, in which FN molecules self-assemble into fibers ranging in diameter from 10 nm to micrometers in width, and lengths up to tens of micrometers.<sup>292</sup> The initiation of FN fiber formation by platelets is not well-understood, but has been studied in the context of fibroblasts. After FN binds to integrin  $\alpha_5\beta_1$  on the cell surface,  $\alpha_5\beta_1$  translocates along the plasma membrane, which mechanically stretches FN dimers to expose cryptic binding sites in type III modules that enable pFN binding, and cells can actively add FN molecules to FN fibers.<sup>291</sup> FN matrix fibers are held together by intermolecular, non-covalent bonds that stabilize these structures in an insoluble state, and FN fibers are believed to act as a provisional scaffold during wound healing.<sup>293</sup>

FN binds to integrins  $\alpha_{\text{IIb}}\beta_3$ ,<sup>294,295</sup>  $\alpha_V\beta_3$ ,<sup>296</sup> and  $\alpha_5\beta_1$ <sup>297</sup> on platelets, fibrillar collagens I and III,<sup>298</sup> FG,<sup>298</sup> fibrin,<sup>298</sup> and TSP-1.<sup>299</sup> Platelet adhesion to FN is mediated by platelet integrins binding to the RGD sequence in the tenth type III module of FN.<sup>300</sup> Immobilized FN supports platelet adhesion under stasis and shear up to  $1300\text{ s}^{-1}$ , with

maximal adhesion observed at  $300 \text{ s}^{-1}$ .<sup>301</sup> Platelet adhesion to FN under stasis or flow involves RGD-dependent binding to  $\alpha_5\beta_1$  and  $\alpha_{IIb}\beta_3$ . Antibody blockade of  $\alpha_5\beta_1$  reduces adhesion to FN by roughly 50%, whereas blockade of  $\alpha_{IIb}\beta_3$  completely abolishes platelet adhesion to FN.<sup>301</sup> Similarly, Glanzmann thrombasthenia (GT) platelets, which lack  $\alpha_{IIb}\beta_3$ , do not adhere to immobilized FN under flow.<sup>301</sup> Platelet adhesion to immobilized FN on its own is a relatively weak interaction compared to platelet adhesion onto fibrillar collagen or cultured subendothelial matrix, and platelets are more easily detached from FN under increased shear stress compared to their detachment from VWF or collagen surfaces.<sup>302</sup> Additionally, FN binding to  $\alpha_{IIb}\beta_3$  requires platelet activation,<sup>295</sup> which induces a shift to the high-affinity conformation of  $\alpha_{IIb}\beta_3$ .

A supporting role of FN has been reported in platelet adhesion to fibrillar collagens or to fibrin. Platelet adhesion to type I or III fibrillar collagen is significantly reduced when platelets are re-suspended in FN-free plasma under a range of shear rates ( $490, 800, \text{ and } 1300 \text{ s}^{-1}$ ),<sup>303,304</sup> and pFN enhances adhesion and aggregate size of washed platelets onto collagen under high shear flow ( $1250 \text{ s}^{-1}$ ) in a dose-dependent manner.<sup>305</sup> In regard to fibrin, pFN becomes tethered to the  $\alpha$ -chain of fibrin in a reaction catalysed by thrombin-activated FXIII,<sup>306</sup> and pFN crosslinked to immobilized fibrin matrices enhances platelet adhesion and aggregate formation compared to fibrin matrices alone. It is postulated that the presence of pFN stabilizes platelet thrombi and enhances platelet cohesion.<sup>206</sup> Activated platelets adherent to immobilized FN, fibrin, or type I collagen are

also able to assemble FN into fibers, whereas platelets adherent to immobilized FG, VN, or VWF suppress pFN assembly.<sup>305,307,308</sup>

Until recently, the ability of FN to modulate platelet aggregation was controversial. pFN binds to thrombin-activated, but not ADP-activated, platelets.<sup>309</sup> Monoclonal anti-FN antibodies inhibit platelet aggregation by thrombin or collagen, but exogenous pFN inhibits thrombin- or collagen-induced platelet aggregation.<sup>310</sup> The adhesive properties of pFN are considered to depend on the conformation of FN, whether it is present as soluble dimers, insoluble fibers, or crosslinked to fibrin. Consequently, a dual role has been proposed for pFN in hemostasis and thrombosis: pFN can switch from an inhibitory role in platelet adhesion and platelet aggregation to a supportive role in the presence of fibrin.<sup>204</sup>

Fibrin is required for pFn dimers to support platelet aggregation, and pFn inhibits platelet aggregation in response to agonists or conditions that do not induce fibrin formation.<sup>160,311</sup> It is postulated that the close proximity of RGD loops on a FN dimer restricts the ability of soluble FN to bind  $\alpha_{IIb}\beta_3$  on adjacent platelets simultaneously, and soluble FN binding to  $\alpha_{IIb}\beta_3$  reduces the availability of binding sites for FG, which inhibits platelet aggregation.<sup>202</sup> A similar inhibitory mechanism has been proposed for plasma VN monomers,<sup>204</sup> which also inhibit platelet aggregation,<sup>203</sup> presumably through occupancy of  $\alpha_{IIb}\beta_3$  on activated platelets. Fibrin acts as a bridging protein that allows soluble FN to bridge platelets by crosslinking to fibrin monomers. This is further

evidenced by studies of triple-deficient  $Vwf^{f^{-}}/Fg^{f^{-}}/pFn^{f^{-}}$  (TKO) mice.<sup>204</sup> Coupled with the absence of Fg and Vwf, TRAP- or collagen-induced platelet aggregation is enhanced in TKO mice compared to double-deficient  $Vwf^{f^{-}}/Fg^{f^{-}}$  controls. Similarly, TKO mice have enhanced platelet adhesion, faster thrombus formation, increased thrombus stability, and shorter vessel occlusion times in response to  $FeCl_3$ -induced vessel injury *in vivo* compared to  $Vwf^{f^{-}}/Fg^{f^{-}}$  mice. It is postulated that *in vivo*, pFn crosslinked to fibrin in the core of thrombi supports platelet aggregation and clot stability, while soluble pFN at the periphery of a growing thrombus inhibits further platelet accumulation to limit thrombus size and prevents vessel occlusion.<sup>159,160,202,311</sup> The switch between inhibitory and supporting roles is suggested to require either self-association of pFN into fibers or crosslinking to fibrin or other matrix proteins.

To date, a single family has been described with partial FN deficiency, but they have normal hemostasis and platelet function.<sup>312</sup> Complete deficiency of FN has not been reported, and global *Fn* inactivation is embryonic lethal in mice,<sup>226</sup> which appears to reflect important roles in embryonic development. Targeted inactivation of *Fn* expression by hepatocytes has been used to generate  $pFn^{f^{-}}$  mice,<sup>207</sup> which develop normally, but have almost no detectable plasma Fn and approximately 80% reduction in platelet Fn following tissue-specific inactivation of *Fn*.  $pFn^{f^{-}}$  mice have no bleeding diathesis, but it is unclear how much the pool of cFn remaining in platelets contributes to hemostasis. Notably, cFN, which contains ED-A, is more active in initiating fiber assembly and incorporating into thrombi.<sup>313,314</sup> In response to  $FeCl_3$ -induced vessel injury, platelet

adhesion is normal in the mesenteric arterioles of *pFn*<sup>-/-</sup> mice, but aggregate formation is significantly delayed, and as a result, vessel occlusion times are delayed compared to wild-type mice.<sup>208</sup> However, thrombi in *pFn*<sup>-/-</sup> mice are stable and stay attached at the site of injury.

### *1.3.1.3 von Willebrand factor*

Von Willebrand factor (VWF) is a large homopolymeric glycoprotein assembled from dimers of two 250 kDa subunits that are encoded by the VWF gene. VWF subunits are synthesized as pre-pro-VWF, which consists of an N-terminal signal peptide, a propeptide, and the mature 2050-aa VWF subunit. The mature VWF subunit consists of four repeating domain structures classified as “A”, “B”, “C”, and “D”, which are organized as D'-D3-A1-A2-A3-D4-C1-C2-C3-C4-C5-C6-CK. Mature VWF monomers assemble into dimers, which subsequently form N-terminal-linked multimers through inter-chain disulfide bonds that can range from 0.5 to 20 MDa in size.<sup>315,316</sup> Although VWF shares some similarities with MMRN1 in that it is a large, multi-domain glycoprotein that forms large, disulfide-linked multimers, VWF and MMRN1 are structurally unrelated.<sup>10</sup>

VWF is synthesized by megakaryocytes and endothelial cells,<sup>317-319</sup> and is present in plasma, within platelet and endothelial cell granules, and in the basement membrane of endothelial cells. VWF multimers circulate in plasma at approximately 10 µg/ml in

humans in a compact, globular conformation.<sup>320</sup> The inactive, globular conformation of plasma VWF conceals the collagen- and GPIb $\alpha$ -binding sites within the A1 and A3 domains.<sup>321–323</sup> As plasma VWF self-associates into larger multimers, shear forces cause the large multimers to begin tumbling and unfolding, which induces unfolding of the cryptic VWF A domains. Upon exposure of VWF A domains in flowing blood, circulating ADAMTS13 cleaves a peptidyl bond in the VWF A2 domain, which reduces VWF multimer size, subsequently regulating both multimer size and conformation.<sup>324–327</sup> ADAMTS13 also regulates VWF multimer size at sites of vessel injury by cleaving ultra-large (UL)VWF multimers released by activated endothelial cells and platelets.

VWF binds to collagens I, III, IV,<sup>328</sup> and VI,<sup>329</sup> GPIb $\alpha$ ,  $\alpha$ <sub>IIb</sub> $\beta$ <sub>3</sub>, fibrin,<sup>330</sup> TSP-1, MMRN1, and FVIII. Through its numerous interactions, VWF contributes to hemostasis and thrombosis in multiple ways. VWF acts as a carrier protein for FVIII in plasma that protects it from proteolytic degradation and can deliver FVIII to sites of vessel injury. VWF also participates in platelet-endothelial cell and leukocyte-endothelial cell interactions, which contribute to inflammatory and angiogenic processes. VWF can be crosslinked to fibrin by FXIIIa, which is suggested to enhance clot stability.<sup>271</sup> Lastly, VWF contributes to platelet adhesion and thrombus formation through its ability to bind platelet GPIb $\alpha$  to localize circulating platelets at sites of injury or onto developing thrombi under high shear flow.

VWF multimers bound to the vessel wall, either to activated endothelial cells or the exposed subendothelium, are considered the critical ligand for initial platelet adhesion. VWF binding to GPIIb $\alpha$  has a fast on-rate that enables transient binding of platelets under conditions of high shear flow,<sup>331</sup> whereas interactions between platelet integrins (e.g.  $\alpha_{IIb}\beta_3$ ,  $\alpha_2\beta_1$ , and  $\alpha_5\beta_1$ ) and other surface-bound extracellular matrix proteins (e.g. FG, fibrin, laminins, collagens, and MMRN1) are not sufficient to support platelet tethering under high shear flow. Platelet adhesion to VWF occurs under a range of shear rates, and the morphology of platelet aggregates on VWF surfaces is typically strings of adherent platelets. Additionally, VWF is able to mediate platelet adhesion to fibrillar collagens, TSP-1, fibrin, and MMRN1 under shear rates that trigger unfolding of VWF multimers (approximately  $\geq 500 \text{ s}^{-1}$ ). Platelet adhesion to collagen under high shear flow requires VWF for platelets to significantly adhere and aggregate onto collagen surfaces.<sup>302,303</sup> Adhesion of human platelets lacking VWF or Vwf-deficient mouse platelets to collagen is abolished under high shear flow.<sup>332</sup> VWF also enhances platelet adhesion and aggregate formation onto MMRN1-coated surfaces under high shear flow,<sup>21</sup> and VWF is required for MMRN1 to enhance platelet adhesion to fibrillar collagen.<sup>2</sup> Platelet adhesion to TSP-1 surfaces involves VWF and GPIIb $\alpha$  under high shear flow, but TSP-1 is considered a counter receptor for GPIIb $\alpha$  in the absence of VWF, and is capable of supporting platelet adhesion under high shear flow through a mechanism involving GPIIb $\alpha$  but not VWF.

Following initial platelet adhesion, large VWF multimers are released from adherent activated platelets, which stably bind through RGD-dependent interactions to activated  $\alpha_{IIb}\beta_3$ .<sup>333</sup> Platelet-bound VWF multimers continue tethering additional circulating platelets to contribute to platelet aggregate growth.<sup>200</sup> VWF multimers also crosslink  $\alpha_{IIb}\beta_3$  on adjacent activated platelets, which enhances the stability of platelet aggregates.<sup>333</sup> As the diameter of the vessel lumen decreases following thrombus formation, the shear rate at the apex of the thrombus significantly increases. VWF is capable of supporting platelet aggregation under extremely high shear ( $\geq 15,000 \text{ s}^{-1}$ ) independent of FG and  $\alpha_{IIb}\beta_3$ ,<sup>177,247</sup> which may play a role in vessel occlusion or thrombus formation in stenotic vessels. Vwf-deficient ( $Vwf^{f/-}$ ) mice fail to form occlusive thrombi due to a channel that forms at the apex of the thrombus that fails to fully occlude.

Quantitative or qualitative defects in VWF cause a variety of bleeding symptoms based on the type of defect, which are collectively referred to as von Willebrand disease (VWD).<sup>334</sup> VWD is divided into types based on the type and severity of the defect. Type 1 VWD is defined as a partial quantitative defect in structurally and functionally normal VWF. Type 2 VWD refers to disorders in which VWF is functionally abnormal, and is further subdivided based on the type of functional defect. Type 3 VWD is the most severe, in which there is near or complete loss of VWF in plasma and cells and, consequently, a reduction of plasma FVIII. Type 3 VWD patients suffer from severe mucocutaneous bleeding and prolonged challenge-related bleeding.<sup>335</sup>  $Vwf^{f/-}$  mice, which are essentially a model of type 3 VWD, develop normally, but have reduced survival due

to spontaneous bleeding.<sup>211,222</sup> In response to injury,  $Vwf^{f/-}$  mice have severely prolonged bleeding compared to wild-type mice.<sup>222,223,332</sup> In response to  $FeCl_3$ -induced injury of mesenteric arterioles,  $Vwf^{f/-}$  mice have impaired platelet adhesion, thrombus formation, and vessel occlusion compared to the wild-type.<sup>211,222</sup>

#### *1.3.1.4 Thrombospondin-1*

Thrombospondin-1 (TSP-1) is a large homotrimeric glycoprotein of approximately 450 kDa. Its domain structure contains an oligomerization domain that is responsible for trimerization, a VWF C domain that shares high homology with FN type 1 modules, numerous thrombospondin type repeats (TSRs), and two EGF-like domains.<sup>336</sup> TSP-1 is synthesized by endothelial cells, smooth muscle cells, and fibroblasts.<sup>337</sup> Consequently, TSP-1 is present in the vessel wall matrix and constitutively secreted into plasma by endothelial cells. Platelets do not synthesize TSP-1, but uptake TSP-1 from plasma, which accounts for roughly 20 to 30% of protein content in  $\alpha$ -granules.<sup>338</sup> Normally, TSP-1 concentrations in plasma range from 0.1 to 0.3  $\mu$ g/ml. Following platelet activation and  $\alpha$ -granule secretion, localized concentrations of TSP-1 increase roughly 100-fold.<sup>339</sup>

Given its complex multi-domain structure, TSP-1 is known to bind to numerous plasma and/or ECM proteins and platelet receptors: integrins  $\alpha_V\beta_3$  and  $\alpha_2\beta_1$ ,<sup>340–342</sup> GPIV (CD36), integrin-associated protein (IAP; CD47), GPIb $\alpha$ , FG,<sup>242,343</sup> fibrin,<sup>343</sup> VWF,<sup>315</sup>

FN,<sup>344</sup> laminins,<sup>345</sup> and collagens.<sup>346</sup> TSP-1 may directly interact with  $\alpha_{IIb}\beta_3$ , but many studies report conflicting results.<sup>340,347–350</sup> In an isolated system, TSP-1 fails to trigger aggregation of  $\alpha_{IIb}\beta_3$ -coated beads,<sup>205</sup> suggesting other proteins are required to mediate this interaction.

TSP-1 is shown to have a non-essential, but supporting role in platelet adhesion and platelet aggregation through its interactions with FG. Pre-treatment with anti-TSP-1 Fab fragments inhibit platelet aggregation in response to collagen and thrombin.<sup>241,351</sup> Anti-TSP-1 Fab fragments decrease the size and number of large aggregates, resulting in more small aggregates and non-aggregated single platelets. TSP-1 binds and crosslinks  $\alpha_{IIb}\beta_3$ -bound FG, which decreases the distance required for cell-cell interactions, increases collision frequency, and localizes additional adhesive proteins that support platelet adhesion.<sup>205</sup> TSP-1 can also switch to an inhibitory role in platelet aggregation by binding to soluble FG, which blocks FG binding to  $\alpha_{IIb}\beta_3$  on platelets.<sup>205</sup> Additionally, TSP-1-coated beads co-aggregate, suggesting that TSP-1 bound to the cell surface is also capable of crosslinking with TSP-1 on adjacent cells. Further, TSP-1 enhances platelet aggregation by blocking the inhibitory effects of NO through its interactions with CD36 and IAP.<sup>352</sup>

TSP-1 supports platelet adhesion under stasis and shear rates up to  $4000\text{ s}^{-1}$  through multiple mechanisms. Platelet adhesion to immobilized TSP-1 increases with shear up to rates of approximately  $1800\text{ s}^{-1}$ , after which platelet adhesion to TSP-1

gradually declines with increasing shear.<sup>299,353</sup> Under high shear flow, monoclonal anti- $\alpha_{IIb}\beta_3$ ,  $-\alpha_v\beta_3$ , and -IAP antibodies do not inhibit platelet adhesion to TSP-1. Antibodies that block CD36 binding or VWF binding to GPIIb $\alpha$  partially inhibit platelet adhesion to TSP-1, whereas monoclonal antibodies that block GPIIb $\alpha$  binding abolish platelet adhesion to TSP-1. Additionally, type 3 VWD platelets adhere normally to TSP-1 under high shear, which shows that GPIIb $\alpha$  supports platelet adhesion to TSP-1 under high shear flow independent of VWF. These data are consistent with *in vivo* observations that *GpIb $\alpha$ <sup>-/-</sup>* mice exhibit a more severe impairment in thrombus formation compared to *Vwf<sup>f/-</sup>* mice. Additionally, TSP-1 binds collagens I-VI and contributes to platelet adhesion to immobilized fibrillar collagen surfaces under flow through its interactions with CD36, which enhance platelet activation, PE expression, and thrombus stability on collagen.<sup>346,354,355</sup> TSP-1 binding to IAP is also shown to enhance platelet activation and aggregation by collagen.<sup>356</sup>

TSP-1 contributes to hemostatic plug formation and thrombosis through multiple mechanisms. TSP-1 binds to thrombin,<sup>357,358</sup> plasminogen,<sup>359</sup> and TFPI,<sup>360</sup> which affect fibrin formation and thrombin-induced platelet activation. TSP-1 interactions with fibrin accelerate the rate of fibrin formation, decrease fibrin fiber diameter and increases the number of fibrin fibers in fibrin networks, and may regulate branching during network formation.<sup>361</sup> TSP-1 also contributes to platelet recruitment to sites of injury or growing thrombi through its interactions with VWF. TSP-1 binds to the A3 domain of VWF and blocks ADAMTS-13 mediated cleavage of the adjacent VWF A2 domain.<sup>225,362</sup> In this

regard, TSP-1 facilitates the maintenance of large VWF multimers at the site of injury, which are more effective at tethering circulating platelets. TSP-1 binding to VWF is also postulated to stabilize platelet adhesion to VWF. *In vivo*, large Vwf multimers released by endothelial cells are more rapidly degraded by Adamts13 in *Tsp1*<sup>-/-</sup> mice compared to the wild-type.<sup>363</sup>

*Tsp1*<sup>-/-</sup> mice are viable and fertile, but exhibit abnormalities in the lungs and thoracic spine,<sup>209</sup> consistent with the high expression levels of TSP-1 in pulmonary tissues. Consequently, *Tsp1*<sup>-/-</sup> mice experience diffuse alveolar hemorrhage, but bleeding in response to injury is similar between *Tsp1*<sup>-/-</sup> and wild-type mice. *Tsp1*<sup>-/-</sup> platelets aggregate normally in response to thrombin, ADP, TxA<sub>2</sub> analogue, or collagen.<sup>209,225</sup> In response to FeCl<sub>3</sub>-induced vessel injury, *Tsp1*<sup>-/-</sup> have a slower rate of thrombus growth and delayed vessel occlusion due to impaired thrombus stability and frequent embolization. Impaired thrombus formation in *Tsp1*<sup>-/-</sup> mice is attributed to loss of the TSP-1/CD36 signalling axis, given that *Tsp1*<sup>-/-</sup> and *CD36*<sup>-/-</sup> mice have a similar phenotype.<sup>354</sup> Although TSP-1 is argued to be a counter-receptor for GPIIb $\alpha$  in the absence of Vwf, double-deficient *Tsp1*<sup>-/-</sup>/*Vwf*<sup>-/-</sup> mice have a similar phenotype to *Vwf*<sup>-/-</sup> mice in response to FeCl<sub>3</sub>-induced vessel injury,<sup>212,364</sup> suggesting that Tsp-1 is not the only counter receptor for GPIIb $\alpha$ .

### *1.3.1.5 Vitronectin*

Vitronectin (VN) is a 75 kDa glycoprotein synthesized by hepatocytes that is present in plasma, platelet  $\alpha$ -granules,<sup>365</sup> and the extracellular matrix of blood vessels.<sup>366–368</sup> VN circulates in plasma at a concentration ranging from 200 to 500  $\mu\text{g/ml}$  in humans.<sup>369,370</sup> Plasma VN circulates as soluble monomers that are constitutively taken up and stored by MKs and platelets in  $\alpha$ -granules.<sup>371</sup> VN exists in two conformations, which regulate its ability to bind ligands and support platelet adhesion and aggregation. Plasma VN monomers have a compact conformation in which their integrin-binding RGD sites are not accessible.<sup>372</sup> VN in platelet  $\alpha$ -granules and the ECM self-associate into multimers that are able to bind integrins.<sup>372,373</sup> Additionally, ligand binding can induce conformational change of plasma VN monomers that enables VN to multimerize and exposes binding sites for platelet integrins,<sup>374</sup> and a small portion (~2%) of the plasma VN pool is present in the active, integrin-binding conformation.

VN binds to  $\alpha_V\beta_3$  and  $\alpha_{IIb}\beta_3$  on platelets,<sup>375</sup> fibrin,<sup>376</sup> fibrillar collagens types I and III,<sup>377</sup> PAI-1,<sup>378</sup> plasminogen, and the thrombin-antithrombin complex. Platelet adhesion to VN requires platelet activation and involves  $\alpha_V\beta_3$  and  $\alpha_{IIb}\beta_3$ . Resting platelets do not adhere to VN under stasis or flow.<sup>265,379</sup> The physiologic role of platelet adhesion to VN on its own is unclear, but VN incorporated into fibrin surfaces enhances platelet adhesion and aggregation onto fibrin through homotypic interactions between platelet-bound VN and fibrin-bound VN.<sup>380</sup> Following platelet activation and  $\alpha$ -granule secretion, the local

VN concentration increases approximately 200-fold, with about 50% of VN remaining bound to the platelet surface.<sup>381</sup> Further, VN is co-localized with fibrin *in vivo* and stabilizes thrombi through its interactions with PAI-1.<sup>382–384</sup> Binding to PAI-1 or thrombin-antithrombin induces conformational change of plasma VN monomers to their active, integrin-binding form.<sup>374,385–387</sup>

Given the conformation-dependent functions of VN, studies have reported conflicting results for the role of VN in platelet aggregation. Monoclonal anti-VN antibodies inhibit platelet aggregation *in vitro*,<sup>380,388</sup> whereas VN is also shown to inhibit platelet aggregation through competition with FG and VWF for binding to  $\alpha_{IIb}\beta_3$ .<sup>229,389</sup> Conflicting results have also been reported for aggregation of Vn-deficient ( $Vn^{-/-}$ ) mouse platelets.  $Vn^{-/-}$  mice develop normally and do not experience spontaneous bleeding or prolonged bleeding in response to injury.<sup>210,229</sup> Initially,  $Vn^{-/-}$  platelets were reported to have normal ADP-induced aggregation, but accelerated thrombin-induced aggregation compared to the wild-type.<sup>229</sup> Later analysis showed that thrombin-induced platelet aggregation is abolished in  $Vn^{-/-}$  platelets, whereas ADP-induced of  $Vn^{-/-}$  platelets is enhanced compared to the wild-type.<sup>203</sup> This discrepancy is reported to result from differences in experimental design and measurement type.

$Vn^{-/-}$  mice were first reported to show significantly shorter vessel occlusion times *in vivo* in response to  $FeCl_3$ -induced vessel injury compared to wild-type mice,<sup>229</sup> which suggests that Vn normally inhibits thrombus formation *in vivo*. Subsequent analyses of

thrombus formation *in vivo* following FeCl<sub>3</sub>-induced vessel injury have demonstrated that thrombus growth and vessel occlusion are delayed in *Vn*<sup>-/-</sup> mice due to frequent dissolution of thrombi, embolization, and vessel re-opening.<sup>203</sup> Similarly, PAI-1-deficient or double-deficient *PAI-1*<sup>-/-</sup>/*Vn*<sup>-/-</sup> mice develop unstable thrombi in response to FeCl<sub>3</sub>-induced vessel injury.<sup>390,391</sup> Following laser-induced vessel injury, fibrin content is lower and unstable in thrombi formed by *Vn*<sup>-/-</sup> mice compared to the wild-type.<sup>203</sup> These studies demonstrate a crucial role of Vn and PAI-1 in supporting thrombus stability. Additionally, it is hypothesized that Vn multimers form macromolecular complexes with other adhesive proteins to increase the avidity of platelet-platelet interactions during thrombus formation to further stabilize thrombi.<sup>203</sup>

### 1.3.2 Platelet adhesive receptors

Transmembrane receptor complexes on the platelet surface are the means through which platelets interact with other cells and the extracellular environment via inside-out signalling, outside-in signalling, or both. In particular, some platelet receptors have been demonstrated to play crucial roles in platelet adhesion and aggregation, such as integrins  $\alpha_{IIb}\beta_3$  and  $\alpha_2\beta_1$ , the GPVI-FcR $\gamma$  complex, and the GPIb/IX/V complex. A supporting, but non-essential role has also been described for  $\alpha_v\beta_3$ , which is expressed on the platelet surface in very low numbers and can bind FG,<sup>244</sup> VN,<sup>392</sup> FN,<sup>296</sup> and MMRN1.<sup>1,2</sup> The relative abundance of these receptors on resting human and mouse platelets is presented in *Figure 4*. Although the functions of various receptors discussed below are not limited

to platelet adhesion and aggregation, the following sections will focus on the mechanisms through which these receptors contribute to these processes.

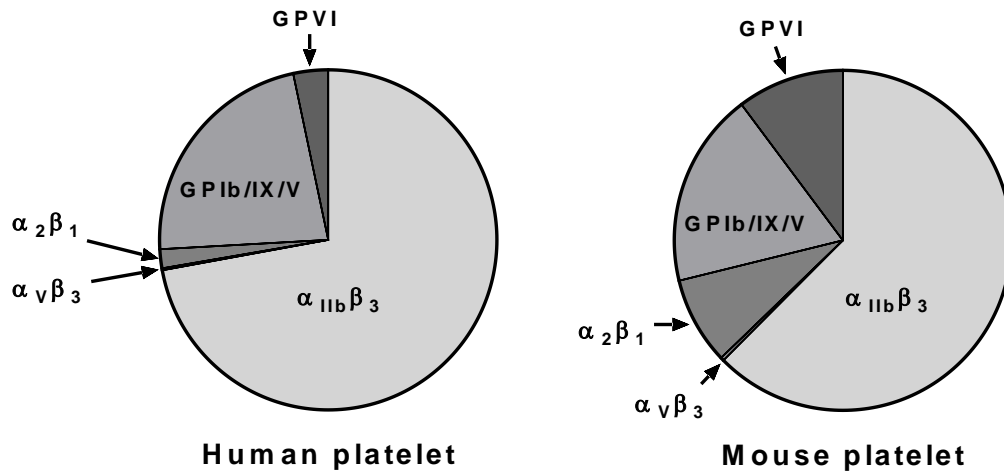


**Figure 4: Estimated relative abundance of major receptors on resting human and mouse platelets.**

#### 1.3.2.1 Alpha-IIb Beta-3

Integrin  $\alpha_{IIb}\beta_3$  (sometimes called GPIIb/IIIa) is a heterodimeric transmembrane receptor complex expressed primarily by MKs and platelets,<sup>393,394</sup> but it is also present on mast cells<sup>395,396</sup> and some tumour cells.<sup>397</sup> In MKs and platelets, the  $\alpha_{IIb}$  and  $\beta_3$  subunits are constitutively synthesized by MKs and are present as a heterodimer on the cell membrane and within  $\alpha$ -granules.<sup>398</sup> On the cell surface, the  $\alpha_{IIb}\beta_3$  complex is capable of outside-in signalling and supporting cell adhesion to extracellular matrix proteins.<sup>399</sup> There are approximately 80,000 copies of  $\alpha_{IIb}\beta_3$  present on the membrane of resting

human platelets and approximately 120,000 copies on a single mouse platelet.<sup>400–403</sup> These numbers increase by approximately 30 to 50% following platelet activation,<sup>404,405</sup> wherein  $\alpha_{IIb}\beta_3$  stored within  $\alpha$ -granules is incorporated into the cell membrane during granule secretion.

Integrin  $\alpha_{IIb}\beta_3$  binds to FG,<sup>406–408</sup> FN,<sup>309,409</sup> VN,<sup>375</sup> VWF,<sup>410</sup> and MMRN1,<sup>1,2</sup> but platelet activation affects the affinity and avidity of these interactions. On resting platelets,  $\alpha_{IIb}\beta_3$  is present in an inactive conformation, in which a genu in each extracellular portion of the  $\alpha_{IIb}$  and  $\beta_3$  subunits allows  $\alpha_{IIb}\beta_3$  to fold into a bent conformation.<sup>411</sup> Platelet activation by agonists such as thrombin, collagen, ADP, or VWF triggers  $\alpha_{IIb}\beta_3$  to shift to an extended, high-affinity conformation through inside-out signalling. Platelet activation also induces clustering of  $\alpha_{IIb}\beta_3$  on the platelet surface, which increases the avidity of  $\alpha_{IIb}\beta_3$ -mediated ligand binding.<sup>412–414</sup>

Integrin  $\alpha_{IIb}\beta_3$  is essential for stable platelet adhesion and aggregate formation. Platelets irreversibly adhere to FG or VWF via activated  $\alpha_{IIb}\beta_3$ ,<sup>174</sup> which stabilizes primary adhesion and subsequent platelet aggregation. The only known exceptions are: 1) conditions of elevated shear ( $>15,000\text{ s}^{-1}$ ) in which reversible platelet aggregation can occur independent of  $\alpha_{IIb}\beta_3$  and platelet activation or 2) mechanical trapping of platelets within a fibrin meshwork that can occur independent of  $\alpha_{IIb}\beta_3$ .<sup>177,247,276</sup> Resting and activated platelets adhere to FG or fibrin via  $\alpha_{IIb}\beta_3$  under conditions of stasis and flow, and platelet activation significantly enhances platelet adhesion and aggregate formation

onto immobilized FG or fibrin surfaces.<sup>174</sup> Resting platelets do not significantly adhere to FN- or VN-coated surfaces under flow, but platelet activation allows platelets to stably adhere to FN or VN via  $\alpha_{IIb}\beta_3$  and other minor receptors ( $\alpha_5\beta_1$  and  $\alpha_V\beta_3$ , respectively) to form aggregates.<sup>265</sup> Similarly, platelet adhesion to MMRN1 under stasis and low shear flow is mediated by  $\alpha_{IIb}\beta_3$  and  $\alpha_V\beta_3$  and requires platelet activation.<sup>2</sup>

A critical role of  $\alpha_{IIb}\beta_3$  in platelet aggregation onto fibrillar collagen under high shear flow has been demonstrated for both human and mouse platelets. Monoclonal anti- $\alpha_{IIb}\beta_3$  antibodies eliminates mouse platelet aggregate formation on fibrillar collagen under high shear flow ( $1300\text{ s}^{-1}$ ),<sup>183</sup> and treatment with peptidomimetic lotrafiban, which blocks the FG/Fg and VWF/Vwf binding site on  $\alpha_{IIb}\beta_3$ , abolishes human or mouse platelet aggregate formation on fibrillar collagen without affecting primary adhesion onto collagen or activation by collagen.<sup>415</sup> Additionally, RGDS peptides inhibit platelet aggregate formation onto collagen under high shear flow ( $1500\text{ s}^{-1}$ ), which suggests the involvement of integrin-binding RGD motifs in platelet aggregate formation on collagen surfaces.

Hereditary or acquired qualitative or quantitative defects in  $\alpha_{IIb}\beta_3$  are referred to as Glanzmann thrombasthenia (GT), which are the cause of severe bleeding symptoms in human patients.<sup>416</sup> Notably, patients with defects in  $\beta_3$  affect both  $\alpha_{IIb}\beta_3$  and  $\alpha_V\beta_3$ , whereas defects in the  $\alpha_{IIb}$  subunit only affect  $\alpha_{IIb}\beta_3$ .<sup>417</sup> Aggregation of GT platelets is severely impaired (typically absent) in response to ADP, thrombin, collagen, and

epinephrine, which further demonstrates the critical role of  $\alpha_{IIb}\beta_3$  in platelet aggregation at low shear. GT platelets agglutinate but do not aggregate in response to ristocetin, which also highlights the ability of VWF to mediate platelet agglutination under conditions sufficient to expose the GPIIb $\alpha$ -binding VWF A1 domain. Beta-3-deficient mice develop normally, but have a severe bleeding phenotype that is similar to GT in human patients.<sup>221</sup> Beta-3-deficient mice exhibit severe bleeding in response to injury and reduced survival due to spontaneous hemorrhage. Additionally,  $\beta_3$ -deficient mice are protected from thrombosis in a large arteries following treatment with FeCl<sub>3</sub> and systemic intravascular thrombosis induced by a variety of agonists.<sup>418</sup>

#### *1.3.2.2 Alpha-2 beta-1*

Integrin  $\alpha_2\beta_1$  is a transmembrane heterodimeric receptor complex composed of the  $\alpha_2$  and  $\beta_1$  subunits, which associate via disulfide linkage on the surface of cells. Alpha-2 beta-1 is one of four known integrins capable of direct binding to collagen.<sup>419,420</sup> The  $\alpha_2$  subunit contains a highly conserved inserted (I)-domain that shares homology with the VWF A domain and is responsible for collagen binding.<sup>420-422</sup> The I-domain contains a metal ion-dependent adhesion site (MIDAS) that requires either Mg<sup>2+</sup> or Mn<sup>2+</sup> to form a complex with collagen.<sup>422,423</sup>

Integrin  $\alpha_2\beta_1$  is expressed on the surface of MKs, platelets, endothelial cells, fibroblasts, and lymphocytes. In contexts other than hemostasis,  $\alpha_2\beta_1$  is referred to as

either very late antigen (VLA)-1 or extracellular matrix receptor (ECMR)-II.<sup>424-426</sup> Endothelial  $\alpha_2\beta_1$  anchors endothelial cells to collagens and laminins in the subendothelial basement membrane, and may contribute to sprouting angiogenesis and wound healing.<sup>427-429</sup> On platelets,  $\alpha_2\beta_1$  is present at approximately 1000 to 3000 copies per platelet and functions primarily as a receptor for various collagens and laminins.<sup>430</sup> Mouse platelets express substantially greater numbers of  $\alpha_2\beta_1$ , with approximately 16,000 copies per platelet.<sup>403</sup> On resting platelets,  $\alpha_2\beta_1$  is present in a low affinity conformation in which the I-domain is inaccessible, but is still capable of binding some high-affinity ligands.<sup>431</sup> Following platelet activation by GPVI or protease-activated receptors (PARs)-1 and -4, inside-out signalling triggers  $\alpha_2\beta_1$  to shift to a high-affinity conformation in which the I-domain is exposed.<sup>432</sup>

Integrin  $\alpha_2\beta_1$  binds to types I-VI and XI collagen and laminins in the extracellular matrix.<sup>433-435</sup> More specifically,  $\alpha_2\beta_1$  preferentially binds types I, II, III, and V collagen, and integrin activation is not required for  $\alpha_2\beta_1$  to bind types I, II, and III collagen. Binding to types IV and VI collagen and laminins requires platelet activation to trigger the high-affinity conformation of  $\alpha_2\beta_1$ . Under stasis and low shear flow,  $\alpha_2\beta_1$  is sufficient to support significant and stable platelet adhesion to fibrillar collagen.<sup>183</sup> Platelet activation enhances  $\alpha_2\beta_1$ -mediated platelet adhesion to fibrillar collagen, but is not required.<sup>436</sup> Under conditions of elevated shear stress, VWF binding to collagen to tether circulating platelets is required for significant platelet adhesion to fibrillar collagen.<sup>332</sup> In the absence

of collagen-bound VWF multimers, platelets adhere individually or in much smaller, nodular aggregates under high shear flow.<sup>175</sup>

Defects in  $\alpha_2\beta_1$  have been reported in human patients that are associated with prolonged bleeding, failure of platelets to aggregate in response to collagen, and failure of platelets to adhere to collagen.<sup>437,438</sup> Alpha-2-deficient mice develop normally without hemostatic complications,<sup>214,439</sup> despite the ubiquitous expression of  $\alpha_2\beta_1$  on fibroblasts and various epithelial cell types. Alpha-2-deficient mice bred on a C57BL/6J background do not experience bleeding,<sup>214</sup> but  $\alpha_2$ -deficient mice of a mixed C57BL/6J/BalbC background show severe bleeding in response to injury.<sup>183</sup> Adhesion of  $\alpha_2$ -deficient platelets to collagen is abolished under low shear, where VWF is not involved, and severely impaired under high shear flow.<sup>183,214,215</sup> Alpha-2-deficient mice also show a delayed aggregation response to collagen,<sup>214,439</sup> which is postulated to arise from the loss of stable adhesion to collagen that facilitates collagen-induced platelet activation by GPVI. In response to FeCl<sub>3</sub>-induced vessel injury, thrombus growth and vessel occlusion are impaired in  $\alpha_2$ -deficient compared to wild-type mice.<sup>215</sup> This has been attributed to a role of  $\alpha_2\beta_1$  in enhancing TxA<sub>2</sub> release within growing thrombi, rather than defects in platelet adhesion to collagen. Similarly, in response to photochemical injury,  $\alpha_2$ -deficient mice have delayed thrombus growth and vessel occlusion compared to the wild-type.<sup>440</sup>

### *1.3.2.3 Glycoprotein VI*

Glycoprotein VI (GPVI) is a transmembrane immunoreceptor that is exclusively expressed by MKs and platelets.<sup>441</sup> It is present on the surface of human platelets in similar numbers as  $\alpha_2\beta_1$  (~1000 to 4000 copies per platelet),<sup>430</sup> whereas mouse platelets express significantly greater numbers of GPVI.<sup>403</sup> GPVI is part of the immunoglobulin (Ig) superfamily and contains two Ig-like domains that are responsible for ligand binding via an immunoreceptor tyrosine-based activation motif (ITAM). GPVI is present in disulfide-linkage with FcR $\gamma$  on the platelet surface. GPVI is relatively small (62 kDa) and lacks a significant intracellular domain. GPVI linkage to FcR $\gamma$  is required for GPVI expression on the platelet surface and the extensive intracellular domain of FcR $\gamma$  is critical for signal transduction of the GPVI/FcR $\gamma$  complex.<sup>442–444</sup> FcR $\gamma$  is a homodimer and a copy of GPVI is linked to each FcR $\gamma$  monomer so that GPVI is present as a dimer on the platelet surface.<sup>445,446</sup> Clustering of GPVI/FcR $\gamma$  complexes also appears to be necessary for collagen binding.<sup>447</sup>

GPVI binds to collagens I-VI,<sup>441,448</sup> laminins,<sup>449,450</sup> FG,<sup>279</sup> and fibrin.<sup>451</sup> GPVI binding to fibrillar collagens I and III induces full activation of platelets, including PS exposure, blebbing, and granule secretion.<sup>452</sup> GPVI binding to laminin, FG, or fibrin does not induce full platelet activation. GPVI binding to laminin may be involved in platelet spreading,<sup>450</sup> whereas a role of GPVI-fibrin interactions in promoting thrombin generation and thrombus stability has been reported.<sup>451</sup> Ligation of the dimeric

GPVI/FcR $\gamma$  complex that crosslinks the Ig-like domains of GPVI results in receptor triggering.<sup>453,454</sup> Ligands capable of binding GPVI but not crosslinking GPVI Ig-like domains do not trigger full platelet activation.<sup>441</sup> Collagen fibers are able to crosslink GPVI Ig-like domains, whereas ligands such as laminins and fibrin do not.

GPVI deficiency has been reported in several human patients with mild bleeding symptoms.<sup>455-460</sup> Platelets from GPVI-deficient patients fail to aggregate in response to collagen, but have normal aggregation responses to thrombin, ADP, and ristocetin.<sup>455,456,459,460</sup> Additionally, platelets from some GPVI-deficient patients fail to adhere to collagen,<sup>455</sup> while platelets from other patients show impaired adhesion to collagen.<sup>460,461</sup> GpVI-deficient (*GpVI*<sup>-/-</sup>) mice bred on a C57BL/6J background have a mild prolongation of bleeding in response to injury,<sup>216,218</sup> and *GpVI*<sup>-/-</sup> BalbC mice exhibit a moderate bleeding phenotype.<sup>183</sup> *GpVI*<sup>-/-</sup> platelets do not aggregate in response to collagen and adhesion of *GpVI*<sup>-/-</sup> platelets to collagen is significantly impaired under a wide range of shear rates (400 to 2600 s<sup>-1</sup>).<sup>183,216,462</sup> Similarly, GpVI-deficiency significantly impairs thrombus formation in response to FeCl<sub>3</sub>-induced injury of small and large arteries,<sup>217,463,464</sup> ligation injury,<sup>465</sup> or intravenous collagen injection.<sup>440</sup> Thrombus growth and vessel occlusion are delayed in *GpVI*<sup>-/-</sup> mice due to thrombus instability and frequent embolization. The role of GPVI in FeCl<sub>3</sub>-induced vessel injury is posited to involve GPVI binding to FG and fibrin to promote thrombin generation and platelet recruitment in addition to its collagen binding functions.<sup>451</sup>

#### 1.3.2.4 Glycoprotein Ib/IX/V complex

The glycoprotein Ib/IX/V complex (GPIb/IX/V) consists of four subunits encoded by four separate genes: GPIb $\alpha$ , GPIb $\beta$ , GPIX, and GPV, which is expressed on the surface of endothelial cells,<sup>466</sup> MKs, and platelets.<sup>467</sup> Approximately 25,000 copies of the GPIb/IX/V complex are present on a single resting human platelets and approximately 36,000 copies on a single resting mouse platelet.<sup>220,403</sup> In addition to its role as an adhesive receptor complex, GPIb-IX-V is a structural component of the platelet cytoskeleton that links the platelet membrane to actin filaments.<sup>468</sup> GPIb $\alpha$  is the most-studied subunit, which contains the binding sites for VWF, TSP-1,<sup>469</sup> P-selectin,<sup>470</sup> thrombin,<sup>471,472</sup> and  $\alpha_M\beta_2$ .<sup>473,474</sup> GPIb $\alpha$  mediates platelet adhesion to activated endothelial cells and activated leukocytes by binding P-selectin and Mac-1, respectively. GPIb $\alpha$  also supports platelet adhesion to endothelial cells and platelet-platelet interactions by binding to the A1 domain of shear-stretched VWF multimers.<sup>475</sup> In the absence of VWF, GPIb $\alpha$  is able to support platelet adhesion and thrombus formation *in vivo*,<sup>220</sup> suggesting that other ligands in the vessel wall or other receptors may contribute to GPIb $\alpha$ -mediated thrombus formation. Additionally, a role of GPV as a collagen receptor has also been reported, but its biological significance has not been explored.<sup>476</sup> Ligation of the GPIb/IX/V complex is able to induce intracellular signals leading to Ca<sup>2+</sup> mobilization, cytoskeletal rearrangement, and activation of  $\alpha_{IIb}\beta_3$ .<sup>477,478</sup>

Mutations in the GPIb $\alpha$ , GPIb $\beta$ , or GPIX subunits of GPIb/IX/V that result in functional loss of VWF binding to GPIb/IX/V give rise to Bernard-Soulier syndrome (BSS):<sup>479</sup> a heterogeneous group of diseases characterized by giant, spherical platelets, mild thrombocytopenia, inability for platelets to aggregate in response to ristocetin, and pronounced bleeding symptoms in human patients.<sup>480</sup> *GpIb $\alpha$ <sup>-/-</sup>* mice similarly exhibit giant platelets, thrombocytopenia, and pronounced bleeding symptoms.<sup>219</sup> Giant platelets characteristic of BSS are postulated to result from the loss GPIb/IX/V-mediated linkage of the cell membrane and actin cytoskeleton of MKs and platelets. Mice expressing a chimeric form of GPIb $\alpha$  that lacks the extracellular ligand-binding domain have structurally normal platelets without thrombocytopenia, but exhibit severe bleeding and severely impaired thrombus formation *in vivo*.<sup>220</sup>

#### 1.4 THE COLLAGEN FAMILY

The collagen family consists of 28 known glycoproteins encoded by at least 45 distinct genes that are grouped together based on domain structure homology.<sup>481–485</sup> Collagens are characterized by the presence of a collagenous (COL) domain, which is a rod-like triple-helical motif composed of GXX' repeats (where X is frequently occupied by proline and X' is frequently occupied by hydroxyproline) of variable length.<sup>483,485</sup> All collagens are trimers composed of three  $\alpha$ -chains.<sup>481–484</sup> The  $\alpha$ -chains of each collagen type are encoded by separate genes, and only  $\alpha$ -chains from the same collagen type associate into trimers.<sup>484,486</sup> The collagen superfamily is subdivided into two broad types

based on the relative length of their COL domain and their ability to self-assemble into fibers: fibrillar and non-fibrillar collagens.<sup>484,486,487</sup> Each collagen is assigned a Roman numeral and each  $\alpha$ -chain is assigned an Arabic numeral based on their order of discovery.<sup>484</sup>

The distribution and amount of collagen types in blood vessels varies between the layers of the vessel wall as well as between veins and arteries.<sup>488–491</sup> Within blood vessels, fibrillar collagens I, III, V, and VIII are mostly present within the tunica media and the adventitia,<sup>488–491</sup> but thin, sparse type I and III collagen fibrils have been detected within the tunica intima (*Table 2*).<sup>489,490</sup> The thickness of the outer layers of the vessel wall, and consequently the amount of collagen, varies depending on the size of the blood vessel and due to the requirement of a thick muscular medial layer in arteries, but not in veins, to modulate vascular tone.<sup>167,491</sup> Smooth muscle cells synthesize the majority of collagens in the tunica media, and fibroblasts and macrophages synthesize collagens in the adventitia.<sup>484</sup> The tunica intima of veins, arteries, and capillaries contains non-fibrillar collagens IV, VI, and VIII in the endothelial cell basement membrane,<sup>481,491,492</sup> which provides a surface for attachment of endothelial cells.<sup>488</sup> Type VI collagen is also synthesized by smooth muscle cells in the elastic laminae of the tunica media,<sup>491</sup> which assists in the integration of matrix components with cells and one another.<sup>481,488</sup> The following sections will discuss the major fibrillar and non-fibrillar collagens in the vessel wall and their contributions to platelet adhesion, hemostasis, and thrombosis.

	Collagen type	Location in the vessel wall	Estimated abundance	Known functions
Fibrillar	I	Media Adventitia	Very high	Tensile strength; <sup>493,494</sup> load resistance; <sup>493,494</sup> platelet adhesion and activation <sup>190,419,430</sup>
	III	Media Adventitia	Low	Elasticity; <sup>493</sup> regulation of fiber size; <sup>495,496</sup> platelet adhesion and activation <sup>190,419,430</sup>
	V	Intima Media Adventitia	Very low	Regulation of collagen assembly <sup>484,497,498</sup>
Non-fibrillar	IV	Intima Media	Moderate	Cell attachment; <sup>499</sup> membrane flexibility <sup>488</sup>
	VI	Intima Media	Moderate	Integration of ECM components and cells <sup>500</sup>
	VIII	Intima Media	Moderate	Compressive strength; <sup>488</sup> angiogenesis <sup>501</sup>

**Table 2: Tissue distribution, estimated abundance, and functions of major fibrillar and non-fibrillar collagens present in the vessel wall.** This table provides estimates on the tissue distribution of collagens at the level of different layers of the vessel wall, which does not account for whether or not these collagens are cell-associated or fibril-associated, and how their distributions vary within each layer itself.<sup>488,492</sup>

#### 1.4.1 Fibrillar collagen structure, synthesis, and assembly

The common feature of fibrillar collagens is that they contain a long, uninterrupted COL domain, which imparts rigidity and high tensile strength to collagen molecules.<sup>484,486</sup> Approximately 30% of proteins in the human body are collagens,<sup>482</sup> and of that, over 90% of the total collagen content in the human body is estimated to be fibrillar type I collagen.<sup>502</sup> Type I collagen is a heterotrimer composed of two  $\alpha_1(\text{I})$  and one  $\alpha_2(\text{I})$  chain, and has a ubiquitous structural role in a variety of tissues, including: skin,

bone, dentin, tendon, blood vessels, cornea, and lungs.<sup>493,494</sup> It is synthesized by a wide range of cell types as procollagen,<sup>485</sup> which includes N- and C-terminal telopeptides that are important for triple helix assembly and regulation of collagen fibril formation.<sup>487,503</sup>

Types I, II, and III fibrillar collagens are highly conserved, but their relative abundance and tissue distributions vary. While type I collagen is the most abundant and most ubiquitous,<sup>485</sup> the distribution of type II collagen is limited to cartilage.<sup>504</sup> Type III collagen is often present in small quantities in tissues alongside type I or II collagen, and is thought to play a role in the regulation of collagen fiber diameter.<sup>495,496</sup> In particular, type III collagen is present in large quantities within the blood vessel wall,<sup>489–491</sup> which is postulated to be because type III collagen is more elastic than type I collagen and its presence would allow for greater extensibility of blood vessels.<sup>488,505</sup> Types V and XI fibrillar collagens are also present in small quantities within collagen fiber networks, and are presumed to function primarily in the regulation of fibril assembly.<sup>495,497,498,506,507</sup>

The synthesis, structure, and assembly of fibrillar collagens have been most studied in regard to type I collagen, but it is postulated that fibrillar collagens II and III assemble into triple helices through similar processes.<sup>487,508</sup> Following translation, each procollagen  $\alpha$ -chain spontaneously assembles into a left-handed helix that lacks intra-chain hydrogen bonds.<sup>487,503,508</sup> The structure is most similar to a polyproline-II helix, or sometimes called a polyglycine II helix,<sup>509–512</sup> in which the pitch of the  $\alpha$ -chain helix roughly corresponds to a single GXX' triplet (three residues).<sup>512,513</sup> Interactions between

the non-collagenous C-terminal globular domains of each  $\alpha$ -chain potentiate their assembly into a right-handed triple superhelix that trimerizes from the C- to the N-terminus.<sup>487,503,508</sup> The tight packaging of  $\alpha$ -chains into the triple helix requires the  $\alpha$ -chains to stagger by a single residue, and every third residue is placed near the common helical axis.<sup>513</sup> Steric constraints require that glycine sits at the centre position within the triple helix because it is the smallest amino acid and almost entirely lacks a side chain.<sup>513</sup> Substitution of glycine residues at any position in the  $\alpha$ -chain causes kinks in the triple helix that have downstream effects on triple helix assembly,<sup>514</sup> glycosylation of procollagen molecules, and triple helix stability.<sup>503,515</sup> Missense mutations of glycine residues in types I or III collagen are the cause of systemic connective tissue disorders that range in severity from mild to embryonic lethal,<sup>516,517</sup> and are discussed in more detail in *section 1.3.5*. Glycosylation and hydroxylation of the procollagen molecule occurs following triple helix assembly,<sup>503,508</sup> and the formation of inter-chain hydrogen bonds by hydroxylated proline residues stabilizes the triple helix.<sup>487,503</sup>

Triple-helical type I procollagen molecules are secreted into extracellular space,<sup>487,503</sup> wherein their N- and C-terminal propeptides prevent their assembly into fibrils. Cleavage of the N- and C-terminal propeptides by ADAMTS2 and bone morphogenetic protein (BMP)-1, respectively,<sup>518,519</sup> in the extracellular environment results in mature collagen molecules of approximately 1000-aa and 300 nm in length, which are able to spontaneously assemble into larger ultrastructures.<sup>481,487</sup> Collagen monomers associate end-to-end to form long strands, which subsequently aggregate

laterally into 5-mer bundles of monomer strands called fibrils.<sup>515</sup> Laterally adjacent monomers overlap by 234 residues, which results in a 67-nm D-period that is the basic repeated structure of a collagen fibril.<sup>515</sup> Collagen fibrils assemble into a larger unit called a fiber, which is the native conformation of fibrillar collagens I, II, and III *in vivo*.<sup>481,515</sup>

#### 1.4.2 Non-fibrillar collagens IV, VI, and VIII

The majority of collagens assemble into polymeric structures, including non-fibrillar collagens, but non-fibrillar types IV, VI, and VIII collagen form different types of ultrastructural networks that serve different functions than fibrillar collagens.<sup>484,487,515</sup>

Type IV collagen molecules are typically heterotrimers consisting of two  $\alpha_1(\text{IV})$  and one  $\alpha_2(\text{IV})$  chain, which associate with one another via their C-terminal globular head into three dimensional networks.<sup>481,499</sup> Type IV collagen is a major component of the basement membranes of many cell types, including the endothelial cell basement membrane.<sup>484,487,489,490</sup> Type IV collagen molecules contain interruptions within their COL domain, which impart flexibility into the collagen molecule. The flexibility of type IV collagen networks imparts elasticity and extensibility to basement membranes.<sup>488,499</sup>

Type VI collagen is a heterotrimer mostly often expressed as an  $\alpha_1(\text{VI})$ ,  $\alpha_2(\text{VI})$ , and  $\alpha_3(\text{VI})$  heterotrimer,<sup>520</sup> but some tissues express isoforms containing  $\alpha_4(\text{VI})$ ,  $\alpha_5(\text{VI})$ , and  $\alpha_6(\text{VI})$  chains in various combinations of trimers.<sup>481,484</sup> Type VI collagen forms

beaded filamentous microfibrils that connect different components of the basement membrane,<sup>521,522</sup> and type VI collagen is abundant within the endothelial cell basement membrane.<sup>481,484</sup> Within the tunica media, type VI collagen microfibrils mediate smooth muscle cell interactions with elastin fibers.<sup>500</sup> Similar to fibrillar collagens, type VI collagen assembly begins intracellularly, but once type VI  $\alpha$ -chains have formed a triple-helical collagen monomer, they aggregate into tetramers before being secreted into extracellular space, where the tetramers associate end-to-end into beaded filaments.<sup>521,522</sup> The filaments then aggregate laterally into beaded microfibrils,<sup>522</sup> which are composite structures that integrate many different molecules within the basement membrane of cells.<sup>523</sup> The tissue distribution of type VI collagen is fairly ubiquitous,<sup>524</sup> and its primary known function is to integrate components of extracellular matrices to one another and to cells.<sup>500</sup>

Type VIII collagen is present as either a homotrimer of  $\alpha_1(\text{VIII})$  chains or as a heterotrimer of  $\alpha_1(\text{VIII})$  and  $\alpha_2(\text{VIII})$  chains that is also an abundant component of the basement membrane of endothelial cells.<sup>481,525,526</sup> Type VIII collagen similarly forms three dimensional networks that are postulated to stabilize the basement membrane and play a role in angiogenesis.<sup>525</sup> Type VIII collagen was originally referred to as “endothelial collagen” because it is abundantly produced and deposited into the tunica intima,<sup>527</sup> but it has since been shown to be produced by other cells.<sup>528</sup> Type VIII collagen molecules consist of a short, rod-like COL with a globular domain at both the C- and N-termini.<sup>481</sup> These globular domains associate with one another into a hexagonal lattice

structure. Type VIII collagen is considered to be important for the resistance of compressive forces,<sup>528</sup> but has also been shown to be synthesized by sprouting endothelial cells, suggesting it may contribute to angiogenesis.<sup>529</sup>

### 1.4.3 Collagens in hemostasis and thrombosis

Collagens have a dual role in hemostasis and thrombosis.<sup>419,492</sup> First, they provide an insoluble scaffold for the attachment of cells and other matrix constituents,<sup>530</sup> which facilitates and maintains a closed system of blood circulation.<sup>492</sup> Second, fibrillar and non-fibrillar collagens within the vessel directly support platelet adhesion and platelet activation.<sup>430,531</sup> Collagens are normally sequestered from flowing blood. Following blood vessel injury, flowing blood is exposed to high local concentrations of collagens in the layers of the vessel wall and connective tissues around vessels and in the tissues that blood is exposed to in a wound.<sup>419,492</sup>

Fibrillar collagens are the only known proteins that can support significant platelet adhesion and full platelet activation.<sup>419,492</sup> Fibrillar collagens are potent agonists of platelet activation that can induce platelet aggregation and fibrin formation.<sup>190</sup> Similar to thrombin-activated platelets, collagen-activated platelets express negatively charged phospholipids on their surface and release  $\alpha$ -granule contents, which supports the assembly of the prothrombinase complex on the platelet surface, leading to thrombin generation and then fibrin formation.<sup>190</sup> Platelets adherent to fibrillar collagen spread,

form extensive lamellipodia, exhibit bleb formation, and release procoagulant TF-bearing microparticles.<sup>419</sup>

Type I-IV collagens are considered the “platelet reactive” collagens due to their ability to support platelet adhesion and induce platelet aggregate formation under low and high shear rates.<sup>302</sup> Platelets are also capable of adhering to types VI-VIII collagen, but platelets do not aggregate onto these collagens, and only adhere as a monolayer under shear rates lower than approximately  $800 \text{ s}^{-1}$ .<sup>532</sup> Notably, although platelets can adhere to and aggregate onto type IV collagen, type IV collagen binding to platelet GPVI does not induce full platelet activation.<sup>533</sup> Fibrillar collagens I and III in the vessel wall are considered the primary mediators of collagen-induced platelet activation.<sup>190,441,492,531</sup>

Collagen receptors on platelets have both adhesive and signaling functions. Accordingly, platelet adhesion to collagen is a dual process that supports both platelet adhesion and activation.<sup>419,531</sup> The classic “two-site, two-step” model of platelet adhesion to collagen states that platelets adhere to collagen via  $\alpha_2\beta_1$  and are activated by GPVI binding to collagen.<sup>430,531</sup> These two processes involve distinct receptors and discrete recognition sites in the triple-helical domain of fibrillar collagens.<sup>430,531,534</sup> However, outside-in signalling following ligation of  $\alpha_2\beta_1$  by collagen has been reported,<sup>535–538</sup> suggesting that  $\alpha_2\beta_1$  may participate to some degree in platelet activation. Similarly, platelet GPVI is capable of supporting platelet adhesion to collagen in the absence of

$\alpha_2\beta_1$ .<sup>539</sup> Therefore, platelet adhesion and activation by collagen should not be considered mutually exclusive processes, each mediated by a single receptor.

Presently, there are three major “adhesive axes” of platelet adhesion to collagen that have been described:  $\alpha_2\beta_1$ -mediated platelet adhesion, GPVI-mediated platelet activation that supports some adhesion and enhances  $\alpha_2\beta_1$ -mediated adhesion, and VWF-mediated platelet adhesion.<sup>175</sup> VWF is sometimes referred to as a collagen receptor due to its ability to mediate platelet adhesion to collagen by binding to collagens and GPIb $\alpha$  on platelets. The primary function of VWF-mediated platelet adhesion to collagen is to facilitate direct platelet-collagen interactions by tethering circulating platelets and allowing them to slowly translocate across the collagen surface under high shear flow.

The use of fragmentation methods (i.e. pepsin digestion or cyanogen bromide hydrolysis) and peptide libraries have been instrumental in identifying the regions in fibrillar collagens that bind various ligands.<sup>540–544</sup> In particular, Collagen Toolkits are peptide libraries that have been used to characterize the precise motifs and key residues in homotrimeric fibrillar collagens that bind VWF,  $\alpha_2\beta_1$ , and GPVI.<sup>436,545–547</sup> Collagen Toolkits are sets of synthetic triple-helical peptides that take advantage of the inherent properties of fibrillar collagen molecules (*Figure 5*). Given the repeated rod-like structure of the COL domain, its sequence can be segmented into short peptides, which, due to the repeating GXX’ motif of the COL domain, causes these peptides to spontaneously assemble into  $\alpha$ -helices and subsequently trimerize into a triple helix that recapitulates the

native conformation of the COL domain of a fibrillar collagen monomer.<sup>548</sup> Stable triple helix formation is facilitated and maintained by the use of (GPP)<sub>5</sub> host sequences, which do not support platelet adhesion or platelet activation.<sup>548</sup> The following sections discuss the various recognition motifs for platelet collagen receptors and their importance in hemostasis and thrombosis. The current scope of recognition motifs in types I and III fibrillar collagen that support platelet adhesion or activation are presented in *Figure 6*, not including MMRN1-binding sequences in fibrillar collagens presented later in this thesis. As part of collaborative studies between the laboratories of Dr. Catherine Hayward and Dr. Richard Farndale, Dr. Subia Tasneem performed analyses of MMRN1 binding to Collagen Toolkit peptides, which identified a GPAGPOGPX motif (where O is hydroxyproline and X is occupied by either valine or glutamine) that is postulated to be the recognition motif in types II and III fibrillar collagen for MMRN1. These experiments are the foundation for some of the work included in this thesis and are discussed in more detail in *section 1.5*.

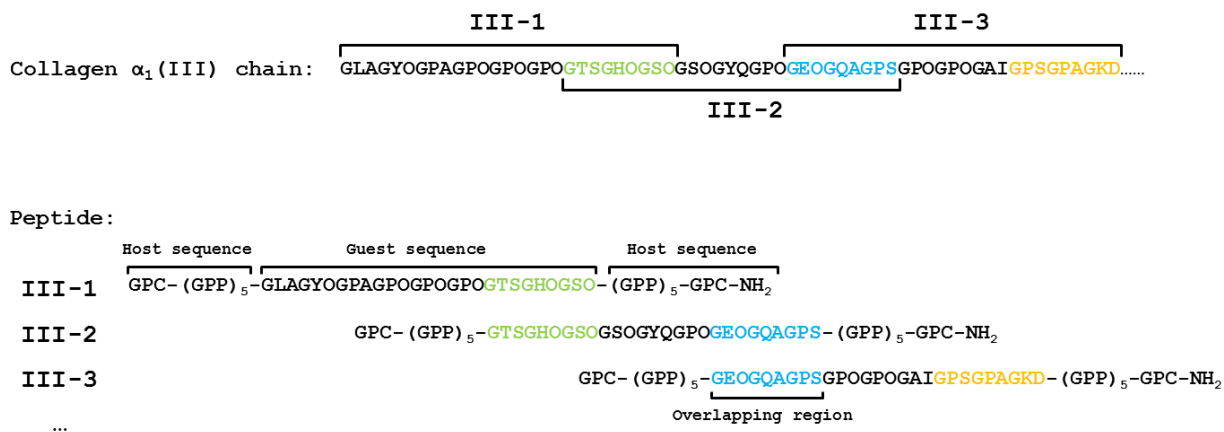


**Figure 5: Structure of Collagen Toolkit III peptides.** The primary sequence of COL  $\alpha_1$ (III) is divided into a set of 57 peptides containing a 27-aa guest sequence within inert

(GPP)<sub>5</sub> sequences. Each guest sequence overlaps with the guest sequence of adjacent peptides by 9-aa to account for the possibility of splitting recognition motifs at the junction of two sequences. The (GPP)<sub>5</sub> host sequences flanking each end of the guest sequence do not support platelet adhesion or activation, but facilitate the formation of a stable triple helix. The cysteine residue on the N- and C-termini of each peptide allows them to crosslink to one another.<sup>549</sup>

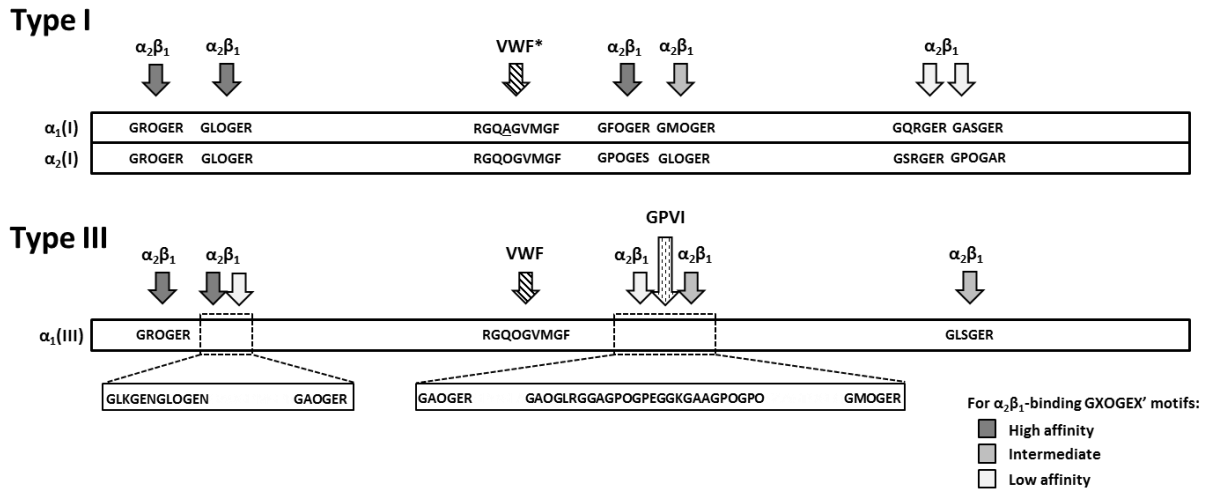


**Figure 6: Recognition motifs in types I and III fibrillar collagens for  $\alpha_2\beta_1$ , GPVI, and VWF.** Arrows are spatially aligned based on their location in the primary sequence of COL  $\alpha_1(I)$ , COL  $\alpha_2(I)$ , and COL  $\alpha_1(III)$ , demonstrating the spatial distinctions between various motifs. \*Postulated to be a VWF-binding sequence,<sup>545</sup> but has not been verified using a heterotrimeric peptide.

#### 1.4.3.1 VWF recognition motifs in fibrillar collagens

VWF binds to types I and III fibrillar collagen via its A3 domain, and a minor role has been attributed to the A1 domain in VWF binding to collagen.<sup>550</sup> Binding of VWF to platelets is required for their adhesion to fibrillar collagen under high shear flow, and monoclonal anti-VWF or anti-GpIb antibodies completely abolish platelet adhesion onto

collagen. Conversely, mice with defective VWF-collagen binding are protected from thrombosis *in vivo*.<sup>551</sup> VWF binding to collagen can occur via direct interaction between collagen and the VWF A3 domain or by self-association of circulating plasma or platelet VWF onto collagen-bound VWF.<sup>552</sup>

VWF binds to the GPRGQOGVMGF sequence in type III collagen (*Figure 6*), and the binding affinity of VWF for GPRGQOGVMGF is similar to the affinity of VWF for full-length type III collagen, suggesting that this motif is the only sequence in fibrillar collagen with which VWF interacts.<sup>545</sup> The GPRGQOGVMGF sequence is capable of supporting platelet tethering and translocation, but not stable adhesion under shear rates between 1000 and 3000 s<sup>-1</sup>,<sup>175</sup> consistent with the requirement of high shear stress to reveal cryptic binding sites in the VWF A1 and A3 domains as well as the requirement of  $\alpha_2\beta_1$  for stable adhesion onto collagen. Under low shear flow (100 to 300 s<sup>-1</sup>), GPRGQOGVMGF synergistically enhances platelet adhesion when co-presented with the  $\alpha_2\beta_1$ -binding GFOGER motif and collagen-related peptide (CRP), which activates platelets via GPVI.<sup>175</sup> The GPRGQOGVMGF sequence in  $\alpha_1(\text{III})$  is mostly conserved in the collagen  $\alpha_1(\text{I})$  chain, except for the hydroxyproline residue in the 5<sup>th</sup> position, but the missing hydroxyproline is present at the corresponding 5<sup>th</sup> position in the  $\alpha_2(\text{I})$  chain, which is predicted to enable VWF binding at this locus.<sup>548</sup> A non-triple-helical derivative of peptide III-23 flanked by (GAP)<sub>5</sub> host sequences does not bind VWF nor platelets, indicating that triple helical conformation is required for the recognition of III-23 by VWF.<sup>545</sup> VWF multimer size also affects its ability to bind fibrillar collagen. ULVWF

multimers preferentially bind collagen compared to smaller VWF multimers,<sup>553</sup> which is likely due to multivalent binding between multiple VWF monomers within a multimer and multiple collagen molecules within a fibril. Accordingly, washed platelets are able to adhere to GPRGQOGVMGF under stasis,<sup>545</sup> consistent with the ability of ULVWF multimers released by platelets or endothelial cells to bind collagen in the absence of shear.

Although VWF co-localizes with type VI collagen in the subendothelium and mediates platelet adhesion to type IV or VI collagen, the interaction of VWF with non-fibrillar type IV and type VI collagens differs from its interactions with fibrillar collagens I and III. Types IV and VI collagen do not possess the GPRGQOGVMGF motif, and VWF binding to types IV and VI collagen requires the VWF A1 domain, but not the VWF A3 domain.<sup>328,329</sup> At present, the functions of VWF binding to types IV and VI collagen are not well characterized.

#### *1.4.3.2 Alpha-2 beta-1 recognition motifs in fibrillar collagens*

Platelet integrin  $\alpha_2\beta_1$  is the only known receptor on platelets that is capable of supporting stable platelet adhesion to collagen by binding directly to collagen.<sup>419</sup> Alpha-2 beta-1 on resting or activated platelets binds with high affinity to the GFOGER sequence in COL  $\alpha_1(I)$ . The GFOGER motif was initially identified as the recognition motif for  $\alpha_2\beta_1$  in type I fibrillar collagen using cyanogen bromide hydrolysed type I collagen

fragments.<sup>540</sup> Following the development of synthetic triple-helical collagen mimetic peptides and Collagen Toolkits, additional  $\alpha_2\beta_1$ -binding motifs have been identified in types I and III fibrillar collagen (*Figure 6*). The consensus recognition motif in collagens for  $\alpha_2\beta_1$  is GXOGEX',<sup>548</sup> and it is present in various forms in types I and III collagens. GFOGER, GROGER, GLOGER, and GLOGEN are high-affinity motifs that can support adhesion of resting or activated platelets.<sup>540,541,546</sup> Additional motifs, such as GLKGEN, GLSGER, GMOGER, GAOGER, GASGER, and GQRGER bind to  $\alpha_2\beta_1$  and support platelet adhesion, but only following platelet activation when  $\alpha_2\beta_1$  is in an active conformation.<sup>436,546</sup> The low affinity GXOGEX' motifs in collagens are considered to be important in stabilizing platelet adhesion to collagen following activation of platelets and  $\alpha_2\beta_1$ .<sup>436</sup> High-affinity GXOGEX' motifs are likely essential to initial adhesion of platelets to collagen when  $\alpha_2\beta_1$  is present in an inactive conformation on the platelet surface. Interestingly, the spatial relationship between GXOGEX' motifs is conserved between COL  $\alpha_1$ (I) and COL  $\alpha_1$ (III), suggesting that the distribution of recognition motifs in the COL domain may be important for  $\alpha_2\beta_1$  function.

#### *1.4.3.3 GPVI recognition motifs in fibrillar collagens*

Monomeric GPVI binds to the GPO motif in the triple-helical COL domain. Given that GPVI is present as a dimer on the platelet surface, each copy of GPVI must bind to a respective GPO triplet in collagen to trigger receptor signalling. A single GPO triplet is insufficient to induce platelet activation via GPVI.<sup>453</sup> The Ig-like domains of

adjacent copies of GPVI are separated by a gap roughly equivalent to three amino acids in length.<sup>441</sup> The smallest GPVI recognition motif in fibrillar collagens is two GPO triplets, either directly adjacent or separated by four GPP repeats. Collagen Toolkit peptide III-30 contains multiple GPO triplets within its 27-aa guest sequence, and is able to bind and activate platelets via GPVI.<sup>547</sup> This region of type III collagen is considered the primary interaction site for GPVI (*Figure 6*). Similar GPO-rich regions are posited to be responsible for platelet activation by type I fibrillar collagen but have not been investigated in depth.

Fibrillar ultrastructure of collagen molecules is required for platelet activation via GPVI. Preparations of collagen that are either non-fibrillar or produce non-fibrillar fragments (i.e. cyanogen bromide treatment) support GPVI binding, but do not activate platelets.<sup>240,554</sup> Similarly, type IV collagen contains many GPO triplets, but does not trigger platelet activation via GPVI because it lacks the quaternary structure of fibrillar collagens.

#### 1.4.4 Fibrillar collagen-related disease states

The Ehlers-Danlos syndromes (EDS) are a heterogeneous group of hereditary connective tissue disorders characterized in part by excessive bruising, hematomas, and increased bleeding despite normal findings for clinical tests of hemostasis.<sup>516,555,556</sup> There are currently six characterized subtypes of EDS,<sup>516</sup> which are linked to causative

mutations in genes encoding the  $\alpha$ -chains of fibrillar collagens or enzymes involved in post-translational modification of collagen molecules. The conventional explanation of EDS-associated bleeding symptoms is that defects in collagen molecules lead to structural abnormalities in collagen fibers, resulting in fragile vessels that are prone to rupture.<sup>557</sup> In particular, type IV EDS, also called “vascular EDS”, generally arises from missense mutations of glycine residues within the  $\alpha_1$  chain of type III collagen, which causes structural defects in blood vessels. Rupture of major arteries, the bowel, or gravid uteri are features of vascular EDS, along with fragile skin that splits easily in response to minor trauma. Over 250 different vascular EDS mutations have been described,<sup>558</sup> the majority of which are point mutations leading to substitutions for glycine in the triple helical domain of type III collagen. Interestingly, a mutation in the MMRN1-binding GPAGPOGPQ sequence (G852C) is associated with type IV EDS, but its potential effects on platelet adhesion are unclear. The possible effects of collagen mutations on MMRN1 binding and platelet adhesion are discussed in more detail in *section 4.5.3*. In mice, global knockout of *Col3a1* results in 90% perinatal mortality, with a reduced lifespan in surviving homozygotes, usually due to spontaneous vascular rupture. Instead, mice heterozygous for *Col3a1* deletion have been used as a model for EDS that recapitulates many key features of vascular EDS in humans.<sup>559</sup>

Osteogenesis imperfecta, also called “brittle bone disease”, is a heterogeneous group of genetic disorders characterized by susceptibility to fracture that varies in severity from mild (type I) to embryonic lethal (type II). Dominantly inherited forms account for

90% of people with OI result from heterogeneous mutations in *COL1A1* or *COL1A2*.<sup>517</sup> The mildest forms of OI generally result in the loss of mRNA from one *COL1A1* allele, whereas severe forms can result from substitution of glycine residues within the COL domain of *COL1A1* or *COL1A2*. OI can sometimes result in a bleeding phenotype that is similar to features of EDS, which is suggested to be caused by defective collagen fibers and vessel fragility. It is currently not known what the specific effects of *COL1A1* and *COL1A2* mutations are on platelet adhesion.

## 1.5 UNANSWERED QUESTIONS REGARDING MMRN1 ADHESIVE FUNCTIONS

Given what is presently known about MMRN1 adhesive functions and platelet adhesion and platelet aggregation, there are numerous unanswered questions regarding the role of MMRN1/Mmrn1 in platelet adhesion. In particular, the observation that the adhesion of *Mmrn1*<sup>-/-</sup> platelets to fibrillar collagen is impaired raised questions regarding the mechanism through which Mmrn1 contributes to platelet adhesion to collagen. It has been argued that the specific roles of ligands involved in platelet adhesion to collagen cannot be resolved by analyses of surface coverage alone.<sup>560</sup> It was previously noted that *Mmrn1*<sup>-/-</sup> platelets showed a tendency toward forming smaller aggregates onto collagen under high shear flow (1500 s<sup>-1</sup>),<sup>4</sup> but a standardized method for quantification of adherent platelet aggregates is not established for this assay. Additionally, the dynamics of the defect in platelet adhesion and aggregate formation onto collagen have not been explored. Endpoint analyses of platelet adhesion are not sensitive to differentiate between

defects in initial platelet tethering onto collagen, rate of aggregate growth, or aggregate stability. It is also unclear if this defect in platelet adhesion to collagen is present under low shear flow, in which VWF is not essential for platelets to significantly aggregate onto fibrillar collagen.

As described in *section 1.3.2.1*, a critical role of  $\alpha_{IIb}\beta_3$  in platelet aggregation onto fibrillar collagen under high shear flow has been demonstrated for both human and mouse platelets. MMRN1 is a ligand for  $\beta_3$  integrins on activated platelets, and *Mmrn1* may contribute to platelet aggregate formation on fibrillar collagens through interactions with  $\alpha_{IIb}\beta_3$  on activated mouse platelets. However, *Mmrn1* lacks the N-terminal RGD site present in MMRN1,<sup>18</sup> meaning it is unclear if *Mmrn1* binds  $\beta_3$  integrins. It is possible that *Mmrn1* may interact with  $\alpha_{IIb}\beta_3$  through RGD-independent mechanisms, similar to FG.

Alternatively, *Mmrn1* could crosslink  $\alpha_{IIb}\beta_3$ -bound adhesive proteins to indirectly support platelet aggregate formation, similar to TSP-1 and multimeric VN released from platelets. Given the complex, multi-domain structure of MMRN1/*Mmrn1* and its ability to form large multimers, it may act as a bridging protein by binding FG on activated platelets to support platelet cohesion through interactions with platelet-bound FG. Potential defects in Fg-dependent platelet adhesion in the absence of *Mmrn1* may also partly explain the antithrombotic phenotype of *Mmrn1*<sup>-/-</sup> mice in response to FeCl<sub>3</sub> arteriolar injury, as Fg-deficient mice similarly show impaired thrombus formation, stability, and vessel occlusion in this model.<sup>211</sup>

Another possible binding partner for MMRN1/Mmrn1 is FN. FN supports platelet adhesion via RGD-dependent binding to  $\alpha_5\beta_1$  and activated  $\alpha_{IIb}\beta_3$ , and MMRN1 may assist in FN-mediated platelet adhesion or possibly compete for ligation of activated  $\alpha_{IIb}\beta_3$ . MMRN1 could potentially act as a bridging protein that would enhance the ability of platelet FN to crosslink platelets or increase the avidity of platelet-platelet interactions by binding to  $\alpha_{IIb}\beta_3$ -bound FN.

Observations from studies of FeCl<sub>3</sub>-treated mesenteric arterioles raised questions regarding the ability of Mmrn1 to support platelet adhesion, aggregation, and thrombus formation *in vivo*. Firstly, the role of collagen in FeCl<sub>3</sub>-induced vessel injury is controversial.<sup>561,562</sup> Some evidence suggests that types IV and VI collagen in the endothelial basal lamina are exposed following exposure to FeCl<sub>3</sub>,<sup>211,563</sup> but FeCl<sub>3</sub>-induced vessel injury has not been shown to induce exposure of fibrillar collagens deeper within the vessel wall. Despite this, platelet adhesion and thrombus formation are significantly impaired in the arterioles of *Mmrn1*<sup>-/-</sup> mice treated with FeCl<sub>3</sub>.<sup>4</sup> The connection between impaired adhesion of *Mmrn1*<sup>-/-</sup> platelets to fibrillar collagen *in vitro* and impaired thrombus formation in mesenteric arterioles *in vivo* is uncertain, but suggests other mechanisms are involved. For example,  $\alpha_2$ -deficient mice have delayed thrombus formation with frequent embolization in FeCl<sub>3</sub>-treated mesenteric arterioles, which is attributed to a reduction in TxA<sub>2</sub> formation, not impaired adhesion to collagens.<sup>215</sup>

Although MMRN1 modulates FV storage and thrombin generation, in the context of platelet adhesion, Mmrn1 binding to FG and FN to enhance or stabilize platelet adhesion may contribute to FeCl<sub>3</sub>-induced thrombus formation. This would provide a link between impaired aggregate formation on collagen *in vitro* and impaired thrombus formation *in vivo* observed in *Mmrn1*<sup>-/-</sup> mice. Another particularly interesting potential Mmrn1 binding partner is fibrin, which is generated in significant quantities in the FeCl<sub>3</sub>-induced vessel injury model. The possibility for Mmrn1 to modulate platelet adhesion and thrombus formation *in vivo* through interactions with fibrin would represent an additional mechanism through which Mmrn1 contributes to platelet thrombus formation, and help reconcile *in vitro* and *in vivo* observations of *Mmrn1*<sup>-/-</sup> mice.

The LTA responses of *Mmrn1*<sup>-/-</sup> mice raised questions regarding how they relate to *in vitro* analyses of platelet adhesion to collagen. *Mmrn1*<sup>-/-</sup> mouse platelets had normal collagen-induced aggregation when tested in PRP, but not using GFP, which is postulated to be due to the presence of other adhesive plasma proteins masking the contribution of Mmrn1.<sup>4</sup> However, in analyses of platelet adhesion to collagen under high shear flow using whole blood, *Mmrn1*<sup>-/-</sup> mice had significantly impaired platelet adhesion to collagen. This could be due to 1) differences in shear rate between the models or 2) differences in how platelets are exposed to collagen (i.e. surface-bound versus soluble agonist). Testing the ability of *Mmrn1*<sup>-/-</sup> and wild-type mouse platelets in whole blood in response to collagen would clarify if using PRP or gel-filtered platelets alters the ability

of *Mmrn1*<sup>-/-</sup> and wild-type platelets to aggregate in response to collagen compared to platelets in whole blood.

Presently, *in vitro* and *in vivo* analyses of *Mmrn1*<sup>-/-</sup> mice have focused on high shear flow (1500 s<sup>-1</sup>), excluding LTA experiments. Immobilized MMRN1 can support adhesion of activated platelets under much higher shear rates ( tested to a maximum of 6000 s<sup>-1</sup>), and fluid shear stress is known to affect MMRN1 adhesive functions.<sup>2</sup> It is intriguing to consider that *Mmrn1* could contribute to platelet aggregation under elevated shear rates, such as at the apex of a developing thrombus, which would provide evidence for a potential mechanism through which *Mmrn1* contributes to thrombus growth and vessel occlusion. As described in *section 1.3.1.2*, VWF is a key mediator of platelet aggregation under elevated shear, and *Vwf*<sup>-/-</sup> mice fail to form occlusive thrombi due to small luminal channels that never fully occlude. Given that MMRN1 binds VWF, *Mmrn1* could similarly bind *Vwf* to enhance *Vwf*-mediated platelet aggregation under elevated shear.

Lastly, there are unanswered questions regarding the ability of MMRN1 to interact with collagens. Previous work by our laboratory has identified a MMRN1-binding GPAGPOGPX sequence in types II and III fibrillar collagens (*outlined in section 1.4.3*), but it is unknown if a similar GPAGPOGPX sequence that binds MMRN1 is present in type I collagen, which is also a ligand for MMRN1. The GPAGPOGPX sequence is spatially and structurally discrete from other recognition motifs in collagen

that support platelet adhesion, but the specificity of GPAGPOGPX for MMRN1/Mmrn1 and its ability to support mouse platelet adhesion have not been evaluated. The ability of MMRN1 to enhance platelet adhesion to fibrillar collagen is intriguing, and could involve MMRN1-mediated platelet-collagen interactions that synergize with other receptors and proteins to enhance platelet adhesion. However, the ability of the MMRN1-binding GPAGPOGPX sequence to enhance platelet adhesion under stasis and flow when presented with other recognition motifs in fibrillar collagens has not been evaluated.

#### 1.5.1 Hypothesis

Based on the considerations described above, I hypothesize that:

Mmrn1 contributes to platelet adhesion and aggregate formation by binding to adhesive proteins in plasma and platelets, such as fibrin(ogen) or fibronectin, contributes to platelet adhesion and aggregation under elevated shear stress, and enhances collagen-dependent platelet adhesion through a mechanism involving Mmrn1-specific motifs in fibrillar collagens.

### 1.5.2 Experimental aims

To test this hypothesis, my specific experimental aims were:

1. Characterize the ability of Mmrn1 to modulate aggregate formation onto fibrillar collagen and determine the dynamics of impaired platelet adhesion to fibrillar collagen shown by *Mmrn1*<sup>-/-</sup> mice, using analyses of:
  - a. Aggregate size of collagen- or Vwf-adherent *Mmrn1*<sup>-/-</sup> and wild-type mouse platelets
  - b. Real-time adhesion of *Mmrn1*<sup>-/-</sup> and wild-type mouse platelets to collagen under high shear flow
  - c. Adhesion of *Mmrn1*<sup>-/-</sup> and wild-type mouse platelets to Horn collagen under low shear flow
  - d. Collagen-induced aggregation of *Mmrn1*<sup>-/-</sup> and wild-type platelets in whole blood
  
2. Test the ability of MMRN1 to bind FG, fibrin, and FN, and assess the ability of Mmrn1 to augment platelet adhesion to FG, fibrin, and FN, using:
  - a. Solid-phase MMRN1 binding assays to FG, fibrin, and FN
  - b. Assays of static and low shear adhesion of *Mmrn1*<sup>-/-</sup> and wild-type platelets to murine Fg, fibrin, and Fn

3. Characterize the role of fluid shear stress in the ability of Mmrn1 to enhance platelet adhesion and aggregate formation.
  - a. Assays of shear-induced aggregation of *Mmrn1*<sup>-/-</sup> and wild-type mouse platelets
  
4. Identify additional GPAGPOGPX-like sequences in type I fibrillar collagen and test their ability to bind MMRN1 and modulate platelet adhesion, using:
  - a. *In silico* analysis of amino acid sequences of type I collagen  $\alpha$ -chains
  - b. Solid-phase MMRN1 binding assays to triple-helical collagen mimetic peptides
  - c. Static and high shear adhesion assays using *Mmrn1*<sup>-/-</sup> and wild-type platelet and triple-helical collagen peptides
  - d. Static adhesion assays using resting and activated human platelets and triple-helical collagen peptides

## CHAPTER 2: MATERIALS AND METHODS

### 2.1 MATERIALS

#### 2.1.1 Reagents and supplies

Reagents and supplies included: prostaglandin E<sub>1</sub> (PGE<sub>1</sub>, Sigma-Aldrich Canada, Oakville, ON, CA), CNBr-activated Sepharose™ 4B (GE Healthcare Bio-Sciences AB, Uppsala, SE), Colorburst™ Blue TMB/peroxide color developing peroxidase substrate (ALerCHEK, Inc., Portland, ME, USA), BioTrace™ NT pure nitrocellulose blotting membrane (Pall Life Sciences, Pensacola, FL, USA), Immobilon™ Western Chemiluminescent horseradish peroxidase (HRP) substrate (Thermo Fisher Scientific, Inc., Waltham, MA, USA), ProLong™ Gold antifade reagent (Invitrogen Canada Inc., Burlington, ON, CA), ketamine (Narketan; Vetoquinol, Lavaltrie, QC, CA), atropine (Arto-SA, Rafter8, Calgary, AB, Canada), xylazine (Rompun™; BayerDVM, Shawnee Mission, KS, USA), polyethylene tubing (PE10; Becton Dickinson and Company, Sparks, MD, USA), 75x25x1 mm single-frosted glass microscope slides (VWR® VistaVision™; VWR International, Radnor, PA, USA), 22x22 mm glass micro cover slides (VWR International, Radnor, PA, USA), Extract-N-Amp™ Tissue Polymerase Chain Reaction (PCR) Kit (Sigma-Aldrich Canada, Oakville, ON, CA), Phe-Pro-Arg-chloromethylketone (PPACK; Haematologic Technologies Inc., Essex Junction, VT, USA), thrombin (Sigma-Aldrich Canada, Oakville, ON, CA), mouse Par4 amide (GYPGKF-NH<sub>2</sub>; Bachem

Americas, Inc., Torrance, CA, USA), phosphatase substrate (p-Nitrophenyl phosphate; Sigma-Aldrich Canada, Oakville, ON, CA), C-Chip DHC-N01 disposable hemocytometer (Incyto, Seonggeo-eup, Seobuk-gu Cheonan-si, Chungnam-do, SK), microtitre plates (Costar<sup>®</sup> 3695; Corning, Inc., Kennebunk, ME, USA; Immulon<sup>®</sup> 2 HB; Thermo Scientific, Rochester, NY, USA), braided silk non-absorbable suture (SP115; Surgical Specialties Corporation<sup>™</sup>, Westwood, MA, USA), Precision Plus Protein<sup>™</sup> dual color standard (Bio-Rad Laboratories [Canada] Ltd., Mississauga, ON, CA), plastic cuvettes (Chrono-Log Corp., Havertown, PA, USA), siliconized stir bars (Chrono-Log Corp., Havertown, PA, USA), 100bp DNA ladder RTU (ready-to-use; GeneDireX, Inc.), Vena8Fluoro+ Biochips (Cellix Ltd., Dublin, IE), 3.2% sodium citrate (Becton, Dickinson and Company, Franklin Lakes, NJ, USA), heparin (Sandoz Canada, Boucherville, QC, CA), 2-Mercaptoethanol (Sigma-Aldrich Canada, Oakville, ON, CA), 3,3'-dihexyloxacarbocyanine iodide (DiOC6[3]; Enzo Life Sciences Inc., Farmingdale, NY, USA), Tween<sup>®</sup> 20 detergent (Sigma-Aldrich Canada, Oakville, ON, CA), Triton X-100 detergent (Sigma-Aldrich Canada, Oakville, ON, CA), AccuStart<sup>™</sup> II GelTrack PCR SuperMix (Quanta Biosciences, Inc., Beverly, MA, USA), and EDTA (Fisher Chemical<sup>™</sup>, Thermo Fisher Scientific, Inc., Waltham, MA, USA).

### 2.1.2 Antibody sources

Antibodies against multimerin 1 included: rabbit polyclonal anti-MMRN1 (sc-367225; Santa Cruz Biotechnology, Inc., Dallas, TX, USA) raised against a MMRN1 C-terminal fragment (residues 1051-1228) that recognizes mouse *Mmrn1*; in-house prepared

monoclonal mouse anti-MMRN1 (JS-1), that recognizes an epitope in the C-terminal region of human MMRN1 (residues 961-1139);<sup>10</sup> and in-house prepared polyclonal rabbit anti-MMRN1 (P155).<sup>15</sup>

HRP-conjugated secondary antibodies used in Western blotting and ELISA included: donkey anti-mouse immunoglobulin G (IgG) and donkey anti-rabbit IgG (Jackson ImmunoResearch Laboratories, Inc., West Grove, PA, USA).

Fluorescently-labelled antibodies against mouse platelet proteins included: phycoerythrin (PE)-labelled hamster anti-mouse  $\beta_3$  (CD61; BD Biosciences, Mississauga, ON, CA); fluorescein isothiocyanate (FITC)-labelled rat anti-mouse GPIIb/IIIa (CD42b; Emfret Analytics GmbH & Co. KG, Eibelstadt, Germany); and FITC-labelled rat anti-mouse P-selectin (CD62P; Emfret Analytics GmbH & Co. KG, Eibelstadt, Germany).

Monoclonal anti-mouse  $\beta_3$  blocking antibody (9D2) was a gift from Dr. Heyu Ni.

### 2.1.3 Purified proteins

#### *2.1.3.1 Recombinant human multimerin 1*

Recombinant human (rh) MMRN1 was prepared by culture of human embryonic kidney (HEK) 293 cells that were stably transfected with the cDNA for prepromultimerin 1 in pCMV5 (pCMV5-multimerin).<sup>12</sup> rhMMRN1 was affinity purified from cell culture media using JS-1 conjugated Sepharose beads as described.<sup>1,20</sup> Captured rhMMRN1 was eluted using 3.5 M MgCl<sub>2</sub>, and desalted and concentrated by two centrifugations. The

concentration of affinity purified rhMMRN1 was evaluated by enzyme-linked immunosorbent assays (ELISA) via comparison to pooled normal platelet lysate as described,<sup>1,21,27</sup> where 1 unit (U) of MMRN1 is defined as the amount of MMRN1 in 10<sup>9</sup> pooled ( $n=20$ ) normal platelets (estimated to be equivalent to 18.5  $\mu\text{g}$ ).<sup>6,20</sup> Costar<sup>®</sup> 96-well half-volume microtitre plates were coated using 0.5  $\mu\text{g}/\text{well}$  JS-1 in carbonate buffer (14.2 mM Na<sub>2</sub>CO<sub>3</sub>, 35 mM NaHCO<sub>3</sub>, pH 9.6) overnight at 4°C. JS-1-bound MMRN1 was detected using 1:1000 polyclonal rabbit antisera against MMRN1 (P-155) followed by 1:2000 HRP-conjugated donkey anti-rabbit IgG. Subunit size of purified rhMMRN1 was assessed by reduced sodium dodecyl sulfate polyacrylamide gel electrophoresis (SDS-PAGE) on a 6% polyacrylamide gel followed by transfer to a nitrocellulose membrane and immunoblotting. Nitrocellulose membranes were probed for rhMMRN1 using 1:5000 JS-1 followed by 1:25,000 HRP-conjugated donkey anti-mouse IgG. Silver staining of polyacrylamide gels to assess purity of rhMMRN1 was performed to assess purity of rhMMRN1 preparations as described.<sup>1,21</sup>

### *2.1.3.2 Triple-helical collagen mimetic peptides*

Triple-helical collagen mimetic peptides were provided by the laboratory of Dr. Richard Farndale and were synthesized by Dr. Dominique Bihan and Dr. Arek Bonna. Collagen Toolkit and other triple-helical collagen peptides were generated using Fmoc solid-phase peptide synthesis and a host-guest strategy as described.<sup>564</sup> Although type II collagen is not found in the vessel wall, sequences from Toolkit II were included in these

analyses because it is homotrimeric and has a high degree of homology with type I collagen (75% identity between the COL domains of  $\alpha_1$ [I] and  $\alpha_1$ [II]). It is presently not feasible to generate heterotrimeric triple-helical collagen peptides so a peptide library for the triple-helical (COL) domain of type I collagen is not available. Triple-helical collagen mimetic peptides used in this thesis are described in *Table 3*. CRP is a potent platelet GPVI agonist, which was used to activate human and mouse platelets in some experiments. GFOGER is a high-affinity ligand for platelet integrin  $\alpha_2\beta_1$ , and was used to measure  $\alpha_2\beta_1$ -dependent adhesion of Mmrn1-deficient platelets or to facilitate stable adhesion when co-presented on a surface with other collagen peptides. Collagen Toolkit peptide III-23, which contains the high-affinity VWF-binding motif GPRGQOGVMGF, was used as a ligand for platelet and plasma VWF. The inert triple-helical peptide GPP, which does not support platelet activation, platelet adhesion, VWF binding, or MMRN1 binding, was used as a negative control peptide.

Peptide	Amino acid sequence			Ligand	Function	Location
	C-terminal Host	Guest sequence	N-terminal Host			
DB304	GPC (GPP) <sub>5</sub>	<u>GPAGPOGPV</u>	(GPP) <sub>5</sub> GPC	MMRN1	-	$\alpha_1$ (III)
CC13	GPC (GPP) <sub>5</sub>	GGSG <u>GPAGPOGPQGVK</u>	(GPP) <sub>5</sub> GPC	MMRN1	-	$\alpha_1$ (III)
AB-24	GPC (GPP) <sub>5</sub>	<u>GPAGPOGFQ</u>	(GPP) <sub>5</sub> GPC	-	-	$\alpha_2$ (I)
AB-25	GPC (GPP) <sub>5</sub>	<u>GPAGSOGFQ</u>	(GPP) <sub>5</sub> GPC	-	-	$\alpha_1$ (I)
AB-30	GPC (GPP) <sub>5</sub>	<u>GPAGPOGPI</u>	(GPP) <sub>5</sub> GPC	-	-	$\alpha_1$ (I)
III-23	GPC (GPP) <sub>5</sub>	GPOG <u>PSGPRGQOGVMGF</u> OGPKGNDGAO	(GPP) <sub>5</sub> GPC	VWF	VWF binding	$\alpha_1$ (III)
GFOGER	GPC (GPP) <sub>5</sub>	<u>GFOGER</u>	(GPP) <sub>5</sub> GPC	$\alpha_2\beta_1$	Platelet adhesion	$\alpha_1$ (I)
CRP	GCO	(GPO) <sub>10</sub>	GOG	GPVI	Platelet activation	N/A
GPP	GPC (GPP) <sub>5</sub>	(GPP) <sub>10</sub>	(GPP) <sub>5</sub> GPC	None known	Inert	N/A

**Table 3: Triple-helical collagen mimetic peptides used in this thesis.** Underlined sections of guest sequences indicate the recognition sequence for each ligand, or residues in the GPAGPOGP(V/Q) motif that are conserved in variant peptides AB-24, AB-25, and AB-30. “-” indicates data not available.

### 2.1.3.3 Other protein sources

Other proteins used in experiments included: human fibrinogen (Haematologic Technologies Inc., Essex Junction, VT, USA), human fibronectin (Haematologic Technologies Inc., Essex Junction, VT, USA), mouse fibrinogen (Fg; Molecular Innovations, Novi, MI, USA), mouse fibronectin (Fn; Molecular Innovations, Novi, MI, USA), Horm collagen reagent (Helena Laboratories, Beaumont, TX, USA), Cultrex<sup>®</sup> rat

collagen I (R&D Systems, Minneapolis, MN, USA), and bovine serum albumin (BSA; Sigma-Aldrich Canada, Oakville, ON, CA).

## 2.2 METHODS

### 2.2.1 Helsinki Declaration on human research

The study was conducted in accordance with the requirements of the revised Helsinki Declaration on human research and the Hamilton Integrated Research Ethics Board (HiREB). Blood samples from human participants were obtained with written informed consent.

### 2.2.2 Animal handling

The animal studies (including the generation and maintenance of mouse colonies, and experiments with mouse tissues) were conducted with the approval of the McMaster University Animal Research Ethics Board (Animal Utilization Protocol 13-02-02, which was subsequently replaced by 16-10-38) and in accordance with the standards set by the Canadian Council on Animal Care. Mice were interbred and housed in the vivaria at the Central Animal Facility within the McMaster University Medical Centre. Animals were housed in rooms with 12-hour dark-light cycles. Breeders and weanlings were housed within sterile ventilated caging before being transferred to specific-pathogen-free non-

sterile caging for general housing. Mice were fed a diet of sterile water and irradiated regular chow *ad libitum* (18% protein rodent diet, Teklad Global Diets, Madison, WI, USA). Gender- and age-mixed wild-type (*Mmrn1*<sup>+/+</sup>) or *Mmrn1*-deficient (*Mmrn1*<sup>-/-</sup>) mice were used in all experiments to obtain representative sample populations. Where possible, experimenters were blinded to the genotype of the mice. Mice not used for experiments or retired breeders were either provided to the Discards program at the Central Animal Facility or euthanized by CO<sub>2</sub> followed by cervical dislocation to confirm death.

### 2.2.3 Generation of multimerin 1-deficient mice

*Mmrn1*-deficient mice were generated using the “knockout-first allele” strategy.<sup>30</sup> Adult mice heterozygous for the *Mmrn1* knockout-first allele were purchased from the European Mutant Mouse Archive (EMMA, EM:05337) and crossed with transgenic Flp mice (B6;J-Tg(ACTFLPe)9205Dym/J) to remove the Frt site flanked *lacZ* and *Neo* regions of the gene-trap cassette, resulting in mice with a floxed third exon of *Mmrn1*. Offspring were then crossed with transgenic global cre mice (B6.C-Tg(CMV-cre)1Cgn/J) to remove the third exon of *Mmrn1*. The resultant exon 3 (E3)-deleted heterozygous mice were crossed with wild-type (C57BL/6J) mice to remove the flp and cre transgenes. Breeding and crossing of mouse strains to generate *Mmrn1*-deficient mice was carried out by Dr. Subia Tasneem, as part of collaborative studies between the laboratories of Dr. Bradley Doble and Dr. Catherine Hayward. The frameshift mutation caused by deletion

of *Mmrn1* E3 is predicted to trigger nonsense-mediated decay of the truncated mutant transcript. *Mmrn1*-deficient mice have no detectable platelet *Mmrn1* by Western blotting, which was performed by Dr. D'Andra Parker.

#### 2.2.4 Genotyping of experimental mice

To confirm genotypes of experimental mice, DNA was extracted from either mouse tails (0.5 to 1 cm of distal tip) or ear notches using Extract-N-AMP™ Tissue PCR Kit according to the manufacturer's protocol, followed by PCR using the oligonucleotide primers: forward (5'-TCTTTCTCTCCCTCTCACCT-3') and reverse (5'-GGCTCCTTTCATTCACAGCC-3'). PCR fragments were resolved on a 2% agarose gel. The PCR products for wild-type and *Mmrn1*-deficient mice were approximately 1038 base pairs (bp) and 336 bp, respectively. Heterozygous null mice displayed bands at both 1038 bp and 336 bp.

#### 2.2.5 Mouse blood collection

Approximately 700 to 900 µl of arterial blood was collected by cannulation of the carotid artery from mice anesthetized with 125 µg/kg ketamine supplemented with 12.5 µg/g xylazine for analgesia and 0.25 µg/g atropine to prevent bradycardia during the procedure.

### 2.2.6 Assays of platelet adhesion under shear

Mouse platelet adhesion was evaluated similar to methods described.<sup>2,21</sup> For flow experiments, blood was perfused through Vena8Fluoro+ microcapillary perfusion chambers (Cellix Ltd., Dublin, IE) at a constant rate using a Cellix Mirus 1.1 Nanopump controlled by VenaFlux™ software (Cellix Ltd., Dublin, IE). Shear stress  $\tau$  (dyne/cm<sup>2</sup>) and shear rate  $\gamma$  (s<sup>-1</sup>) were calculated automatically by VenaFlux™ software based on the estimated viscosity of whole blood samples ( $\mu = 0.045$  dynes/cm<sup>2</sup>) and the geometry of microcapillaries (channel width: 0.04 cm, channel height: 0.01 cm).

For analyses of endpoint adhesion of fluorescently-labelled platelets, Vena8Fluoro+ microcapillary channels were coated overnight at 4°C in a humidified box using 100  $\mu$ g/ml Horm collagen (coated using 0.01 M acetic acid), 10 U/ml recombinant murine Vwf (coated using PBS), or 100  $\mu$ g/ml mouse fibrinogen or mouse fibronectin (coated using carbonate buffer). In some channels, immobilized mouse fibrinogen was converted to fibrin *in situ* using 200 mU/ml human thrombin for 15 minutes before channels were washed with Tris-buffered saline (TBS) containing 10 U/ml heparin, similar to methods described. Prior to perfusion, microcapillary channels were blocked for one hour at 37°C in a humidified box using HEPES-buffered Tyrode's solution (137 mM NaCl, 2 mM KCl, 0.3 mM NaH<sub>2</sub>PO<sub>4</sub>, 1 mM MgCl<sub>2</sub>, 2 mM CaCl<sub>2</sub>, 5.5 mM glucose, 5 mM HEPES, 12 mM NaHCO<sub>3</sub>) containing 5% (m/v) BSA. For analyses of platelet adhesion to Horm collagen, whole blood was collected into 93  $\mu$ M (50  $\mu$ g/ml) PPACK

and 2 U/ml heparin. For analyses of platelet adhesion to rVwf, fibrinogen, fibrin, and fibronectin, whole blood was collected into 93  $\mu\text{M}$  PPACK. Platelets were labelled using 4  $\mu\text{M}$  DiOC6(3) for 10 minutes at 37°C before blood was perfused through microcapillary channels (Horm collagen: 1500  $\text{s}^{-1}$ , 3 minutes; rVwf: 1500  $\text{s}^{-1}$ , 5 minutes; mouse fibrinogen, fibrin, and fibronectin: 300  $\text{s}^{-1}$ , 3 minutes). In some experiments, platelets were pre-activated using 30  $\mu\text{M}$  murine TRAP for 5 minutes at 37°C. Channels were subsequently washed using HEPES-buffered Tyrode's solution containing 1 U/ml heparin to remove non-adherent platelets. Experiments to measure endpoint adhesion to Horm collagen or rVwf under high shear flow (1500  $\text{s}^{-1}$ ) were carried out by Dr. D'Andra Parker, as part of her doctoral thesis work under the supervision of Dr. Catherine Hayward. Additional analyses of the data were performed as part of this thesis to evaluate aggregate sizes.

For real-time adhesion experiments, whole blood was collected into 10 U/ml heparin as described<sup>3</sup> and labelled using 4  $\mu\text{M}$  DiOC6(3) for 10 minutes at 37°C. Perfusions were similarly performed using a Cellix Mirus 1.1 Nanopump controlled by VenaFlux™ software. Images were captured every 50 ms using a Zeiss Axiovert S 100 inverted epifluorescence microscope coupled to a VS4-1845 image intensifier assembly (Video Scope International Ltd., Sterling, VA, USA) and a Hamamatsu C9300 digital camera (Hamamatsu Corporation USA, Bridgewater, NJ, USA), controlled by SlideBook 6 software (Intelligent Imaging Innovations, Inc., Denver, CO, USA). Focus was set to the bottom surface of the microcapillary and capture was initiated before collagen-coated

microcapillaries were perfused for 5 minutes under high shear flow ( $1500 \text{ s}^{-1}$ ). Data were analyzed by placing a  $450 \times 450$  pixel (equivalent to  $\sim 45 \text{ mm}^2$ ) mask over the centre of the microcapillary. Background fluorescence was determined by measuring the fluorescent signal before blood was perfused, which was subtracted from each image to correct for background fluorescence intensity. Mean, sum, and maximum fluorescence intensity at each 100 ms time-point were calculated automatically using the Mask Statistics tool. Erroneous spikes in fluorescence due to platelets or small aggregates passing directly through the frame, but outside of the focal plane, were removed manually after plotting data. Data are expressed as the sum of fluorescence intensities in a single, representative experiment.

#### 2.2.7 Quantification of platelet adhesion and aggregate size

A total of 15 images were captured of endpoint platelet adhesion in microcapillaries coated with Horm collagen using a x40 objective or 10 images using a x20 objective for rVwf, fibrinogen, fibrin, fibronectin, and collagen peptides, accounting for  $\sim 10\%$  of the total surface area of microcapillary channels. Percent surface area covered by platelets was estimated in each image, similar to methods described,<sup>2,3,21</sup> using ImageJ (National Institutes of Health, Bethesda, MD, USA) to obtain a mean. Number and size of captured platelet aggregates were estimated using representative regions (Horm collagen, 40x objective:  $\sim 60 \text{ mm}^2$  square,  $1020 \times 1020$  pixels; rVwf, fibrinogen, fibrin, fibronectin, and collagen peptides, 20x objective:  $\sim 60 \text{ mm}^2$  square,  $515 \times 515$

pixels) at the center of microcapillary channels, avoiding areas out of focus. Grayscale images were converted to binary using the Threshold tool before separating features using the Watershed tool and quantification using the Analyze Particles tool. As the size of platelet aggregates on Horm collagen varied greatly (~1 to 40,000  $\mu\text{m}^2$ ), data were binned and frequency plots were used to evaluate data. As the size of platelet aggregates captured onto rVwf, fibrinogen, fibrin, fibronectin, and collagen peptides were more uniform (~1 to 5000  $\mu\text{m}^2$ ), mean feature size per image was used to evaluate data.

#### 2.2.8 Assays of collagen-induced platelet aggregation in whole blood

Collagen-induced aggregation of mouse whole blood was evaluated by impedance aggregometry using a Chrono-Log<sup>®</sup> Model 700 Whole Blood/Optical Lumi-Aggregometer and Aggro/Link<sup>®</sup>8 software (Chrono-log Corporation, Haverton, PA, USA), according to the manufacturer's recommended settings for whole blood, which was collected into 1:10 (v/v) 3.2% sodium citrate and diluted 1:1 (v/v) with 0.9% NaCl. Samples were warmed to 37°C under constant stirring (1200 rpm) and once the baseline measurement had stabilized, 5 or 10  $\mu\text{g}/\text{ml}$  Horm collagen was added. Aggregation responses were measured up to 15 minutes and reported in  $\Omega$  of electrical resistance.

### 2.2.9 Assays of shear-induced platelet aggregation

Shear-induced platelet aggregation was evaluated using a HAAKE Mars rheometer (Thermo Electron Corporation, Waltham, MA, USA) fitted with a C35/0.5° Ti (35 mm diameter) cone. Shear stress  $\tau$  and shear rate  $\dot{\gamma}$  were calculated automatically by HAAKE RheoWin 3 software. Approximately 900  $\mu$ l of whole blood was collected in 1:10 (v/v) 3.2% sodium citrate (1 ml final), and split into four autologous samples that were exposed to different shear rates: 0, 5000, 10000, or 15000  $s^{-1}$ . Samples were supplemented with 5 mM  $CaCl_2$  and 93  $\mu$ M PPACK (to promote aggregation and prevent clotting, respectively) immediately before loading 220  $\mu$ l onto the plate of the rheometer. Because pilot studies indicated that platelets in citrate-anticoagulated whole blood failed to significantly aggregate in response to shear, and PPACK-anticoagulated blood showed some degree of platelet aggregation in unsheared (resting) samples, blood was collected in citrate and then recalcified immediately prior to exposure to shear. Recalcified whole blood was sheared by the rotating cone in a 0.3 mm gap for 1 minute at room temperature before fixation using 1:4 (v/v) 0.625% paraformaldehyde (PFA; 0.5% final). Fixed platelets were labelled in the dark using either 1:8.3 (v/v) of anti-mouse GpIb $\alpha$  (CD42b, Emfret Analytics, Eibelstadt, Germany) for 15 minutes for flow cytometry or labelled with 4  $\mu$ M DiOC6(3) for fluorescence microscopy. Samples for flow cytometry were diluted 1:200 (v/v) in PBS and BD™ Liquid Counting Beads (165 beads/ $\mu$ l, Becton, Dickinson and Company, BD Biosciences, San Jose, CA, USA) were added by gentle pipetting before samples were analyzed by collecting 50,000 events with a Beckman

Coulter® Epics® XL-MCL™ flow cytometer and Expo32™ software (Beckman Coulter, Brea, CA, USA).

Collected events were sequentially gated for FITC-positive single platelets using FlowJo™ 10 (Becton, Dickinson and Company, Franklin Lakes, NJ, USA) based on forward and side scatter characteristics. PE-positive counting beads were gated separately to determine the number of collected beads/sample so that platelet concentration could be estimated as follows:

$$\text{platelets/ml} = \frac{\text{single platelet events}}{\text{bead events}} \times \frac{\text{bead events}}{\mu\text{l}} \times 1000 \times \text{dilution factor}$$

Recalcified resting samples were also analyzed to determine the baseline platelet count. Percent loss of platelets at each shear rate was determined by calculating the % reduction of platelet concentration in sheared samples relative to the untreated sample. Aggregate size of platelets in samples subjected to shear was determined by fluorescence microscopy with comparison to untreated samples. DiOC6(3)-labelled fixed platelets were deposited as a monolayer onto 75x25x1 mm VWR® VistaVision™ glass slides using the Shandon™ Cytospin® 3 Cell Preparation System according to the manufacturer's instructions (1000 rpm for 5 minutes at room temperature, Thermo Fisher Scientific, Waltham, MA, USA). Slides were allowed to dry for 30 minutes in the dark before 1-2 drops of ProLong™ Gold anti-fade reagent was added and slides were covered with a 22x22 mm glass coverslip. Images of platelet aggregates were captured using a

Zeiss Axiovert 200 inverted epifluorescent microscope coupled to an AxioCam MRc and Axiovision software (Carl Zeiss Canada Ltd., Toronto, CA).

#### 2.2.10 Protein binding assays

Solid-phase protein binding assays were used to assess rhMMRN1 binding to immobilized collagen, fibrinogen, fibrin, fibronectin, triple-helical collagen peptides, or bovine serum albumin (BSA, negative control) similar to methods described, with the following modifications: wells of Immulon<sup>®</sup> 2 HB flat-bottom plates were coated overnight at 4°C with 1 µg/well of protein or peptide. Collagen, Collagen Toolkit peptides, and triple-helical collagen peptides were coated using 0.01 M acetic acid. Fibrinogen and fibronectin were coated using carbonate buffer (14.2 mM Na<sub>2</sub>CO<sub>3</sub>, 35 mM NaHCO<sub>3</sub>, pH 9.6). In some wells, bound fibrinogen was converted to fibrin *in situ* using 200 mU/ml of human thrombin for 15 minutes as described. Wells were blocked for one hour using 2% BSA in tris- (collagen and collagen peptides) or phosphate- (other proteins) buffered saline with 0.05% Tween<sup>®</sup> 20. Bound rhMMRN1 was detected using 0.14 µg/well of JS-1 followed by 0.04 µg/well of HRP-conjugated donkey anti-mouse IgG and then 3,3',5,5'-tetramethylbenzidine (TMB). The reaction was stopped after 10 minutes using 1 M H<sub>2</sub>SO<sub>4</sub> and absorbance was measured at 450 nm using a Sunrise<sup>™</sup> microplate absorbance reader and Magellan<sup>™</sup> software (Tecan Austria GmbH, Grödig, AU). rhMMRN1 binding was tested in triplicate within each experiment to obtain a mean

and data are expressed as the mean optical density (OD) at a wavelength of 450 nm  $\pm$  standard deviation (SD).

#### 2.2.11 *In silico* analyses of collagen amino acid sequences

Amino acid sequences for collagen were obtained from the Universal Protein Knowledgebase (UniProtKB), which obtains sequence data from translated coding sequences submitted to the EMBL-Bank/GenBank/DDJ nucleotide sequences resources (International Nucleotide Sequence Database Collaboration). Alignments, sequence similarity, and sequence identity were determined using Clustal Omega software.

#### 2.2.12 Assays of static platelet adhesion using human or mouse platelets

Human and mouse blood for assays of static platelet adhesion were collected into 1:10 (v/v) acid citrate dextrose (ACD) anticoagulant. ACD-anticoagulated mouse blood was supplemented with 500  $\mu$ l of platelet wash buffer (2.35 mM citric acid, 5.5 mM D-glucose, 128 mM NaCl, 4.26 mM Na<sub>2</sub>HPO<sub>4</sub>·H<sub>2</sub>O, 7.46 mM NaH<sub>2</sub>PO<sub>4</sub>·H<sub>2</sub>O, 4.77 mM trisodium citrate dihydrate, 0.35% (m/v) BSA, 3  $\mu$ M PGE<sub>1</sub>, pH 6.5) before blood was centrifuged to obtain platelet-rich plasma (PRP) diluted in buffer (260 x g, 5 minutes, room temperature). The remaining blood was supplemented once more with 500  $\mu$ l of platelet wash buffer and centrifuged a second time to collect the remaining platelets in buffer (260 x g, 5 minutes, room temperature). Platelets were pelleted and washed twice

using platelet wash buffer before final resuspension in adhesion buffer (50 mM Tris, 140 mM NaCl, 2 mM MgCl<sub>2</sub>, 25 μM CaCl<sub>2</sub>, 0.1% BSA, pH 7.4) at a concentration of  $1.8 \times 10^8$  platelets/ml. Platelet concentration for final resuspension was estimated using a C-Chip DHC-N01 disposable hemocytometer and a Zeiss Axiovert 25 inverted light microscope fitted with a x10 objective lens (Carl Zeiss Canada Ltd., Toronto, CA). Mouse platelets in buffer were left to rest at room temperature for 20 minutes to allow the effects of inhibitors to wear off as described.<sup>423,540,545</sup> For some experiments, mouse platelets were pre-activated using either 10 μg/ml CRP or murine TRAP (AYPGKF-NH<sub>2</sub>) for 5 minutes at 37°C to induce Mmrn1 release and activate platelet integrins. In experiments using monoclonal anti-mouse β<sub>3</sub> blocking antibody 9D2, platelets were simultaneously incubated with 10 μg/ml CRP and 10 μg/ml of antibody 9D2 for 5 minutes at 37°C.

ACD-anticoagulated human blood (20 ml/donor) was collected from the antecubital vein of general population controls, after obtaining written informed consent, then centrifuged (140 x g, 15 minutes, room temperature) to obtain PRP. PRP was supplemented with platelet wash buffer before pelleting and washing the platelets twice (740 x g, 10 minutes, room temperature) using platelet wash buffer. Pelleted platelets were resuspended at  $1.6 \times 10^8$  platelets/ml in adhesion buffer and similarly left to rest for 20 minutes at room temperature. Human platelet concentration was estimated using a Coulter AcT diff Hematology Analyzer (Beckman Coulter, Inc., Brea, CA, USA) for final

resuspension. Where indicated, platelets were pre-activated using 10 µg/ml CRP (5 minutes, 37°C).

Static platelet adhesion was evaluated colourimetrically as described,<sup>423,436,540,545,565</sup> using wells pre-coated overnight at 4°C with 1 µg/well of: Horm collagen, rhMMRN1, mouse fibrinogen, mouse fibronectin, or collagen peptides. In experiments in which two or more collagen peptides were coated onto the well surface, 0.5 µg/well of each peptide was used for two peptides or 0.33 µg/well of each peptide for three peptides. In some experiments, MMRN1-binding GPAGPOGPX peptides were tested for platelet adhesion using a range of molarities (0.02 to 4 mM/well). Horm collagen and collagen peptides were coated using 0.1 M acetic acid, and rhMMRN1, mouse fibrinogen and mouse fibronectin were coated using carbonate buffer. In some wells, immobilized mouse fibrinogen was converted to fibrin *in situ* using 200 mU/ml of human thrombin, similar to methods described.<sup>174</sup> Wells were blocked for one hour using 5% BSA in TBS before 50 µl of platelet suspension was added to each well. After one hour, wells were washed to remove non-adherent platelets and the remaining adherent platelets were lysed using lysis buffer (30 mM citric acid, 70 mM trisodium citrate, 0.1% Triton™ X-100) containing 5 mM p-nitrophenyl phosphate. After one hour, the reaction was stopped by 2 M NaOH and absorbance was measured at 405 nm using a Sunrise™ microplate absorbance reader and Magellan™ software. Platelet adhesion was tested in triplicate within each experiment to obtain a mean, and data are expressed as the mean OD at a wavelength of 405 nm ± SEM.

### 2.2.13 Assays of platelet adhesion under high shear using collagen peptides

Mouse blood was collected into 1:10 (v/v) ACD and similarly supplemented with buffer and centrifuged twice (260 x g, 5 minutes, room temperature) to obtain PRP diluted in buffer before final resuspension at a concentration of  $3 \times 10^8$  platelets/ml in adhesion buffer. The remaining red blood cells (RBCs) were pelleted and washed twice (1000 x g, 4 minutes, room temperature) using RBC washing buffer (140 mM Na<sub>2</sub>CO<sub>3</sub>, 35 mM NaHCO<sub>3</sub>, 100 mu/ml apyrase).

Vena8 Fluoro+ microcapillary perfusion chambers were coated overnight at 4°C using 1 µg/channel of triple-helical collagen peptide dissolved in 0.01 M acetic acid. Chambers were coated with combinations of two triple-helical peptides, maintaining a total peptide amount of 1 µg/channel, as described previously.<sup>175</sup> In channels where only one adhesive peptide was presented, GPP (0.5 µg/channel) was added to maintain the total peptide amount at 1 µg/channel. Channels were blocked with 5% (m/v) BSA in adhesion buffer for 30 minutes prior to the experiment.

Platelets were labelled using 4 µM DiOC6(3) for 10 minutes at 37°C before pre-activation with 10 µg/ml of CRP for 5 minutes at 37°C. The platelet suspension was subsequently gently mixed with 1:1.2 (v/v) pelleted autologous washed RBCs immediately prior to perfusion. Each channel was perfused at a constant shear rate using a Cellix Mirus 1.1 Nanopump controlled by VenaFlux™ software. Channels were

subsequently washed with HEPES-buffered Tyrode's solution containing 1 U/ml heparin to remove non-adherent platelets before imaging.

### 2.3 STATISTICAL ANALYSES

Two-tailed Student's t-tests (paired or independent) were used for comparisons of two groups of data with normal distributions. Mann-Whitney U tests were used to evaluate data with non-normal distributions. Normality was determined visually by plotting data to assess spread and skewness and using the Shapiro-Wilk test. One-way or repeated measures ANOVA were used to evaluate data with more than two groups. In all single comparisons,  $\alpha < 0.05$  was considered significant. Bonferroni correction was used for *post hoc* multiple comparisons where  $k \leq 6$  or the Holm-Sidak method where  $k > 6$ , with  $\alpha < 0.05$  considered significant for each family of comparisons. Statistical tests were performed using Prism 6 (GraphPad Software, San Diego, CA, USA). Data are reported as the mean  $\pm$  standard error of the mean (SEM), unless otherwise stated.

## CHAPTER 3: RESULTS

### 3.1 MULTIMERIN 1-DEFICIENT MICE

Some aspects of the phenotype of selective *Mmrn1*-deficient (*Mmrn1*<sup>-/-</sup>) mice were characterized by Dr. D'Andra Parker as part of her doctoral thesis work at McMaster University under the supervision of Dr. Catherine Hayward and are outlined in *section 1.1.3*.

Similar to previous observations, mice homozygous for the E3-deleted *Mmrn1* allele (*Mmrn1*<sup>-/-</sup>) used in these studies were viable and fertile without overt developmental abnormalities, spontaneous bleeding, or reduced survival. Each mouse used in experiments was confirmed to possess the predicted P1-P2 fragment size based on their *Mmrn1* genotype, consistent with previous analyses of this strain (*Figure 7*).

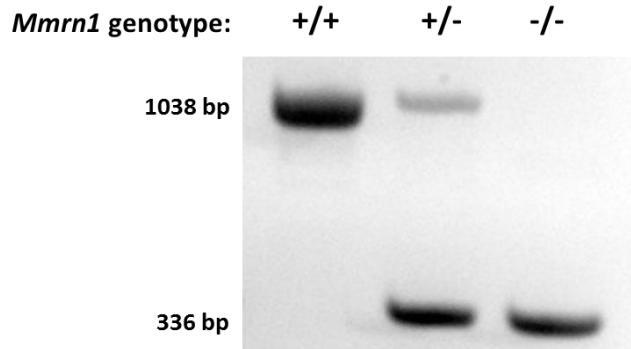


**Figure 7: Electrophoretic mobility of P1-P2 fragments from *Mmrn1*<sup>+/+</sup>, *Mmrn1*<sup>+/-</sup>, and *Mmrn1*<sup>-/-</sup> mice.** The 1038 bp *Mmrn1* P1-P2 fragment represents the intact allele, and the 336 bp P1-P2 fragment represents the E3-deleted *Mmrn1* allele. Heterozygous mice show a darker band for the 336 bp fragment because smaller sequences are favoured in PCR, which results in greater amplification of the 336 bp P1-P2 fragment relative to the wild-type allele.

### 3.2 AGGREGATE FORMATION OF WILD-TYPE AND *Mmrn1*<sup>-/-</sup> MOUSE

#### PLATELETS ON HORM COLLAGEN AND VWF UNDER HIGH SHEAR FLOW

Experiments measuring endpoint platelet adhesion to Horm collagen or recombinant (r)Vwf under high shear flow (1500 s<sup>-1</sup>) were performed by Dr. D’Andra Parker (as described in section 1.1.3). I expanded upon these analyses by developing a method to quantify the size and number of fluorescently-labelled platelet aggregates, and I performed additional experiments to clarify the mechanism of the defect in platelet adhesion to Horm collagen exhibited by *Mmrn1*<sup>-/-</sup> mice.

*Mmrn1*<sup>-/-</sup> mice formed significantly smaller aggregates onto collagen at the end of perfusions (p≤0.004, Figure 8). Because MMRN1 is a ligand for VWF<sup>21</sup> and enhances

platelet adhesion to Horm collagen under high shear flow ( $1500 \text{ s}^{-1}$ ) through a mechanism involving both VWF and GPIIb/IIIa, <sup>2</sup> platelet aggregate formation on rVwf surfaces was similarly tested. On average, *Mmrn1*<sup>-/-</sup> platelets formed significantly smaller aggregates compared to wild-type platelets ( $p < 0.0001$ , *Figure 9A*). The similar adhesion ( $p = 0.7$ ) but smaller size of platelet aggregates ( $p < 0.0001$ , *Figure 9B*) adherent to rVwf for *Mmrn1*<sup>-/-</sup> platelets was also observed in experiments using washed platelets reconstituted in washed red blood cells (RBCs) to rVwf.

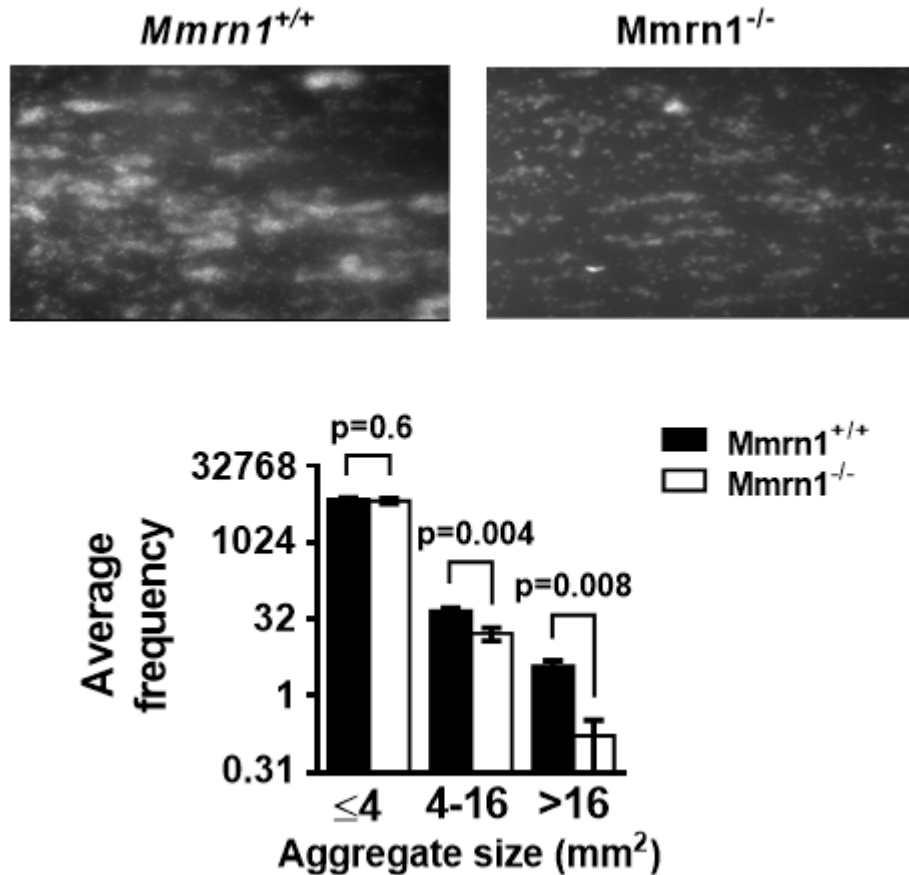


**Figure 8: Aggregate size of wild-type versus *Mmrn1*<sup>-/-</sup> mouse platelets adherent to Horm collagen under high shear flow (1500 s<sup>-1</sup>).** (A) Representative images (original magnification x40) showing adhesion of wild-type and *Mmrn1*<sup>-/-</sup> platelets tested in whole blood to assess adhesion to Horm collagen, and (B) quantitative analysis of average frequency of different-sized platelet aggregates captured ( $n = 7$  mice/group)  $\pm$  SEM.

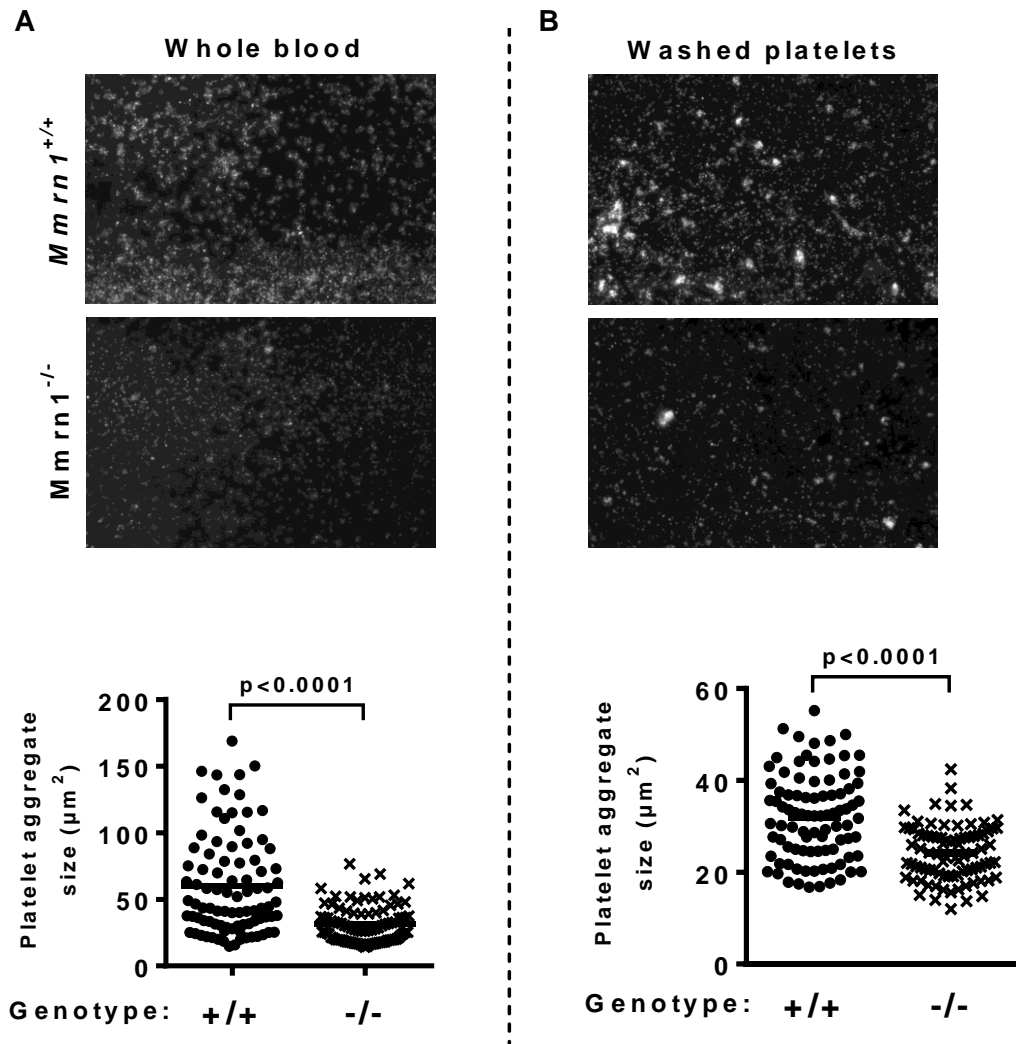


**Figure 9: Aggregate size of wild-type versus *Mmrn1*<sup>-/-</sup> mouse platelets adherent to recombinant (r)Vwf under high shear flow (1500 s<sup>-1</sup>).** Representative images (original magnification x20) showing adhesion of wild-type and *Mmrn1*<sup>-/-</sup> platelets in (A) whole blood or (B) as preparations of washed platelets reconstituted with washed RBCs. Quantitative data shown compares the average frequency of different-sized platelet aggregates captured onto rVwf (*n* = 6 mice/group) ± SEM. Symbols indicate *Mmrn1* genotype (circles: *Mmrn1*<sup>+/+</sup>; x's: *Mmrn1*<sup>-/-</sup>).

It was unclear if the defect in endpoint adhesion to Horm collagen observed for *Mmrn1*<sup>-/-</sup> platelets was due to: 1) impaired platelet tethering and/or primary adhesion, 2) slower aggregate growth mediated via platelet-platelet interactions, 3) aggregate instability or embolization during perfusions, or a combination of multiple factors. I performed assays of platelet adhesion under high shear flow in real-time to measure the rate and amount of platelet accumulation onto immobilized Horm collagen. *Mmrn1*<sup>-/-</sup> platelets showed decreased primary adhesion to Horm collagen (*Figure 10A,B*, as indicated by a lower initial spike in fluorescence), and a slower rate of accumulation of fluorescent platelets during the 5-minute perfusion (*Figure 10A,B*).

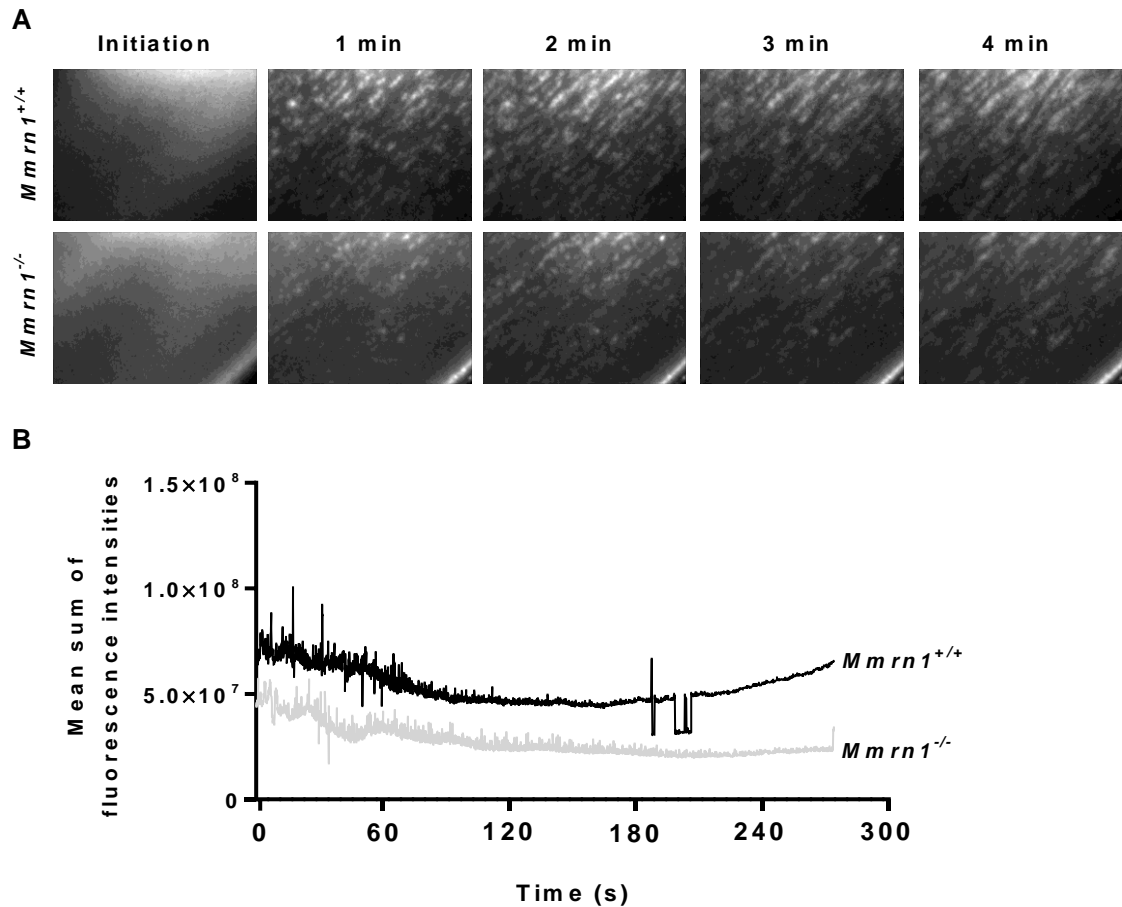


**Figure 10: Real-time adhesion of wild-type versus *Mmrn1*<sup>-/-</sup> mouse platelets to Horm collagen under high shear flow (1500 s<sup>-1</sup>).** (A) Representative time series images and (B) quantitative analyses of platelet adhesion to Horm collagen. The mean sum of fluorescence intensities, captured every 50 ms in a 450x450 pixel field at the centre of the microcapillary, was calculated for each biological replicate. The data are presented as the mean for each group ( $n = 3$  mice/group). Time zero denotes induction of DiOC6(3)-labelled platelets in whole blood into the collagen-coated microcapillary, which spikes due to initial focus blur. The time at which blood was inducted into the microcapillary during the recording time was manually aligned for each replicate.

Platelet adhesion was also tested under low shear flow ( $300 \text{ s}^{-1}$ ) to determine if the effects of *Mmrn1* loss on adhesion and aggregate formation on fibrillar collagen required high shear flow. *Mmrn1*<sup>-/-</sup> platelets formed visually smaller aggregates compared to wild-type platelets under low shear flow, although the morphology of captured aggregates (which extended through multiple planes of focus) for both wild-type and *Mmrn1* deficient platelets prevented similar quantitative analysis of captured 2D images (*Figure 11*). Interestingly, long fluorescent strings were visible following perfusion of collagen with PPACK-anticoagulated wild-type mouse blood, which appeared to extend into the lumen of the chamber. These strings were not present in chambers perfused with *Mmrn1*<sup>-/-</sup> blood, and the morphology of *Mmrn1*<sup>-/-</sup> platelet aggregates on collagen was more nodular.

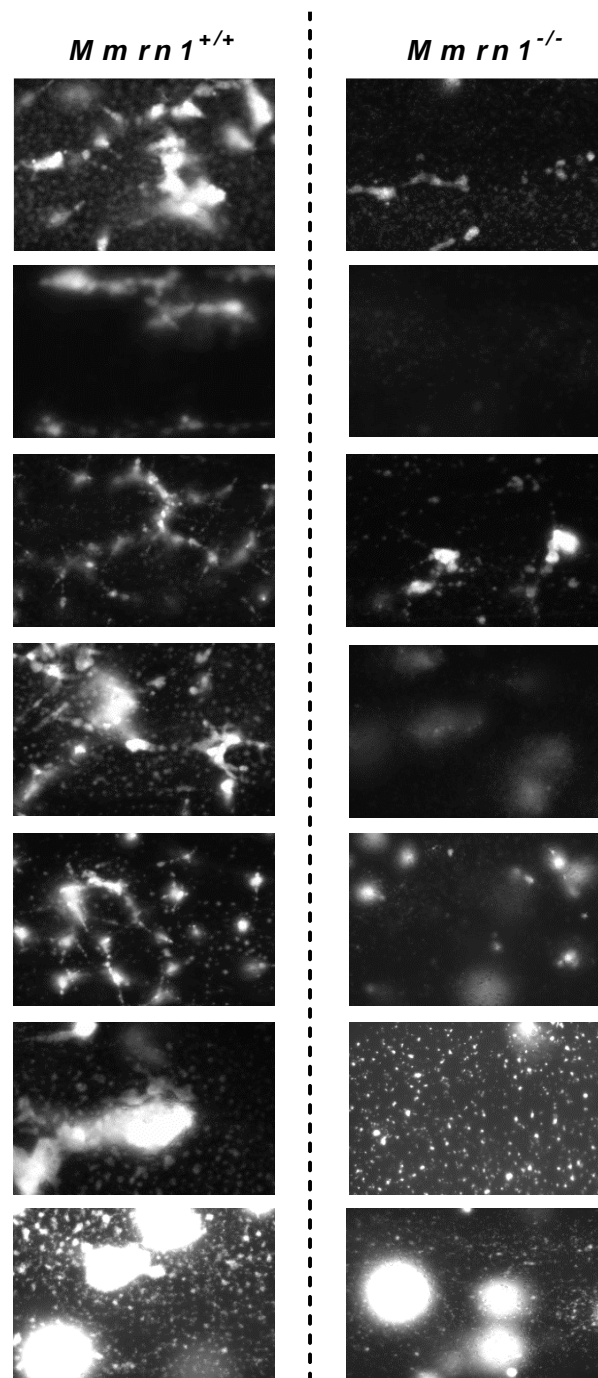


**Figure 11: Adhesion of wild-type versus *Mmrn1*<sup>-/-</sup> mouse platelets to Horm collagen under low shear flow (300 s<sup>-1</sup>).** Representative images showing adhesion of wild-type (left) and *Mmrn1*<sup>-/-</sup> (right) platelets for each biological replicate tested (*n* = 7 mice/group) after focusing the image at the chamber surface.

### 3.3 ADHESION OF WILD-TYPE AND *Mmrn1*<sup>-/-</sup> MOUSE PLATELETS TO FIBRINOGEN, FIBRIN, AND FIBRONECTIN

I investigated the possibility that *Mmrn1* affects aggregate formation on collagen and rVwf by influencing stable platelet-platelet interactions involving fibrinogen and/or fibronectin. First, I performed binding assays to determine if MMRN1 is a ligand for fibrinogen and/or fibronectin, before proceeding to whole blood perfusion assays to test the impact of *Mmrn1* loss on platelet adhesion to immobilized fibrinogen or fibronectin. Fibrin was also included in these analyses to further elucidate the mechanism of impaired thrombus formation in FeCl<sub>3</sub>-injured vessels of *Mmrn1*<sup>-/-</sup> mice.

rhMMRN1 showed dose-dependent binding to human fibrinogen, fibrin, and fibronectin FN that was significantly greater than non-specific binding to BSA ( $p < 0.05$ , *Figure 12*). Under static conditions, activated *Mmrn1*<sup>-/-</sup> and wild-type showed similar adhesion to immobilized murine fibrinogen (Fg,  $p = 0.32$ ), fibrin ( $p = 0.14$ ), and murine fibronectin (Fn,  $p = 0.32$ , *Figure 13*).

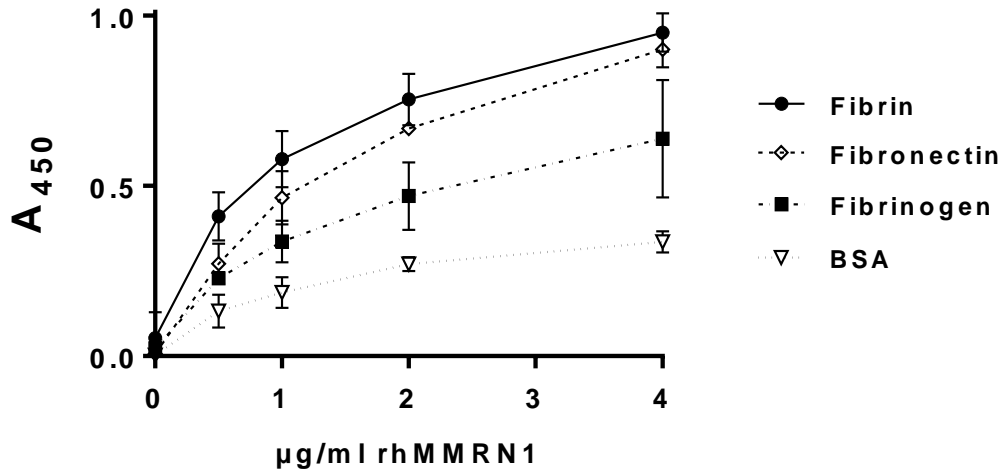


**Figure 12: rhMMRN1 binding to human FG, fibrin, or FN.** Absorbance values are reported as the mean of three independent experiments  $\pm$  SD. Within each experiment, determinations were performed in triplicate to obtain a mean.

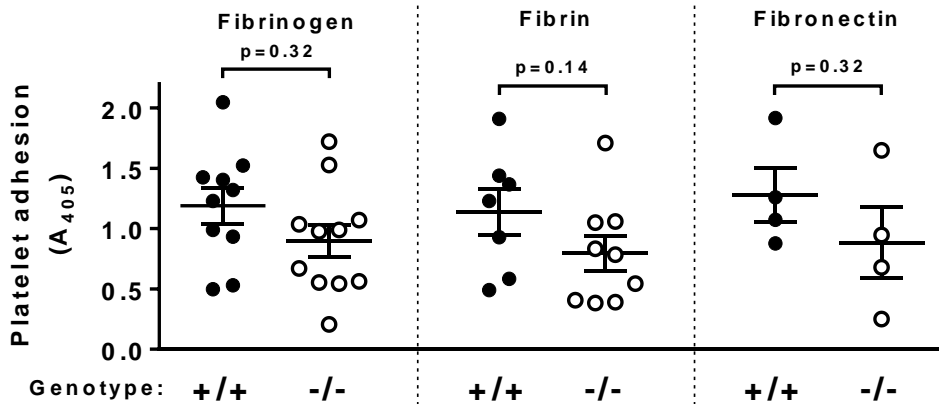


**Figure 13: Static adhesion of wild-type versus *Mmrn1*<sup>-/-</sup> CRP-activated mouse platelets to murine Fg, fibrin, and Fn.** Data are shown as mean absorbance measured in each sample, each tested in triplicate with each protein to obtain a mean. Washed wild-type and *Mmrn1*-deficient platelets were pre-activated with 10 µg/ml CRP to induce release of platelet  $\alpha$ -granule proteins, including *Mmrn1*, and to activate platelet integrins. Symbols indicate *Mmrn1* genotype (closed: *Mmrn1*<sup>+/+</sup>; open: *Mmrn1*<sup>-/-</sup>).

Under low shear flow ( $300 \text{ s}^{-1}$ ), untreated *Mmrn1*<sup>-/-</sup> and wild-type platelets in whole blood showed similar surface coverage ( $p=0.31$ , *Figure 14*) and aggregate formation ( $p=0.2$ , *Figure 15A*) onto immobilized Fg, however, significantly fewer *Mmrn1*<sup>-/-</sup> platelets than wild-type platelets adhered to Fg ( $p<0.0001$ , *Figure 15B*). When platelets were pre-activated with  $30 \mu\text{M}$  murine TRAP (AYPGKF-NH<sub>2</sub>) to induce the release of  $\alpha$ -granule contents and pre-activate platelet integrins, the surface coverage of *Mmrn1*<sup>-/-</sup> platelets was significantly reduced compared to wild-type platelets ( $p=0.03$ , *Figure 14B*). TRAP-activated *Mmrn1*<sup>-/-</sup> platelets also formed smaller aggregates on Fg compared to activated wild-type platelets ( $p=0.007$ , *Figure 15A*). Lastly, significantly fewer *Mmrn1*<sup>-/-</sup> platelet aggregates adhered to Fg compared to wild-type platelets ( $p=0.03$ , *Figure 15B*).

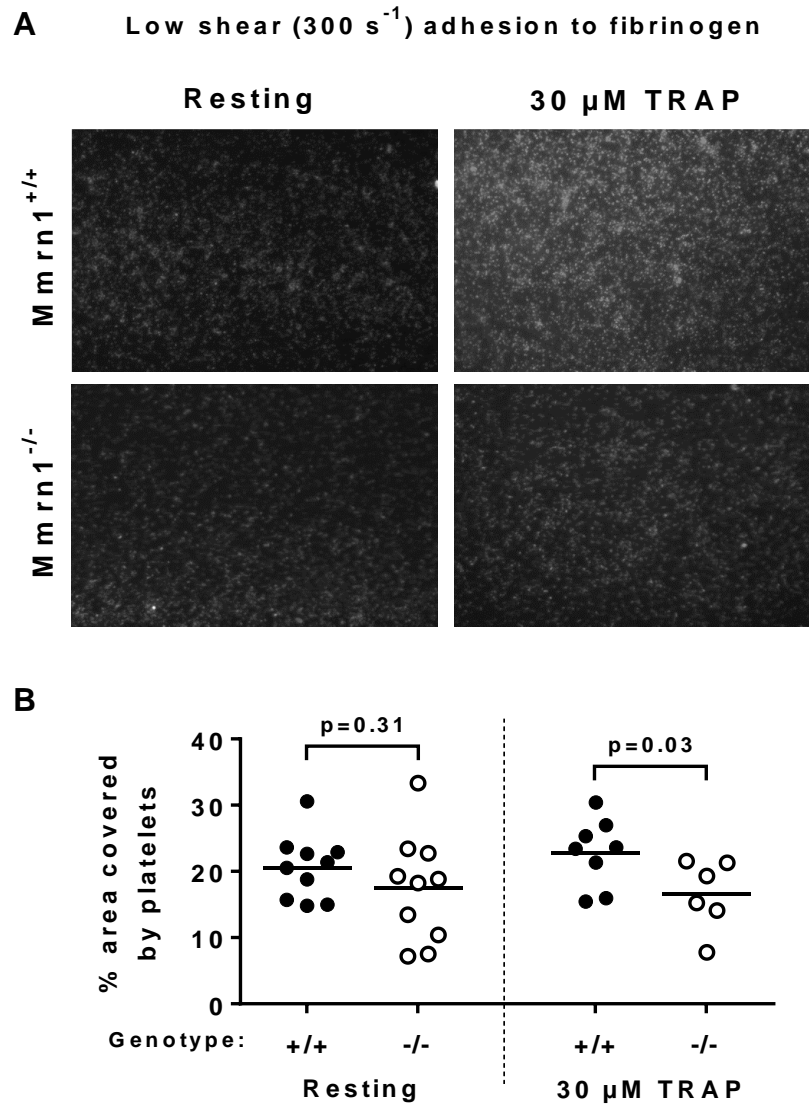


**Figure 14: Wild-type versus *Mmrn1*<sup>-/-</sup> mouse platelet adhesion to immobilized murine fibrinogen under low shear flow ( $300 \text{ s}^{-1}$ ).** (A) Representative images (original magnification x20) and (B) quantitative analyses of % surface area covered by platelets. PPACK-anticoagulated whole blood samples were perfused over fibrinogen for 3 minutes under constant shear and subsequently washed to remove non-adherent platelets. Data represent the mean % area covered ( $n=10$  images per mouse) for each biological replicate and bars indicate sample mean. Symbols in panel B indicate *Mmrn1* genotype (closed: *Mmrn1*<sup>+/+</sup>; open: *Mmrn1*<sup>-/-</sup>).

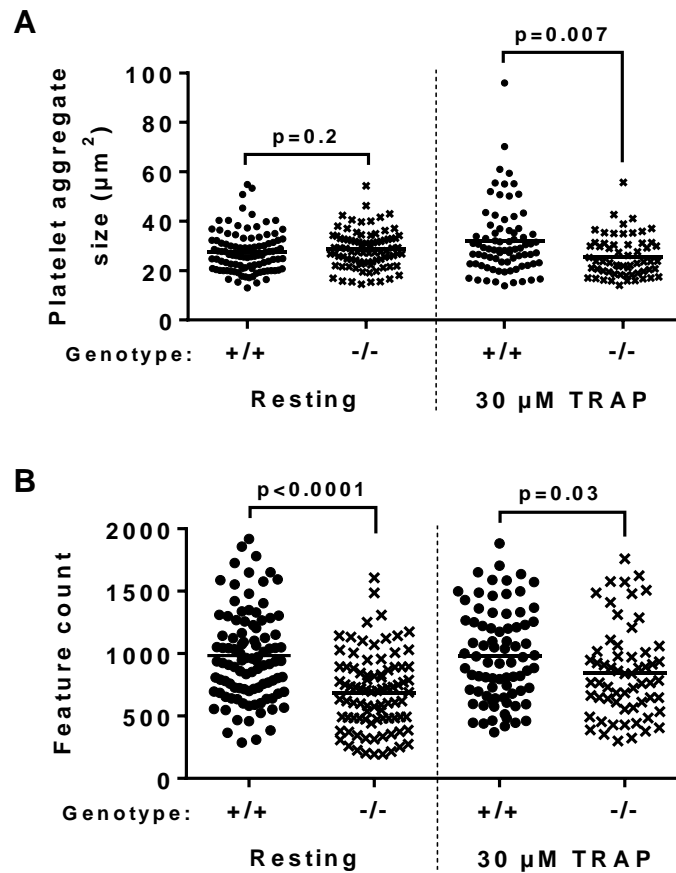


**Figure 15: Wild-type versus *Mmrn1*<sup>-/-</sup> mouse platelet aggregate size and feature count captured onto immobilized murine fibrinogen under low shear flow (300 s<sup>-1</sup>).** Data indicate (A) the mean feature size and (B) the feature count in each image captured for wild-type resting ( $n=10$  mice) and TRAP-activated ( $n=8$  mice) and for *Mmrn1*<sup>-/-</sup> resting ( $n=10$  mice) and TRAP-activated ( $n=6$  mice) samples. Symbols indicate *Mmrn1* genotype (circles: *Mmrn1*<sup>+/+</sup>; x's: *Mmrn1*<sup>-/-</sup>).

Further experiments indicated that *Mmrn1*<sup>-/-</sup> and wild-type platelets in whole blood showed similar adhesion (p=0.84, *Figure 16*), aggregate formation (p=0.16, *Figure 17A*), and numbers of platelet features (p=0.73, *Figure 17B*) when perfused over immobilized murine fibrin. The pre-activation of platelets with 30  $\mu$ M TRAP did not significantly alter these parameters (respective p values: adhesion: 0.41, *Figure 16B*; aggregate 0.18, *Figure 17A*; platelet features 0.72, *Figure 17B*).

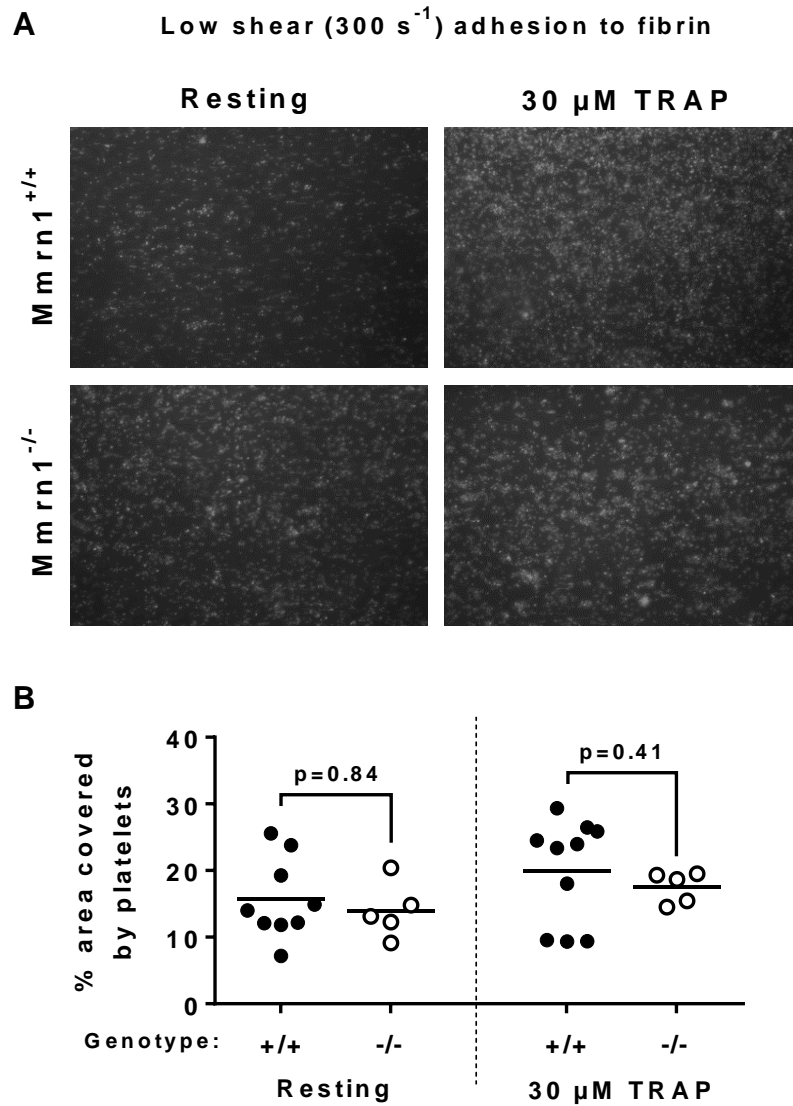


**Figure 16: Wild-type versus *Mmrn1*<sup>-/-</sup> mouse platelet adhesion to immobilized murine fibrin under low shear flow ( $300 \text{ s}^{-1}$ ).** (A) Representative images (original magnification x20) and (B) quantitative analyses of % surface area covered by platelets. PPACK-anticoagulated whole blood samples were perfused over fibrin for 3 minutes under constant shear and subsequently washed to remove non-adherent platelets. Data represent the mean % area covered by platelets ( $n=10$  images per mouse) for each biological replicate and bars indicate sample mean. Symbols in panel B indicate *Mmrn1* genotype (closed: *Mmrn1*<sup>+/+</sup>; open: *Mmrn1*<sup>-/-</sup>).

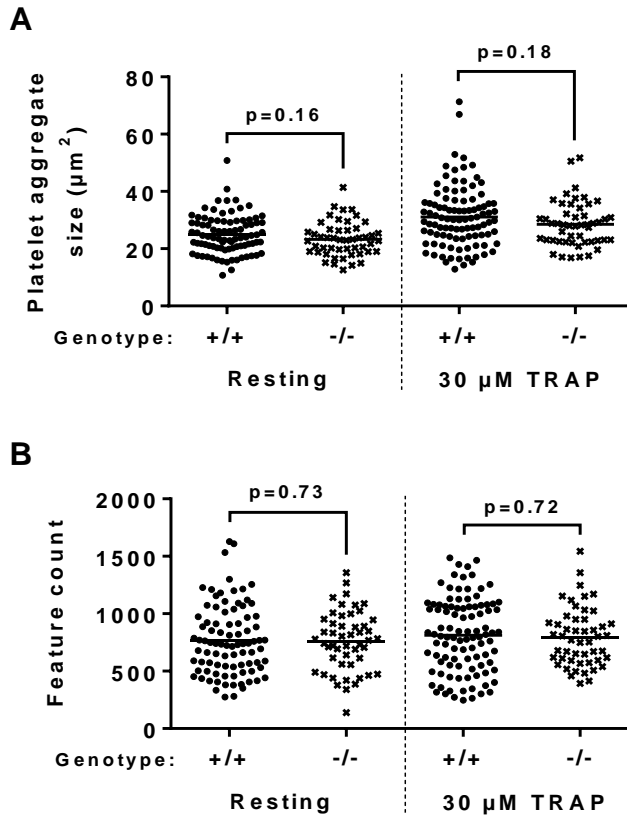


**Figure 17: Wild-type versus *Mmrn1*<sup>-/-</sup> mouse platelet aggregate size and feature count captured onto immobilized murine fibrin under low shear flow (300 s<sup>-1</sup>).** Data indicate (A) the mean feature size and (B) the feature count in each image captured for wild-type resting (*n*=9 mice) and TRAP-activated (*n*=10 mice) and for *Mmrn1*<sup>-/-</sup> resting (*n*=5 mice) and TRAP-activated (*n*=5 mice) samples. Symbols indicate *Mmrn1* genotype (circles: *Mmrn1*<sup>+/+</sup>; x's: *Mmrn1*<sup>-/-</sup>).

Labelled mouse platelets in whole blood showed less adhesion to immobilized murine fibronectin under low shear flow (300 s<sup>-1</sup>) compared to fibrinogen- or fibrin-coated surfaces, and adhesion of resting or TRAP-activated platelets to fibronectin was similar between *Mmrn1*<sup>-/-</sup> and wild-type samples (*p*=0.69 and *p*=0.62, respectively, *Figure 18*). Platelets tended to adhere individually, and did not form larger aggregates on

fibronectin surfaces following TRAP activation. Resting *Mmrn1*<sup>-/-</sup> platelets formed significantly larger aggregates on fibronectin compared to wild-type platelets (p=0.03), and TRAP-activated *Mmrn1*<sup>-/-</sup> platelets formed significantly smaller aggregates on fibronectin compared to wild-type platelets (p=0.03, *Figure 19A*). However, the mean differences in aggregate size were negligible: 4.5  $\mu\text{m}^2$  for resting platelets and 0.78  $\mu\text{m}^2$  for TRAP-activated platelets. Feature counts were similar between *Mmrn1*<sup>-/-</sup> and wild-type samples for resting (p=0.64) and TRAP-activated (p=0.92) platelets (*Figure 19B*). Pre-activation with TRAP did not significantly increase the number of adherent *Mmrn1*<sup>-/-</sup> (p=0.48) or wild-type (p=0.23) platelets.

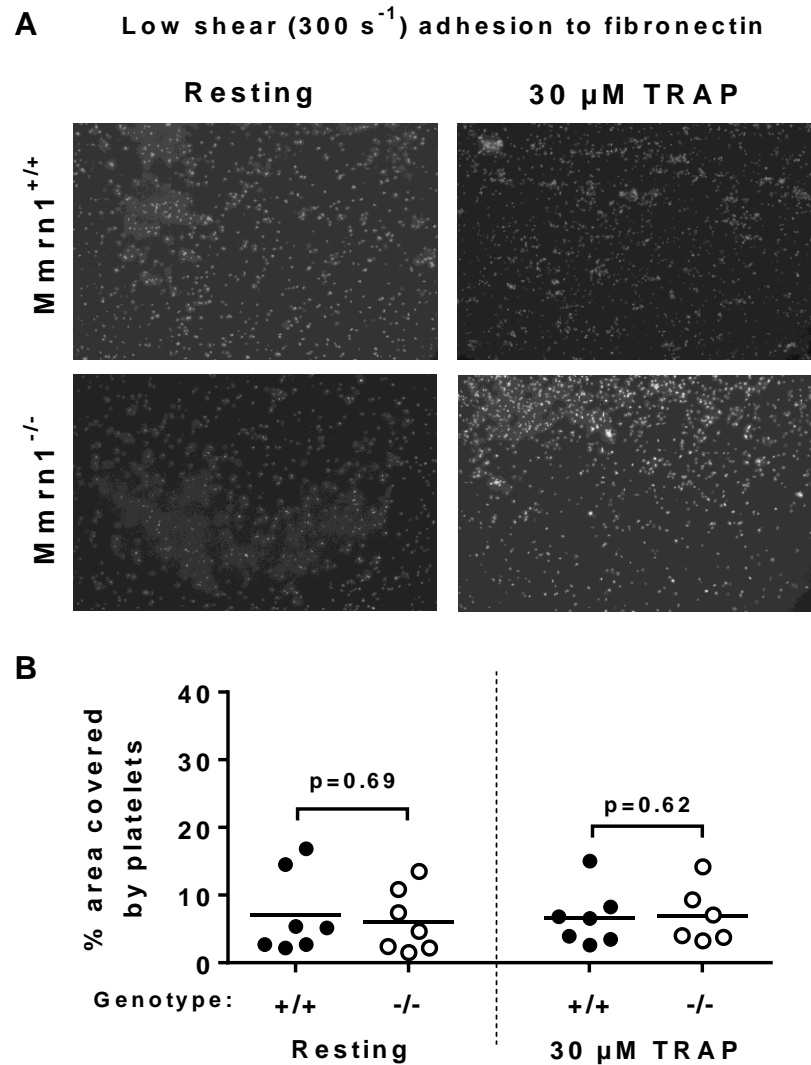


**Figure 18: Wild-type versus *Mmrn1*<sup>-/-</sup> mouse platelet adhesion to immobilized murine fibronectin under low shear flow ( $300 \text{ s}^{-1}$ ).** (A) Representative images (original magnification x20) and (B) quantitative analyses of % surface area covered by platelets. PPACK-anticoagulated whole blood samples were perfused over fibronectin for 3 minutes under constant shear and subsequently washed to remove non-adherent platelets. Data represent the mean % area covered by platelets ( $n=10$  images per mouse) for each biological replicate and bars indicate sample mean. Symbols in panel B indicate *Mmrn1* genotype (closed: *Mmrn1*<sup>+/+</sup>; open: *Mmrn1*<sup>-/-</sup>).

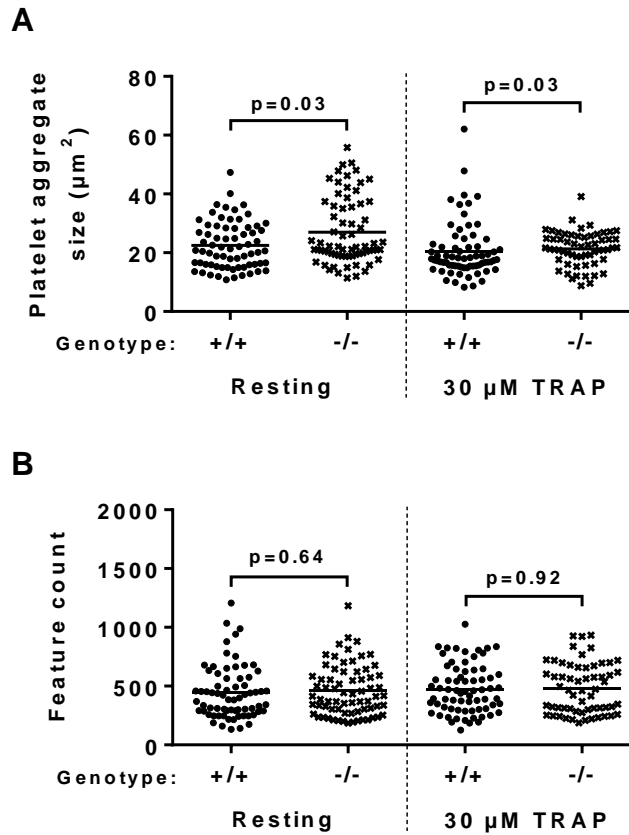


**Figure 19: Wild-type versus *Mmrn1*<sup>-/-</sup> mouse platelet aggregate size and feature count captured onto immobilized murine fibronectin under low shear flow (300 s<sup>-1</sup>).** Data indicate (A) the mean feature size and (B) the feature count in each image captured for wild-type resting and TRAP-activated ( $n=7$  mice) and for *Mmrn1*<sup>-/-</sup> resting ( $n=7$  mice) and TRAP-activated ( $n=6$  mice) samples. Symbols indicate *Mmrn1* genotype (circles: *Mmrn1*<sup>+/+</sup>; x's: *Mmrn1*<sup>-/-</sup>).

### 3.4 EFFECT OF INTEGRIN ALPHA-IIIB BETA-3 ON STATIC ADHESION OF ACTIVATED WILD-TYPE AND *Mmrn1*<sup>-/-</sup> MOUSE PLATELETS

I performed assays of static platelet adhesion with and without anti-mouse  $\beta_3$  blocking antibody 9D2 to determine if mouse platelet adhesion to Mmrn1 is mediated by  $\beta_3$  integrins. In the absence of platelet Mmrn1, activated *Mmrn1*<sup>-/-</sup> and wild-type platelets showed similar adhesion to immobilized rhMMRN1 (p=0.49), indicating that platelet Mmrn1 is not essential for this adhesion. Antibody 9D2 inhibited adhesion of both *Mmrn1*<sup>-/-</sup> and wild-type platelets to rhMMRN1, by 35.7±5.3% and 45.1±3.5%, respectively (p=0.15, *Figure 20*). 9D2 similarly inhibited the static adhesion of *Mmrn1*<sup>-/-</sup> versus wild-type mice to Fg (% inhibition for *Mmrn1*<sup>-/-</sup> vs. *Mmrn1*<sup>+/+</sup>: 77±7.5 vs. 67.4±3.7, p=0.3), fibrin (% inhibition for *Mmrn1*<sup>-/-</sup> vs. *Mmrn1*<sup>+/+</sup>: 75.7±7.6 vs. 63.7±2.0, p=0.17), and Fn (% inhibition for *Mmrn1*<sup>-/-</sup> vs. *Mmrn1*<sup>+/+</sup>: 68.6±5.0 vs. 63±3.3, p=0.39), which were tested as positive controls for  $\beta_3$ -dependent adhesion. These data suggest that under these conditions, Mmrn1-mediated adhesion involves other, unidentified ligands. Additionally, inhibition of static platelet adhesion to rhMMRN1 did not increase with increasing amount of blocking antibody (*Figure 21*), indicating that 9D2 binding to platelets was saturable at the concentration tested to induce  $\beta_3$  inhibition.

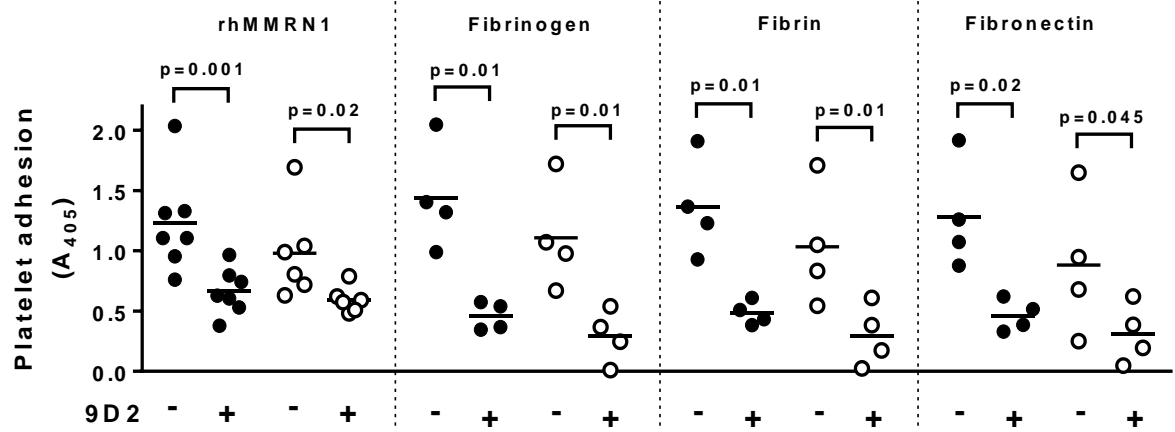


**Figure 20: Effect of anti-mouse  $\beta_3$  blocking antibody 9D2 on static adhesion of wild-type versus *Mmrn1*<sup>-/-</sup> CRP-activated mouse platelets.** Data are shown as mean absorbance of each biological replicate, each tested in triplicate for each protein to obtain a mean. Platelets were pre-activated with CRP, in order to induce *Mmrn1* release, and incubated with antibody 9D2 (5 minutes, 37°C) to block  $\beta_3$ -mediated adhesion. Symbols indicate the *Mmrn1* genotype (solid: +/+; open: -/-).

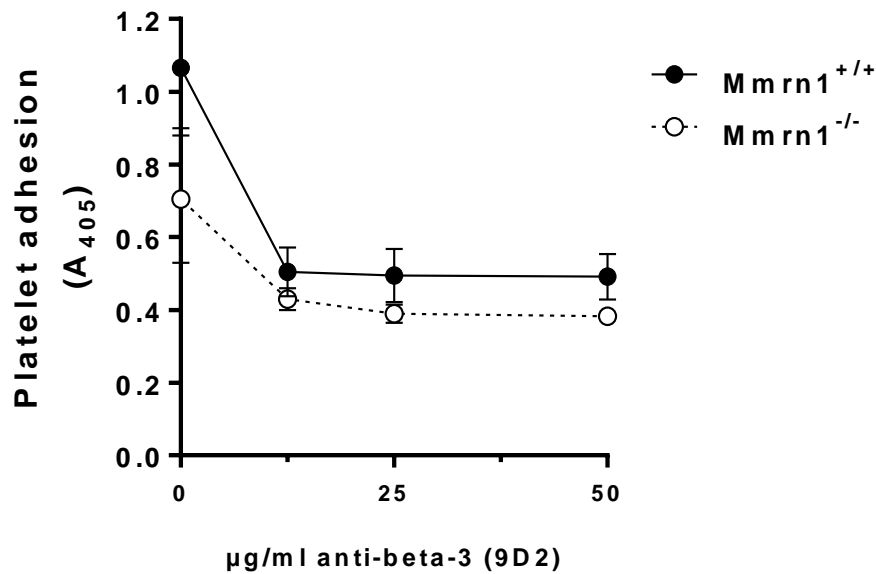


**Figure 21: Effect of 9D2 concentration on static adhesion of wild-type versus *Mmrn1*<sup>-/-</sup> CRP-activated mouse platelets to immobilized rhMMRN1.** Data are shown as mean absorbance of  $n=3$  mice/genotype  $\pm$  SEM. Within each experiment, determinations were performed in triplicate to obtain a mean. Symbols indicate the *Mmrn1* genotype (solid: +/+; open: -/-).

### 3.5 COLLAGEN-INDUCED AGGREGATION OF WILD-TYPE AND *Mmrn1*<sup>-/-</sup> PLATELETS IN WHOLE BLOOD

I performed assays of collagen-induced platelet aggregation to determine if *Mmrn1* contributes to collagen-induced platelet aggregation in whole blood samples. *Mmrn1*<sup>-/-</sup> and wild-type mice showed similar aggregation profiles and similar maximal aggregation responses to 5  $\mu\text{g/ml}$  ( $p=0.48$ ) or 10  $\mu\text{g/ml}$  ( $p=0.36$ ) Horm collagen (*Figure 22*).

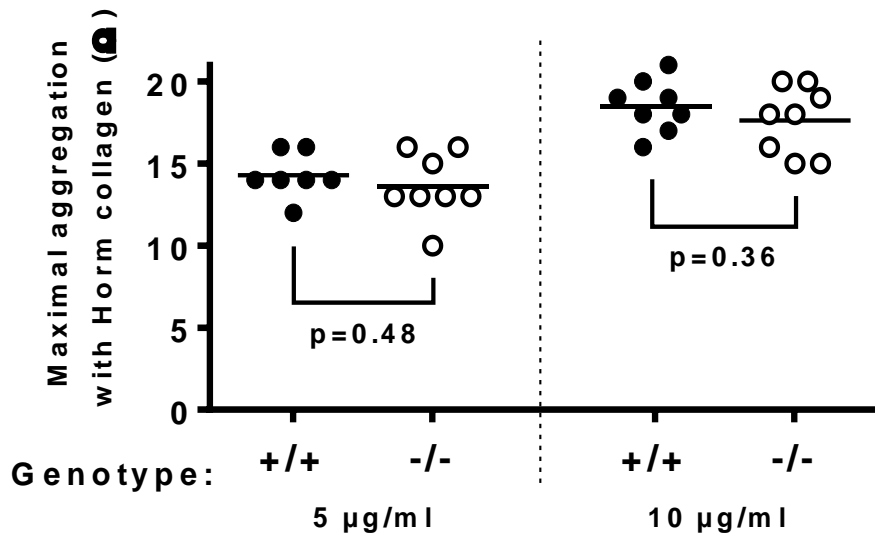


**Figure 22: Aggregation responses of wild-type versus *Mmrn1*<sup>-/-</sup> mouse platelets tested in whole blood to Horm collagen.** Maximal aggregation responses of mouse platelets to Horm collagen measured by electrical impedance ( $\Omega$ ) ( $n=7-8$  mice/genotype). Symbols indicate *Mmrn1* genotype (closed: *Mmrn1*<sup>+/+</sup>; open: *Mmrn1*<sup>-/-</sup>).

### 3.6 SHEAR-INDUCED AGGREGATION OF WILD-TYPE AND *Mmrn1*<sup>-/-</sup> MOUSE PLATELETS

I tested whether *Mmrn1* loss influences platelet aggregate formation under high and pathological levels of mechanical shear stress using assays of shear-induced platelet aggregation in whole blood. Samples from wild-type and *Mmrn1*<sup>-/-</sup> mice showed similar platelet counts in resting whole blood samples (*Mmrn1*<sup>+/+</sup> vs. *Mmrn1*<sup>-/-</sup>  $\pm$  SEM:  $638 \pm 119$  vs.  $652 \pm 115$ ,  $p=0.94$ ). With both types of platelets, the detection of CD42b<sup>+</sup> single platelets decreased incrementally with exposure to increasing shear rate (Figure 23). The % loss of single platelets, relative to the resting samples, was not significantly different

between *Mmrn1*<sup>-/-</sup> and wild-type platelets at 5000 s<sup>-1</sup> (p=0.81), 10000 s<sup>-1</sup> (p=0.6), or 15000 s<sup>-1</sup> (p=0.94, *Figure 24B*). Fluorescent microscopic analyses of SIPA similarly showed that *Mmrn1*<sup>-/-</sup> or wild-type platelets in whole blood formed aggregates with similar morphology, which, on average, increased in size with increasing shear rate (*Figure 24C*). To test SIPA in combination with collagen-induced platelet aggregation, samples in some experiments were sheared immediately after pre-treatment with varying concentrations of Horm collagen or CRP, but pre-activation coupled with shear stress caused samples to clot, which made retrieval for analysis unfeasible.

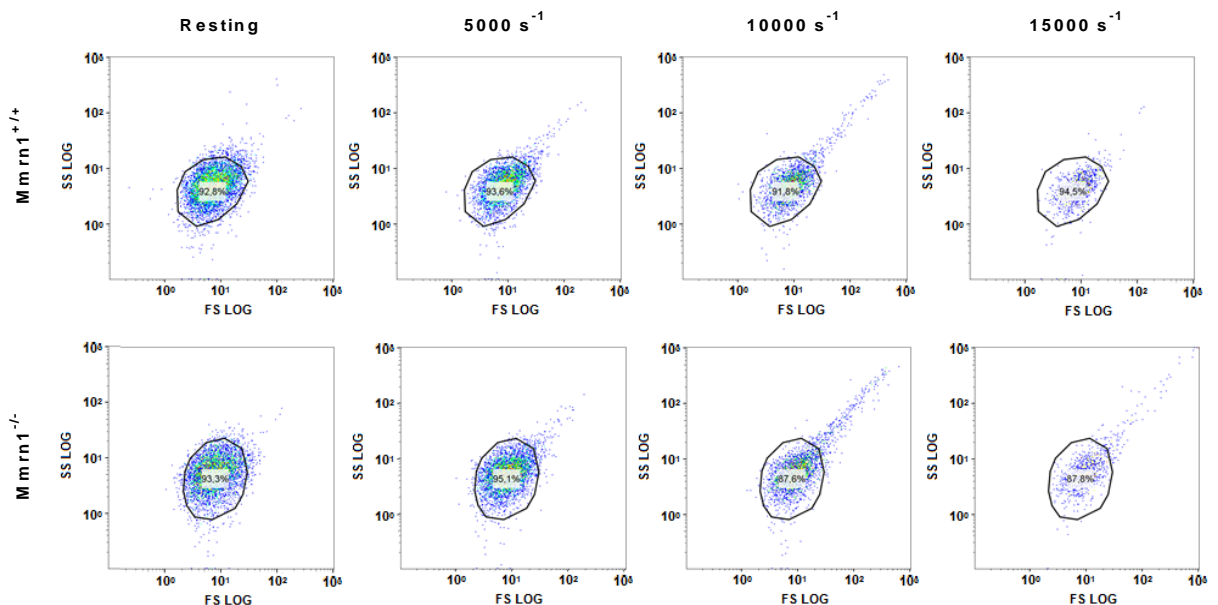


**Figure 23: Representative scatterplots showing the effects of shear on wild-type versus *Mmrn1*<sup>-/-</sup> mouse platelets detected by flow cytometry.** A total of 50,000 events were collected and gated for FITC-positive events using autologous unlabelled samples.

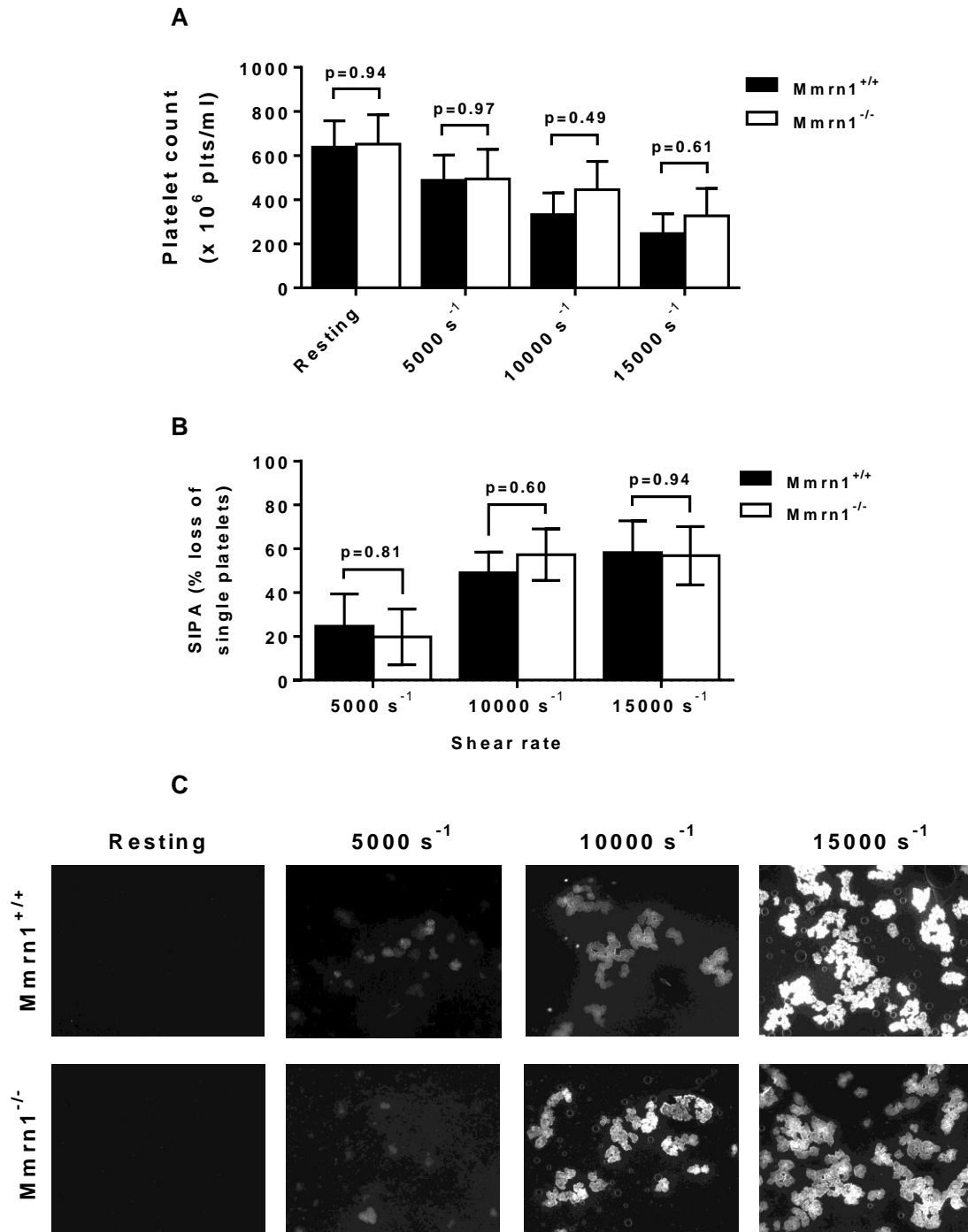


**Figure 24: Aggregation of wild-type versus *Mm rn1*<sup>-/-</sup> mouse platelets in whole blood in response to variable shear rates.** Shear-induced aggregation of mouse platelets shown by (A) platelet counts and (B) % loss of single platelets in whole blood samples.

Bars and whiskers represent the mean and SEM, respectively. (C) Representative images showing aggregate size of fixed, DiOC6(3)-labelled platelets following exposure to variable shear rates. In panels A,B, bars and whiskers represent the mean and SEM, respectively ( $n=8$  mice/group).

### 3.7 *IN SILICO* ANALYSIS OF COLLAGEN AMINO ACID SEQUENCES AND MMRN1 BINDING TO VARIANT SEQUENCES OF GPAGPOGPX

I performed *in silico* searches for candidate sequences type I collagen to test for MMRN1 binding. Searches indicated that the GPAGPOGPX sequence is unique to fibrillar collagens: it is not present in any other human or mouse proteins, and both GPAGPOGPV in type II collagen and GPAGPOGPQ in type III collagen are highly conserved (*Table 4*). Many GPAGPOGPX-like sequences were present in peptides from Toolkits II and III, which narrowed the search for potential recognition motifs in the  $\alpha$ -chains of type I collagen. Although there is high homology between the COL domains of fibrillar collagens I, II, and III, alignments indicated that the GPAGPOGPV locus (helix residues 151 to 159) from type II collagen is poorly conserved in collagens I and III. In total, three highly conserved GPAGPOGPX-like sequences were identified in type I collagen: GPAGPOGPI at helix residues 667 to 675 in D-period 3 of the  $\alpha_1(I)$  triple helix, and GPAGSOGFQ in D-period 2 at residues 457 to 465 that aligns with a conserved GPAGPOGFQ sequence in  $\alpha_2(I)$  (*Table 4*). In particular, GPAGPOGPI in collagen I overlaps in sequence alignments with GPAGPOGPQ (helix residues 682 to 690) in collagen III, which has a 9-residue extension at its N-terminus, offsetting helix numbering. Additionally, substitution of the hydrophobic residue valine for isoleucine is a conservative mutation,<sup>566</sup> further suggesting that GPAGPOGPI could support MMRN1 binding.

**Collagen alpha-1(I) chain: GPAGPOGPI**

UniProtKB ID:		
P02452	Human ( <i>H. sapiens</i> )	842 GPAGPAGPPGPIGNV
P11087	Mouse ( <i>M. musculus</i> )	831 GPAGPAGPPGPIGNV
P02454	Rat ( <i>R. norvegicus</i> )	831 GPAGPAGPPGPIGNV
P02453	Cow ( <i>B. taurus</i> )	841 GPAGPAGPPGPIGNV
Q9XSJ7	Dog ( <i>C. lupus familiaris</i> )	838 GPAGPTGPPGPIGNV
		*****

**Collagen alpha-1(I) chain: GPAGSOGFQ**

UniProtKB ID:		
P02452	Human ( <i>H. sapiens</i> )	631 GEQGPAGSPGFQGLP
P11087	Mouse ( <i>M. musculus</i> )	631 GEQGPAGSPGFQGLP
P02454	Rat ( <i>R. norvegicus</i> )	631 GEQGPAGSPGFQGLP
P02453	Cow ( <i>B. taurus</i> )	630 GEQGPAGSPGFQGLP
Q9XSJ7	Dog ( <i>C. lupus familiaris</i> )	628 GEQGPAGSPGFQGLP
		*****

**Collagen alpha-2(I) chain: GP(A/P)GPOGFQ**

UniProtKB ID:		
P08123	Human ( <i>H. sapiens</i> )	543 GEQGPAGPPGFQGLP
Q01149	Mouse ( <i>M. musculus</i> )	549 GEQGPAGPPGFQGLP
P02466	Rat ( <i>R. norvegicus</i> )	549 GEQGPAGPPGFQGLP
P02465	Cow ( <i>B. taurus</i> )	541 GEQGPAGPPGFQGLP
O46392	Dog ( <i>C. lupus familiaris</i> )	543 GEQGPAGPPGFQGLP
		*****

**Collagen alpha-1(II) chain: GPAGPOGPIV**

UniProtKB ID:		
P02458	Human ( <i>H. sapiens</i> )	348 GQPGPAGPPGPIVGA
P28481	Mouse ( <i>M. musculus</i> )	348 GQPGPAGPPGPIVGA
P05539	Rat ( <i>R. norvegicus</i> )	280 GQPGPAGPPGPIVGA
P02459	Cow ( <i>B. taurus</i> )	348 GQPGPAGPPGPIVGA
		*****

**Collagen alpha-1(III) chain: GPAGPOGPQ**

UniProtKB ID:		
P02461	Human ( <i>H. sapiens</i> )	845 GSGPAGPPGPGVVK
P08121	Mouse ( <i>M. musculus</i> )	844 GSGPAGPPGPGVVK
P13941	Rat ( <i>R. norvegicus</i> )	844 GSGPAGPPGPGVVK
P04258	Cow ( <i>B. taurus</i> )	689 GSGPAGPPGPGVVK
		* *****

**Table 4: Conservation of GPAGPOGPX sequences in types I, II, and III fibrillar collagens.** Sequences were retrieved from UniProtKB. Sequence alignment was performed using the Align tool and sequence similarity was calculated automatically by UniProtKB.

These three variant sequences were synthesized as homotrimeric triple-helical peptides and tested for rhMMRN1 binding. GPAGPOGPI supported rhMMRN1 binding significantly more than inert control peptide GPP ( $p=0.0002$ ), whereas GPAGPOGFQ and GPAGSOGFQ did not ( $p=0.12$  and  $p=0.52$ , respectively, *Figure 25*).

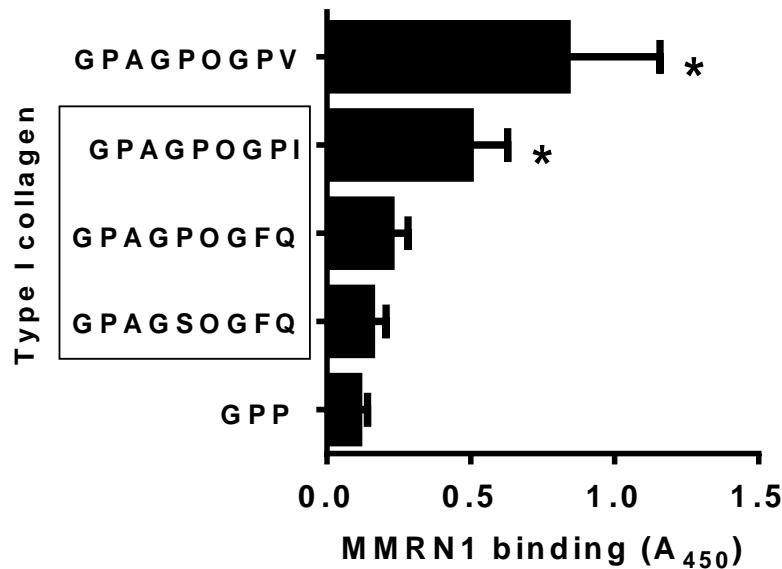


**Figure 25: rhMMRN1 binding to homotrimeric triple-helical peptides derived from GPAGPOGPX-like motifs in the alpha-chains of type I collagen.** Bars and whiskers represent the mean and SD of three independent experiments, respectively, performed with a single preparation of rhMMRN1. Within each experiment, determinations were performed in triplicate to obtain a mean. Asterisks (\*) indicate statistical significance compared to GPP, using multiple paired  $t$ -tests and the Bonferroni correction, where number of comparisons  $k = 4$  and  $\alpha = 0.0125$  in each comparison. A total of 4 preparations of rhMMRN1 were tested, each yielding equivalent results (data not shown).

### 3.8 STATIC ADHESION OF ACTIVATED WILD-TYPE AND *Mmrn1*<sup>-/-</sup> PLATELETS TO GPAGPOGPX, GFOGER, AND FULL-LENGTH FIBRILLAR COLLAGEN

The GPAGPOGPX motifs that bound rhMMRN1 are fully conserved in murine collagens, and mouse *Mmrn1* shares 67% sequence similarity with human MMRN1. I tested the specificity of these peptides for *Mmrn1* using assays of static adhesion of wild-type and *Mmrn1*<sup>-/-</sup> platelets, pre-activated with CRP to induce *Mmrn1* release and activation of platelet integrins. Wild-type platelets showed dose-dependent adhesion to GPAGPOGPQ or GPAGPOGPI, unlike *Mmrn1*<sup>-/-</sup> platelets, which showed minimal adhesion to GPAGPOGPX peptides ( $p < 0.05$ , *Figure 26A,B*). Additionally, CRP-activated *Mmrn1*<sup>-/-</sup> platelets also showed impaired platelet adhesion to collagen (tested as a positive control for maximal adhesion) under stasis compared to wild-type platelets ( $p = 0.03$ , *Figure 26C*). Despite this, additional testing showed that the ability of *Mmrn1*<sup>-/-</sup> platelets to adhere to GFOGER was not impaired ( $p = 0.49$ , *Figure 27*).

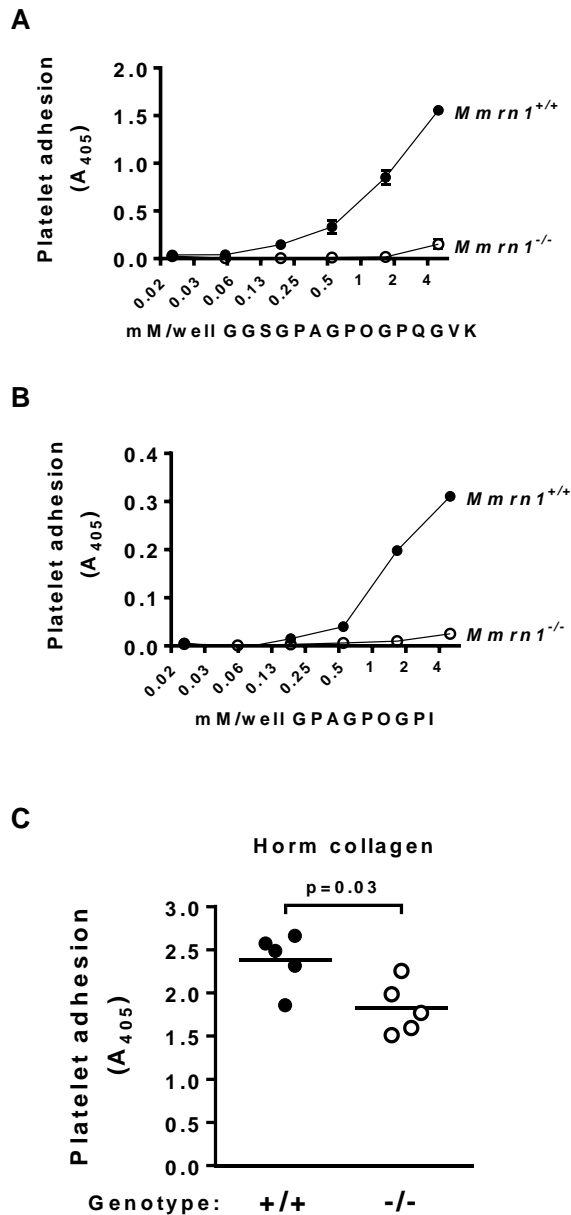


**Figure 26: Static adhesion of wild-type versus *Mmrn1*<sup>-/-</sup> CRP-activated mouse platelets to triple-helical collagen mimetic peptides or Horm collagen.** (A) Specificity of MMRN1-binding peptide GGSGPAGPOGPQGVK for wild-type (n = 4 mice) or *Mmrn1*<sup>-/-</sup> (n = 3 mice) platelets. (B) Specificity of MMRN1-binding peptide GPAGPOGPI for wild-type or *Mmrn1*<sup>-/-</sup> (n = 3 mice/genotype) platelets. (C) Adhesion of CRP-activated wild-type (n = 5) and *Mmrn1*<sup>-/-</sup> (n = 5) to Horm collagen. In panels A,B absorbance values are corrected for non-specific adhesion by subtracting adhesion to GPP

at each concentration tested. In panels A-C, symbols indicate *Mmrn1* genotype (closed: *Mmrn1*<sup>+/+</sup>; open: *Mmrn1*<sup>-/-</sup>).

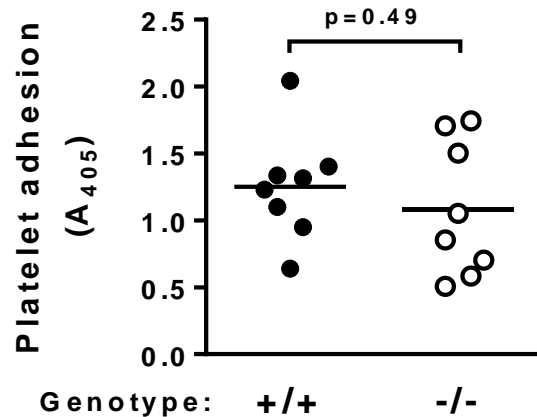


**Figure 27: Static adhesion of CRP-activated mouse platelets to  $\alpha_2\beta_1$ -binding peptide GFOGER.** Data show the mean absorbance value of each biological replicate (n = 8 mice/group). Within each experiment, determinations were performed in triplicate to obtain a mean. Symbols indicate *Mmrn1* genotype (closed: *Mmrn1*<sup>+/+</sup>; open: *Mmrn1*<sup>-/-</sup>).

### 3.9 ADHESION OF WILD-TYPE AND *Mmrn1*<sup>-/-</sup> MOUSE PLATELETS TO TRIPLE-HELICAL COLLAGEN PEPTIDES UNDER HIGH SHEAR FLOW (1500 s<sup>-1</sup>)

I performed assays of platelet adhesion with washed, CRP-activated mouse platelets to test the effects of GPAGPOGPX on adhesion of wild-type platelets under high shear flow (1500 s<sup>-1</sup>). Presented on its own, GPAGPOGPQ was insufficient to support platelet adhesion (*Figure 28A*). On surfaces co-coated with GFOGER and GPAGPOGPQ, the presence of GPAGPOGPQ increased size of captured wild-type (p<0.0001), but not *Mmrn1*<sup>-/-</sup> (p=0.06), platelet aggregates compared to surfaces co-coated with GFOGER and GPP (*Figure 28B*), providing further evidence that adhesion to GPAGPOGPQ

requires Mmrn1. On surfaces coated with GFOGER and GPP, *Mmrn1*<sup>-/-</sup> platelets formed smaller aggregates than wild-type platelets (p <0.001), suggesting that Mmrn1 also supports GPAGPOGPX-independent platelet-platelet interactions. In order to recapitulate the conditions of platelet adhesion to fibrillar collagen *in vivo*, experiments were performed in which wild-type or *Mmrn1*<sup>-/-</sup> anticoagulated whole blood was perfused over surfaces coated with combinations of collagen peptides, including CRP to activate platelets (data not shown). Under these conditions, mouse platelets failed to adhere to peptide-coated surfaces, even when peptide coating concentration was increased or if blood was collected into PPACK or citrate. This may reflect the presence of molecules and pathways in murine whole blood that normally inhibit platelet adhesion to collagen, or that fibrillar ultrastructure could be required for resting mouse platelets in whole blood to adhere to collagen.

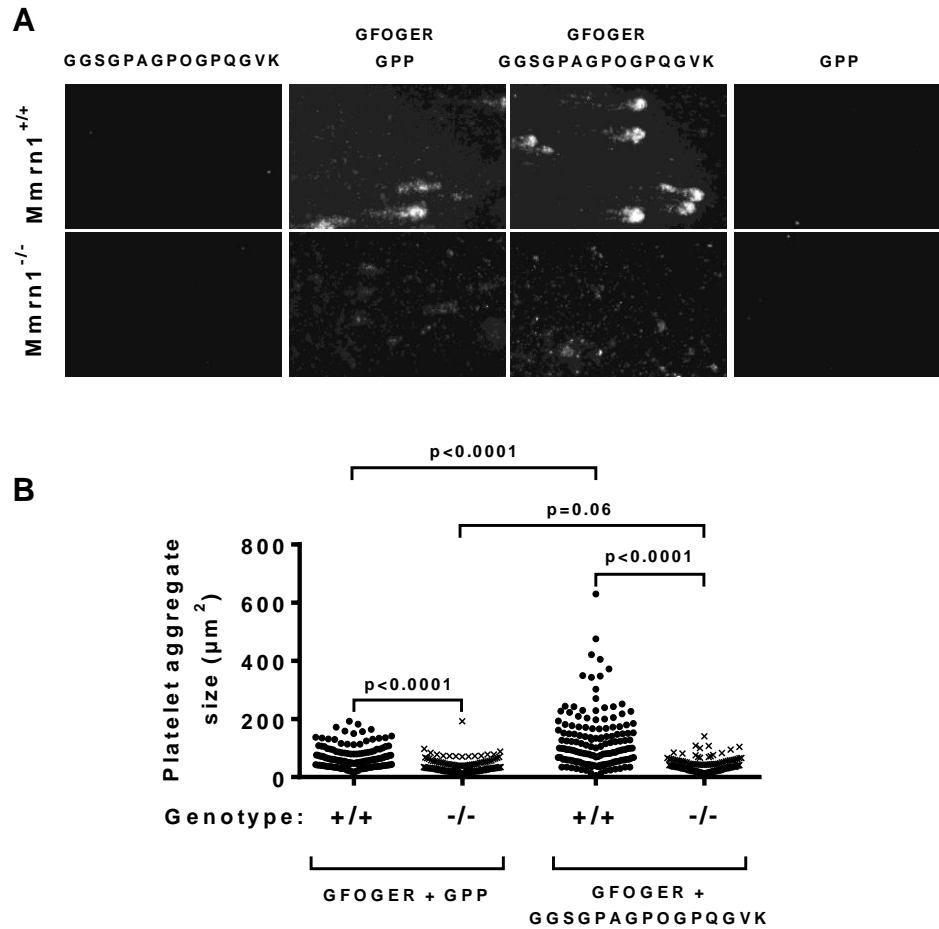


**Figure 28: Adhesion of washed, CRP-activated mouse platelets to triple-helical collagen mimetic peptides under high shear flow ( $1500 \text{ s}^{-1}$ ).** (A) Representative images (original magnification  $\times 20$ ) and (B) quantitative analyses of wild-type and *Mmrn1*<sup>-/-</sup> platelet aggregates captured onto immobilized triple-helical collagen peptides. In panel B, data represent the mean feature size in each captured image ( $n = 15$  images per experiment,  $n = 5$  mice/group).

### 3.10 STATIC ADHESION OF HUMAN PLATELETS TO TRIPLE-HELICAL COLLAGEN PEPTIDES

I performed static adhesion assays to characterize the ability of GPAGPOGPX peptides to support or enhance adhesion of human platelets. When presented alone, GPAGPOGPX peptides did not support significant adhesion of CRP-activated human platelets (*Figure 29A*). When co-presented with the  $\alpha_2\beta_1$ -binding peptide GFOGER, GPAGPOGPX peptides significantly enhanced human platelet adhesion compared to GFOGER + GPP ( $p < 0.002$ ), similar to GFOGER co-presented with the VWF-binding peptide III-23 (*Figure 29B*). In comparison, co-presentation of III-23 with GPAGPOGPX peptides did not support significant adhesion of activated human platelets compared to III-23 + GPP (*Figure 29B*). When presented together, GFOGER, III-23, and GPAGPOGPX peptides synergistically enhanced adhesion of activated human platelets (*Figure 29C*). The enhancing effect of GPAGPOGPX peptides co-presented with GFOGER was significantly increased by platelet activation to induce MMRN1 release ( $p < 0.007$ , *Figure 30A*). The effect of platelet activation was similar whether human platelets were pre-treated with CRP or exposed to CRP coated in wells ( $p > 0.24$ , *Figure 30B*).

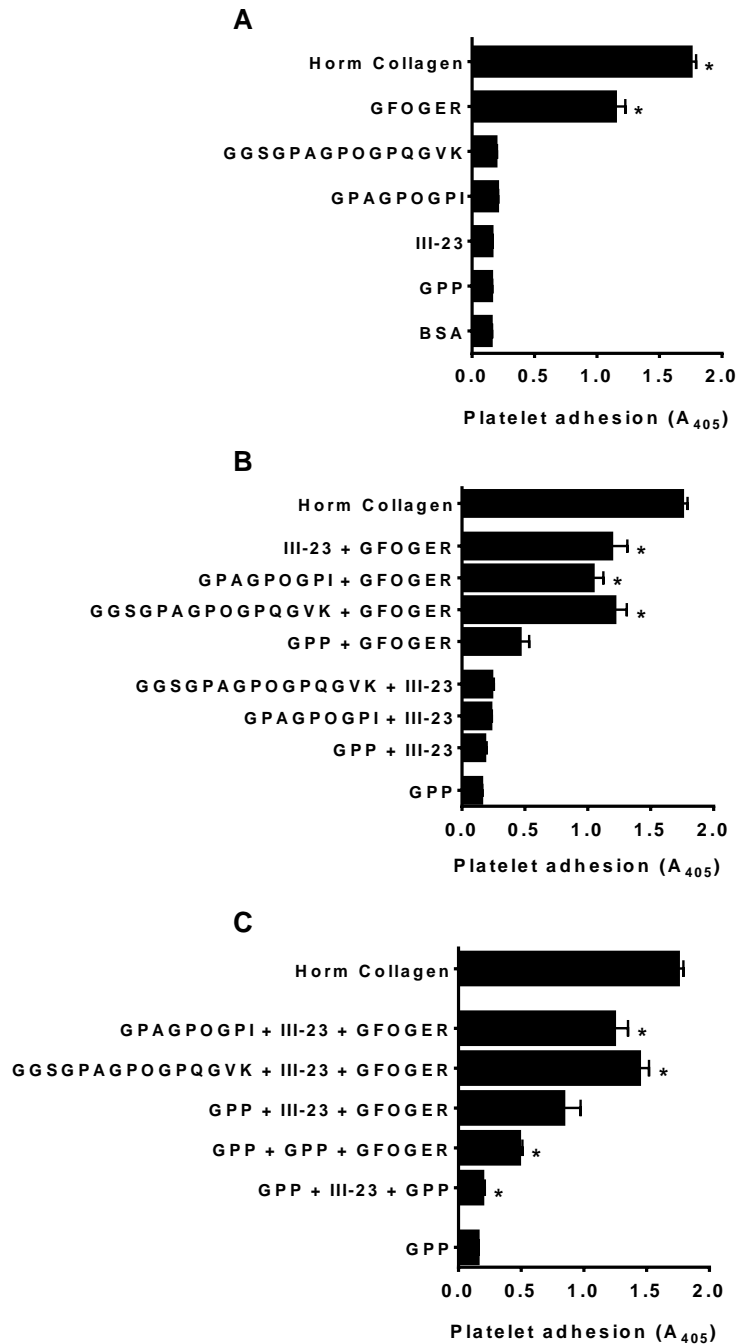


**Figure 29: Synergistic effects of triple-helical peptide combinations on static adhesion of CRP-activated human platelets.** Bars and whiskers represent the mean absorbance and SEM, respectively ( $n = 3$  healthy controls). Asterisks (\*) indicate statistical significance using multiple paired  $t$ -tests and the Bonferroni correction for

family-wise error. In panel A, statistical comparisons are relative to GPP. In panel B, statistical comparisons are relative to GPP + GFOGER (top) or GPP + III-23 (bottom). In panel C, statistical comparisons are relative to GPP + III-23 + GFOGER.

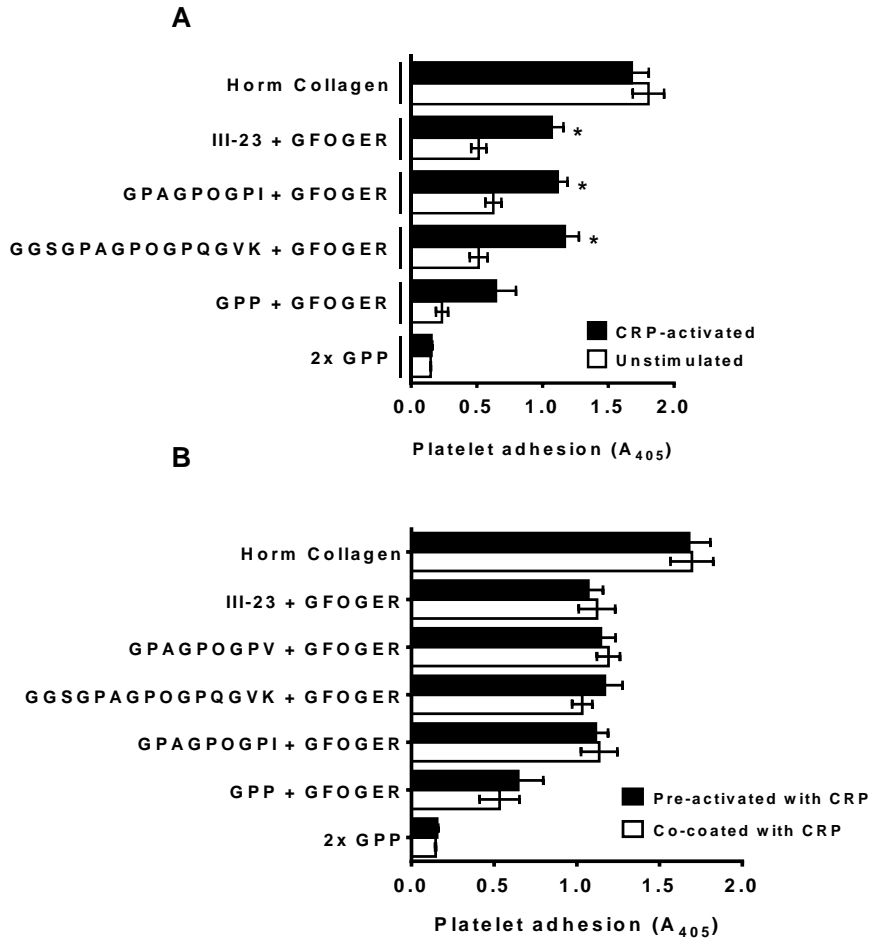


**Figure 30: Effect of CRP activation on static adhesion of human platelets.** Bars and whiskers represent the mean absorbance and SEM, respectively ( $n = 3$  healthy controls). Asterisks (\*) indicate statistical significance between CRP-activated and unstimulated samples using multiple paired  $t$ -tests and the Bonferroni correction for family-wise error ( $k = 5$ ,  $\alpha = 0.01$  in each comparison). In panel A, comparison of adhesion of CRP-activated versus unstimulated platelets to GPP + GFOGER approached, but did not reach, significance ( $p=0.07$ ).

## CHAPTER FOUR: DISCUSSION

### 4.1 SUMMARY OF THESIS WORK AND KEY OBSERVATIONS

This thesis aimed to further characterize the role of MMRN1/Mmrn1 in platelet adhesion and platelet aggregation, specifically through its interactions with fibrillar collagens, identifying additional potential binding partners for MMRN1, testing the effects of fluid shear stress on MMRN1 adhesive functions, identifying novel MMRN1-binding motifs in type I collagen, and assess the specificity and functions of MMRN1-binding GPAGPOGPX sequences in platelet adhesion. The main findings of this thesis were that *Mmrn1*<sup>-/-</sup> platelets had impaired aggregate formation on Horm collagen under high shear flow (1500 s<sup>-1</sup>), which was due in part to reduced initial adhesion and a slower rate of platelet accumulation onto collagen. Additionally, *Mmrn1*<sup>-/-</sup> platelets formed significantly smaller aggregates on immobilized rVwf under high shear flow (1500 s<sup>-1</sup>), regardless of whether or not plasma Vwf was present. Impaired adhesion of *Mmrn1*<sup>-/-</sup> platelets to Horm collagen was also observed under low shear flow (300 s<sup>-1</sup>) and stasis, suggesting that Mmrn1 could enhance platelet adhesion to collagen through additional, Vwf-independent mechanisms.

rhMMRN1 was found to be a ligand for human FG, fibrin, and FN. Additionally, *Mmrn1*<sup>-/-</sup> platelets had significantly impaired adhesion and aggregate formation onto murine Fg, but not fibrin, under low shear flow (300 s<sup>-1</sup>), tested after platelets were pre-

activated to expose  $\alpha$ -granule contents and activate platelet integrins. Contrary to expectations, activated *Mmrn1*<sup>-/-</sup> platelets had similar adhesion and aggregate formation onto Fn. Wild-type and *Mmrn1*<sup>-/-</sup> platelets were found to adhere to rhMMRN1 through mechanisms involving, but not requiring,  $\beta_3$  integrins, suggesting the involvement of other receptors and/or proteins. Although MMRN1 is a ligand for VWF, platelet aggregation under elevated shear stress, which is sufficient to induce  $\alpha$ -granule release, was similar between *Mmrn1*<sup>-/-</sup> and wild-type platelets at all shear rates tested, indicating that high-shear induced platelet aggregation is Vwf- but not *Mmrn1*-dependent.

Fibrillar type I collagen was found to contain a conserved GPAGPOGPI sequence that binds rhMMRN1 and aligns with the MMRN1-binding GPAGPOGPQ sequence in type III collagen. Both GPAGPOGPI and GPAGPOGPQ show high specificity for *Mmrn1* as wild-type but not *Mmrn1*<sup>-/-</sup> platelets adhered to this motif under stasis and high shear flow (1500 s<sup>-1</sup>). GPAGPOGPX peptides enhanced static adhesion of human platelets when co-presented with  $\alpha_2\beta_1$ -binding peptide GFOGER or GFOGER and VWF-binding peptide III-23 together, which was significantly enhanced by platelet activation, which is required to release MMRN1 from  $\alpha$ -granules.

The following sections discuss the proposed roles of MMRN1/*Mmrn1* in platelet adhesion to collagen and present an updated model of the recognition motifs in collagen that support platelet adhesion or activation in light of these findings. Next, the strengths

and limitations of the approaches and techniques used in this thesis will be considered, along with potential future experiments to address questions raised by this thesis.

## 4.2 CONTRIBUTIONS OF MULTIMERIN 1 IN PLATELET ADHESION TO COLLAGEN

### 4.2.1 Potential roles of Mmrn1 in primary platelet adhesion and platelet tethering onto fibrillar collagen

As described in *section 1.4.3*, platelet adhesion to fibrillar collagen under high shear flow requires VWF to bind to the collagen surface, which tethers circulating platelets and reduces their velocity to facilitate stable adhesion onto collagen. Although MMRN1 (which is not detectable in normal plasma) is sequestered within platelet and endothelial cell granules until activation-induced release, with platelet activation at sites of injury, the local concentrations of MMRN1 likely rise so that it can participate with other ligands in platelet attachment. Vessel injury that results in activation or rupture of endothelial cells would also release MMRN1 locally, and it is difficult to exclude that *in vivo*, a small amount of MMRN1 is constitutively secreted into the subendothelium after biosynthesis by endothelial cells.<sup>1,17</sup> In these ways, MMRN1 may contribute to the initial “protein wave” of hemostasis that primes the site of injury for adhesion prior to initial platelet attachment. Additionally, in thrombotic diseases in which endothelial cells are

pathologically activated, MMRN1 would similarly be exposed to flowing blood by endothelial cells prior to platelet activation.

One important consideration is that *in vitro* perfusion experiments using resting platelets lack any initial presence of Mmrn1 on the adhesive substrate before contact with platelets. In experiments testing adhesion of resting murine platelets to Horm collagen under high shear flow, Mmrn1 is likely only released from  $\alpha$ -granules following contact with collagen. While the ligation of VWF to GPIb $\alpha$  is able to induce activation of  $\alpha_{IIb}\beta_3$  and Ca<sup>2+</sup> mobilization in platelets, it is insufficient to induce  $\alpha$ -granule release from platelets.<sup>186,567</sup> Collagen-activated platelets would express Mmrn1 on their surface and may also release some Mmrn1 downstream of the site of attachment. Moreover, at sites of injury, there are likely multiple triggers to platelet activation. Thus, it is quite possible that Mmrn1 contributes to both early and later steps of platelet adhesion onto collagen. *Figure 31* outlines potential mechanisms for the role of MMRN1/Mmrn1 in primary platelet adhesion onto collagen under high shear flow based on previous data and observations described in this thesis.

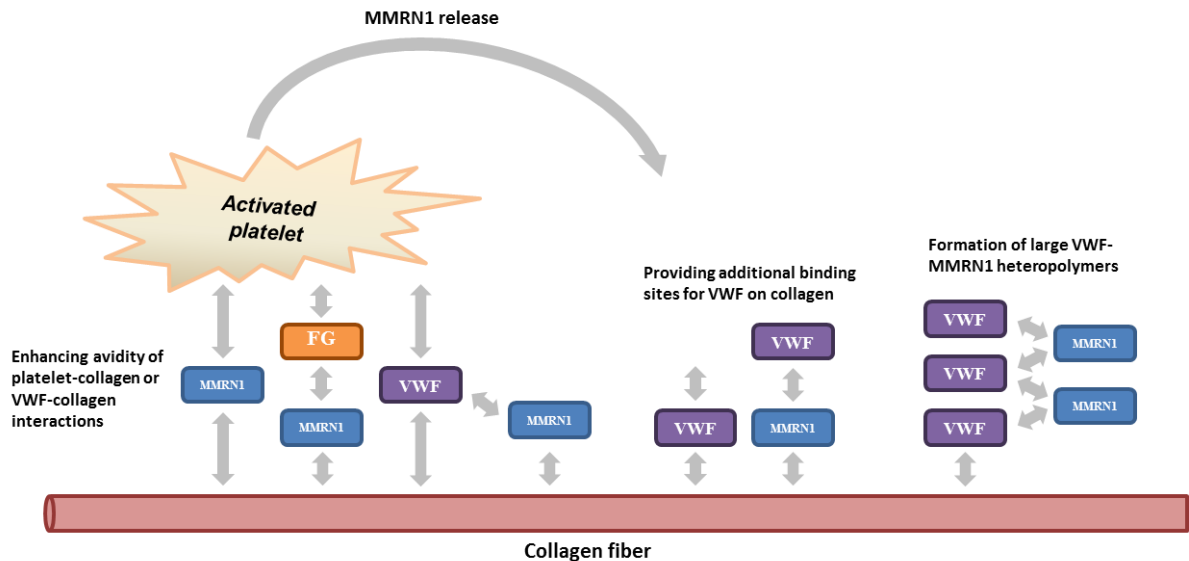


**Figure 31: Potential mechanisms through which MMRN1/Mmrn1 enhances primary platelet adhesion to fibrillar collagen under high shear flow.**

Mmrn1 that remains bound to the platelet surface following platelet activation could bind to GPAGPOGPX motifs in collagen fibers to stabilize platelet adhesion to collagen. Each type I or III collagen molecule contains a single, discrete VWF-binding GPRGQOGVMGF that is distinct from the MMRN1-binding GPAGPOGP(I/Q) motif. Mmrn1 binding to collagen could enhance the avidity of Vwf binding to collagen by providing additional bonds between Vwf and the collagen molecule to stabilize Vwf-collagen interactions. Additionally, Mmrn1 could mediate the binding of  $\alpha_{IIIb}\beta_3$ -bound Fg on the activated platelet surface to collagen fibers to further stabilize platelet adhesion.

A second possible mechanism is that Mmrn1 released from the platelet surface could enhance Vwf-dependent tethering onto collagen by increasing the availability of

Vwf-binding sites on collagen fibrils downstream of attachment. Mmrn1 released into circulation by stably-adherent platelets would be able to bind GPAGPOGPX motifs in fibrillar collagen molecules downstream to essentially double the availability of Vwf-binding sites on collagen fibrils. This idea is particularly intriguing because the collagen-binding and MMRN1-binding regions of VWF involve the same domains: VWF A1 and VWF A3, meaning that MMRN1-bound VWF would be anchored in a similar way as collagen-bound VWF. Further, it is already shown that plasma VWF multimers can self-associate onto collagen-bound VWF through homotypic interactions to enhance platelet adhesion to collagen.<sup>552</sup> Although MMRN1 is not in direct competition for the same binding sequence on a single collagen molecule as other ligands, the steric parameters of VWF and MMRN1 binding to collagen are unclear. Both VWF and MMRN1 form large homopolymers, which can exceed millions of Daltons in size.<sup>11,13,18,568,569</sup> In particular, VWF multimers can reach up to 15  $\mu\text{m}$  in length,<sup>570</sup> whereas a mature human type I or III fibrillar collagen molecule is approximately 300 nm in length. Large VWF and MMRN1 homopolymers likely engage multiple copies of their respective recognition motifs on a series of crosslinked, end-to-end collagen molecules within a collagen fibril. While it is possible that large MMRN1 homopolymers may be able to block VWF-binding to collagen or *vice versa*, the observations described in this thesis suggest that Vwf and Mmrn1 cooperatively enhance platelet adhesion to collagen. Previous studies also indicate that adding exogenous rhMMRN1 enhances platelet adhesion to Horn collagen,<sup>2</sup> further suggesting that VWF and MMRN1 homopolymers cooperatively support platelet adhesion to collagen. Collagen fibrils are quarter-staggered 5-mers of end-to-end

crosslinked collagen molecules that aggregate into bundles of fibrils, which would present an abundance of binding sites for both VWF and MMRN1 multimers, potentially rendering competition for collagen binding moot. *In vivo*, the stoichiometry of collagen, VWF, and MMRN1 is likely to be highly variable, dependent on a number of factors, including: the tissue in which the hemostatic or thrombotic response is occurring (i.e. collagen-rich or collagen-poor), the localized platelet concentration (the amount of platelet MMRN1 available for release), and the platelet activation state (how much platelet MMRN1 is released). Based on these considerations, it is difficult to conclude whether MMRN1 and VWF cooperatively or competitively support platelet adhesion to collagen in some or all situations, or if competition would be irrelevant due to a molar excess of collagen in most collagen-containing tissues. Fluid-phase competition assays could be useful for understanding how MMRN1, VWF, and  $\alpha_2\beta_1$  cooperatively enhance platelet adhesion to collagen, but would be complicated to perform and interpret given that MMRN1 and VWF bind to one another. Instead, assays where varying concentrations of rhMMRN1 or BSA are incubated with or perfused over Horm collagen before perfusion with fluorescently-labelled VWF could be used to determine if MMRN1 can enhance VWF binding to collagen fibers.

The idea that adhesive plasma or platelet proteins bind one another to form large, macromolecular complexes has been proposed as a possible explanation for the supportive role of multimeric platelet VN,<sup>203</sup> TSP-1,<sup>205</sup> and insoluble (crosslinked) plasma FN<sup>204,206,208</sup> in platelet aggregate formation, as well as in platelet adhesion to

collagen.<sup>303,304</sup> It is possible that Mmrn1 either bound to the platelet surface or released into circulation could bind to shear-stretched Vwf multimers to form larger, heteropolymers to enhance platelet tethering and adhesion. Larger heteropolymers composed of Vwf and Mmrn1 would likely extend further into the lumen, which would increase the probability and frequency of encountering circulating platelets. Similar to Tsp-1, Mmrn1 may also bind to the A1 and A3 domains of Vwf to block cleavage of immobilized, shear-stretched Vwf multimers by Adamts13. This would facilitate the formation and maintenance of ultra-large Vwf multimers on the exposed collagen surface, which are more effective at supporting platelet adhesion.<sup>571</sup> As outlined in *section 1.2.3*, TSP-1 competitively binds to the VWF A2 and A3 domains to block VWF A2 cleavage by ADAMTS13,<sup>362</sup> and *Tsp-1<sup>-/-</sup>* mice show rapid degradation of ultra-large Vwf multimers released from endothelial cells following photochemical injury *in vivo*, which is restored by adding back recombinant TSP-1 or anti-ADAMTS13-antibodies.<sup>225</sup> Mmrn1 may function in a similar way to inhibit the regulation of Vwf multimer size by Adamts13. This possibility is discussed further in *section 4.5.1*. Another important consideration is the potential role of MMRN1 in thrombotic thrombocytopenic purpura (TTP), in which quantitative or qualitative defects in ADAMTS13 impair the regulation of plasma VWF multimer size, resulting in increased platelet adhesion to ULVWF multimers that underlie the microangiopathy of TTP. Given that MMRN1 binds to the VWF A1 and A3 domains, and the ability of Mmrn1 to contribute to platelet aggregate formation onto Vwf under flow, this raises the possibility that MMRN1/Mmrn1 could be

involved in the pathogenesis of TTP if it alters VWF cleavage by ADAMTS13 or the stability of platelet aggregates adherent to ULVWF multimers.

Lastly, it is interesting to consider that differently-sized *Mmrn1* multimers could fulfil different adhesive functions. For example, larger MMRN1 multimers preferentially stay bound to the platelet surface, whereas smaller multimers tend to be released into the milieu,<sup>15</sup> which may have biological significance. Large, platelet-bound MMRN1 multimers could locally enhance or stabilize platelet adhesion, whereas smaller MMRN1 multimers might be more important for facilitating primary adhesion of additional platelets downstream of MMRN1 release.

The mechanisms through which *Mmrn1* contributes to primary platelet adhesion under low shear likely differ in some respects because platelet adhesion and aggregate formation on collagen can occur independent of VWF under shear rates of approximately  $\leq 1000 \text{ s}^{-1}$ .<sup>175</sup> Under low shear flow ( $300 \text{ s}^{-1}$ ) and stasis, *Mmrn1*<sup>-/-</sup> platelets visually showed reduced adhesion to collagen and formed smaller aggregates compared to wild-type platelets. These data suggest that *Mmrn1* may enhance platelet adhesion to collagen through additional mechanisms than those that support Vwf adhesive functions. In regard to primary platelet adhesion to collagen, it is possible that *Mmrn1* binding to collagen and to platelets may be sufficient to mediate platelet adhesion to collagen on its own under stasis and low shear flow. This could be tested using a model of combined *Mmrn1* and Vwf deficiency compared to single-deficient *Vwf*<sup>-/-</sup> mice to eliminate the contribution of

ultra-large platelet Vwf to platelet adhesion to collagen, with and without anti-mouse  $\alpha_2\beta_1$  and GpVI blocking antibodies to control the contribution of platelet collagen receptors.

#### 4.2.2 Potential roles of Mmrn1 in supporting platelet aggregate formation onto fibrillar collagen

An important observation from this thesis is that the presence of Mmrn1 enhanced the size of platelet aggregates formed on Horm collagen surfaces under high and low shear flow. This suggests that in addition to supporting initial platelet adhesion to collagen, Mmrn1 has a role in enhancing the size or stability of platelet aggregates formed under flow. Within the context of platelet adhesion to collagen, Mmrn1 interactions with collagen and platelets might also facilitate platelet activation, which is suggested by the observation of enhanced stable primary platelet adhesion to collagen in the presence compared to the absence of Mmrn1. Platelet activation is an important modulator of platelet adhesion and aggregation onto collagen, given that it induces conformational changes in platelet integrins, which increases the affinity of  $\alpha_2\beta_1$  for collagen and increases the affinity of  $\alpha_{IIb}\beta_3$ . This is supported by observations that GpVI- or FcR $\gamma$ -deficient mouse platelets (which do not express platelet GpVI) fail to form aggregates on collagen under high shear flow,<sup>182,415,464</sup> and show significantly reduced  $\alpha_2\beta_1$ -mediated stable adhesion onto collagen in real-time.<sup>415</sup> It is also supported by observations that blockade of P2Y<sub>12</sub> and P2Y<sub>1</sub> significantly reduces platelet aggregation onto collagen.<sup>573</sup> Mmrn1 may assist in primary adhesion onto collagen to facilitate

platelet activation by collagen, which would enhance the rate and amount of platelet aggregate formation. The transient on/off binding of VWF to GPIIb/IIIa and the relatively weak interaction between collagen and GPVI means that additional ligands are required to facilitate stable adhesion and subsequent activation, partly evidenced by the delay in collagen-induced platelet aggregation observed in  $\alpha_2$ -deficient mice.<sup>574</sup>

Notably, the ability of Mmrn1 to enhance platelet aggregate size under flow is not limited to immobilized collagen surfaces, which suggests that Mmrn1 may play a dual role in enhancing platelet adhesion and aggregate formation onto collagen by: 1) mediating platelet adhesion onto collagen through interactions with collagen and/or Vwf, and 2) enhancing platelet aggregate formation on collagen by supporting platelet-platelet interactions. The ability of MMRN1 to bind FG, fibrin, and FN indicates MMRN1/Mmrn1 could feasibly enhance platelet aggregate growth through multiple potential mechanisms. Similar to TSP-1, multimeric VN, and fibrillar FN, MMRN1 may be able to crosslink  $\alpha_{IIb}\beta_3$  or  $\alpha_{IIb}\beta_3$ -bound FG on adjacent platelets. *Figure 32* outlines potential mechanisms through which MMRN1/Mmrn1 could support platelet-platelet interactions to enhance platelet aggregate formation. Large MMRN1/Mmrn1 multimers bound to the surface of activated platelets would decrease the distance required for platelet-platelet interactions to occur, which would facilitate greater platelet-platelet interactions. Increasing the number of platelet crosslinks would also enhance the avidity of platelet-platelet interactions. Lastly, MMRN1/Mmrn1 may bind to FG or FN to form larger complexes that are more effective at supporting platelet-platelet interactions.

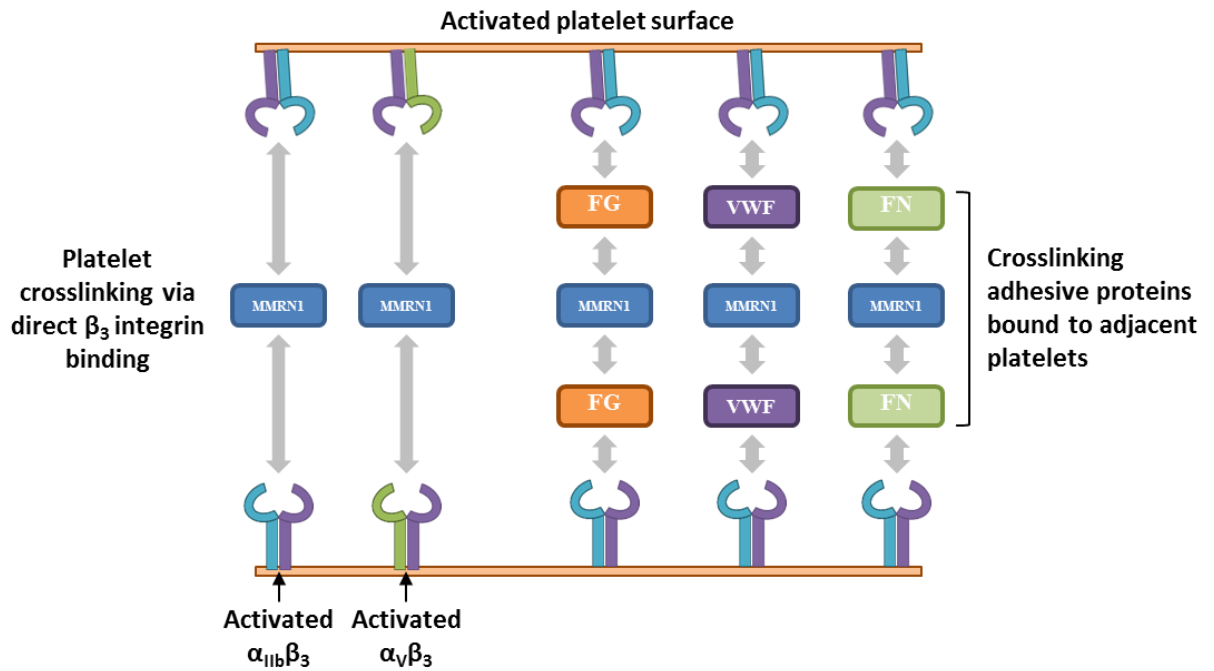


**Figure 32: Potential mechanisms through which MMRN1/Mmrn1 enhances aggregate formation onto fibrillar collagens and other adhesive substrates.**

Assays of static platelet adhesion using pre-activated mouse platelets to induce Mmrn1 release indicated that Mmrn1 was not required for stable adhesion to Fg, fibrin, or Fn, although the absence of Mmrn1 impaired platelet adhesion and aggregate formation onto Fg under low shear flow. This discrepancy could arise from the type of model and unit of measurement to measure adhesion in static adhesion and perfusion assays. Static adhesion assays commonly estimate platelet adhesion by quantifying conversion of p-Nitrophenyl phosphate by acid phosphatases released from lysed adherent platelets,<sup>565</sup> whereas perfusion assays directly visualize the quantity and extent of fluorescently-labelled platelets onto a protein surface. Another possible explanation is differences in the

binding kinetics of mouse platelet receptors to their respective ligands under stasis versus shear stress. Under conditions of low shear flow, the ability of Mmrn1 to enhance adhesion and aggregate size of activated but not resting platelets onto immobilized Fg is consistent with the requirement of platelet activation to release Mmrn1 from platelet  $\alpha$ -granules. Additionally, it is possible that the active conformation of  $\alpha_{IIb}\beta_3$  may be required for platelets to bind Mmrn1, similar to observations of human platelet adhesion to MMRN1.<sup>1,2</sup> These data indicate that Mmrn1 may have a supportive role in platelet adhesion to Fg, which would be immobilized onto the outer surface of a growing platelet aggregate. The binding site(s) of MMRN1 on FG are unknown, meaning it is presently unclear if MMRN1 bound to FG could prevent engagement of  $\alpha_{IIb}\beta_3$  by the FG  $\gamma$ -chain. Future studies using recombinant FG domains, recombinant  $\alpha_{IIb}$  and  $\beta_3$ , and rhMMRN1 could unravel this question.

Platelet adhesion to Fg, fibrin, and Fn were tested under low shear flow to recapitulate conditions that are favourable for  $\alpha_{IIb}\beta_3$ -mediated platelet adhesion, mostly independent of Vwf/GpIb $\alpha$ -mediated platelet tethering. FG-, fibrin-, or FN-coated surfaces do not support significantly platelet adhesion or aggregate formation under high shear rates,<sup>174,265</sup> which require VWF and GPIb $\alpha$ . Low shear perfusion assays are ideal for testing the effects of platelet Mmrn1 on platelet adhesion and aggregate formation through mechanisms involving FG and  $\alpha_{IIb}\beta_3$ . Although perfusion assays using Horn collagen or Vwf surfaces were performed at high shear, some comparisons can be made between high shear and low shear perfusion experiments. Following VWF/GPIb $\alpha$ -

mediated platelet tethering under high shear flow, stable platelet-collagen and platelet-platelet interactions mediate adhesion, which involve FG and VWF binding to  $\alpha_{IIb}\beta_3$  on activated platelets either arrested onto collagen or slowly translocating along the collagen surface. In this way, stable platelet adhesion and platelet aggregate formation onto collagen under high shear flow also involves static or low-velocity interactions.

Analyses of *Mmrn1*<sup>-/-</sup> and wild-type platelet adhesion indicate that Mmrn1 contributes to platelet adhesion and aggregate formation onto immobilized Fg when platelets are pre-activated to release Mmrn1. TRAP activation prior to perfusion likely primes the platelet surface with large Mmrn1 multimers and releases some Mmrn1 into solution. Similar to previously discussed, Mmrn1 could decrease the distance required for platelets to contact surface-bound Fg, and also increase the frequency of platelet-platelet interactions to enhance the rate of aggregate formation. It is possible that Mmrn1 may also contribute to the stability of platelet aggregates formed on Fg surfaces. Additional experiments could be performed to answer this question, in which *Mmrn1*<sup>-/-</sup> and wild-type platelet adhesion to Fg under low shear is quantified by fluorescence microscopy and chambers are subsequently washed under elevated shear stress to quantify aggregate dissolution and platelet detachment. Lastly, Mmrn1 released from the platelet surface could even bind pFn to inhibit its ability to compete with FG for ligation of  $\alpha_{IIb}\beta_3$ ,<sup>211</sup> thereby indirectly supporting FG-dependent platelet adhesion and aggregation.

Interestingly, *Mmrn1*<sup>-/-</sup> and wild-type platelet adhesion to fibrin was similar using resting or TRAP-activated platelets. Differences in the ultrastructure of surface-adsorbed Fg versus fibrin and/or differences in Fg- and fibrin- $\alpha_{IIb}\beta_3$  binding interactions could account for this divergence. Surface-adsorbed FG is shown to unfold into a highly adhesive conformation that supports platelet adhesion via RGD-independent mechanisms.<sup>280</sup> Conversely, fibrin forms large polymers that branch and crosslink into three-dimensional networks, and platelet adhesion to fibrin is predominantly mediated by  $\alpha_{IIb}\beta_3$  binding to the RGD motifs in fibrin.

*Mmrn1*<sup>-/-</sup> and wild-type platelet adhesion to Fn is consistent with previous observations that FN does not support significant platelet adhesion and platelets do not aggregate on FN surfaces. This is hypothesized to be a result of the weak interaction between platelet receptors  $\alpha_{IIb}\beta_3$  and  $\alpha_V\beta_3$  with FN. Platelet adhesion to FN is mediated by its RGD sequence binding to  $\beta_3$  integrins. Although  $\alpha_5\beta_1$  on the platelet surface binds FN, it is not the key mediator of platelet adhesion to FN under stasis or flow. The molar ratio of FG to FN likely affects platelet adhesion to FN. Plasma FG concentrations range from 2 to 4 mg/ml in humans, whereas plasma FN concentrations range from 100 to 300  $\mu\text{g/ml}$ . The affinity of FG for activated  $\alpha_{IIb}\beta_3$  is so high that  $\alpha_{IIb}\beta_3$  is likely immediately occupied by FG following platelet activation. As a result, in whole blood perfusion assays, plasma FG likely inhibits platelet adhesion onto FN, resulting in poor adhesion. Although MMRN1 binds to FN, it does not appear to affect the ability of platelets to adhere to or aggregate onto Fn under stasis or low shear flow. It could be that pFn

requires co-presentation with other proteins to modulate platelet adhesion. For example, pFn crosslinked to fibrin surfaces induces fibrillar matrix formation of pFn monomers that significantly enhances platelet adhesion,<sup>575</sup> and pFn requires fibrin in order to enhance platelet aggregation.<sup>204</sup> On its own, pFn is insufficient to induce fiber formation, and does not support significant adhesion. Similarly, VN incorporated into fibrin matrices enhances platelet adhesion, whereas it supports little adhesion on its own.<sup>380</sup> It is possible that *Mmrn1* could modulate platelet adhesion to fibrillar Fn to synergistically enhance platelet adhesion and aggregate formation on surfaces with multiple adhesive proteins present, and a model of platelet adhesion to Fn alone is insufficient to detect an effect of *Mmrn1* on Fn adhesive functions.

Although MMRN1 binds to  $\alpha_{IIb}\beta_3$  and  $\alpha_V\beta_3$  on activated human platelets, it is interesting that static adhesion of *Mmrn1*<sup>-/-</sup> and wild-type platelets to rhMMRN1 is only partially inhibited by blockade of  $\alpha_{IIb}\beta_3$ . When presented with immobilized rhMMRN1, which contains the N-terminal integrin-binding RGD site, static adhesion was only inhibited by  $\leq 45\%$  on average for both wild-type and *Mmrn1*<sup>-/-</sup> platelets. This observation differs from previous studies of human platelets (*Table 5*). Differences in antibody epitopes or affinity could account for this discrepancy, but it is possible that additional mechanisms are involved in murine platelet adhesion to MMRN1/*Mmrn1*. One possibility is that, because MMRN1 is a ligand for FN, platelet Fn could potentially mediate platelet adhesion to MMRN1 by binding  $\alpha_5\beta_1$  on platelets. Additionally, ULVWF secreted from activated platelets is able to bind platelets in the absence of shear stress,<sup>576</sup> and could

potentially bridge platelet-MMRN1 interactions, but stable platelet adhesion to VWF is mediated by  $\alpha_{IIb}\beta_3$  binding to the RGD motif in the VWF C4 domain,<sup>569</sup> which may be inaccessible in the absence of high shear flow. Lastly, other platelet receptors, either known or uncharacterized, could bind MMRN1/Mmrn1. In analyses of human platelet adhesion to MMRN1, combined blockade of  $\alpha_{IIb}\beta_3$  and  $\alpha_V\beta_3$  on activated human platelets only inhibited adhesion by 77% on average,<sup>1</sup> which led the authors to suggest the presence of other receptors for MMRN1 on human platelets.

Protein surface	ADP-activated human platelets		CRP-activated WT mouse platelets
	Monoclonal anti-human $\alpha_{IIb}\beta_3$	Monoclonal anti-human $\alpha_{IIb}\beta_3/\alpha_V\beta_3$	Monoclonal anti-mouse $\alpha_{IIb}\beta_3$
MMRN1	75.5 ± 4.4	76.8 ± 4.9	45.1 ± 3.5
FG/Fg	82.6 ± 6.4	81.1 ± 7.2	67.4 ± 3.4
FN/Fn	67.2 ± 3.5	69.3 ± 4.3	63.6 ± 2.0

**Table 5: Comparison of inhibition of static adhesion of ADP-activated human platelets to MMRN1, FG, and FN with inhibition of static adhesion of CRP-activated mouse platelets to MMRN1, murine Fg, and murine Fn.** Methods, antibody sources, and data reported for ADP-activated human platelets are described in Adam *et al.*<sup>1</sup> In both sets of experiments, wells were coated overnight at 4°C using 100  $\mu$ l of 110  $\mu$ g/ml protein (1  $\mu$ g/well) and platelets were incubated with 10  $\mu$ g/ml of monoclonal antibodies before adding to microtiter wells. In experiments using CRP-activated mouse platelets, adhesion was tested using murine Fg or Fn.

Collagen-induced aggregation of *Mmrn1*<sup>-/-</sup> and wild-type platelets tested in whole blood was similar to studies of collagen-induced aggregation of *Mmrn1*<sup>-/-</sup> and wild-type platelets tested by LTA.<sup>4</sup> It was previously hypothesized that adhesive proteins in plasma, such as VWF and FG, mask the ability to detect a defect in platelet aggregation due to loss of platelet Mmrn1. Similarly, studies of human platelets show that adding plasma concentrations of purified FG or FN to washed platelets reduces platelet adhesion to MMRN1 by 50% or 23%, respectively, and adding plasma to washed platelets reduces platelet adhesion to MMRN1 by 88%.<sup>1</sup> Together, these data indicate that other proteins in plasma, such as FG and FN, likely compete with MMRN1 for ligation of the promiscuous  $\alpha_{IIb}\beta_3$  receptor. This may account for why *Mmrn1*<sup>-/-</sup> platelets show normal aggregation responses in models wherein adhesive plasma proteins are present. In regard to how these findings relate to observations from *in vitro* perfusion experiments using whole blood, aggregometry testing measures either turbidity or electrical resistance, which measure the rate of aggregation and maximal aggregation, but these tests are not sensitive to detect changes in aggregate size or morphology. For example, anti-TSP-1 antibodies impair collagen- or thrombin-induced platelet aggregation measured by turbidity, but a striking feature is that anti-TSP-1 antibodies impair the size of aggregates formed when assessed by microscopy.<sup>241,351</sup> It is possible that Mmrn1 modulates aggregate size, but not the rate and amount of maximal aggregation in these assays. Analyses to measure the size of fixed platelet aggregates by fluorescence microscopy following LTA or whole blood aggregation tests could be used to answer this question.

It is surprising that *Mmrn1* deficiency did not affect SIPA, considering that SIPA is initiated by VWF-mediated aggregation, followed by platelet activation,  $\alpha$ -granule release, and  $\alpha_{IIb}\beta_3$ -mediated stabilization of platelet aggregates.<sup>320,577</sup> Under these conditions, it is anticipated that *Mmrn1* would be released following platelet activation, which could contribute to platelet-platelet interactions and bind to plasma Vwf multimers to assist in further Vwf-mediated aggregation. The presence of adhesive platelet  $\alpha$ -granule and plasma proteins such as Fg, Fn, Tsp-1, and Vn, could mask the ability of *Mmrn1* to contribute to SIPA or even inhibit *Mmrn1* binding to activated platelets via competition for ligation of  $\alpha_{IIb}\beta_3$ . However, whole blood was selected for these experiments because it is the most physiologic model to test SIPA. The data presented in this thesis suggests that platelet *Mmrn1* does not significantly contribute to SIPA, but further experiments using washed platelets could determine if *Mmrn1* modulates SIPA in the absence of adhesive plasma proteins. The time in which blood is exposed to shear affects the amount of SIPA, although SIPA was similar between *Mmrn1*<sup>-/-</sup> and wild-type samples when sheared for 30 s or 90 s (data not shown), in addition to the studies included herein that sheared samples for 60 s. It is possible that measuring SIPA at a greater number of time points could reveal a significant difference in SIPA between *Mmrn1*<sup>-/-</sup> and wild-type samples.

Part of the observed reduction in platelet number in response to high shear stress could be due to either receptor shedding or platelet fragmentation in addition to SIPA. Shedding of platelet GPIb/IX/V and  $\alpha_{IIb}\beta_3$  occur following platelet activation, and

receptor shedding has also been reported under conditions of pathological shear stress.<sup>578,579</sup> In many experiments, smaller events were visible on scatterplots (*Figure 23*), which could reflect either platelet fragmentation or the release of CD42b-bearing platelet microparticles by activated platelets in response to elevated shear stress.<sup>579</sup> Notably, platelet count can also impact the degree of SIPA.<sup>247,580</sup> Platelet-platelet collisions are required for aggregation to occur, and 2-body collision theory asserts that collision frequency is proportional to the cell concentration at a given shear rate.<sup>581,582</sup> Variability in mouse platelet counts in whole blood could account for some variability in measurements of SIPA, which would make detection of less pronounced changes in SIPA due to *Mmrn1* loss require extremely large sample sizes to reach statistical significance. Using platelet count-adjusted PRP for SIPA experiments could be useful for controlling variability in SIPA due to underlying differences in platelet count, but generating PRP requires sample manipulations that expose whole blood to shear stress (i.e. centrifugation), and eliminates the potential role of erythrocytes in SIPA, unless PRP is reconstituted with washed erythrocytes. Importantly, the upper limit of detection for particle size on the flow cytometer used to measure SIPA is may be insufficient to detect larger aggregates. Following exposure to a shear rate of  $15,000 \text{ s}^{-1}$ , the aggregates detected by fluorescence microscopy in some experiments could reach up to  $11,000 \mu\text{m}^2$  in size. This likely explains why samples show a significantly smaller number of CD42b+ events, but not a significant shift in the size distribution of collected events. Pilot experiments to detect P-selectin expression by flow cytometry as a measure of shear-induced platelet activation (SIPAct) failed to detect significant P-selectin expression on

the events collected by flow cytometry (data not shown), which suggests that most activated platelets expressing P-selectin are likely incorporated into large aggregates not detectable by flow cytometry. Detection of P-selectin expression on fixed platelet aggregates by fluorescence microscopy in future studies could answer this question.

#### 4.3 UPDATED MODEL OF RECOGNITION MOTIFS IN FIBRILLAR COLLAGENS INVOLVED IN PLATELET ADHESION OR ACTIVATION

The GPAGPOGPX sequences in types I and III vessel wall fibrillar collagens are structurally and spatially distinct from other recognition motifs in collagen that support platelet adhesion or activation (*Figure 33*). Toolkit peptide III-38 containing GPAGPOGPQ does not bind VWF,<sup>545</sup> integrin  $\alpha_2\beta_1$ ,<sup>546</sup> or GPVI.<sup>547</sup> Similarly, rhMMRN1 does not bind to peptides containing the VWF-binding GPRGQOGVMGF sequence,  $\alpha_2\beta_1$ -binding GXOGEX' sequences, or the GPVI-binding peptides CRP and III-30 (Subia Tasneem, unpublished data). The MMRN1-binding GPAGPOGPQ motif in Toolkit peptide III-38 is also distinct from other recognition motifs in collagen that have been identified using Collagen Toolkits.<sup>583-590</sup> The only other known ligand that binds to the region in collagen containing GPAGPOGPQ is leukocyte-associated Ig-like receptor-1 (LAIR-1), which binds to the discontinuous GPO repeats in Toolkit peptide III-38,<sup>586</sup> not specifically to the GPAGPOGPQ sequence.

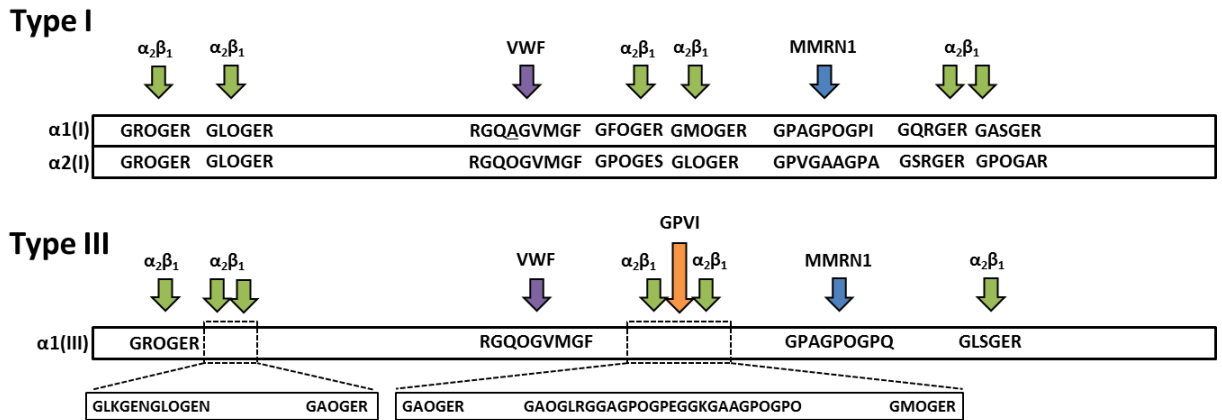


**Figure 33: Updated model of recognition motifs on fibrillar collagens that support platelet adhesion.**

The GPAGPOGPI (helix residues 667 to 675) sequence lies at the same locus as GPAGPOGPQ (helix residues 682 to 690) in D-period 3 of the collagen  $\alpha_1(I)$  chain. At this locus, two copies of GPAGPOGPI would be present in a native heterotrimeric type I collagen molecule. The third  $\alpha_2(I)$  chain of the heterotrimer has a corresponding GPVGAAGPA sequence at this position, but it is unclear if this sequence is involved in MMRN1 binding. Testing a triple-helical homotrimeric GPVGAAGPA peptide for MMRN1 binding would not be sufficient to answer this question, which is why it was not synthesized for testing. Specific residues from the COL  $\alpha_2(I)$  chain GPVGAAGPA may enhance the ability of GPAGPOGPI to bind MMRN1, but not necessarily substitute for this sequence in MMRN1 binding. Interestingly, a homotrimeric isotype of type I collagen composed of three  $\alpha_1(I)$  chains has been reported during wound healing, embryonically, and in certain tumour cell lines,<sup>591</sup> but its potential relevance to MMRN1 is unclear. In the absence of a Collagen Toolkit for the heterotrimeric type I collagen,

other techniques (e.g. cyanogen bromide fragmentation) have been used to map recognition motifs in type I collagen.<sup>540</sup> In some cases, recognition motifs have been inferred from data obtained using Collagen Toolkit III due to the high homology between types I and III collagen.<sup>436,545,546</sup> Similar to the GPAGPOGPQ sequence in type III collagen, GPAGPOGPI is spatially and structural distinct from  $\alpha_2\beta_1$ -binding GXOGEX' sequences in collagen  $\alpha_1(I)$ <sup>436,541,546</sup> and a postulated VWF-binding GPRGQAGVMGF sequence in collagen  $\alpha_1(I)$  that aligns with GPRGQOGVMGF in  $\alpha_2(I)$  and provides the necessary hydroxyproline residue at the 6<sup>th</sup> position.<sup>545</sup> Interaction “hot spots” have been reported in type I collagen, and GPAGPOGPI is directly adjacent to the C-terminal interaction hot spot (helix residues 680 to 830).<sup>502,592</sup> In general, more ligand-binding sites have been identified on the C-terminal half of type I collagen. Fibrillar collagen molecules trimerize from the C- to the N-terminus, and mutations within the COL domain that disrupt helix assembly can affect downstream helix assembly toward the N-terminus. As a result, it is hypothesized that mutations near the C-terminus that disrupt triple helix assembly are less tolerated than N-terminal mutations because they have more significant downstream effects of helix assembly.<sup>593</sup> Consequently, ligand-binding sites have predominantly evolved closer to the C-terminus. Together, these data suggest GPAGPOGPI may be the primary interaction site between type I collagen and MMRN1.

The ability of wild-type but not *Mmrn1*<sup>-/-</sup> platelets to adhere to GPAGPOGPX peptides in static adhesion assays provides further evidence that these sequences in fibrillar collagens are specific recognition motifs for MMRN1/Mmrn1. The overall poor

adhesion of wild-type platelets to GPAGPOGPI compared to GPAGPOGPQ may be a consequence of synthesizing the GPAGPOGPI sequence as a homotrimeric triple-helical peptide. As stated above, it is unclear if the corresponding GPVGAAGPA in the  $\alpha_2(I)$  chain of type I collagen contributes key residues that are important for MMRN1 binding. Similarly, in solid-phase binding assays, MMRN1 binding to GPAGPOGPI was consistently lower compared to GPAGPOGPQ or GPAGPOGPV. This may be a result of using synthetic collagen mimetic peptides rather than full-length collagen fibrils. Toolkit and other triple-helical collagen mimetic peptides contain Cys residues at both the N- and C-termini, which allows them to crosslink to one another, but they do not aggregate into native fibrils. The dynamics of polyvalent binding of MMRN1 multimers to collagen fibrils may be important for the amount and stability of MMRN1 binding to GPAGPOGPX sequences, which could result in poor binding between MMRN1 and GPAGPOGPI peptides. The reduction in static adhesion of *Mmrn1*<sup>-/-</sup> to Horn collagen, which is predominantly composed of type I collagen (~95%), under stasis suggests that *Mmrn1* is involved in platelet adhesion to type I collagen, likely through interactions with the GPAGPOGPI/GPVGAAGPV heterotrimer. Another possibility is that there may be MMRN1-binding motifs in type I collagen that are structurally distinct from GPAGPOGPX that support or enhance MMRN1 binding to collagen, which *in silico* searches for GPAGPOGPX-like sequences would not be sensitive to detect.

Fibrillar collagens are unlike many ligands because of their rod-like COL domain that encompasses almost its entire sequence and the propensity of collagens to form large

ultrastructures. This means that collagens have many possible interactions along the entire length of a collagen fiber, many of which would be low affinity, multi-valent interactions. As a result, GPAGPOGPI may be the single, physiologic ligand for MMRN1 in type I collagen, but polyvalent binding between numerous MMRN1 monomers in a larger polymer along the length of a collagen fiber may be required for GPAGPOGPI to support significant MMRN1 binding or platelet adhesion. Another consideration is that, as a consequence of ultrastructural organization of collagen molecules into D-periods, binding sites for platelet receptors and other molecules are not uniformly distributed across the fiber surface. It is hypothesized that binding sites may be presented as coherent bands around the circumference of the fiber,<sup>594</sup> allowing platelet receptors to be recruited in closely packed clusters, which may be required to induce signalling. Clustering of GPAGPOGPX motifs on a fiber surface may similarly be important for MMRN1 binding. Moreover, it is unclear what regions of the collagen monomer are accessible on the fiber surface. Collagen fibrils contain many inter-chain crosslinking sites, and additional molecules, such as type V collagen, are bound to the fibril surface to regulate its function. Some recognition motifs may be concealed by the architecture of a collagen fiber,<sup>595</sup> or, conversely, some motifs may only be present in a suitable conformation when collagen molecules are assembled into fibers.

Testing platelet adhesion to GPAGPOGPX peptides under high shear flow provided further evidence of a potential dual role of Mmrn1 in platelet adhesion to collagen, while also demonstrating specificity of GPAGPOGPQ for Mmrn1 under

laminar flow. Although VWF is considered to be required for significant platelet adhesion under high shear flow, the GPAGPOGPQ-containing peptide was able to enhance the formation of platelet aggregates in the absence of a surface ligand for Vwf when co-presented with GFOGER. It is possible that Mmrn1 released from activated platelets could bind to GPAGPOGPX to provide a surface for attachment of Vwf, which would allow for some degree of platelet tethering in the absence of a surface ligand for Vwf. Additionally, Mmrn1 multimers bound to the platelet surface or bound to GPAGPOGPQ may contribute to platelet tethering that is able to enhance  $\alpha_2\beta_1$ -mediated adhesion to GFOGER under high shear flow. However, it would be expected that if Mmrn1 released into solution binds to GPAGPOGPX to provide a surface for Vwf attachment and platelet tethering, presentation of the GPAGPOGPQ sequence alone would support some degree of platelet adhesion, with morphology similar to surfaces coated with either GPRQOGVMGF or immobilized Vwf. Following perfusion under high shear flow, strings of platelets can be observed on immobilized VWF, rVwf, and GPRQOGVMGF. Wild-type and *Mmrn1*<sup>-/-</sup> platelets failed to adhere to the GPAGPOGPQ-containing peptide under high shear flow, which suggests that Mmrn1 cannot substitute for Vwf in the absence of an additional adhesive ligand, such as GFOGER.

An important observation was that *Mmrn1*<sup>-/-</sup> platelets had impaired aggregate formation on GFOGER surfaces in the absence of a surface ligand for other proteins or receptors. These data provide further evidence that Mmrn1 plays a supporting role in platelet aggregate formation onto adhesive substrates. *Mmrn1*<sup>-/-</sup> platelets have similar

expression of  $\beta_1$  integrin compared to wild-type platelets,<sup>4</sup> and static adhesion of activated *Mmrn1*<sup>-/-</sup> and wild-type platelets to GFOGER is also similar, which indicates the inability of *Mmrn1*<sup>-/-</sup> platelets to form large aggregates on GFOGER surfaces is likely not due to alterations in  $\alpha_2\beta_1$  expression or the ability of  $\alpha_2\beta_1$  to bind GFOGER.

In assays of static platelet adhesion using mouse platelets and triple-helical collagen peptides, GFOGER alone supported adhesion of CRP-activated mouse platelets as well as full-length Horm collagen, which hindered the ability to detect synergy between combinations of triple-helical peptides. In comparison, GFOGER supported roughly 50% of adhesion of CRP-activated human platelets compared to Horm collagen, which provided a sufficient model to test the synergistic effects of GFOGER, GPRQOGVMGF, and GPAGPOGPX on platelet adhesion. These differences between human and mouse platelets may result from the significantly higher copy number of  $\alpha_2\beta_1$  on murine platelets (~16000 copies per platelet)<sup>403</sup> versus human platelets (~1000 to 3000 copies per platelet, *Figure 3*).<sup>430</sup> Even when the relative concentration of GFOGER compared to GPAGPOGPI/Q was titrated down to 10% of GPAGPOGPX concentrations, it was not possible to detect synergy between GFOGER and GPAGPOGPX peptides using CRP-activated mouse platelets. Titration curves indicated that adhesion of activated mouse platelets to GFOGER was nearly all-or-nothing, in that adhesion jumped from no adhesion to maximal adhesion in a window of 0.9  $\mu$ M. In assays using human platelets, GPAGPOGPX peptides were able to synergistically enhance platelet adhesion when presented with GFOGER or GFOGER and III-23. These data provide further evidence

that MMRN1 is able to additively enhance platelet adhesion to collagen without inhibiting VWF- or  $\alpha_2\beta_1$ -mediated adhesion to their respective recognition motifs in collagen. However, as these experiments were performed with triple-helical collagen peptides, it is unclear how the spatial arrangement of immobilized peptides versus native collagen fibrils impacts these findings.

The effect of platelet activation on static adhesion to combinations of triple-helical peptides is consistent with the requirement for platelet activation to release MMRN1. These data provide indirect evidence that GPAGPOGPX sequences may also have high specificity for MMRN1. Ligands with high specificity for MMRN1 would be expected to support minimal adhesion in the absence of MMRN1 on the surface of activated platelets unless the ligand can support adhesion through other mechanisms. Notably, a modest increase in the endpoint adhesion of washed, unstimulated human platelets to GPAGPOGPX peptides co-presented with GFOGER was observed, which may be the result of a small degree of platelet activation inevitably occurring during platelet preparation and less likely, other, unidentified adhesive molecules that can bind this motif to supporting platelet adhesion. The effect of platelet activation on platelet adhesion to GFOGER is also consistent with the observation that platelet activation induces conformational change in  $\alpha_2\beta_1$  that increases the affinity of  $\alpha_2\beta_1$  for GFOGER.<sup>436</sup>

With regard to the MMRN1-binding GPAGPOGPV sequence in type II collagen, it is unclear whether or not this sequence is physiologically relevant to platelet adhesion.

The GPAGPOGPV peptide was able to synergistically enhance platelet adhesion similar to either GPAGPOGPI or GPAGPOGPQ, but the tissue distribution of type II collagen is restricted to cartilage in mammals: fibrocartilage in cartilaginous joints of the pelvis and spine, hyaline cartilage on the articular surface of joints, in the trachea, or in the nose, and elastic cartilage in the epiglottis and outer ear. MMRN1 would likely only contact the GPAGPOGPV sequence in instances wherein flowing blood enters a type II collagen-rich joint capsule or when flowing blood is exposed to cartilaginous structures in the nose, ear, or trachea. Sequence conservation is not necessarily a good indicator of preservation of function for fibrillar collagens because of its repeating structure. Approximately 33% of the triple-helical domain of fibrillar collagens is composed of glycine.<sup>485</sup> Given the requirement of proline in each  $\alpha$ -chain for the formation of a polyproline II-like helix, much of the COL domain is composed of highly conserved proline residues. As a result, fibrillar collagens tend to have highly conserved COL domains because of their structural requirements, and mutations in glycine and proline residues are not well-tolerated due to its ubiquitous distribution and essential developmental and structural role.

#### 4.4 STRENGTHS AND LIMITATIONS OF THIS THESIS

The use of *in vitro* experimentation allows for the control and isolation of specific variables contributing to complex outcomes. MMRN1/Mmrn1 is a multipotent adhesive ligand that binds to adhesive proteins in platelets, plasma, and extracellular matrices, but also has potential roles in supporting thrombin generation and coagulation. It is difficult

to dissect the specific contributions of *Mmrn1* in platelet adhesion using *in vivo* models that involve thrombin generation and coagulation, such as the  $\text{FeCl}_3$ -induced vessel injury model and the tail transection model. These models measure outcomes of thrombosis and hemostasis, respectively, which may be insensitive to detect specific alterations in platelet *Mmrn1* adhesive functions, rather than measuring a holistic outcome. This is evidenced by studies of other supporting proteins in platelet adhesion, such as *Tsp-1*<sup>-/-</sup>, *pFn*<sup>-/-</sup>, and *Vn*<sup>-/-</sup> mice, which have normal bleeding times and only somewhat altered thrombus formation (*Table 1*), despite numerous *in vitro* studies that demonstrate more complex supporting roles of these proteins in platelet adhesion and platelet aggregation.

The experiments performed in this thesis have the advantage of inhibiting or removing specific components of hemostatic or thrombotic responses (i.e. thrombin generation, platelet activation, presence or absence of plasma, or composition of extracellular matrices). These conditions enable the study of platelet adhesion at varying levels of complexity: whole blood vs. washed platelets, resting vs. pre-activated platelets, with or without antibody blockade of specific receptors, and control over the composition of immobilized adhesive substrates. *In vitro* experiments also enable strict control over rheological parameters (i.e. shear rate, tube diameter, and pulsatile vs. constant flow), which greatly affect platelet adhesive properties. Further, the use of triple-helical collagen mimetic peptides allows for the manipulation of individual recognition motifs in collagen independent of one another in order to define their specific and synergistic roles, and eliminates the variability observed between different fibrillar collagen preparations.<sup>596</sup>

Consequently, triple-helical collagen mimetic peptides have been instrumental in the current understanding of the type I, II, and III collagen interactomes as well as the functional properties of recognition motifs in collagens.<sup>548</sup> The use of purified proteins are useful for elucidating specific mechanisms, but it is equally important to consider that protein-coated surfaces fail to reflect the integrated function of all components present in the extracellular matrix of the vessel wall.

A major limitation in studying platelet adhesion and platelet-collagen interactions is establishing the relevance of *in vitro* findings using *in vivo* models. Fibrillar collagen exposure would be most evident in extravascular injuries, that is, when platelets in flowing blood are exposed to: 1) the collagen-rich structures of the tunica media and adventitia of blood vessels, 2) type I collagen-rich dense and loose fibrous tissues (i.e. skin, tendons, and ligaments), 3) type III collagen-rich reticular meshwork of adipose tissue, and 4) type II collagen-rich cartilage. The most commonly used *in vivo* models of arterial thrombosis include FeCl<sub>3</sub> treatment of the carotid artery<sup>229,464,563,597</sup> or mesenteric arterioles,<sup>3,204,208,211,215</sup> laser-induced injury of cremaster muscle arterioles,<sup>33,203,204,598–600</sup> or photochemical injury of the carotid artery following injection of Rose-Bengal dye.<sup>440,601,602</sup> Within these models, the degree and extent of collagen exposure is not well-understood and these models assess thrombosis, not hemostasis. Collagen-induced thrombosis can be measured directly by intravenous injection of collagen or collagen-like peptides,<sup>310,440</sup> but these models fail to recapitulate the conditions of exposed, insoluble collagen fibers in the vessel wall following injury. A major limitation of commonly used

murine models of thrombosis is that they induce platelet adhesion artificially within intact vessels. A model involving exposure of adventitial fibrillar collagen exposure to flowing blood has been reported,<sup>603</sup> which may be useful for studying *Mmrn1* contributions to collagen-induced thrombosis in arteries and veins, but thrombosis also occurs within vessel lumina in this model.

An *in vivo* model has been developed to visualize hemostatic plug formation on the inner and outer surfaces of the vessel wall following puncture of the jugular vein in mice.<sup>604</sup> The findings of these studies highlight major differences in the architecture of hemostatic plugs versus thrombi formed within vessels, specifically that the collagen-rich outer surface of the vessel wall is the primary site of platelet activation,  $\alpha$ -granule release, thrombin generation, and fibrin formation, whereas the luminal surface of the plug is composed predominantly of resting, discoid platelets that show minimal  $\alpha$ -granule release and fibrin formation.<sup>604</sup>

The development of transgenic or knockout mouse models to study the importance of GPAGPOGPX sequences *in vivo* is particularly limited by the inherent properties of fibrillar collagens. Due to the ubiquitous distribution of fibrillar collagens, which make up approximately 30% of total protein mass in humans, mutations or deletions in collagen genes have systemic, often lethal consequences. Developing a mouse model in which GXOGEX', GPRQOGVMGF, and/or GPAGPOGPX sequences are mutated or deleted would likely have systemic, potentially lethal consequences.

Further, it would be difficult to interpret whether bleeding diatheses in collagen mutant mice are due to defects in platelet adhesion or because of vessel fragility as a consequence of compromised collagen triple-helices, which are pronounced clinical features of collagen-related diseases EDS and OI and in a mouse model of EDS.<sup>516,593,605,606</sup> Together, these considerations make it difficult to the effects of MMRN1-binding GPAGPOGPX motifs in fibrillar collagens through *in vivo* experimentation. As a result, this thesis relies on *in vitro* evidence to characterize the mechanisms through which *Mmrn1* supports platelet adhesion to collagen via GPAGPOGPX sequences in fibrillar collagens.

#### 4.5 CONCLUSIONS AND FUTURE DIRECTIONS

The questions addressed in this thesis contribute to the fundamental understanding of platelet adhesion, which is a critical first step in cessation of blood loss following injury or in the development of platelet-rich thrombi. Many of the mechanisms involved in hemostasis are conserved in thrombosis, making it crucially important to develop therapies for the prevention or treatment of thrombotic diseases that do not significantly compromise hemostasis. MMRN1 is an attractive potential therapeutic target because *in vivo* evidence suggests that *Mmrn1* deficiency is anti-thrombotic without significantly impairing hemostasis. Future therapies that block the functions of “supporting proteins” such as MMRN1, TSP-1, multimeric platelet VN, or platelet FN could be useful in combination therapy to enhance the efficacy of anti-platelet drugs without significantly

impacting hemostasis. More specifically, given that MMRN1/*Mmrn1* contributes to platelet adhesion to collagen, anti-MMRN1 therapy may be useful for exploring in the treatment of atherothrombosis, in which the type I collagen-rich fibrous cap formed over an atherosclerotic plaque ruptures and is exposed to flowing blood. Equally, it is important to consider that species differences may affect the phenotype of qualitative or quantitative defects in MMRN1 versus *Mmrn1*.

Although selective MMRN1 deficiency has not been described in human patients, the causes of many inherited platelet function disorders (PFDs) are uncharacterized.<sup>607</sup> It is possible that selective defects in MMRN1 could be the cause of some cases of PFD, but all of what is presently known about the phenotype of selective MMRN1 deficiency comes from studies of *Mmrn1* knockout mice. Based on studies of *Mmrn1*<sup>-/-</sup> mice, specific types of analyses (i.e. testing platelet adhesion to collagen under high shear flow or collagen-induced aggregation of gel-filtered platelets) would be required to suggest involvement of MMRN1. Typical laboratory tests of platelet function would not be sensitive to detect MMRN1 deficiency in human patients,<sup>608</sup> making it unlikely that a selective defect in MMRN1 would be identified through routine laboratory testing for platelet function disorders.

It has also been argued that mechanisms of platelet adhesion to fibrillar collagens are redundant in hemostasis,<sup>531</sup> based on the relatively mild phenotypes of transgenic and knockout mouse models and cases of human patients with deficiencies or defects in

platelet collagen receptors. What is not often considered is the process of wound healing, in which fibroblasts and smooth muscle cells infiltrate the area of injury to regenerate and remodel the damaged extracellular matrix structures. For example, in addition to the role of FN in platelet adhesion and aggregation, FN fibers are a normal part of extracellular matrices of connective tissues that appear to play an important role in wound healing.<sup>275,609</sup> Similarly, the role of MMRN1 may not be limited to the processes of platelet adhesion and aggregation in hemostasis, and may have important functions in the wound healing process during and following the dissolution of a hemostatic plug. Other proteins in the EMILIN/Multimerin family are normal constituents of extracellular matrices containing elastic fibers, including the outer layers of arteries and veins. Given the high homology between EMILINs and MMRN1, it is possible that platelet MMRN1 released at sites of injury may serve similar functions following hemostatic plug formation.

The results described in this thesis raised numerous questions regarding additional mechanisms of MMRN1 in platelet adhesion and identified a need for verifying *in vitro* data using models of collagen-mediated hemostasis or collagen-induced thrombosis *in vivo*. It is also interesting to consider how mutations in collagens might have effects on platelet adhesion and contribute to part of the bleeding phenotype exhibited by some patients with EDS or OI. The following sections will discuss additional studies that could be performed to answer some of these questions.

#### 4.5.1 Possible effect of multimerin 1 on VWF multimer size

As suggested in *section 4.2.1*, *Mmrn1* may contribute to platelet adhesion and thrombus formation partly by binding plasma and platelet Vwf, which could: 1) generate large, highly adhesive heteropolymers composed of *Mmrn1* and Vwf, or 2) prevent ADAMTS13-mediated cleavage of Vwf to facilitate the formation of and maintain the size of ULVwf multimers at sites of injury. First, the ability of MMRN1 to form large heteropolymers with VWF/Vwf could be tested *in vitro* using recombinant VWF or Vwf and rhMMRN1. Purified VWF or VWF in normal or ADAMTS13-deficient plasma could be exposed to ristocetin or shear to induce exposure of the cryptic MMRN1-binding sites in VWF A1 and A3 in the presence or absence of varying concentrations of rhMMRN1. Multimer size could then be resolved using non-reduced agarose-acrylamide gel electrophoresis and Western blotting. There is also a possibility that *Mmrn1* augments Vwf multimer size within platelet and endothelial cell storage granules, although studies of *Tsp-1<sup>-/-</sup>* mice generated on different background strains have reported conflicting results.<sup>225,363</sup> *Tsp-1<sup>-/-</sup>* C57BL/6J mice show smaller Vwf multimers in platelets and endothelial cells compared to the wild-type, but Vwf multimer size is similar between *Tsp-1<sup>-/-</sup>* and wild-type Swiss mice. TSP-1 has been demonstrated to block VWF A2 cleavage by ADAMTS13 *in vitro*,<sup>362</sup> which has been demonstrated *in vivo* using *Tsp-1<sup>-/-</sup>* mice.<sup>225</sup> These assays could be adapted to test the ability of MMRN1 to competitively bind VWF to prevent cleavage by ADAMTS13 in a dose-dependent manner *in vitro* and measure ultra-large Vwf degradation *in vivo* using *Mmrn1<sup>-/-</sup>* mice. These experiments

would clarify part of the mechanism through which MMRN1 supports VWF adhesive functions.

#### 4.5.2 Generation and testing of additional mouse models

The ability of *Mmrn1* to augment platelet adhesion and thrombus formation following exposure to fibrillar collagens *in vivo* could be investigated using methods described in *section 4.4*. The jugular vein puncture model is most appropriate for studying the effects of *Mmrn1* on platelet adhesion to collagens because it best recapitulates conditions of extravascular injury involving collagen-rich matrices. It may also be possible to modify this model to assess hemostatic plug formation in arteries or differently-sized vessels. Additionally, there is a collagen-induced thrombosis model in which a section of the epigastric artery is dissected from donor mice and inserted into the carotid artery or femoral vein of anesthetized recipient mice to induce thrombus formation by exposure of the fibrillar collagen-rich adventitia of the epigastric artery to flowing blood.<sup>603</sup> However, this model involves intravascular thrombus formation, which might be useful as a model for studying collagen-induced thrombosis, but not for studies of hemostatic plug formation. The collagen-dependent thrombosis model that measures pulmonary embolism following collagen or peptide injection is less appealing because it would not directly test platelet adhesion to immobilized fibrillar collagen surfaces at a site of injury.

The presence of *Mmrn1* in both platelet and endothelial cell granules combined with its proposed contributions to Fv storage and thrombin generation complicates interpretations of *in vivo* observations. Using global *Mmrn1* knockout animals, it is difficult to ascertain whether defects in platelet adhesion are due to platelet *Mmrn1* loss or if the endothelial cell pool of *Mmrn1* plays an important, or potentially greater, role in platelet adhesion and thrombus formation. The specific contributions of platelet *Mmrn1* in fibrillar collagen-dependent thrombus formation could be studied using bone marrow transplantation, which has already been used to identify the relative contributions of platelet vs. endothelial cell Vwf in thrombosis.<sup>332</sup> These studies would untangle the relative importance of platelet vs. endothelial cell *Mmrn1* in experimental models of thrombosis, and help orient the findings of this thesis in an *in vivo* setting, which centre on platelet *Mmrn1*. The jugular vein puncture model, coupled with the generation of cell type-specific *Mmrn1* knockout mice, could be used to validate some of the results in this thesis *in vivo* and address some ambiguities of the results obtained using the FeCl<sub>3</sub>-induced mesenteric vessel injury model and global *Mmrn1*<sup>-/-</sup> mice.

#### 4.5.3 Impact of triple-helical conformation and mutations in MMRN1 binding to GPAGPOGPX sequences

Triple-helical conformation is required for GPVI binding to GPO repeats or  $\alpha_2\beta_1$  binding to GFOGER.<sup>540,543</sup> It may be similarly required for MMRN1 binding to GPAGPOGPX motifs. As previously reported, synthesizing GPAGPOGPX peptides

within (GAP)<sub>5</sub> host sequences, which do not spontaneously assemble into triple-helices, could be used to determine if triple-helical conformation of GPAGPOGPX peptides is required for MMRN1 binding. Although the GPAGPOGPI and GPAGPOGPQ sequences are unique to collagen, there may be non-triple-helical GPAGPOGPX-like sequences in other proteins. The substitution of the hydrophobic residue V to another hydrophobic residue I is a conservative mutation,<sup>566</sup> and both the GPAGPOGPV and GPAGPOGPI peptides support MMRN1 binding. It could be that other proteins contain GPAGPOGPX sequences where X is occupied by a different hydrophobic residue, which could consequently support MMRN1 binding. An *in silico* search for sequences containing GPAGPOGPX sequences where X is occupied by any of the amino acids with a hydrophobic side chain could reveal additional MMRN1-binding motifs in other proteins. Interestingly, substitution of V to Q is not a conservative mutation,<sup>566</sup> but both GPAGPOGPV and GPAGPOGPQ support MMRN1 binding very well, meaning that residues in the X position may not be limited to hydrophobic residues alone. Further, without performing studies of site-directed mutagenesis of the GPAGPOGPX motif, it is unclear which residues in this sequence are critical for MMRN1 binding. This means that while GPAGPOGP(I/V/Q) is unique to collagens, there could be other variants of this sequence that possess the key residues for MMRN1 binding, but differ dramatically in others, which would make detection of these types of potential MMRN1-binding sequences by *in silico* analyses difficult. Firstly, determining whether or not linear (non-triple-helical) GPAGPOGPX peptides bind MMRN1 would provide evidence for whether

or not linear GPAGPOGPX-like sequences in other proteins could potentially support MMRN1 binding.

As mentioned in *section 4.3*, mutations in the MMRN1-binding GPAGPOGPX motifs could affect MMRN1 binding and platelet adhesion, similar to reports of Gly mutations in the GFOGER sequence.<sup>610,611</sup> Disease-causing mutations have been reported in the GPAGPOGPI and GPAGPOGPQ sequences. Mutations in the GPAGPOGPI motif (G845R and G848R) are associated with type II (perinatal lethal) OI<sup>517</sup> and a mutation in GPAGPOGPQ (G852C) is associated with type IV (vascular type) EDS. The effects of missense Gly mutations within and surrounding the GFOGER sequence on integrin binding have been tested using recombinant bacteria that express a triple-helical collagen-like protein, and this model could be applied to study the effects of Gly mutations in GPAGPOGPX motifs on MMRN1 binding. In these studies, mutation of either Gly residue in GFOGER abolishes  $\alpha_2\beta_1$  binding and results in disruption of inter-chain hydrogen bonds within the affected portion of the triple helix.<sup>610</sup> Additionally, substitution of Gly residues to the N-terminal side of the inserted GFOGER sequence is able to impair  $\alpha_2\beta_1$  binding.<sup>611</sup> It has been previously postulated that mutations in fibrillar collagens that locally disrupt triple helix assembly could have systemic consequences on ligand binding at other areas within the COL domain.<sup>593</sup> It is therefore difficult to conclude how specific mutations might affect other ligand binding sites in collagen, and consequently, different aspects of platelet adhesion to collagen. Other studies have used cultured fibroblasts from patients with fibrillar collagen mutations to test their effects on

ligand binding and cell adhesion. Cell databases could be accessed to obtain fibroblasts from patients with COL domain mutations in recognition motifs in collagens that support platelet adhesion or activation in order to study the systemic effects of various collagen mutations on platelet adhesion and MMRN1 binding to collagen.

## REFERENCES

1. Adam F, Zheng S, Joshi N, et al. Analyses of cellular multimerin 1 receptors: in vitro evidence of binding mediated by  $\alpha$ IIb $\beta$ 3 and  $\alpha$ V $\beta$ 3. *Thromb. Haemost.* 2005;94:1004–1011.
2. Tasneem S, Adam F, Minullina I, et al. Platelet adhesion to multimerin 1 in vitro: influences of platelet membrane receptors, von Willebrand factor and shear. *J. Thromb. Haemost.* 2009;7:685–692.
3. Rehemian A, Tasneem S, Ni H, Hayward CPM. Mice with deleted multimerin 1 and  $\alpha$ -synuclein genes have impaired platelet adhesion and impaired thrombus formation that is corrected by multimerin 1. *Thromb. Res.* 2010;125(5):e177–e183.
4. Parker DN. Functions of multimerin 1 (MMRN1) in platelet adhesion and thrombus formation, through interactions with von Willebrand factor (VWF). 2017;
5. Jeimy SB, Fuller N, Tasneem S, et al. Multimerin 1 binds factor V and activated factor V with high affinity and inhibits thrombin generation. *Thromb. Haemost.* 2008;100(6):1058–1067.
6. Hayward CPM, Rivard GE, Kane WH, et al. An autosomal dominant, qualitative platelet disorder associated with multimerin deficiency, abnormalities in platelet factor V, thrombospondin, von Willebrand factor, and fibrinogen and an epinephrine aggregation defect. *Blood.* 1996;87(12):4967–4978.
7. Hayward CPM, Furmaniak-Kazmierczak E, Cieutat AM, et al. Factor V is complexed with multimerin in resting platelet lysates and colocalizes with multimerin in platelet  $\alpha$ -granules. *J. Biol. Chem.* 1995;270(33):19217–19224.
8. Braghetta P, Ferrari A, De Gemmis P, et al. Overlapping, complementary and site-specific expression pattern of genes of the EMILIN/Multimerin family. *Matrix Biol.* 2004;22:549–556.
9. Colombatti A, Spessotto P, Doliana R, et al. The EMILIN/multimerin family. *Front. Immunol.* 2012;2(JAN):1–13.
10. Hayward CPM, Hassell JA, Denomme GA, et al. The cDNA sequence of human endothelial cell multimerin. *J. Biol. Chem.* 1995;270(31):18246–18251.
11. Hayward CPM, Bainton DF, Smith JW, et al. Multimerin is found in the  $\alpha$ -granules of resting platelets and is synthesized by a megakaryocytic cell line. *J. Clin. Invest.* 1993;91:2630–2639.
12. Hayward CPM, Song Z, Zheng S, et al. Multimerin processing by cells with and without pathways for regulated Protein secretion. *Blood.* 1999;94:1337–1347.
13. Kika Veljkovic D, Cramer EM, Fichelson S, Massé J-M, Hayward CPM. Studies of  $\alpha$ -granule proteins in cultured human megakaryocytes. *Thromb. Haemost.* 2003;90(5):844–852.
14. Hayward CPM, Warkentin TE, Horsewood P, Kelton JG. Multimerin: a series of large disulfide-linked multimeric proteins within platelets. *Blood.* 1991;77(12):2556–2560.
15. Hayward CPM, Smith JW, Horsewood P, Warkentin TE, Kelton JG. P-155, a multimeric platelet protein that is expressed on activated platelets. *J. Biol. Chem.*

- 1991;266(11):7114–7120.
16. Hayward CPM, Kelton JG. Multimerin: A Multimeric Protein Stored in Platelet Alpha-granules. *Platelets*. 1995;6:1–10.
  17. Hayward CPM, Cramer EM, Song Z, et al. Studies of multimerin in human endothelial cells. *Blood*. 1998;91(0006-4971 (Print)):1304–1317.
  18. Jeimy SB, Tasneem S, Cramer EM, Hayward CPM. Multimerin 1. *Platelets*. 2008;19(2):83–95.
  19. Hayward CPM. Platelet multimerin and its proteolytic processing. *Thromb. Haemost.* 1999;82:1779–1780.
  20. Hayward CPM, Fuller N, Zheng S, et al. Human platelets contain forms of factor V in disulfide-linkage with multimerin. *Thromb. Haemost.* 2004;92(6):1349–1357.
  21. Parker DN, Tasneem S, Farndale RW, et al. The functions of the A1A2A3 domains in von Willebrand factor include multimerin 1 binding Cellular Haemostasis and Platelets. *Thromb. Haemost.* 2016;116:87–95.
  22. Pawlikowska M. Characterization of the mechanisms that support multimerin 1 binding to collagen in vitro. 2010;
  23. Jeimy SB, Woram RA, Fuller N, et al. Identification of the MMRN1 binding region within the C2 domain of human factor V. *J. Biol. Chem.* 2004;279(49):51466–51471.
  24. Camire RM, Bos MHA. The molecular basis of factor V and VIII procofactor activation. *J. Thromb. Haemost.* 2009;7(12):1951–1961.
  25. Jeimy SB, Quinn-Allen MA, Fuller N, Kane WH, Hayward CPM. Location of the multimerin 1 binding site in coagulation factor V: an update. *Thromb. Res.* 2008;123:352–354.
  26. Jeimy SB, Krakow EF, Fuller N, Tasneem S, Hayward CPM. An acquired factor V inhibitor associated with defective factor V function, storage and binding to multimerin 1. *J. Thromb. Haemost.* 2008;6(2):395–397.
  27. Hayward CPM, Weiss HJ, Lages B, et al. The storage defects in grey platelet syndrome and  $\alpha\delta$ -storage pool deficiency affect  $\alpha$ -granule factor V and multimerin storage without altering their proteolytic processing. *Br. J. Haematol.* 2001;113(4):871–877.
  28. Specht CG, Schoepfer R. Deletion of multimerin-1 in  $\alpha$ -synuclein-deficient mice. *Genomics*. 2004;83(6):1176–1178.
  29. Park SM, Jung HY, Kim HO, et al. Evidence that  $\alpha$ -synuclein functions as a negative regulator of  $\text{Ca}^{++}$ -dependent  $\alpha$ -granule release from human platelets. *Blood*. 2002;100(7):2506–2514.
  30. Skarnes WC, Rosen B, West AP, et al. A conditional knockout resource for the genome-wide study of mouse gene function. *Nature*. 2011;474(7351):337–344.
  31. Testa G, Schaft J, Van Der Hoeven F, et al. A Reliable lacZ Expression Reporter Cassette for Multipurpose, Knockout-First Alleles. *Genesis*. 2004;38(3):151–158.
  32. Diamandis M, Veljkovic DK, Maurer-Spurej E, Rivard GE, Hayward CPM. Quebec platelet disorder: features, pathogenesis and treatment. *Blood Coagul. Fibrinolysis*. 2008;19(2):109–119.
  33. Kahr WHA, Lo RW, Li L, et al. Abnormal megakaryocyte development and

- platelet function in *Nbeal2*<sup>-/-</sup> mice. *Blood*. 2013;122(19):3349–3358.
34. Albers CA, Cvejic A, Favier R, et al. Exome sequencing identifies NBEAL2 as the causative gene for Gray Platelet Syndrome. *Nat. Gen.* 2012;43(8):735–737.
  35. Kahr WHA, Hinckley J, Li L, et al. Mutations in NBEAL2, encoding a BEACH protein, cause gray platelet syndrome. *Nat. Genet.* 2011;43(8):738–740.
  36. Monteferrario D, Bolar NA, Marneth AE, et al. A dominant-negative GFI1B mutation in the gray platelet syndrome. *N. Engl. J. Med.* 2014;370(3):245–253.
  37. Tubman VN, Levine JE, Campagna DR, et al. X-linked gray platelet syndrome due to a GATA1 Arg216Gln mutation. *Blood*. 2007;109(8):3297–3299.
  38. Lee AC. Idiopathic purpura with gray platelets: an acquired form or Gray Platelet Syndrome. *J. Pediatr. Hematol. Oncol.* 2019;41(1):47–50.
  39. Malicdan MC, Markello TC, Gunay-aygun M, William A. Combined alpha-delta platelet storage pool deficiency is associated with mutations in GFI1b. *Mol. Genet. Metab.* 2017;120(3):288–294.
  40. Lentaigne C, Greene D, Sivapalaratnam S, et al. Germline mutations in the transcription factor IKZF5 cause thrombocytopenia. *Blood*. 2019;134(23):2070–2081.
  41. Versteeg HH, Heemskerk JWM, Levi M, Reitsma PH. New fundamentals in hemostasis. *Physiol. Rev.* 2013;93:327–358.
  42. Beckman MG, Hooper WC, Critchley SE, Ortel TL. Venous Thromboembolism. A Public Health Concern. *Am. J. Prev. Med.* 2010;38(4 SUPPL.):S495–S501.
  43. Benjamin EJ, Muntner P, Alonso A, et al. Heart Disease and Stroke Statistics-2019 Update: A Report From the American Heart Association. 2019.
  44. Heron M. National Vital Statistics Reports Deaths: leading causes for 2013. *Natl. vital Stat. reports from Centers Dis. Control Prev. Natl. Cent. Heal. Stat. Natl. Vital Stat. Syst.* 2016;65(2):1–95.
  45. Undas A, Ariëns RAS. Fibrin clot structure and function: A role in the pathophysiology of arterial and venous thromboembolic diseases. *Arterioscler. Thromb. Vasc. Biol.* 2011;31(12):88–99.
  46. MacFarlane FG. An enzyme cascade in the blood clotting mechanism. and its function as a biochemical amplifier. *Nature*. 1964;202:498–499.
  47. Davie EW, Ratnoff OD. Waterfall sequence for intrinsic blood clotting. *Science (80- )*. 1964;145(3638):1310–1312.
  48. Butenas S, Orfeo T, Mann KG. Tissue factor in coagulation: Which? where? when? *Arterioscler. Thromb. Vasc. Biol.* 2009;29(12):1989–1996.
  49. Wilcox JN, Smith KM, Schwartz SM, Gordon D. Localization of tissue factor in the normal vessel wall and in the atherosclerotic plaque. *Proc. Natl. Acad. Sci. U. S. A.* 1989;86(8):2839–2843.
  50. Fleck RA, Rao L V., Rapaport SI, Varki N. Localization of human tissue factor antigen by immunostaining with monospecific, polyclonal anti-human tissue factor antibody. *Thromb. Res.* 1990;59(2):421–437.
  51. Drake TA, Morrissey JH, Edgington TS. Selective cellular expression of tissue factor in human tissues. Implications for disorders of hemostasis and thrombosis. *Am. J. Pathol.* 1989;134(5):1087–1097.

52. Maynard JR, Dreyer BE, Stemerman MB, Pitlick FA. Tissue-factor coagulant activity of cultured human endothelial and smooth muscle cells and fibroblasts. *Blood*. 1977;50(3):387–396.
53. Panes O, Matus V, Saez CG, et al. Human platelets synthesize and express functional tissue factor. *Blood*. 2007;109(12):5242–5250.
54. Camera M, Frigerio M, Toschi V, et al. Platelet activation induces cell-surface immunoreactive tissue factor expression, which is modulated differently by antiplatelet drugs. *Arterioscler. Thromb. Vasc. Biol.* 2003;23(9):1690–1696.
55. Brambilla M, Camera M, Colnago D, et al. Tissue factor in patients with acute coronary syndromes: Expression in platelets, leukocytes, and platelet-leukocyte aggregates. *Arterioscler. Thromb. Vasc. Biol.* 2008;28(5):947–953.
56. Kirchhofer D, Tschopp TB, Hadvary P, Baumgartner HR. Endothelial cells stimulated with tumor necrosis factor- $\alpha$  express varying amounts of tissue factor resulting in inhomogenous fibrin deposition in a native blood flow system. Effects of thrombin inhibitors. *J. Clin. Invest.* 1994;93(5):2073–2083.
57. Parry GCN, Mackman N. Transcriptional regulation of tissue factor expression in human endothelial cells. *Arterioscler. Thromb. Vasc. Biol.* 1995;15(5):612–621.
58. Nawroth P, Handley DA, Esmon CT, Stern DM. Interleukin 1 induces endothelial cell procoagulant activity while suppressing cell-surface anticoagulant activity. *Proc. Natl. Acad. Sci. U. S. A.* 1986;83(10):3460–2464.
59. Gregory SA, Morrissey JH, Edgington TS. Regulation of tissue factor gene expression in the monocyte procoagulant response to endotoxin. *Mol. Cell. Biol.* 1989;9(6):2752–2755.
60. Haynes LM, Dubief YC, Mann KG. Membrane binding events in the initiation and propagation phases of tissue factor-initiated zymogen activation under flow. *J. Biol. Chem.* 2012;287(8):5225–5234.
61. Iino M, Foster DC, Kisiel W. Functional consequences of mutations in Ser-52 and Ser-60 in human blood coagulation factor VII. *Arch. Biochem. Biophys.* 1998;352(2):182–192.
62. Stern DM, Drillings M, Kisiel W, et al. Activation of factor IX bound to cultured bovine aortic endothelial cells. *Proc. Natl. Acad. Sci. U. S. A.* 1984;81(3):913–917.
63. White II GC, Marder VJ, Schulman S, Aird WC, Bennett JS. Overview of basic coagulation and fibrinolysis. *Hemost. Thromb. Basic Princ. Clin. Pract.* 2013;104–109.
64. Morrissey JH, Smith SA. Polyphosphate as modulator of hemostasis, thrombosis, and inflammation. *J. Thromb. Haemost.* 2015;13(Suppl 1):S92-97.
65. Miller G, Silverberg M, Kaplan AP. Autoactivatability of human Hageman factor (factor XII). *Biochem. Biophys. Res. Commun.* 1980;92(3):803–810.
66. Kurachi K, Davie EW. Activation of human factor XI (plasma thromboplastin antecedent) by factor XIIa (activated Hageman factor). *Biochemistry.* 1977;16(26):5831–5839.
67. Kurachi K, Fujikawa K, Davie EW. Mechanism of activation of bovine factor XI by factor XII and factor XIIa. *Biochemistry.* 1980;19(7):1330–1338.
68. Davie EW, Kulman JD. An overview of the structure and function of thrombin.

- Semin. Thromb. Hemost.* 2006;32(Suppl 1):3–15.
69. Naito K, Fujikawa K. Activation of human blood coagulation factor XI independent of factor XII. Factor XI is activated by thrombin and factor XIa in the presence of negatively charged surfaces. *J. Biol. Chem.* 1991;266(12):7353–7358.
  70. Zhu S, Travers RJ, Morrissey JH, Diamond SL. FXIa and platelet polyphosphate as therapeutic targets during human blood clotting on collagen/tissue factor surfaces under flow. *Blood.* 2015;126(12):1494–1502.
  71. Nemerson Y. Tissue factor and the initiation of blood coagulation. *Adv. Exp. Med. Biol.* 1987;214:83–94.
  72. Rapaport SI. The initiation of the tissue factor dependent pathway of coagulation. *Adv. Exp. Med. Biol.* 1990;281:97–103.
  73. Edgington TS, Ruf W, Rehemtulla A, Mackman N. The molecular biology of initiation of coagulation by tissue factor. *Curr. Stud. Hematol. Blood Transfus.* 1991;58:15–21.
  74. Nesheim ME, Taswell JB, Mann KG. The contribution of bovine factor V and factor Va to the activity of prothrombinase. *J. Biol. Chem.* 1979;254(21):10952–10962.
  75. Rosing J, Tans G, Govers-Riemslog JW, Zwaal RF, Hemker HC. The role of phospholipids and factor Va in the prothrombinase complex. *J. Biol. Chem.* 1980;255(1):274–283.
  76. van Dieijen G, Tans G, Rosing J, Hemker HC. The role of phospholipid and factor VIIIa in the activation of bovine factor X. *J. Biol. Chem.* 1981;256(7):3433–3442.
  77. Ren M, Li R, Chen N, et al. Platelet-derived factor V is a critical mediator of arterial thrombosis. *J. Am. Heart Assoc.* 2017;6(7):1–9.
  78. Duckers C, Simioni P, Spiezia L, et al. Residual platelet factor V ensures thrombin generation in patients with severe congenital factor V deficiency and mild bleeding symptoms. *Blood.* 2010;115(4):879–886.
  79. Hantgan RR, Fowler WE, Erickson HP, Hermans J. Fibrin assembly: a comparison of electron microscopic and light scattering results. *Thromb. Haemost.* 1980;44(3):119–124.
  80. Hantgan RR, Hermans J. Assembly of fibrin. A light scattering study. *J. Biol. Chem.* 1979;254(22):11272–11281.
  81. Greenberg CS, Miraglia CC, Rickles FR, Shuman MA. Cleavage of blood coagulation factor XIII and fibrinogen by thrombin during in vitro clotting. *J. Clin. Invest.* 1985;75(5):1463–1470.
  82. Lahav J, Tvito A, Bagoly Z, Dardik R, Inbal A. Factor XIII improves platelet adhesion to fibrinogen by protein disulfide isomerase-mediated activity. *Thromb. Res.* 2013;131(4):338–341.
  83. Esmon CT. The protein C pathway. *Chest.* 2003;124(Suppl 3):S26–32.
  84. Madonna R, De Caterina R. Potential roles of vessel wall heparan sulfate proteoglycans in atherosclerosis. *Vascul. Pharmacol.* 2014;60(2):49–51.
  85. Jin L, Abrahams JP, Skinner R, et al. The anticoagulant activation of antithrombin by heparin. *Proc. Natl. Acad. Sci. U. S. A.* 1997;94(26):14683–14688.
  86. Gross PL, Murray RK, Weil A, Rand ML. Hemostasis & thrombosis. *Harper's*

- Illus. Biochem.* 2015;713–723.
87. Chapin JC, Hajjar KA. Fibrinolysis and the control of blood coagulation. *Blood Rev.* 2015;29(1):17–24.
  88. Stricker RB, Wong D, Shiu DT, Reyes PT, Shuman MA. Activation of plasminogen by tissue plasminogen activator on normal and thrombasthenic platelets: effects on surface proteins and platelet aggregation. *Blood.* 1986;68:275–280.
  89. Andrade-Gordon P, Strickland S. Interaction of heparin with plasminogen activators and plasminogen: effects on the activation of plasminogen. *Biochemistry.* 1986;25(14):4033–4040.
  90. Mann KG, Jenny RJ, Krishnaswamy S. Cofactor proteins in the assembly and expression of blood clotting enzyme complexes. *Annu. Rev. Biochem.* 1988;57:915–956.
  91. Morrissey JH, Tajkhorshid E, Rienstra CM. Nanoscale studies of protein-membrane interactions in blood clotting. *J. Thromb. Haemost.* 2011;9(Suppl 1):162–167.
  92. Huang M, Rigby AC, Morelli X, et al. Structural basis of membrane binding by Gla domains of vitamin K-dependent proteins. *Nat. Struct. Biol.* 2003;10(9):751–756.
  93. Zwaal RF, Comfurius P, Bevers EM. Lipid-protein interactions in blood coagulation. *Biochim. Biophys. Acta.* 1998;1376(3):433–453.
  94. Mann KG, Nesheim ME, Church WR, Haley P, Krishnaswamy S. Surface-dependent reactions of the vitamin K-dependent enzyme complexes. *Blood.* 1990;76(1):1–16.
  95. Heemskerk JWM, Bevers EM, Lindhout T. Platelet activation and blood coagulation. *Thromb. Haemost.* 2002;88:186–193.
  96. Krishnaswamy S. Prothrombinase complex assembly. Contributions of protein-protein and protein-membrane interactions toward complex formation. *J. Biol. Chem.* 1990;265(7):3708–3718.
  97. Berndt MC, Metharom P, Andrews RK. Primary haemostasis: Newer insights. *Haemophilia.* 2014;20(S4):15–22.
  98. Vinholt PJ. The role of platelets in bleeding in patients with thrombocytopenia and hematological disease. *Clin. Chem. Lab. Med.* 2019;57(12):1808–1817.
  99. Slichter SJ. Relationship between platelet count and bleeding risk in thrombocytopenic patients. *Transfus. Med. Rev.* 2004;18(3):153–167.
  100. Ho-Tin-Noé B, Jadoui S. Spontaneous bleeding in thrombocytopenia: is it really spontaneous? *Transfus. Clin. Biol.* 2018;25(3):210–216.
  101. Terpening C. An appraisal of dual antiplatelet therapy with clopidogrel and aspirin for prevention of cardiovascular events. *J. Am. Board Fam. Med.* 2009;22(1):51–56.
  102. ESPRIT study group, Halkes PH, van Gijn J, et al. Aspirin plus dipyridamole versus aspirin alone after cerebral ischaemia of arterial origin (ESPRIT): randomised controlled trial. *Lancet.* 2006;367(9523):1665–1673.
  103. Schneider DJ. Anti-platelet therapy: glycoprotein IIb-IIIa antagonists. *Br. J. Clin.*

- Pharmacol.* 2011;72(4):672–682.
104. Wijeyeratne YD, Heptinstall S. Anti-platelet therapy: ADP receptor antagonists. *Br. J. Clin. Pharmacol.* 2011;72(4):647–657.
  105. McNicol A, Israels SJ. Platelets and anti-platelet therapy. *J. Pharmacol. Sci.* 2003;93(4):381–396.
  106. Daly M. Determinants of platelet count in humans. *Haematologica.* 2011;96(1):10–13.
  107. Frojmovic MM, Milton JG. Human platelet size, shape, and related functions in health and disease. *Physiol. Rev.* 1982;62(1):185–261.
  108. Peters LL, Cheever EM, Ellis HR, et al. Large-scale, high-throughput screening for coagulation and hematologic phenotypes in mice. *Physiol. Genomics.* 2002;11(3):185–193.
  109. Levin J. The evolution of mammalian platelets. *Platelets.* 2013;
  110. Italiano JEJ, Hartwig JH. Megakaryocyte development and platelet formation. *Platelets.* 2013;
  111. Choi ES, Nichol JL, Hokom MM, Hornkohl AC, Hunt P. Platelets generated in vitro from proplatelet-displaying human megakaryocytes are functional. *Blood.* 1995;85:402–413.
  112. Cramer EM, Norol F, Guichard J, et al. Ultrastructure of platelet formation by human megakaryocytes cultured with the Mpl ligand. *Blood.* 1997;89(7):2336–2346.
  113. Tablin F, Castro M, Leven RM. Blood platelet formation in vitro: the role of the cytoskeleton in megakaryocyte fragmentation. *J. Cell Sci.* 1990;97:59–70.
  114. Becker RP, DeBruyn PP. The transmural passage of blood cells into myeloid sinusoids and the entry of platelets into the sinusoidal circulation: a scanning electron microscopic investigation. *Am. J. Anat.* 1976;145:1046–1052.
  115. Lichtman MA, Chamberlain JK, Simon W, Santillo PA. Parasinusoidal location of megakaryocytes in marrow: a determinant of platelet release. *Am. J. Hematol.* 1978;4:303–312.
  116. Junt T, Schulze H, Chen Z, et al. Dynamic visualization of thrombopoiesis within bone marrow. *Science (80-. ).* 2007;317(5845):1767–1770.
  117. Scurfield G, Radley JM. Aspects of platelet formation and release. *Am. J. Hematol.* 1981;10:285–296.
  118. Lefrancais E, Ortiz-Munoz G, Caudrillier A, et al. The lung is a site of platelet biogenesis and a reservoir for hematopoietic progenitors Emma. *Nature.* 2017;544(7648):105–109.
  119. Grozovsky R, Giannini S, Falet H, Hoffmeister KM. Regulating billions of blood platelets: glycans and beyond. *Blood.* 2015;126(16):1877–1884.
  120. Cohen JA, Leeksa CH. Determination of the life span of human blood platelets using labelled diisopropylfluorophosphonate. *J. Clin. Invest.* 1956;35(9):964–969.
  121. Odell TTJ, McDonald TP. Life span of mouse blood platelets. *Proc. Soc. Exp. Biol.* 1961;106:107–108.
  122. Aranda E, Pizarro M, Pereira J, Mezzano D. Accumulation of 5-hydroxytryptamine by aging platelets: studies in a model of suppressed thrombopoiesis in dogs.

- Thromb. Haemost.* 1994;71:488–492.
123. Rand M, Greenberg J, Packham M, Mustard J. Density subpopulations of rabbit platelets: size, protein, and sialic acid content, and specific radioactivity changes following labelling with <sup>35</sup>S-sulfate in vivo. *Blood.* 1981;57:741–746.
  124. Ludany A, Kellermayer M. Protein synthesis in human platelets. *Clin. Biochem.* 1988;21(2):107–110.
  125. Siegel A, Luscher EF. Non-identity of the alpha-granules of human blood platelets with typical lysosomes. *Nature.* 1967;215(5102):745–747.
  126. Tranzer JP, Da Prada M, Pletscher A. Ultrastructural localization of 5-hydroxytryptamine in blood platelets. *Nature.* 1966;212(5070):1574–1575.
  127. Reed GL. Platelet secretory mechanisms. *Semin. Thromb. Hemost.* 2004;30(4):441–450.
  128. King SM, Reed GL. Development of platelet secretory granules. *Semin. Cell Dev. Biol.* 2002;13(4):293–302.
  129. Blair P, Flaumenhaft R. Platelet  $\alpha$ -granules: Basic biology and clinical correlates. *Blood Rev.* 2009;23(4):177–189.
  130. Coppinger JA, Cagney G, Toomey S, et al. Characterization of the proteins released from activated platelets leads to localization of novel platelet proteins in human atherosclerotic lesions. *Blood.* 2004;103(6):2096–2104.
  131. Piersma SR, Broxterman HJ, Kapci M, et al. Proteomics of the TRAP-induced platelet releasate. *J. Proteomics.* 2009;72(1):91–109.
  132. Holmsen H, Weiss HJ. Secretable storage pools in platelets. *Annu. Rev. Med.* 1979;30:119–134.
  133. Ruiz FA, Lea CR, Oldfield E, Docampo R. Human platelet dense granules contain polyphosphate and are similar to acidocalcisomes of bacteria and unicellular eukaryocytes. *J. Biol. Chem.* 2004;279(43):44250–44257.
  134. Rondina MT, Weyrich AS, Zimmerman GA. Platelets as cellular effectors of inflammation in vascular diseases. *Circ. Res.* 2013;112:1506–1519.
  135. Nurden AT. Platelets, inflammation and tissue regeneration. *Thromb. Haemost.* 2011;105(SUPPL. 1):13–33.
  136. Gros A, Ollivier V, Ho-Tin-Noé B. Platelets in inflammation: Regulation of leukocyte activities and vascular repair. *Front. Immunol.* 2015;6(JAN):1–8.
  137. Speth C, Loffler J, Krappmann S, Lass-Flörl C, Rambach G. Platelets as immune cells in infectious diseases. *Future Microbiol.* 2013;8:1431–1451.
  138. Gardiner EE, Andrews RK. Platelets: envoys at the infection frontline. *J. Infect. Dis.* 2013;208:871–873.
  139. Wong CHY, Jenne CN, Petri B, Chrobok NL, Kubes P. Nucleation of platelets with blood-borne pathogens on Kupffer cells precedes other innate immunity and contributes to bacterial clearance. *Nat. Immunol.* 2013;14:785–792.
  140. Kikuchi L, Kieran MW, Wheatley E, et al. Platelets actively sequester angiogenesis regulators. *Blood.* 2009;113(12):2835.
  141. Repsold L, Pool R, Karodia M, Tintinger G, Joubert AM. An overview of the role of platelets in angiogenesis, apoptosis and autophagy in chronic myeloid leukaemia. *Cancer Cell Int.* 2017;17(1):1–12.

142. Sabrkhany S, Griffioen AW, oude Egbrink MGA. The role of blood platelets in tumor angiogenesis. *Biochim. Biophys. Acta - Rev. Cancer*. 2011;1815(2):189–196.
143. McNicol A, Israels SJ. Beyond Hemostasis: The Role of Platelets in Inflammation, Malignancy and Infection. *Cardiovasc. Haematol. Disord. Targets*, 2008, 8, 99–117. 2008;1–19.
144. Menter DG, Kopetz S, Hawk E, et al. Platelet “first responders” in wound response, cancer, and metastasis. *Cancer Metastasis Rev*. 2017;36(2):199–213.
145. Li N. Platelets in cancer metastasis: To help the “villain” to do evil. *Int. J. Cancer*. 2016;138(9):2078–2087.
146. Jackson SP, Nesbitt WS, Westein E. Dynamics of platelet thrombus formation. *J. Thromb. Haemost.* 2009;7(SUPPL. 1):17–20.
147. Marcus AJ, Safier LB, Kaminski WE, et al. Principles of thromboregulation: control of platelet reactivity in vascular disease. *Adv. Prostaglandin. Thromboxane. Leukot. Res*. 1995;23:413–418.
148. Marcus AJ, Safier LB. Thromboregulation: multicellular modulation of platelet reactivity in hemostasis and thrombosis. *FASEB J*. 1993;7(6):516–522.
149. Marcus AJ, Broekman MJ, Drosopoulos JH, et al. Heterologous cell-cell interactions: thromboregulation, cerebroprotection and cardioprotection by CD39 (NTPDase-1). *J. Thromb. Haemost.* 2003;1(12):2497–2509.
150. Hamilos M, Petousis S, Parthenaki F. Interaction between platelets and endothelium: from pathophysiology to new therapeutic options. *Cardiovasc. Diagnosis Ther*. 2018;8(5):568–580.
151. Alphonsus CS, Rodseth RN. The endothelial glycocalyx: a review of the vascular barrier. *Anaesthesia*. 2014;69(7):777–784.
152. Dogne S, Flamion B, Caron N. Endothelial glycocalyx as a shield against diabetic vascular complications: involvement of hyaluronan and hyaluronidases. *Arterioscler. Thromb. Vasc. Biol*. 2018;38(7):1427–1439.
153. Clemetson KJ. Platelets and primary haemostasis. *Thromb. Res*. 2012;129(3):220–224.
154. Jenne CN, Urrutia R, Kubes P. Platelets: Bridging hemostasis, inflammation, and immunity. *Int. J. Lab. Hematol*. 2013;35(3):254–261.
155. Xu XR, Zhang D, Oswald BE, et al. Platelets are versatile cells: New discoveries in hemostasis, thrombosis, immune responses, tumor metastasis and beyond. *Crit. Rev. Clin. Lab. Sci*. 2016;53(6):409–430.
156. Ruggeri ZM. Platelet adhesion under flow. *Microcirculation*. 2011;16(1):58–83.
157. Nieswandt B, Pleines I, Bender M. Platelet adhesion and activation mechanisms in arterial thrombosis and ischaemic stroke. *J. Thromb. Haemost.* 2011;9(1 S):92–104.
158. Kaplan ZS, Jackson SP. The role of platelets in atherothrombosis. *Hematology Am. Soc. Hematol. Educ. Program*. 2011;2011:51–61.
159. Hou Y, Carrim N, Wang Y, Gallant RC, Marshall A. Platelets in hemostasis and thrombosis: Novel mechanisms of fibrinogen-independent platelet aggregation and fibronectin-mediated protein wave of hemostasis. *J. Biomed. Res*. 2015;29(August):437–444.

160. Wang Y, Carrim N, Ni H. Fibronectin orchestrates thrombosis and hemostasis. *Oncotarget*. 2015;6(23):6–7.
161. Xu XR, Carrim N, Antonio M, et al. Platelets and platelet adhesion molecules : novel mechanisms of thrombosis and anti-thrombotic therapies. *Thromb. J*. 2016;14(Suppl 1):37–46.
162. Rakshit S, Sivasankar S. Biomechanics of cell adhesion: How force regulates the lifetime of adhesive bonds at the single molecule level. *Phys. Chem. Chem. Phys*. 2014;16(6):2211–2223.
163. Ruggeri ZM, Mendolicchio GL. Interaction of von willebrand factor with platelets and the vessel wall. *Hamostaseologie*. 2015;35(3):211–224.
164. Tangelder GJ, Slaaf DW, Arts T, Reneman RS. Wall shear rate in arterioles in vivo: least estimates from platelet velocity profiles. *Am. J. Physiol*. 1988;254(6 Pt 2):H1059-1064.
165. Strony J, Beaudoin A, Brands D, Adelman B. Analysis of shear stress and hemodynamic factors in a model of coronary artery stenosis and thrombosis. *Am. J. Physiol*. 1993;265(5 Pt 2):H1787-1796.
166. Peterson LH. The dynamics of pulsatile blood flow. *Circ. Res*. 1954;2(2):127–139.
167. Brozovich F V., Nicholson CJ, Degen C V., et al. Mechanisms of vascular smooth muscle contraction and the basis for pharmacologic treatment of smooth muscle disorders. *Pharmacol. Rev*. 2016;68(2):476–532.
168. Nesbitt WS, Westein E, Tovar-Lopez FJ, et al. A shear gradient-dependent platelet aggregation mechanism drives thrombus formation. *Nat. Med*. 2009;15(6):665–673.
169. Bark DL, Ku DN. Wall shear over high degree stenoses pertinent to atherothrombosis. *J. Biomech*. 2010;43(15):2970–2977.
170. Kefayati S, Milner JS, Holdsworth DW, Poepping TL. In vitro shear stress measurements using particle image velocimetry in a family of carotid artery models: effect of stenosis severity, plaque eccentricity, and ulceration. *PLoS One*. 2014;9(7):e98209.
171. Murray CD. The physiological principle of minimum work I. The vascular system and the cost of blood volume. *Proc. Natl. Acad. Sci. U. S. A*. 1926;12(3):207–214.
172. Doutel E, Pinto SIS, Campos JBLM, Miranda JM. Link between deviations from Murray’s Law and occurrence of low wall shear stress regions in the left coronary artery. *J. Theor. Biol*. 2016;402:89–99.
173. Sandoo A, Veldhuijzen van Zanten JJCS, Metsios GS, Carroll D, Kitas GD. The endothelium and its role in regulating vascular tone. *Open Cardiovasc. Med. J*. 2010;4:302–312.
174. Savage B, Saldívar E, Ruggeri ZM. Initiation of platelet adhesion by arrest onto fibrinogen or translocation on von Willebrand factor. *Cell*. 1996;84(2):289–297.
175. Pugh N, Simpson AMC, Smethurst PA, et al. Synergism between platelet collagen receptors defined using receptor-specific collagen-mimetic peptide substrata in flowing blood. *Blood*. 2010;115(24):5069–5079.
176. Schneider SW, Nuschele S, Wixforth A, et al. Shear-induced unfolding triggers adhesion of von Willebrand factor fibers. *Proc. Natl. Acad. Sci*.

- 2007;104(19):7899–7903.
177. Ruggeri ZM, Orje JN, Habermann R, Federici AB, Reininger AJ. Activation-Independent Platelet Adhesion and Aggregation under Elevated Shear Stress  
Running title : Platelet adhesion and aggregation in flowing blood. *Blood*. 2006;108(6):1903–1911.
  178. Andrews RK, Berndt MC. Platelet adhesion: a game of catch and release. *J. Clin. Invest.* 2008;118:3009–3011.
  179. Nightingale T, Cutler D. The secretion of von Willebrand factor from endothelial cells; an increasingly complicated story. *J. Thromb. Haemost.* 2013;11(SUPPL.1):192–201.
  180. Bryckaert M, Rosa JP, Denis C V., Lenting PJ. Of von Willebrand factor and platelets. *Cell. Mol. Life Sci.* 2015;72(2):307–326.
  181. Ruggeri ZM, Mendolicchio GL. Adhesion mechanisms in platelet function. *Circ. Res.* 2007;100(12):1673–1685.
  182. Kuijpers MJE, Schulte V, Bergmeier W, et al. Complementary roles of platelet glycoprotein VI and integrin alpha2beta1 in collagen-induced thrombus formation in flowing whole blood ex vivo. *FASEB.* 2003;
  183. Sarratt KL, Chen H, Zutter MM, et al. GPVI and  $\alpha 2\beta 1$  play independent critical roles during platelet adhesion and aggregate formation to collagen under flow. *Blood*. 2005;106(4):1268–1277.
  184. Yap CL, Hughan SC, Cranmer SL, et al. Synergistic adhesive interactions and signaling mechanisms operating between platelet glycoprotein Ib/IX and integrin  $\alpha \text{IIb}\beta 3$ : Studies in human platelets and transfected Chinese hamster ovary cells. *J. Biol. Chem.* 2000;275(52):41377–41388.
  185. Mazzucato M, Pradella P, Cozzi MR, De Marco L, Ruggeri ZM. Sequential cytoplasmic calcium signals in a 2-stage platelet activation process induced by the glycoprotein Iba mechanoreceptor. *Blood*. 2002;100(8):2793–2800.
  186. Nesbitt WS, Kulkarni S, Giuliano S, et al. Distinct glycoprotein Ib/V/IX and integrin  $\alpha \text{IIb}\beta 3$ -dependent calcium signals cooperatively regulate platelet adhesion under flow. *J. Biol. Chem.* 2002;277(4):2965–2972.
  187. Jakus Z, Simon E, Frommhold D, Sperandio M, Mócsai A. Critical role of phospholipase  $\text{C}\gamma 2$  in integrin and Fc receptor-mediated neutrophil functions and the effector phase of autoimmune arthritis. *J. Exp. Med.* 2009;206(3):577–593.
  188. Oberfell A, Judd BA, Del Pozo MA, et al. The Molecular Adapter SLP-76 Relays Signals from Platelet Integrin  $\alpha \text{IIb}\beta 3$  to the Actin Cytoskeleton. *J. Biol. Chem.* 2001;276(8):5916–5923.
  189. Goncalves I, Hughan SC, Schoenwaelder SM, et al. Integrin  $\alpha \text{IIb}\beta 3$ -dependent calcium signals regulate platelet-fibrinogen interactions under flow: Involvement of phospholipase  $\text{C}\gamma 2$ . *J. Biol. Chem.* 2003;278(37):34812–34822.
  190. Farndale RW. Collagen-induced platelet activation. *Blood Cells, Mol. Dis.* 2006;36(2):162–165.
  191. Brass LF. Thrombin and platelet activation. *Chest.* 2003;124(Suppl 3):S18-25.
  192. De Candia E. Mechanisms of platelet activation by thrombin: a short history. *Thromb. Res.* 2012;129(3):250–256.

193. Golebiewska EM, Poole AW. Platelet secretion: From haemostasis to wound healing and beyond. *Blood Rev.* 2015;29(3):153–162.
194. Jarvis GE, Atkinson BT, Snell DC, Watson SP. Distinct roles of GPVI and integrin  $\alpha 2 \text{b} 1$  in platelet shape change and aggregation induced by different collagens. 2002;2:107–117.
195. Heemskerk JWM, Vuist WMJ, Feijge MAH, Reutelingsperger CPM, Lindhout T. Collagen but not fibrinogen surfaces induce bleb formation, exposure of phosphatidylserine, and procoagulant activity of adherent platelets: evidence for regulation by protein tyrosine kinase-dependent  $\text{Ca}^{2+}$  responses. *Blood.* 1997;90(7):2615–2625.
196. Thiagarajan P, Tait JF. Collagen-induced exposure of anionic phospholipid in platelets and platelet-derived microparticles. *J. Biol. Chem.* 1991;266(36):24302–24307.
197. Ruggeri ZM. The role of von Willebrand factor in thrombus formation. *Thromb. Res.* 2007;120(SUPPL. 1):1–10.
198. Ruggeri ZM. Platelet interactions with vessel wall components during thrombogenesis. *Blood Cells, Mol. Dis.* 2006;36(2):145–147.
199. Mendolicchio GL, Ruggeri ZM. New perspectives on von Willebrand factor functions in hemostasis and thrombosis. *Semin. Hematol.* 2005;42(1):5–14.
200. Ruggeri ZM, Jackson SP. Platelet thrombus formation in flowing blood. *Platelets.* 2013;
201. Furie B, Furie BC. Mechanisms of thrombus formation. *N. Engl. J. Med.* 2008;359(9):938–949.
202. Wang Y, Ni H. Fibronectin maintains the balance between hemostasis and thrombosis. *Cell. Mol. Life Sci.* 2016;73(17):3265–3277.
203. Rehemian A, Gross PL, Yang H, et al. Vitronectin stabilizes thrombi and vessel occlusion but plays a dual role in platelet aggregation. *J. Thromb. Haemost.* 2005;3:875–883.
204. Rehemian A, Yang H, Zhu G, et al. Plasma fibronectin depletion enhances platelet aggregation and thrombus formation in mice lacking fibrinogen and von Willebrand factor. *Blood.* 2009;113(8):1809–1817.
205. Bonnefoy A, Hantgan R, Legrand C, Frojmovic MM. A Model of Platelet Aggregation Involving Multiple Interactions of Thrombospondin-1, Fibrinogen, and GPIIb/IIIa Receptor. *J. Biol. Chem.* 2001;276(8):5605–5612.
206. Cho J, Mosher DF. Enhancement of thrombogenesis by plasma fibronectin cross-linked to fibrin and assembled in platelet thrombi. 2019;107(9):3555–3564.
207. Sakai T, Johnson KJ, Murozono M, et al. Plasma fibronectin supports neuronal survival and reduces brain injury following transient focal cerebral ischemia but is not essential for skin-wound healing and hemostasis. *Nat. Med.* 2001;7(3):324–330.
208. Ni H, Yuen PST, Papalia JM, et al. Plasma fibronectin promotes thrombus growth and stability in injured arterioles. *Proc. Natl. Acad. Sci.* 2003;100(5):2415–2419.
209. Lawler J, Sunday M, Thibert V, et al. Thrombospondin-1 is required for normal murine pulmonary homeostasis and its absence causes pneumonia. *J. Clin. Invest.*

- 1998;101:982–992.
210. Zheng X, Saunders TL, Camper SA, Samuelson LC, Ginsburg D. Vitronectin is not essential for normal mammalian development and fertility. *Proc. Natl. Acad. Sci.* 1995;92:12426–12430.
  211. Ni H, Denis C V., Subbarao S, et al. Persistence of platelet thrombus formation in arterioles of mice lacking both von Willebrand factor and fibrinogen. *J. Clin. Invest.* 2000;106:385–392.
  212. Prakash P, Kulkarni PP, Chauhan AK. Thrombospondin 1 requires von Willebrand factor to modulate arterial thrombosis in mice. *Blood.* 2015;125(2):399–406.
  213. Yang H, Reheman A, Chen P, et al. Fibrinogen and von Willebrand factor-independent platelet aggregation in vitro and in vivo. *J. Thromb. Haemost.* 2006;4:2230–2237.
  214. Chen J, Diacovo TG, Grenache DG, Santoro S a., Zutter MM. The  $\alpha 2$  Integrin Subunit-Deficient Mouse. *Am. J. Pathol.* 2002;161(1):337–344.
  215. Kuijpers MJE, Pozgajova M, Cosemans JMEM, et al. Role of murine integrin  $\alpha 2\beta 1$  in thrombus stabilization and embolization: contribution of thromboxane A<sub>2</sub>. *Thromb. Haemost.* 2007;98:1072–1080.
  216. Lockyer S, Okuyama K, Begum S, et al. GPVI-deficient mice lack collagen responses and are protected against experimentally induced pulmonary thromboembolism. *Thromb. Res.* 2006;118(3):371–380.
  217. Dubois C, Panicot-Dubois L, Merrill-Skoloff G, Furie B, Furie BC. Glycoprotein VI-dependent and -independent pathways of thrombus formation in vivo. *Blood.* 2006;107:3902–3906.
  218. Kato K, Kanaji T, Russell S, et al. The contribution of glycoprotein VI to stable platelet adhesion and thrombus formation illustrated by targeted gene deletion. *Blood.* 2003;102:1701–1707.
  219. Ware J, Russell S, Ruggeri ZM. Generation and rescue of a murine model of platelet dysfunction: The Bernard-Soulier syndrome. *Proc. Natl. Acad. Sci.* 2000;97(6):2803–2808.
  220. Bergmeier W, Piffath CL, Goerge T, et al. The role of platelet adhesion receptor GPIIb far exceeds that of its main ligand, von Willebrand factor, in arterial thrombosis. *Proc. Natl. Acad. Sci.* 2006;103(45):16900–16905.
  221. Hodivala-Dilke KM, McHugh KP, Tsakiris DA, et al.  $\beta 3$ -integrin-deficient mice are a model for Glanzmann thrombasthenia showing placental defects and reduced survival. *J. Clin. Invest.* 1999;103(2):229–238.
  222. Denis C, Methia N, Frenette PS, et al. A mouse model of severe von Willebrand disease: Defects in hemostasis and thrombosis. *Proc. Natl. Acad. Sci.* 1998;95(16):9524–9529.
  223. Marx I, Christophe OD, Lenting PJ, et al. Altered thrombus formation in von Willebrand factor deficient mice expressing von Willebrand factor variants with defective binding to collagen or GPIIbIIIa. *Blood.* 2008;112(3):603–609.
  224. Pimanda JE, Ganderton T, Maekawa A, et al. Role of thrombospondin-1 in control of von Willebrand factor multimer size in mice. *J. Biol. Chem.* 2004;279(20):21439–21448.

225. Bonnefoy A, Daenens K, Feys HB, et al. Thrombospondin-1 controls vascular platelet recruitment and thrombus adherence in mice by protecting (sub)endothelial VWF from cleavage by ADAMTS13. *Blood*. 2006;107:955–964.
226. George EL, Georges-Labouesse EN, Patel-King RS, Rayburn H, Hynes RO. Defects in mesoderm, neural tube and vascular development in mouse embryos lacking fibronectin. *Development*. 1993;119:1079–1091.
227. Suh TT, Holmback K, Jensen NJ, et al. Resolution of spontaneous bleeding events but failure of pregnancy in fibrinogen-deficient mice. *Genes Dev*. 1995;9(2020–2033):.
228. Zheng X, Saunders TL, Camper SA, Samuelson LC, Ginsburg D. Vitronectin is not essential for normal mammalian development and fertility. *Proc. Natl. Acad. Sci. U. S. A.* 1995;92(26):12426–12430.
229. Fay WP, Parker a C, Ansari MN, Zheng X, Ginsburg D. Vitronectin inhibits the thrombotic response to arterial injury in mice. *Blood*. 1999;93(6):1825–30.
230. Weisel JW, Litvinov RI. Fibrin formation, structure and properties. *Subcell. Biochem*. 2017;82:405–456.
231. Medved L, Weisel JW. Recommendations for nomenclature on fibrinogen and fibrin. *J. Thromb. Haemost.* 2009;7(2):355–359.
232. Hall CE, Slayter HS. The fibrinogen molecule: its size, shape, and mode of polymerization. *J. Biophys. Biochem. Cytol.* 1959;5(1):11–27.
233. Takeda Y. Studies of the metabolism and distribution of fibrinogen in healthy men with autologous 125-I-labeled fibrinogen. *J. Clin. Invest.* 1966;45(1):103–111.
234. Ogston CM, Ogston D. Plasma fibrinogen and plasminogen levels in health and in ischaemic heart disease. *J. Clin. Pathol.* 1966;19(4):352–356.
235. Gullledge AA, McShea C, Schwartz T, Koch G, Lord ST. Effects of hyperfibrinogenemia on vasculature of C57BL/6 mice with and without atherogenic diet. *Arterioscler. Thromb. Vasc. Biol.* 2003;23:130–135.
236. Machlus KR, Cardenas JC, Church FC, Wolberg AS. Causal relationship between hyperfibrinogenemia, thrombosis, and resistance to thrombolysis in mice. *Blood*. 2011;117(18):4953–4963.
237. Kerlin B, Cooley BC, Isermann BH, et al. Cause-effect relation between hyperfibrinogenemia and vascular disease. *Blood*. 2004;103(5):1728–1734.
238. Harrison P, Wilbourn B, Debili N, et al. Uptake of plasma fibrinogen into the alpha granules of human megakaryocytes and platelets. *J. Clin. Invest.* 1989;84(4):1320–1324.
239. Makogonenko E, Tsurupa G, Ingham K, Medved L. Interaction of fibrin(ogen) with fibronectin: further characterization and localization of the fibronectin-binding site. *Biochemistry*. 2002;41(25):7907–7913.
240. Engvall E, Ruoslahti E, Miller EJ. Affinity of fibronectin to collagens of different genetic types and to fibrinogen. *J. Exp. Med.* 1978;147(6):1584–1595.
241. Leung LLK. Role of thrombospondin in platelet aggregation. *J. Clin. Invest.* 1984;74(5):1764–1772.
242. Bacon-Baguley T, Ogilvie ML, Gartner TK, Walz DA. Thrombospondin binding to specific sequences within the A alpha- and B beta-chains of fibrinogen. *J. Biol.*

- Chem.* 1990;265(4):2317–2323.
243. Sasaki T, Page IH, Shainoff JR. Stable complex of fibrinogen and fibrin. *Science* (80-. ). 1966;152(3725):1069–1071.
  244. Suehiro K, Gailit J, Plow EF. Fibrinogen is a ligand for integrin alpha5beta1 on endothelial cells. *J. Biol. Chem.* 1997;272(8):5360–5366.
  245. Albert F, Christopher N F. The platelet fibrinogen receptor: from megakaryocyte to the mortuary. *JRSM Cardiovasc. Dis.* 2012;1(2):1–13.
  246. Kloczewiak M, Timmons S, Lukas TJ, Hawiger J. Platelet receptor recognition site on human fibrinogen. Synthesis and structure-function relationship of peptides corresponding to the carboxy-terminal segment of the gamma chain. *Biochemistry.* 1984;23(8):1767–1774.
  247. Ikeda Y, Handa M, Kawano K, et al. The role of von Willebrand factor and fibrinogen in platelet aggregation under varying shear stress. *J. Clin. Invest.* 1991;87(4):1234–1240.
  248. Bennett JS. Platelet-fibrinogen interactions. *Ann. N. Y. Acad. Sci.* 2001;936:340–354.
  249. Farrell DH, Thiagarajant P, Chung DW, Davie EW. Role of fibrinogen a and y chain sites in platelet aggregation. *Proc. Natl. Acad. Sci. U. S. A.* 1992;89:10729–10732.
  250. Weisel JW, Nagaswami C, Vilaire G, Bennett JS. Examination of the platelet membrane glycoprotein IIb-IIIa complex and its interaction with fibrinogen and other ligands by electron microscopy. *J. Biol. Chem.* 1992;267(23):16637–16643.
  251. Springer TA, Zhu J, Xiao T. Structural basis for distinctive recognition of fibrinogen  $\gamma$ C peptide by the platelet integrin  $\alpha$ IIb $\beta$ 3. *J. Cell Biol.* 2008;182(4):791–800.
  252. Rooney MM, Farrell DH, van Hemel BM, de Groot PG, Lord ST. The contribution of the three hypothesized integrin-binding sites in fibrinogen to platelet-mediated clot retraction. *Blood.* 1998;92(7):2374–2381.
  253. Rooney MM, Parise L V., Lord ST. Dissecting clot retraction and platelet aggregation. *J. Biol. Chem.* 1996;271(15):8553–8555.
  254. Carr Jr. ME. Development of platelet contractile force as a research and clinical measure of platelet function. *Cell Biochem. Biophys.* 2003;38(1):55–78.
  255. Hantgan RR, Mousa SA. Inhibition of platelet-mediated clot retraction by integrin antagonists. *Thromb. Res.* 1998;89:271–279.
  256. Matsunaga S, Takai Y, Seki H. Fibrinogen for the management of critical obstetric hemorrhage. *J. Obstet. Gynaecol. Res.* 2018;45(1):13–21.
  257. Ranucci M, Pistuddi V, Baryshnikova E, Colella D, Bianchi P. Fibrinogen levels after cardiac surgery proceduresL association with postoperative bleeding, trigger values, and target values. *Ann. Thorac. Surg.* 2016;102(1):78–85.
  258. Geck MJ, Singh D, Gunn H, Stokes JK, Truumees E. Relationship between preoperative plasma fibrinogen concentration, perioperative bleeding, and transfusions in elective adult spinal deformity correction. *Spine Deform.* 2019;7(5):788–795.
  259. Faraoni D, Willems A, Savan V, et al. Plasma fibrinogen concentration is

- correlated with postoperative blood loss in children undergoing cardiac surgery. A retrospective review. *Eur. J. Anaesthesiol.* 2014;31(6):317–326.
260. Pillai RC, Fraser JF, Bhaskar B. Influence of circulating levels of fibrinogen and perioperative coagulation parameters on predicting postoperative blood loss in cardiac surgery: a prospective observational study. *J. Card. Surg.* 2014;29(2):189–195.
261. Rahe-Meyer N, Pichlmaier M, Haverich A, et al. Bleeding management with fibrinogen concentrate targeting a high-normal plasma fibrinogen level: a pilot study. *Br. J. Anaesthesia.* 2009;102(6):785–792.
262. Fries D, Martini WZ. Role of fibrinogen in trauma-induced coagulopathy. *Br. J. Anaesthesia.* 2010;105(2):116–121.
263. Martinez J. Congenital dysfibrinogenemia. *Curr. Opin. Hematol.* 1997;4:357–365.
264. Kamphuisen PW, Eikenboom JC, Vos HL, et al. Increased levels of factor VIII and fibrinogen in patients with venous thrombosis are not caused by acute phase reactions. *Thromb. Haemost.* 1999;81(5):680–683.
265. Zaidi TN, McIntire L V., Farrell DH, Thiagarajan P. Adhesion of platelets to surface-bound fibrinogen under flow. *Blood.* 1996;88(8):2967–2972.
266. Jen CJ, Lin JS. Direct observation of platelet adhesion to fibrinogen- and fibrin-coated surfaces. *Am. J. Physiol.* 1991;261:1457–1463.
267. Medved L, Ugarova TP, Veklich Y, Lukinova N, Weisel JW. Electron microscope investigation of the early stages of fibrin assembly. *J. Mol. Biol.* 1990;216(3):503–509.
268. Fowler WE, Hantgan RR, Hermans J, Erickson HP. Structure of the fibrin protofibril. *Proc. Natl. Acad. Sci. U. S. A.* 1981;78(8):4872–4876.
269. Mosesson MW, DiOrio JP, Muller MF, et al. Studies on the ultrastructure of fibrin lacking fibrinopeptide B (beta-fibrin). *Blood.* 1987;69(4):1073–1081.
270. Weisel JW. Fibrin assembly. Lateral aggregation and the role of the two pairs of fibrinopeptides. *Biophys. J.* 1986;50(6):1079–1093.
271. Hada M, Kaminski M, Bockenstedt PL, McDonagh J. Covalent crosslinking of von Willebrand factor to fibrin. *Blood.* 1986;68(1):95–101.
272. Hook P, Litvinov RI, Kim O V., et al. Strong binding of platelet integrin alphaIIb beta3 to fibrin clots: potential target to destabilize thrombi. *Sci. Rep.* 2017;7:.
273. Languino LR, Plescia J, Duperray A, et al. Fibrinogen mediates leukocyte adhesion to vascular endothelium through an ICAM-1-dependent pathway. *Cell.* 1993;73(7):1423–1434.
274. Altieri DC. Regulation of leukocyte-endothelium interaction by fibrinogen. *Thromb. Haemost.* 1999;82(2):781–786.
275. Zollinger AJ, Smith ML. Fibronectin, the extracellular glue. *Matrix Biol.* 2017;60–61:27–37.
276. Jarvis GE, Atkinson BT, Frampton J, Watson SP. Thrombin-induced conversion of fibrinogen to fibrin results in rapid platelet trapping which is not dependent on platelet activation of GPIIb. *Br. J. Pharmacol.* 2003;138:574–583.
277. Alshehri OM, Hughes CE, Montague S, et al. Fibrin activates GPVI in human and

- mouse platelets. 2018;126(13):1601–1609.
278. Induruwa I, Moroi M, Bonna A, et al. Platelet collagen receptor Glycoprotein VI-dimer recognizes fibrinogen and fibrin through their D-domains, contributing to platelet adhesion and activation during thrombus formation. *J. Thromb. Haemost.* 2018;16:1–16.
  279. Mangin PH, Onselaer M-B, Receveur N, et al. Immobilized fibrinogen activates human platelets through glycoprotein VI. *Haematologica.* 2018;103(5):898–907.
  280. Sivaraman B, Latour RA. The relationship between platelet adhesion on surfaces and the structure versus the amount of adsorbed fibrinogen. *Biomaterials.* 2010;31(5):832–839.
  281. Hughes CE, Finney BA, Koentgen F, Lowe KL, Watson SP. The N-terminal SH2 domain of Syk is required for (hem) ITAM, but not integrin, signaling in mouse platelets. *Blood.* 2015;125(1):144–155.
  282. Zhi H, Rauova L, Hayes V, et al. Cooperative integrin/ITAM signaling in platelets enhances thrombus formation in vitro and in vivo. *Blood.* 2013;121(10):1858–1867.
  283. Potts JR, Campbell ID. Fibronectin structure and assembly. *Curr. Opin. Cell Biol.* 1994;6(5):648–655.
  284. Romberger DJ. Fibronectin. *Int. J. Biochem. Cell Biol.* 1997;29(I):939–943.
  285. Chen CI, Federici AB, Cramer EM, et al. Studies of multimerin in patients with von Willebrand disease and platelet von Willebrand factor deficiency. *Br. J. Haematol.* 1998;103(1):20–28.
  286. Mosher DF. Organization of the provisional fibronectin matrix: control by products of blood coagulation. *Thromb. Haemost.* 1995;74:529–533.
  287. Bae E, Sakai T, Mosher DF. Assembly of exogenous fibronectin by fibronectin-null cells is dependent on the adhesive substrate. *J. Biol. Chem.* 2004;279(35749–35759):.
  288. Tamkun JW, Hynes RO. Plasma fibronectin in synthesized and secreted by hepatocytes. *J. Biol. Chem.* 1983;258(7):4641–4647.
  289. Johnson KJ, Sage H, Briscoe G, Erickson HP. The compact conformation of fibronectin is determined by intramolecular ionic interactions. *J. Biol. Chem.* 1999;274(22):15473–15479.
  290. Yang JT, Rayburn H, Hynes RO. Embryonic mesodermal defects in alpha5 integrin-deficient mice. *Development.* 1993;119:1093–1105.
  291. Moretti FA, Chauhan AK, Iaconcig A, Porro F, Baralle FE. A major fraction of fibronectin present in the extracellular matrix of tissues is plasma-derived\*. *J. Biol. Chem.* 2007;282(38):28057–28062.
  292. Theocharis AD, Skandalis SS, Gialeli C, Karamanos NK. Extracellular matrix structure. *Adv. Drug Deliv. Rev.* 2016;97:4–27.
  293. Pickering JG, Chow LH, Li S, et al. alpha5beta1 integrin expression and luminal edge fibronectin matrix assembly by smooth muscle cells after arterial injury. *Am. J. Pathol.* 2000;156(2):453–465.
  294. Parise L V., Philips DR. Fibronectin-binding properties of the purified platelet glycoprotein IIb-IIIa complex. *J. Biol. Chem.* 1986;261:14011–14017.

295. Gardner JM, Hynes RO. Interaction of fibronectin with its receptor on platelets. *Cell*. 1985;42(2):439–448.
296. Charo IF, Nannizzi L, Smith JW, Cheresch DA. The vitronectin receptor alpha v beta 3 binds fibronectin and acts in concert with alpha 5 beta 1 in promoting cellular attachment and spreading on fibronectin. *J. Cell Biol*. 1990;111(6 Pt 1):2795–2800.
297. Wayner EA, Carter WG, Piotrowicz RS, Kunicki TJ. The function of multiple extracellular matrix receptors in mediating cell adhesion to extracellular matrix: Preparation of monoclonal antibodies to the fibronectin receptor that specifically inhibit cell adhesion to fibronectin and react with platelet gly. *J. Cell Biol*. 1988;107:1881.
298. Engvall E, Ruoslahti E, Miller EJ. Affinity of fibronectin to collagens of different genetic types and to fibrinogen. *J. Exp. Med*. 1978;147(6):1584–1595.
299. Agbanyo FR, Sixma JJ, De Groot PG, Languino LR, Plow EF. Thrombospondin-platelet interactions: role of divalent cations, wall shear rate, and platelet membrane glycoproteins. *J. Clin. Invest*. 1993;92(1):288–296.
300. Obara M, Kang MS, Yamada KM. Site-directed mutagenesis of the cell-binding domain of human fibronectin: separable, synergistic sites mediate adhesive function. *Cell*. 1988;53:649–657.
301. Beumer BS, Ijsseldijk MJW, Groot PG De, Sixma JJ. Platelet Adhesion to Fibronectin in Flow: Dependence on Surface Concentration and Shear Rate, Role of Platelet Membrane Glycoproteins GP IIb/IIIa and VLA-5, and Inhibition by Heparin. 2018;84(11):3724–3733.
302. Wu YP, De Groot PG, Sixma JJ. Shear-stress-induced detachment of blood platelets from various surfaces. *Arterioscler. Thromb. Vasc. Biol*. 1997;17(11):3202–3207.
303. Houdijk WPM et al. Role of vWf and fibronectin in the interaction of platelets in flowing blood with monomeric and fibrillar collagen. *J. Clin. Invest*. 1985;75(2):531–540.
304. Bastida E, Escolar G, Ordinas A, Sixma JJ. Fibronectin is required for platelet adhesion and for thrombus formation on subendothelium and collagen surfaces. *Blood*. 1987;70(5):1437–1442.
305. Cho J, Mosher DF. Impact of fibronectin assembly on platelet thrombus formation in response to type I collagen and von Willebrand factor. *Blood*. 2006;108:2229–2236.
306. Mosher DF. Cross-linking of cold-insoluble globulin by fibrin-stabilizing factor. *J. Biol. Chem*. 1975;250(16):6614–6621.
307. Cho J, Degen JL, Collier BS, Mosher DF. Fibrin but not adsorbed fibrinogen supports fibronectin assembly by spread platelets. *J. Biol. Chem*. 2005;280(42):35490–35498.
308. Olorundare OE, Peyruchaud O, Albrecht RM, Mosher DF. Assembly of a fibronectin matrix by adherent platelets stimulated by lysophosphatidic acid and other agonists. *Blood*. 2001;98:117–124.
309. Plow EF, Ginsberg MH. Specific and saturable binding of plasma fibronectin to

- thrombin-stimulated human platelets. *J. Biol. Chem.* 1981;256:9477–9482.
310. Moon DG, Kaplan JE, Mazurkewicz JE. The inhibitory effect of plasma fibronectin on collagen-induced platelet aggregation. *Blood.* 1986;67(2):450–457.
311. Wang Y, Rehemian A, Spring CM, et al. Plasma fibronectin supports hemostasis and regulates thrombosis. *J. Clin. Invest.* 2014;124(10):4281–4293.
312. Shirakami A, Hirai Y, Kawauchi S, et al. Plasma fibronectin deficiency in eight members of one family. *Lancet.* 1986;327(8479):473–474.
313. Chauhan AK, Kisucka J, Cozzi MR, et al. Prothrombotic effects of fibronectin isoforms containing the EDA domain. *Arterioscler. Thromb. Vasc. Biol.* 2008;28(2):296–301.
314. Prakash P, Kulkarni PP, Lentz SR, Chauhan AK. Cellular fibronectin containing extra domain A promotes arterial thrombosis in mice through platelet Toll-like receptor 4. *Blood.* 2015;125(20):3164–3172.
315. Xie L, Chesterman CN, Hogg PJ. Control of von Willebrand factor multimer size by thrombospondin-1. *J. Exp. Med.* 2001;193(12):1341–1350.
316. Counts RB, Paskell SL, Elgee SK. Disulfide bonds and the quaternary structure of factor VIII/von Willebrand factor. *J. Clin. Invest.* 1978;62(3):702–709.
317. Hoyer LW, De los Santos RP, Hoyer JR. Antihemophilic factor antigen. Localization in endothelial cells by immunofluorescent microscopy. *J. Clin. Invest.* 1973;52(11):2737–2744.
318. Jaffe EA, Hoyer LW, Nachman RL. Synthesis of von Willebrand Factor by Cultured Human Endothelial Cells. *Proc. Natl. Acad. Sci. U. S. A.* 1974;71(5):1906–1909.
319. Sporn LA, Chavin SI, Marder VJ, Wagner DD. Biosynthesis of von Willebrand Protein by Human Endothelial Cells. *J. Biol. Chem.* 1985;258(4):2065–67.
320. Shankaran H, Alexandridis P, Neelamegham S. Aspects of hydrodynamic shear regulating shear-induced platelet activation and self-association of von Willebrand factor in suspension. *Blood.* 2003;101(7):2637–2645.
321. Cruz MA, Handin RI, Wise RJ. The interaction of the von Willebrand factor A1 domain with platelet glycoprotein Ib/IX: the role of glycosylation and disulfide bonding in a monomeric recombinant A1 domain protein. *J. Biol. Chem.* 1993;268:21238–21245.
322. Morales LD, Martin C, Cruz MA. The interaction of von Willebrand factor A1 domain with collagen: mutation G1324S (type 2M von Willebrand disease) impairs the conformational change in A1 domain induced by collagen. *J. Thromb. Haemost.* 2006;4:417–425.
323. Bonnefoy A, Romijn RA, Vandervoort PA, et al. von Willebrand factor A1 domain can adequately substitute for A3 domain in recruitment of flowing platelets to collagen. *J. Thromb. Haemost.* 2006;4:2151–2161.
324. Furlan M, Robles R, Lammle B. Partial purification and characterization of a protease from human plasma cleaving von Willebrand factor to fragments produced by in vivo proteolysis. *Blood.* 1996;87:4223–4234.
325. Tsai HM. Physiologic cleavage of von Willebrand factor by a plasma protease is dependent on its conformation and requires calcium ion. *Blood.* 1996;87:4235–

- 4244.
326. Soejima K, Mimura N, Hirashima M, et al. A novel human metalloprotease synthesized in the liver and secreted into the blood: possibly, the von Willebrand factor protease? *J. Biochem.* 2001;130(4):475–480.
  327. Zheng X, Chung D, Takayama TK, et al. Structure of von Willebrand factor-cleaving protease (ADAMTS13), a metalloprotease involved in thrombotic thrombocytopenic purpura. *J. Biol. Chem.* 2001;276:41059–41063.
  328. Flood VH, Schlauderaff AC, Haberichter SL, et al. Crucial role for the VWF A1 domain in binding to type IV collagen. *Blood.* 2015;125(14):2297–2304.
  329. Flood VH, Gill JC, Christopherson PA, et al. Critical von Willebrand factor A1 domain residues influence type VI collagen binding. *J. Thromb. Haemost.* 2012;10(7):1417–1424.
  330. Endenberg SC, Hantgan RR, Lindeboom-Blokzijl L, et al. On the role of von Willebrand factor in promoting platelet adhesion to fibrin in flowing blood. *Blood.* 1995;86:4158–4165.
  331. Kumar RA, Dong JF, Thaggard JA, et al. Kinetics of GPIIb $\alpha$ -vWF-A1 Tether Bond under Flow: Effect of GPIIb $\alpha$  Mutations on the Association and Dissociation Rates. *Biophys. J.* 2003;85(6):4099–4109.
  332. Kanaji S, Fahs SA, Shi Q, Haberichter SL, Montgomery RR. Contribution of platelet versus endothelial VWF to platelet adhesion and hemostasis. *J. Thromb. Haemost.* 2012;10(8):1646–1652.
  333. Lenting PJ, Pegon JN, Groot E, de Groot PG. Regulation of von Willebrand factor-platelet interactions. *Thromb. Haemost.* 2010;104(3):449–455.
  334. Ng C, Motto DG, Di Paola J. Diagnostic approach to von Willebrand disease. *Blood.* 2015;125(13):2029–2037.
  335. Leebeek FWG, Atig F. How I manage severe von Willebrand disease. *Br. J. Haematol.* 2019;187(4):418–430.
  336. Carlson CB, Lawler J, Mosher DF. Structures of thrombospondins. *Cell. Mol. Life Sci.* 2008;65(5):672–686.
  337. Reed MJ, Iruela-Arispe L, O'Brien ER, et al. Expression of thrombospondins by endothelial cells: Injury is correlated with TSP-1. *Am. J. Pathol.* 1995;147(4):1068–1080.
  338. Baenziger NL, Brodie GN, Majerus PW. Isolation and properties of a thrombin-sensitive protein of human platelets. *J. Biol. Chem.* 1972;247(9):2723–2731.
  339. Dubernard V, Arbeille B, Lemesle M, Legrand C. Evidence for an alpha-granular pool of the cytoskeletal protein alpha-actinin in human platelets that redistributes with the adhesive glycoprotein thrombospondin-1 during the exocytotic process. *Arterioscler. Thromb. Vasc. Biol.* 1997;17(10):2293–2305.
  340. Kowalska MA, Tuszynski GP. Interaction of thrombospondin with platelet glycoproteins GPIa-IIa and GPIIb-IIIa. *Biochem. J.* 1993;295(3):725–730.
  341. Lawler J, Hynes RO. An integrin receptor on normal and thrombasthenic platelets that binds thrombospondin. *Blood.* 1989;74(6):2022–2027.
  342. Tuszynski GP, Kowalska MA. Thrombospondin-induced adhesion of human platelets. *J. Clin. Invest.* 1991;87(4):1387–1394.

343. Dixit VM, Grant GA, Frazier WA, Santoro SA. Isolation of the fibrinogen-binding region of platelet thrombospondin. *Biochem. Biophys. Res. Commun.* 1984;119(3):1075–1081.
344. Dardik R, Lahav J. Multiple domains are involved in the interaction of endothelial cell thrombospondin with fibronectin. *Eur. J. Biochem.* 1989;185(3):581–588.
345. Aho S, Uitto J. Two-hybrid analysis reveals multiple direct interactions for thrombospondin 1. *Matrix Biol.* 1998;17(6):401–412.
346. Galvin NJ, Vance PM, Dixit VM, Fink B, Frazier WA. Interaction of human thrombospondin with types I-V collagen: direct binding and electron microscopy. *J. Cell Biol.* 1987;104(5):1413–1422.
347. Karczewski J, Knudsen KA, Smith L, et al. The interaction of thrombospondin with platelet glycoprotein GPIIb-IIIa. *J. Biol. Chem.* 1989;264(35):21322–21326.
348. Beiso P, Pidard D, Fournier D, Dubernard V, Legrand C. Studies on the interaction of platelet glycoprotein IIb-IIIa and glycoprotein IV with fibrinogen and thrombospondin: a new immunochemical approach. *Biochim. Biophys. Acta.* 1990;1033(1):7–12.
349. Rybak ME. Glycoproteins IIb and IIIa and platelet thrombospondin in a liposome model of platelet aggregation. *Thromb. Haemost.* 1986;55(2):240–245.
350. Pytela R, Pierschbacher MD, Ginsberg MH, Plow EF, Ruoslahti E. platelet membrane glycoprotein IIb/IIIa: member of a family of Arg-Gly-Asp--specific adhesion receptors. *Science (80-. ).* 1986;231(4745):1559–1562.
351. Legrand C, Morandi V, Mendelovitz S, et al. Selective inhibition of platelet macroaggregate formation by a recombinant heparin-binding domain of human thrombospondin. *Arterioscler. Thromb. Vasc. Biol.* 1994;14(11):1784–1791.
352. Isenberg JS, Romeo MJ, Yu C, et al. Thrombospondin-1 stimulates platelet aggregation by blocking the antithrombotic activity of nitric oxide/cGMP signaling. *Blood.* 2008;111:613–623.
353. Jurk K, Clemetson KJ, Groot PG De, et al. Thrombospondin-1 mediates platelet adhesion at high shear via glycoprotein Ib (GPIb): an alternative/backup mechanism to von Willebrand factor. 2003;
354. Kuijpers MJE, De Witt S, Nergiz-Unal R, et al. Supporting roles of platelet thrombospondin-1 and CD36 in thrombus formation on collagen. *Arterioscler. Thromb. Vasc. Biol.* 2014;34(6):1187–1192.
355. Faye C, Chautard E, Olsen BR, Ricard-Blum S. The first draft of the endostatin interaction network. *J. Biol. Chem.* 2009;284(33):22041–22047.
356. Chung J, Wang XQ, Lindberg FP, Frazier WA. Thrombospondin-1 acts via IAP/CD47 to synergize with collagen in alpha 2 beta 1-mediated platelet activation. *Blood.* 1999;94(2):642–648.
357. Milev Y, Essex DW. Protein disulfide isomerase catalyzes the formation of disulfide-linked complexes of thrombospondin-1 with thrombin-antithrombin III. *Arch. Biochem. Biophys.* 1999;361(120–126):.
358. Lawler J, Connolly JE, Ferro P, Derick LH. Thrombin and chymotrypsin interactions with thrombospondin. *Ann. N. Y. Acad. Sci.* 1986;485:273–287.
359. Silverstein RL, Leung LL, Harpel PC, Nachman RL. Complex formation of

- platelet thrombospondin with plasminogen. Modulation of activation by tissue activator. *J. Clin. Invest.* 1984;74(5):1625–1633.
360. Mast AE, Stadanlick JE, Lockett JM, et al. Tissue factor pathway inhibitor binds to platelet thrombospondin-1. *J. Biol. Chem.* 2000;275(41):31715–31721.
361. Bale MD, Mosher DF. Effects of thrombospondin on fibrin polymerization and structure. *J. Biol. Chem.* 1986;261(2):862–868.
362. Wang A, Liu F, Dong N, et al. Thrombospondin-1 and ADAMTS13 competitively bind to VWF A2 and A3 domains in vitro. *Thromb. Res.* 2010;126(4):e260–e265.
363. Pimanda JE, Ganderton T, Maekawa A, et al. Role of thrombospondin-1 in control of von Willebrand factor multimer size in mice. *J. Biol. Chem.* 2004;279(20):21439–21448.
364. Prakash P, Nayak MK, Chauhan AK. P-selectin can promote thrombus propagation independently of both von Willebrand factor and thrombospondin-1 in mice. *J. Thromb. Haemost.* 2017;15:388–394.
365. Preissner KT, Holzhter S, Justus C, Miller-Berghaus G. Identification and partial characterization of platelet vitronectin: evidence for complex formation with platelet-derived plasminogen activator inhibitor-1. *Blood.* 1989;74:1989–1996.
366. Seiffert D. Constitutive and regulated expression of vitronectin. *Histol. Histopathol.* 1997;12:787–797.
367. Suzuki S, Oldberg A, Hayman EG, Pierschbacher MD, Ruoslahti E. Complete amino acid sequence of human vitronectin deduced from cDNA. Similarity of cell attachment sites in vitronectin and fibronectin. *EMBO J.* 1985;4:2519–2524.
368. Seiffert D, Keeton M, Eguchi Y, Sawdey M, Loskutoff DJ. Detection of vitronectin mRNA in tissues and cells of the mouse. *Proc. Natl. Acad. Sci. U. S. A.* 1991;88:9402–9406.
369. Preissner KT, Wassmuth R, Miller-Berghaus G. Physicochemical characterization of human S-protein and its function in the blood coagulation system. *Biochem. J.* 1985;231:349–355.
370. Conlan MG, Tomasini BR, Schultz RL, Mosher DF. Plasma vitronectin polymorphism in normal subjects and patients with disseminated intravascular coagulation. *Blood.* 1988;72:185–190.
371. Hill SA, Shaughnessy SG, Ribau JP, Austin RC, Podor TJ. Differential mechanisms targeting type 1 plasminogen activator inhibitor and vitronectin into the storage granules of a human megakaryocytic cell line. *Blood.* 1996;87:5061–5073.
372. Seiffert D, Schleef RR. Two functionally distinct pools of vitronectin (VN) in the blood circulation: Identification of a heparin-binding competent population of VN within platelet  $\alpha$ -granules. *Blood.* 1996;88:552–560.
373. Stockman A, Hess S, Declerck P, Timpl R, Preissner KT. Multimeric vitronectin. Identification and characterization of conformation-dependent self-association of the adhesive protein. *J. Biol. Chem.* 1993;268:22874–22882.
374. Seiffert D, Loskutoff DJ. Type 1 plasminogen activator inhibitor induces multimerization of plasma vitronectin - a suggested mechanism for the generation of the tissue form of vitronectin in vivo. *J. Biol. Chem.* 1996;271(47):29644–

- 29651.
375. Seiffert D, Smith JW. The cell adhesion domain in plasma vitronectin is cryptic. *J. Biol. Chem.* 1997;272:13705–13710.
  376. Schwartz I, Seger D, Maik-Rachline G, Kreizman T, Shaltiel S. Truncated vitronectins: binding to immobilized fibrin and to fibrin clots, and their subsequent interaction with cells. *Biochem. Biophys. Res. Commun.* 2002;290:682–689.
  377. Izumi M, Shimo-Oka T, Morishita N, Ii I, Hayashi M. Identification of the collagen-binding domain of vitronectin using monoclonal antibodies. *Cell Struct. Funct.* 1988;13(3):217–225.
  378. Declerck P, De Mol M, Alessi MC, et al. Purification and characterization of a plasminogen activator inhibitor 1 binding protein from human plasma. Identification as a multimeric form of S protein (vitronectin). *J. Biol. Chem.* 1988;263(30):15454–15461.
  379. Thiagarajan P, Kelly KL. Exposure of binding sites for vitronectin on platelets following stimulation. *J. Biol. Chem.* 1988;263(6):3035–3038.
  380. Wu Y-P, Bloemendal HJ, Voest EE, et al. Fibrin-incorporated vitronectin is involved in platelet adhesion and thrombus formation through homotypic interactions with platelet-associated vitronectin. *Blood.* 2004;104(4):1034–1041.
  381. Parker CJ, Stone OL, White VF, Bernshaw NJ. Vitronectin (S protein) is associated with platelets. *Br. J. Haematol.* 1989;71:245–252.
  382. Morgenstern E, Gnad U, Preissner KT, et al. Localization of protein kinase A and vitronectin in resting platelets and their translocation onto fibrin fibers during clot formation. *Eur. J. Cell Biol.* 2001;80(1):87–98.
  383. Wohn KD, Schmidt T, Kanse SM, et al. The role of plasminogen activator inhibitor-1 as inhibitor of platelet and megakaryoblastic cell adhesion. *Br. J. Haematol.* 1999;104(4):901–908.
  384. Podor TJ, Campbell S, Chindemi P, et al. Incorporation of vitronectin into fibrin clots. Evidence for a binding interaction between vitronectin and gamma A/gamma' fibrinogen. *J. Biol. Chem.* 2002;277(9):7520–7528.
  385. Tomasini BR, Mosher DF, Owen MC, Fenton JW. Conformational lability of vitronectin: Induction of an antigenic change by a-thrombin-serpin complexes and by proteolytically modified thrombin. *Biochemistry.* 1989;28:823–842.
  386. Tomasini BR, Mosher DF. Conformational states of vitronectin: Preferential expression of an antigenic epitope when vitronectin is covalently and noncovalently complexed with thrombin-antithrombin III or treated with urea. *Blood.* 1988;72:903–912.
  387. deBoer HC, de Groot PG, Bouma BN, Preissner KT. Ternary vitronectin-thrombin-antithrombin III complexes in human plasma: Detection and mode of association. *J. Biol. Chem.* 1993;268:1279–1283.
  388. Asch E, Podack E. Vitronectin Binds to Activated Human Platelets and Plays a Role in Platelet Aggregation. 1990;85(May):1372–1378.
  389. Mohri H, Ohkubo T. How vitronectin binds to activated glycoprotein IIb-IIIa complex and its functions in platelet aggregation. *Am. J. Clin. Pathol.* 1991;96(5):605–609.

390. Konstantinides S, Schafer K, Thinnes T, Loskutoff DJ. Plasminogen activator inhibitor-1 and its cofactor vitronectin stabilize arterial thrombi after vascular injury in mice. *Circulation*. 2001;103:576–583.
391. Koschnick S, Konstantinides S, Schäfer K, Crain K, Loskutoff DJ. Thrombotic phenotype of mice with a combined deficiency in plasminogen activator inhibitor 1 and vitronectin. *J. Thromb. Haemost.* 2005;3(10):2290–2295.
392. Cherny RC, Honan MA, Thiagarajan P. Site-directed mutagenesis of the arginine-glycine-aspartic acid in vitronectin abolishes cell adhesion. *J. Biol. Chem.* 1993;268(13):9725–9729.
393. Uzan G, Prenant M, Prandini M-H, Martin F, Marguerie G. Tissue-specific expression of the platelet GPIIb gene. *J. Biol. Chem.* 1991;266(14):8932–8939.
394. Butler-Zimrin AE, Bennett JS, Poncz M, et al. Isolation and characterization of cDNA clones for the platelet membrane glycoproteins IIb and IIIa. *Thromb. Haemost.* 1987;58(1):319a.
395. Oki T, Kitaura J, Eto K, et al. Integrin  $\alpha$ IIb $\beta$ 3 induces the adhesion and activation of mast cells through interaction with fibrinogen. *J. Immunol.* 2006;176(1):52–60.
396. Oki T, Eto K, Yamanishi Y, et al. Evidence that integrin  $\alpha$ IIb  $\beta$ 3-dependent interaction of mast cells with fibrinogen exacerbates chronic inflammation. *J. Biol. Chem.* 2009;284(45):31463–31472.
397. Sheldrake HM, Patterson LH. Function and antagonism of  $\beta$ 3 integrins in the development of cancer therapy. *Curr. Cancer Drug Targets.* 2009;9(4):519–540.
398. Duperray A, Berthier R, Chagnon E, et al. Biosynthesis and processing of platelet GPIIb-IIIa in human megakaryocytes. *J. Cell Biol.* 1987;104(6):1665–1673.
399. Jin J, Quinton TM, Zhang J, Rittenhouse SE, Kunapuli SP. Adenosine diphosphate (ADP)-induced thromboxane A<sub>2</sub> generation in human platelets requires coordinated signaling through integrin  $\alpha$ IIb $\beta$ 3 and ADP receptors. *Blood.* 2002;99(1):193–198.
400. Niiya K, Hodson E, Bader R, et al. Increased surface expression of the membrane glycoprotein IIb/IIIa complex induced by platelet activation. Relationship to the binding of fibrinogen and platelet aggregation. *Blood.* 1987;70(2):475–483.
401. Wagner CL, Mascelli MA, Neblock DS, et al. Analysis of GPIIb/IIIa receptor number by quantification of 7E3 binding to human platelets. *Blood.* 1996;88:907–914.
402. Stouffer GA, Smyth SS. Effects of thrombin on interactions between  $\beta$ 3-integrins and extracellular matrix in platelets and vascular cells. *Arterioscler. Thromb. Vasc. Biol.* 2003;23:1971–1978.
403. Zeiler M, Moser M, Mann M. Copy Number Analysis of the Murine Platelet Proteome Spanning the Complete Abundance Range. *Mol. Cell. Proteomics.* 2014;13(12):3435–3445.
404. Wencel-Drake JD, Plow EF, Kunicki TJ, et al. Localization of internal pools of membrane glycoproteins involved in platelet adhesive responses. *Am. J. Pathol.* 1986;124(2):324–334.
405. Woods Jr. VL, Wolff LE, Keller DM. Resting platelets contain a substantial

- centrally located pool of glycoprotein IIb-IIIa complex which may be accessible to some but not other extracellular proteins. *J. Biol. Chem.* 1986;261:15242–15251.
406. Bennett JS, Vilaire G. Exposure of platelet fibrinogen receptors by ADP and epinephrine. *J. Clin. Invest.* 1979;64:1393–1401.
407. Harfenist EJ, Packham MA, Mustard JF. Reversibility of the association of fibrinogen with rabbit platelets exposed to ADP. *Blood.* 1980;56:189–198.
408. Marguerie G, Plow EF, Edgington TS. Human platelets possess an inducible and saturable receptor specific for fibrinogen. *J. Biol. Chem.* 1979;254:5357–5363.
409. Ginsberg MH, Forsyth J, Lightsey A, Chediak J, Plow EF. Reduced surface expression and binding of fibronectin by thrombin-stimulated thrombasthenic platelets. *J. Clin. Invest.* 1983;71(3):619–624.
410. Ruggeri ZM, Bader R, De Marco L. Glanzmann thrombasthenia: deficient binding of von Willebrand factor to thrombin-stimulated platelets. *Proc. Natl. Acad. Sci. U. S. A.* 1982;79:6038–6041.
411. Kamata T, Handa M, Ito S, et al. Structural requirements for activation in  $\alpha$ IIb $\beta$ 3 integrin. *J. Biol. Chem.* 2010;285(49):38428–38437.
412. Hato T, Pampori N, Shattil SJ. Complementary roles for receptor clustering and conformational change in the adhesive and signaling functions of integrin  $\alpha$ IIb $\beta$ 3. *J. Cell Biol.* 1998;141:1685–1595.
413. Buensucesco C, de Virgilio M, Shattil SJ. Detection of integrin alpha IIb beta 3 clustering in living cells. *J. Biol. Chem.* 2003;278:15217–15224.
414. Carman C V., Springer TA. Integrin avidity regulation: are changes in affinity and conformation underemphasized? *Curr. Opin. Cell Biol.* 2003;15:547–556.
415. Auger JM. Adhesion of human and mouse platelets to collagen under shear: a unifying model. *FASEB J.* 2005;22:1–22.
416. Nurden AT. Glanzmann Thrombasthenia. *Orph.* 2006;1(10):.
417. Collier BS, Seligsohn U, Little PA. Type I Glanzmann thrombasthenia patients from the Iraqi-Jewish and Arab populations in Israel can be differentiated by platelet glycoprotein IIIa immunoblot analysis. *Blood.* 1987;69:1696–1703.
418. Smyth SS, Reis ED, Väänänen H, Zhang W, Collier BS. Variable protection of  $\beta$ 3-integrin-deficient mice from thrombosis initiated by different mechanisms. *Blood.* 2001;98(4):1055–1062.
419. Farndale RW, Sixma J, Barnes MJ, De Groot PG. The role of collagen in thrombosis and hemostasis. *J. Thromb. Haemost.* 2004;2:561–573.
420. Dickeson SK, Walsh JJ, Santoro SA. Binding of the alpha 2 integrin I domain to extracellular matrix ligands: structural and mechanistic differences between collagen and laminin binding. *Cell Adhes. Commun.* 1998;5(4):273–281.
421. Smith C, Estavillo D, Emsley J, et al. Mapping the Collagen-binding Site in the I Domain of the Glycoprotein Ia / IIa ( Integrin  $\alpha$ 2  $\beta$ 1 )\* collagen binds to a groove on the upper surface of the I. 2000;275(6):4205–4209.
422. Kamata T, Liddington RC, Takada Y. Interaction between collagen and the alpha(2) I-domain of integrin alpha(2)beta(1). Critical role of conserved residues in the metal ion-dependent adhesion site (MIDAS) region. *J. Biol. Chem.* 1999;274:32108–32111.

423. Onley DJ, Knight CG, Tuckwell DS, Barnes MJ, Farndale RW. Micromolar Ca<sup>2+</sup> concentrations are essential for Mg<sup>2+</sup>-dependent binding of collagen by the integrin  $\alpha 2\beta 1$  in human platelets. *J. Biol. Chem.* 2000;275(32):24560–24564.
424. Goldman R, Harvey J, Hogg N. VLA-2 is the integrin used as a collagen receptor by leukocytes. *Eur. J. Immunol.* 1992;22(5):1109–1114.
425. O’Connell PJ, Faull R, Russ GR, D’Apice AJ. VLA-2 is a collagen receptor on endothelial cells. *Immunol. Cell Biol.* 1991;69(Pt 2):103–110.
426. Takada Y, Wayner EA, Carter WG, Hemler ME. Extracellular matrix receptors, ECMRII and ECMRI, for collagen and fibronectin correspond to VLA-2 and VLA-3 in the VLA family of heterodimers. *J. Cell. Biochem.* 1988;37(4):385–393.
427. Senger DR, Claffey KP, Benes JE, et al. Angiogenesis promoted by vascular endothelial growth factor: Regulation through  $\alpha 1\beta 1$  and  $\alpha 2\beta 1$  integrins. *Proc. Natl. Acad. Sci. U. S. A.* 1997;94(25):13612–13617.
428. Saarialho-Kere UK, Kovacs SO, Pentland AP, et al. Cell-matrix interactions modulate interstitial collagenase expression by human keratinocytes actively involved in wound healing. *J. Clin. Invest.* 1993;92(6):2858–2866.
429. Enestein J, Kramer RH. Confocal microscopic analysis of integrin expression on the microvasculature and its sprouts in the neonatal foreskin. *J. Invest. Dermatol.* 1994;103(3):381–386.
430. Farndale RW, Siljander PRM, Onley DJ, et al. Collagen-platelet interactions: recognition and signalling. *Biochem. Soc. Symp.* 2003;70:81–94.
431. Emsley J, Knight CG, Farndale RW, Barnes MJ. Structural basis of collagen recognition by integrin  $\alpha 2\beta 1$ . *Cell.* 2000;101:47–56.
432. Jin M, Andricioaei I, Springer TA. Conversion between three conformational states of integrin I domains with a C-terminal pull spring studied with molecular dynamics. *Structure.* 2004;12:2137–2147.
433. Jokinen J, Dadu E, Nykvist P, et al. Integrin-mediated cell adhesion to type I collagen fibrils. *J. Biol. Chem.* 2004;279(30):31956–31963.
434. Kern A, Eble J, Golbik R, Kuhn K. Interaction of type IV collagen with the isolated integrins  $\alpha 1\beta 1$  and  $\alpha 2\beta 1$ . *Eur. J. Biochem.* 1993;215(1):151–159.
435. Edelman JM, Chan BM, Uniyal S, et al. The mouse VLA-2 homologue supports collagen and laminin adhesion but not virus binding. *Cell Adhes. Commun.* 1994;2(2):131–143.
436. Siljander PRM, Hamaia S, Peachey AR, et al. Integrin activation state determines selectivity for novel recognition sites in fibrillar collagens. *J. Biol. Chem.* 2004;279(46):47763–47772.
437. Nieuwenhuis HK, Akkerman JWN, Houdijk WPM, Sixma JJ. Human blood platelets showing no response to collagen fail to express surface glycoprotein Ia. *Nature.* 1985;318(6045):470–472.
438. Nieuwenhuis HK, Sakariassen KS, Houdijk WPM, Nievelstein PF, Sixma JJ. Deficiency of platelet membrane glycoprotein Ia associated with a decreased platelet adhesion to subendothelium: a defect in platelet spreading. *Blood.* 1986;68(3):692–695.
439. Holtkötter O, Nieswandt B, Smyth N, et al. Integrin  $\alpha 2$ -deficient mice develop

- normally, are fertile, but display partially defective platelet interaction with collagen. *J. Biol. Chem.* 2002;277(13):10789–10794.
440. He L, Pappan LK, Grenache DG, et al. The contributions of the alpha 2 beta 1 integrin to vascular thrombosis in vivo. *Blood.* 2003;102(10):3652–3657.
441. Jung SM, Moroi M. Platelet glycoprotein VI. 2008.
442. Berlanga O, Tulasne D, Bori T, et al. The Fc receptor  $\gamma$ -chain is necessary and sufficient to initiate signalling through glycoprotein VI in transfected cells by the snake C-type lectin, convulxin. *Eur. J. Biochem.* 2002;269(12):2951–2960.
443. Bori-Sanz T, Inoue KS, Berndt MC, Watson SP, Tulasne D. Delineation of the region in the glycoprotein VI tail required for association with the Fc receptor  $\gamma$ -chain. *J. Biol. Chem.* 2003;278(38):35914–35922.
444. Nieswandt B, Bergmeier W, Schulte V, et al. Expression and function of the mouse collagen receptor glycoprotein VI is strictly dependent on its association with the Fc $\gamma$  chain. *J. Biol. Chem.* 2000;275(31):23998–24002.
445. Berlanga O, Bori-Sanz T, James JR, et al. Glycoprotein VI oligomerization in cell lines and platelets. *J. Thromb. Haemost.* 2007;5(5):1026–1033.
446. Feng J, Garrity D, Call ME, Moffett H, Wucherpfennig KW. Convergence on a distinctive assembly mechanism by unrelated families of activating immune receptors. *Immunity.* 2005;22(4):427–438.
447. Chen H, Locke D, Liu Y, Liu C, Kahn ML. The platelet receptor GPVI mediates both adhesion and signaling responses to collagen in a receptor density-dependent fashion. *J. Biol. Chem.* 2002;277(4):3011–3019.
448. Jung SM, Takemura Y, Imamura Y, et al. Collagen-type specificity of glycoprotein VI as a determinant of platelet adhesion. *Platelets.* 2008;19(1):32–42.
449. Inoue O, Suzuki-Inoue K, Ozaki Y. Redundant mechanism of platelet adhesion to laminin and collagen under flow: Involvement of von Willebrand factor and glycoprotein Ib-IX-V. *J. Biol. Chem.* 2008;283(24):16279–16282.
450. Inoue O, Suzuki-inoue K, Mccarty OJT, et al. Laminin stimulates spreading of platelets through integrin alpha-6 beta-1-dependent activation of GPVI. 2019;107(4):1405–1413.
451. Mammadova-Bach E, Ollivier V, Loyau S, et al. Platelet glycoprotein VI binds to polymerized fibrin and promotes thrombin generation. *Blood.* 2015;126(5):683–691.
452. Siljander P, Farndale RW, Feijge MAH, et al. Platelet adhesion enhances the glycoprotein VI-dependent procoagulant response: Involvement of p38 MAP kinase and calpain. *Arterioscler. Thromb. Vasc. Biol.* 2001;21(4):618–627.
453. Smethurst PA, Onley DJ, Jarvis GE, et al. Structural basis for the platelet-collagen interaction: The smallest motif within collagen that recognizes and activates platelet Glycoprotein VI contains two glycine-proline-hydroxyproline triplets. *J. Biol. Chem.* 2007;282(2):1296–1304.
454. Jung SM, Moroi M, Soejima K, et al. Constitutive dimerization of glycoprotein VI (GPVI) in resting platelets is essential for binding to collagen and activation in flowing blood. *J. Biol. Chem.* 2012;287(35):30000–30013.
455. Moroi M, Jung SM, Okuma M, Shinmyozu K. A patient with platelets deficient in

- glycoprotein VI that lack both collagen-induced aggregation and adhesion. *J. Clin. Invest.* 1989;84(5):1440–1445.
456. Sugiyama T, Okuma M, Ushikubi F, et al. A novel platelet aggregating factor found in a patient with defective collagen-induced platelet aggregation and autoimmune thrombocytopenia. *Blood.* 1987;69(6):1712–1720.
457. Hermans C, Wittevrongel C, Thys C, et al. A compound heterozygous mutation in glycoprotein VI in a patient with a bleeding disorder. *J. Thromb. Haemost.* 2009;7(8):1356–1363.
458. Dumont B, Lasne D, Rothschild C, et al. Absence of collagen-induced platelet activation caused by compound heterozygous GPVI mutations. *Blood.* 2009;114(9):1900–1903.
459. Ryo R, Yoshida A, Sugano W, et al. Deficiency of P62, a putative collagen receptor, in platelets from a patient with defective collagen-induced platelet aggregation. *Am. J. Hematol.* 1992;39(1):25–31.
460. Arai M, Yamamoto N, Moroi M, et al. Platelets with 10% of the normal amount of glycoprotein VI have an impaired response to collagen that results in a mild bleeding tendency. *Br. J. Haematol.* 1995;89(1):124–130.
461. Siljander PRM, Munnix ICA, Smethurst PA, et al. Platelet receptor interplay regulates collagen-induced thrombus formation in flowing human blood. *Blood.* 2004;103:1333–1341.
462. Poole A, Gibbins JM, Turner M, et al. The Fc receptor  $\gamma$ -chain and the tyrosine kinase Syk are essential for activation of mouse platelets by collagen. *EMBO J.* 1997;16(9):2333–2341.
463. Munnix ICA, Strehl A, Kuijpers MJE, et al. The glycoprotein VI-phospholipase C $\gamma$ 2 signaling pathway controls thrombus formation induced by collagen and tissue factor in vitro and in vivo. *Arterioscler. Thromb. Vasc. Biol.* 2005;25(12):2673–2678.
464. Konstantinides S, Ware J, Marchese P, et al. Distinct antithrombotic consequences of platelet glycoprotein Iba $\alpha$  and VI deficiency in a mouse model of arterial thrombosis. *J. Thromb. Haemost.* 2006;4:2014–2021.
465. Massberg S, Gawaz M, Gruner S, et al. A crucial role of glycoprotein VI for platelet recruitment to the injured arterial wall in vivo. *J. Exp. Med.* 2003;197:41–49.
466. Wu G, Essex DW, Meloni FJ, et al. Human endothelial cells in culture and in vivo express on their surface all four components of the glycoprotein Ib/IX/V complex. *Blood.* 1997;90(7):2660–2669.
467. Modderman PW, Admiraal LG, Sonnenberg A, von dem Borne AE. Glycoproteins V and Ib-IX form a noncovalent complex in the platelet membrane. *J. Biol. Chem.* 1992;267(1):364–369.
468. Hartwig JH. The platelet cytoskeleton. *Platelets.* 2013;
469. Jurk K, Clemetson KJ, de Groot PG, et al. Thrombospondin-1 mediates platelet adhesion at high shear via glycoprotein Ib (GPIb): an alternative/backup mechanism to von Willebrand factor. *FASEB J.* 2003;17(11):1490–1492.
470. Romo GM, Dong J, Schade AJ, et al. The glycoprotein Ib-IX-V complex is a

- platelet counterreceptor for P-selectin. *J. Exp. Med.* 1999;190(6):803–813.
471. Takamatsu J, Horne MK, Gralnick HR. Identification of the thrombin receptor on human platelets by chemical crosslinking. *J. Clin. Invest.* 1986;77(2):362–368.
472. Yamamoto N, Greco NJ, Barnard MR, et al. Glycoprotein Ib (GPIb)-dependent and GPIb-independent pathways of thrombin-induced platelet activation. *Blood.* 1991;77(8):1740–1748.
473. Simon DI, Chen Z, Xu H, et al. Platelet glycoprotein Iba is a counterreceptor for the leukocyte integrin Mac-1 (CD11b/CD18). *J. Exp. Med.* 2000;192(2):193–204.
474. Wang Y, Sakuma M, Chen Z, et al. Leukocyte engagement of platelet glycoprotein Iba via the integrin Mac-1 is critical for the biological response to vascular injury. *Circulation.* 2005;112(19):2993–3000.
475. Ju L, Chen Y, Zhou F, et al. Von Willebrand factor-A1 domain binds platelet glycoprotein Iba in multiple states with distinctive force-dependent dissociation kinetics. *Thromb. Res.* 2015;136(3):606–612.
476. Moog S, Mangin P, Lenain N, et al. Platelet glycoprotein V binds to collagen and participates in platelet adhesion and aggregation. *Blood.* 2001;98(4):1038–1046.
477. Andrews RK, Shen Y, Gardiner EE, et al. The glycoprotein Ib-IX-V complex in platelet adhesion and signaling. *Thromb. Haemost.* 1999;82(2):357–364.
478. Ozaki Y, Asazuma N, Suzuki-Inoue K, Berndt MC. Platelet GPIb-IX-V-dependent signaling. *J. Thromb. Haemost.* 2005;3(8):1745–1751.
479. Savoia A, Kunishima S, De Rocco D, et al. Spectrum of the mutations in Bernard-Soulier syndrome. *Hum. Mutat.* 2014;35(9):1033–1045.
480. Andrews RK, Berndt MC. Bernard-Soulier syndrome: an update. *Semin. Thromb. Hemost.* 2013;39(6):656–662.
481. Birk DE, Bruckner P. Collagen suprastructures. *Top. Curr. Chem.* 2005;247:185–205.
482. Ricard S. The Collagen Family. *Cold Spring Harb. Perspect. Biol.* 2011;3(1):1–19.
483. Ricard-Blum S, Ruggiero F, Van Der Rest M. The collagen superfamily. *Top. Curr. Chem.* 2005;247:35–84.
484. Birk DE, Bruckner P. Collagens, suprastructures, and collagen fibril assembly. *Extracell. Matrix an Overv.* 2011;77–115.
485. Myllyharju J, Kivirikko KI. Collagens, modifying enzymes and their mutations in humans, flies and worms. *Trends Genet.* 2004;20(1):33–43.
486. Corral-Rodríguez MÁ, Bock PE, Hernández-Carvajal E, Gutiérrez-Gallego R, Fuentes-Prior P. Structural basis of thrombin-mediated factor V activation: The Glu 666-Glu672 sequence is critical for processing at the heavy chain - B domain junction. *Blood.* 2011;117(26):7164–7173.
487. Hulmes DJS. Collagen diversity, synthesis and assembly. *Collagen.* 2008;15–47.
488. Holzapfel GA. Collagen in arterial walls: biomechanical aspects. *Collagen.* 2008;285–324.
489. Shekhonin B V., Domogatsky SP, Muzykantov VR, Idelson GL, Rukosuev VS. Distribution of Type I, III, IV and V Collagen in Normal and Atherosclerotic Human Arterial Wall: Immunomorphological Characteristics. *Top. Catal.* 1985;5(4):355–368.

490. Shekhonin B V., Domogatsky SP, Idelson GL, Koteliansky VE, Rukosuev VS. Relative distribution of fibronectin and type I, III, IV, V collagens in normal and atherosclerotic intima of human arteries. *Atherosclerosis*. 1987;67(1):9–16.
491. Howard PS, Macarak EJ. Localization of collagen types in regional segments of the bovine aorta. *Lab. Investig.* 1989;61:548–555.
492. Manon-Jensen T, Kjeld NG, Karsdal MA. Collagen-mediated hemostasis. *J. Thromb. Haemost.* 2016;14(3):438–448.
493. Fratzl P. Collagen: structure and mechanics, an introduction. *Collagen*. 2008;1–14.
494. Fratzl P. Cellulose and collagen: from fibres to tissues. *Curr. Opin. Colloid Interface Sci.* 2003;8:32–39.
495. Romanic AM, Adachi E, Kadler KE, Hojima Y, Prockop DJ. Copolymerization of pNcollagen III and collagen I. *J. Biol. Chem.* 1991;266:12703–12709.
496. Liu X, Wu H, Byrne M, Krane S, Jaenisch R. Type III collagen is crucial for collagen I fibrillogenesis and for normal cardiovascular development. *Proc. Natl. Acad. Sci.* 1997;94:1852–1856.
497. Birk DE, Fitch JM, Babiarz JP, Doane KJ, Linsenmayer TF. Collagen fibrillogenesis in vitro: interaction of types I and V collagen regulates fibril diameter. *J. Cell Sci.* 1990;95(Pt 4):649–657.
498. Birk DE. Type V collagen: heterotypic type I/V collagen interactions in the regulation of fibril assembly. *Micron*. 2001;32(3):223–237.
499. Khoshnoodi J, Pedchenko V, Hudson BG. Mammalian collagen IV. *Microsc. Res. Tech.* 2008;71(5):357–370.
500. Kielty CM, Grant ME. The collagen family: structure, assembly, and organization in the extracellular matrix. *Connect. Tissue its Heritable Disord.* 2002;159–222.
501. Iruela-Arispe ML, Sage EH. Expression of type VIII collagen during morphogenesis of the chicken and mouse heart. *Dev. Biol.* 1991;144(1):107–118.
502. Di Lullo GA, Sweeney SM, Korkko J, Ala-Kokko L, San Antonio JD. Mapping the ligand-binding sites and disease-associated mutations on the most abundant protein in the human, type I collagen. *J. Biol. Chem.* 2002;277(6):4223–4231.
503. Koide T, Nagata K. Collagen biosynthesis. *Top. Curr. Chem.* 2005;247:85–114.
504. Eyre DR. Collagens of articular cartilage. *Arthritis Res.* 2002;4:30–35.
505. Silver FH, Landis WJ. Viscoelasticity, energy storage and transmission and dissipation by extracellular matrices in vertebrates. *Collagen*. 2008;133–154.
506. Blaschke UK, Eikenberry EF, Hulmes DJS, Galla HJ, Bruckner P. Collagen XI nucleates self-assembly and limits lateral growth of cartilage fibrils. *J. Biol. Chem.* 2000;275:10370–10378.
507. Li Y, Lacerda DA, Warman ML, et al. A fibrillar collagen gene, *Col11a1*, is essential for skeletal morphogenesis. *Cell*. 1995;80(3):423–430.
508. Myllyharju J. Intracellular post-translational modifications of collagens. *Top. Curr. Chem.* 2005;247:115–147.
509. Cowan PM, McGavin S. Structure of poly-L-proline. *Nature*. 1955;176:501–503.
510. Crick FH, Rich A. Structure of polyglycine II. *Nature*. 1955;176:780–781.
511. Ramachandran GN, Sasisekharan V, Ramakrishnan C. Molecular structure of polyglycine II. *Biochim. Biophys. Acta*. 1966;112:168–170.

512. Adzhubei AA, Sternberg MJ, Makarov AA. Polyproline-II helix in proteins: structure and function. *J. Mol. Biol.* 2013;425:2100–2132.
513. Bella J. Collagen structure: new tricks from a very old dog. *Biochem. J.* 2016;473(8):1001–1025.
514. Vogel BE, Doelz R, Kadler KE, et al. A substitution of cysteine for glycine 748 of the alpha 1 chain produces a kink at this site in the procollagen molecule and an altered N-proteinase cleavage site over 225 nm away. *J. Biol. Chem.* 1988;263(35):19249–19255.
515. Wess TJ. Collagen fibrillar structure and hierarchies. *Collagen.* 2008;49–80.
516. De Paepe A, Malfait F. The Ehlers-Danlos syndrome, a disorder with many faces. *Clin. Genet.* 2012;82(1):1–11.
517. Bodian DL, Chan TF, Poon A, et al. Mutation and polymorphism spectrum in osteogenesis imperfecta type II: Implications for genotype-phenotype relationships. *Hum. Mol. Genet.* 2009;18(3):463–471.
518. Porter S, Clark IM, Kevorkian L, Edwards DR. The ADAMTS metalloproteinases. *Biochem. J.* 2005;386:15–27.
519. Hopkins DR, Keles S, Greenspan DS. The bone morphogenetic protein 1/Tolloid-like metalloproteinases. *Matrix Biol.* 2007;26:508–523.
520. Chu M, Mann K, Deutzmann R, et al. Characterization of three constituent chains of collagen type VI by peptide sequences and cDNA clones. *Eur. J. Biochem.* 1987;168(2):309–317.
521. Furthmayr H, Wiedemann H, Timpl R, Odermatt E, Engel J. Electron-microscopical approach to a structural model of intima collagen. *Biochem. J.* 1983;211(2):303–311.
522. Baldock C, Sherratt MJ, Shuttleworth CA, Kielty CM. The supramolecular organization of collagen VI microfibrils. *J. Mol. Biol.* 2003;330:297–307.
523. Bruns RR, Press W, Engvall E, Timpl R, Gross J. Type VI collagen in extracellular, 100-nm periodic filaments and fibrils: identification by immunoelectron microscopy. *J. Cell Biol.* 1986;103(2):393–404.
524. von der Mark H, Aumailley M, Wick G, Fleischmajer R, Timpl R. Immunocytochemistry, gene size, and tissue localization of collagen VI. *Eur. J. Biochem.* 1984;142(3):493–502.
525. Shuttleworth CA. Type VIII Collagen. *Int. J. Biochem. Cell Biol.* 1997;29(10):1145–1148.
526. Sawada H, Konomi H, Hirosawa K. Characterization of the collagen in the hexagonal lattice of Descemet's Membrane : its relation to type VIII collagen. *J. Cell Biol.* 1990;110:219–227.
527. Sage H, Trueb B, Bornstein P. Biosynthetic and structural properties of endothelial cell type VIII collagen. *J. Biol. Chem.* 1983;258:13391–13401.
528. Plenz GAM, Deng MC, Robenek H, Völker W. Vascular collagens: Spotlight on the role of type VIII collagen in atherogenesis. *Atherosclerosis.* 2003;166(1):1–11.
529. Iruela-Arispe ML, Sage EH. Expression of type VIII collagen during morphogenesis of the chicken and mouse heart. *Dev. Biol.* 1991;144(1):107–118.
530. Eyre DR, Wu JJ. Collagen cross-links. *Top. Curr. Chem.* 2005;247:207–229.

531. Watson SP, Farndale RW, Moroi M, Jung SM. Platelet collagen receptors. *Hemost. Thromb. Basic Princ. Clin. Pract.* 2013;420–430.
532. Saelman EUM, Kehrel B, Hese KM, et al. Platelet adhesion to collagen and endothelial cell matrix under flow conditions is not dependent on platelet glycoprotein IV. *Blood.* 1994;83(11):3240–3244.
533. Jung SM, Tsuji K, Moroi M. Glycoprotein (GP) VI dimer as a major collagen-binding site of native platelets: Direct evidence obtained with dimeric GPVI-specific Fabs. *J. Thromb. Haemost.* 2009;7(8):1347–1355.
534. Nuyttens BP, Thijs T, Deckmyn H, Broos K. Platelet adhesion to collagen. *Thromb. Res.* 2011;127(SUPPL. 2):S26–S29.
535. Ichinohe T, Takayama H, Ezumi Y, et al. Collagen-stimulated activation of Syk but not c-Src is severely compromised in human platelets lacking membrane glycoprotein VI. *J. Biol. Chem.* 1997;272:63–68.
536. Kamiguti AS, Markland FS, Zhou Q, et al. Proteolytic cleavage of the beta1 subunit of platelet alpha2beta1 integrin by the metalloproteinase jararhagin compromises collagen-stimulated phosphorylation of pp72. *J. Biol. Chem.* 1997;272:32599–32605.
537. Keely PJ, Parise L V. The alpha2beta1 integrin is a necessary co-receptor for collagen-induced activation of Syk and the subsequent phosphorylation of phospholipase Cgamma2 in platelets. *J. Biol. Chem.* 1996;271:26668–26676.
538. Suzuki-Inoue K, Ozaki Y, Kainoh M, et al. Rhodocytin induces platelet aggregation by interacting with glycoprotein Ia/IIa (GPIa/IIa, integrin alpha 2 beta 1). Involvement of GPIa/IIa-associated Src and protein tyrosine phosphorylation. *J. Biol. Chem.* 2001;276:1643–1652.
539. Nieswandt B, Brakebusch C, Bergmeier W, et al. Glycoprotein VI but not alpha2beta1 integrin is essential for platelet interaction with collagen. *EMBO J.* 2001;20(9):2120–2130.
540. Knight CG, Morton LF, Peachey AR, et al. The collagen-binding a-domains of integrins alpha1/beta1 and alpha2/beta1 recognize the same specific amino acid sequence, GFOGER, in native (triple-helical) collagens. *J. Biol. Chem.* 2000;275(1):35–40.
541. Xu Y, Gurusiddappa S, Rich RL, et al. Multiple binding sites in collagen type I for the integrins alpha1beta1 and alpha2beta1. *J. Biol. Chem.* 2000;275(50):38981–38989.
542. Morton LF, Peachey AR, Zijenah LS, et al. Conformation-dependent platelet adhesion to collagen involving integrin alpha 2 beta 1-mediated and other mechanisms: multiple alpha 2 beta 1-recognition sites in collagen type I. *Biochem J.* 1994;299 ( Pt 3):791–797.
543. Asselin J, Knight CG, Farndale RW, Barnes MJ, Watson SP. Monomeric (glycine-proline-hydroxyproline)<sub>10</sub> repeat sequence is a partial agonist of the platelet collagen receptor glycoprotein VI. *Biochem. J.* 1999;339:413–418.
544. Knight CG, Morton LF, Onley DJ, et al. Collagen-platelet interaction: Gly-Pro-Hyp is uniquely specific for platelet Gp VI and mediates platelet activation by collagen. *Cardiovasc. Res.* 1999;41(2):450–457.
545. Lisman T, Raynal N, Groeneveld D, et al. A single high-affinity binding site for von Willebrand factor in collagen III, identified using synthetic triple-helical

- peptides. *Blood*. 2006;108:3753–3756.
546. Raynal N, Hamaia SW, Siljander PRM, et al. Use of synthetic peptides to locate novel integrin  $\alpha 2\beta 1$ -binding motifs in human collagen III. *J. Biol. Chem.* 2006;281(7):3821–3831.
547. Jarvis GE, Raynal N, Langford JP, et al. Identification of a major GpVI-binding locus in human type III collagen. *Blood*. 2008;111(10):4986–4996.
548. Farndale RW, Lisman T, Bihan D, et al. Cell–collagen interactions: the use of peptide Toolkits to investigate collagen–receptor interactions. *Biochem. Soc. Trans.* 2008;36(2):241–250.
549. Slatter DA, Bihan D, Jarvis GE, et al. The properties conferred upon triple-helical collagen-mimetic peptides by the presence of cysteine residues. *Peptides*. 2012;36:86–93.
550. Cruz MA, Yuan H, Lee JR, Wise RJ, Handin RI. Interaction of the von Willebrand Factor (vWF) with Collagen. *J. Biol. Chem.* 1995;270(18):10822–10827.
551. De Meyer SF, Schwarz T, Deckmyn H, et al. Binding of von Willebrand factor to collagen and glycoprotein Iba, but not to glycoprotein IIb/IIIa, contributes to ischemic stroke in mice-brief report. *Arterioscler. Thromb. Vasc. Biol.* 2010;30(10):1949–1951.
552. Savage B, Sixma JJ, Ruggeri ZM. Functional self-association of von Willebrand factor during platelet adhesion under flow. *Proc. Natl. Acad. Sci.* 2002;99(1):425–430.
553. Santoro SA. Preferential binding of high molecular weight forms of von Willebrand factor to fibrillar collagen. *Biochim. Biophys. Acta.* 1983;756(1):123–126.
554. Zijenah LS, Barnes MJ. Platelet-reactive sites in human collagens I and III: evidence for cell-recognition sites in collagen unrelated to RGD and like sequences. *Thromb. Res.* 1990;59(3):553–566.
555. Germain DP. Ehlers-Danlos syndrome type IV. *Orphanet J. Rare Dis.* 2007;2(1):1–9.
556. De Paepe A, Malfait F. Bleeding and bruising in patients with Ehlers-Danlos syndrome and other collagen vascular disorders. *Br. J. Haematol.* 2004;127(5):491–500.
557. Malfait F, De Paepe A. Bleeding in the heritable connective tissue disorders: mechanisms, diagnosis and treatment. *Blood Rev.* 2009;23(5):191–197.
558. Dalglish R. The Human Collagen Mutation Database. *Nucleic Acids Res.* 1998;26(1):253–255.
559. Jeong SJ, Li S, Luo R, Strokes N, Piao X. Loss of Col3a1, the gene for ehlers-danlos syndrome type IV, results in neocortical dyslamination. *PLoS One.* 2012;7(1):1–7.
560. Pugh N, Bihan D, Perry DJ, Farndale RW. Dynamic analysis of platelet deposition to resolve platelet adhesion receptor activity in whole blood at arterial shear rate. *Platelets.* 2015;26(3):216–219.
561. Barr JD, Chauhan AK, Schaeffer G V., Hansen JK, Motto DG. Red blood cells mediate the onset of thrombosis in the ferric chloride murine model. *Blood.*

- 2013;121(18):3733–3741.
562. Ciciliano JC, Sakurai Y, Myers DR, et al. Resolving the multifaceted mechanisms of the ferric chloride thrombosis model using an interdisciplinary microfluidic approach. *Blood*. 2015;126:817–824.
563. Eckly A, Hechler B, Freund M, et al. Mechanisms underlying FeCl<sub>3</sub>-induced arterial thrombosis. *J. Thromb. Haemost.* 2011;9(4):779–789.
564. Shah NK, Ramshaw JAM, Kirkpatrick A, Shah C, Brodsky B. A host-guest set of triple-helical peptides: Stability of Gly-X-Y triplets containing common nonpolar residues. *Biochemistry*. 1996;35(32):10262–10268.
565. Bellavite P, Andrioli G, Guzzo P, et al. A colorimetric method for the measurement of platelet adhesion in microtiter plates. *Anal. Biochem.* 1994;216:444–450.
566. Henikoff S, Henikoff JG. Amino acid substitution matrices from protein blocks. *Proc. Natl. Acad. Sci.* 1992;89(22):10915–10919.
567. Lowell CA, Li Z, Berndt MC, et al. Src family tyrosine kinase Lyn mediates VWF/GPIb-IX-induced platelet activation via the cGMP signaling pathway. *Blood*. 2008;112(4):1139–1146.
568. Huck V, Schneider MF, Gorzelanny C, Schneider SW. The various states of von Willebrand factor and their function in physiology and pathophysiology. *Thromb. Haemost.* 2014;111(4):598–609.
569. Springer TA. Review Article von Willebrand factor , Jedi knight of the bloodstream. 2016;124(9):1412–1426.
570. Springer TA. Biology and physics of von Willebrand factor concatamers. *J. Thromb. Haemost.* 2011;9(1 S):130–143.
571. Stocksclaeder M, Schneppenheim R, Budde U. Update on von Willebrand factor multimers: Focus on high-molecular-weight multimers and their role in hemostasis. *Blood Coagul. Fibrinolysis*. 2014;25(3):206–216.
572. Sadler JE, Moake JL, Miyata T, George JN. Recent advances in thrombotic thrombocytopenic purpura. *Hematology Am. Soc. Hematol. Educ. Program*. 2004;407–423.
573. Turner NA, Moake JL, McIntire L V. Blockade of adenosine diphosphate receptors P2Y<sub>12</sub> and P2Y<sub>1</sub> is required to inhibit platelet aggregation in whole blood under flow. *Blood*. 2001;98(12):3340–3345.
574. Chen J, Diacovo TG, Grenache DG, Santoro SA, Zutter MM. The  $\alpha$ 2 integrin subunit-deficient mouse: A multifaceted phenotype including defects of branching morphogenesis and hemostasis. *Am. J. Pathol.* 2002;161(1):337–344.
575. Cho J, Mosher DF. Characterization of fibronectin assembly by platelets adherent to adsorbed laminin-111. *J. Thromb. Haemost.* 2006;4:943–951.
576. Arya M, Anvari B, Romo GM, et al. Ultralarge multimers of von Willebrand factor form spontaneous high-strength bonds with the platelet glycoprotein Ib-IX complex: Studies using optical tweezers. *Blood*. 2002;99(11):3971–3977.
577. Maxwell MJ, Westein E, Nesbitt WS, et al. Identification of a 2-stage platelet aggregation process mediating shear-dependent thrombus formation. *Blood*. 2007;109(2):566–576.

578. Chen Z, Mondal NK, Ding J, et al. Paradoxical effect of non-physiological shear stress on platelets and von Willebrand factor. *Artif. Organs.* 2016;40:659–668.
579. Miyazaki Y, Nomura S, Miyake T, et al. High shear stress can initiate both platelet aggregation and shedding of procoagulant containing microparticles. *Blood.* 1996;88:3456–3464.
580. Goto S, Ikeda Y, Saldívar E, Ruggeri ZM. Distinct mechanisms of platelet aggregation as a consequence of different shearing flow conditions. *J. Clin. Invest.* 1998;101:479–486.
581. Neelamegham S, Taylor AD, Shankaran H, Smith CW, Simon SI. Shear and time-dependent changes in Mac-1, LFA-1, and ICAM-3 binding regulate neutrophil homotypic adhesion. *J. Immunol.* 2000;164(7):3798–3805.
582. Smoluchowski M V. Versuch einer mathematischen theorie der koagulationskinetik. *Zeitschrift fur Phys. Chemie.* 1917;92:129–168.
583. Konitsiotis AD, Raynal N, Bihan D, et al. Characterization of high affinity binding motifs for the discoidin domain receptor DDR2 in collagen. *J. Biol. Chem.* 2008;283(11):6861–6868.
584. Hamaia SW, Pugh N, Raynal N, et al. Mapping of potent and specific binding motifs, GLOGEN and GVOGEA, for integrin  $\alpha\beta 1$  using collagen toolkits II and III. *J. Biol. Chem.* 2012;287(31):26019–26028.
585. Xu H, Raynal N, Stathopoulos S, et al. Collagen binding specificity of the discoidin domain receptors: Binding sites on collagens II and III and molecular determinants for collagen IV recognition by DDR1. *Matrix Biol.* 2011;30(1):16–26.
586. Lebbink RJ, Raynal N, de Ruyter T, et al. Identification of multiple potent binding sites for human leukocyte associated Ig-like receptor LAIR on collagens II and III. *Matrix Biol.* 2009;28:202–210.
587. Howes JM, Bihan D, Slatter DA, et al. The recognition of collagen and triple-helical toolkit peptides by MMP-13: Sequence specificity for binding and cleavage. *J. Biol. Chem.* 2014;289(35):24091–24101.
588. Barrow AD, Raynal N, Andersen TL, et al. OSCAR is a collagen receptor that costimulates osteoclastogenesis in DAP12-deficient humans and mice. *J. Clin. Invest.* 2011;121(9):3505–3516.
589. Vadon-Le Goff S, Kronenberg D, Bourhis JM, et al. Procollagen C-proteinase enhancer stimulates procollagen processing by binding to the C-propeptide region only. *J. Biol. Chem.* 2011;286(45):38932–38938.
590. Giudici C, Raynal N, Wiedemann H, et al. Mapping of SPARC/BM-40/osteonectin-binding sites on fibrillar collagens. *J. Biol. Chem.* 2008;283(28):19551–19560.
591. Haralson MA, Jacobson HR, Hoover RL. Collagen polymorphisms in cultured rat kidney mesangial cells. *Lab. Invest.* 1987;57(5):513–523.
592. Sweeney SM, Orgel JP, Fertala A, et al. Candidate cell and matrix interaction domains on the collagen fibril, the predominant protein of vertebrates. *J. Biol. Chem.* 2008;283(30):21187–21197.
593. Byers PH, Wallis GA, Willing MC. Osteogenesis imperfecta: translation of

- mutation to phenotype. *J. Med. Genet.* 1991;28(7):433–42.
594. Herr AB, Farndale RW. Structural insights into the interactions between platelet receptors and fibrillar collagen. *J. Biol. Chem.* 2009;284(30):19781–19785.
595. Perumal S, Antipova O, Orgel JP. Collagen fibril architecture, domain organization, and triple-helical conformation govern its proteolysis. *Proc. Natl. Acad. Sci. U. S. A.* 2008;105:2824–2829.
596. Savage B, Ginsberg MH, Ruggeri ZM. Influence of fibrillar collagen structure on the mechanisms of platelet thrombus formation under flow. *Blood.* 1999;94(8):2704–15.
597. Cooley BC, Chen CY, Schmeling G. Increased venous versus arterial thrombosis in the Factor V Leiden mouse. *Thromb. Res.* 2007;119(6):747–751.
598. Rand ML, Wang H, Pluthero FG, et al. Diannexin, an annexin A5 homodimer, binds phosphatidylserine with high affinity and is a potent inhibitor of platelet-mediated events during thrombus formation. *J. Thromb. Haemost.* 2012;10:1109–1119.
599. Falati S, Gross PL, Merrill-Skoloff G, Furie BC, Furie B. Real-time in vivo imaging of platelets, tissue factor and fibrin during arterial thrombus formation in the mouse. *Nat. Med.* 2002;8(10):1175–1180.
600. Falati S, Patil S, Gross PL, et al. Platelet PECAM-1 inhibits thrombus formation in vivo. *Blood.* 2006;107:535–541.
601. Pérez P, Alarcón M, Fuentes E, Palomo I. Thrombus formation induced by laser in a mouse model. *Exp. Ther. Med.* 2014;8(1):64–68.
602. Rosen ED, Raymond S, Zollman A, et al. Laser-induced noninvasive vascular injury models in mice generate platelet- and coagulation-dependent thrombi. *Am. J. Pathol.* 2001;158(5):1613–1622.
603. Cooley BC. Collagen-induced thrombosis in murine arteries and veins. *Thromb. Res.* 2013;131(1):49–54.
604. Tomaiuolo M, Matzko CN, Poventud-Fuentes I, Weisel JW, Brass LF. Interrelationships between structure and function during the hemostatic response to injury. *Proc. Natl. Acad. Sci.* 2019;116(6):2243–2252.
605. Wenstrup RJ, Florer JB, Davidson JM, et al. Murine model of the Ehlers-Danlos syndrome: col5a1 haploinsufficiency disrupts collagen fibril assembly at multiple stages. *J. Biol. Chem.* 2006;281(18):12888–12895.
606. Cooper TK, Zhong Q, Krawczyk M, et al. The haploinsufficient Col3a1 mouse as a model for vascular Ehlers-Danlos syndrome. 2010.
607. Gresele P, Harrison P, Bury L, et al. Diagnosis of suspected inherited platelet function disorders: results of a worldwide survey. *J. Thromb. Haemost.* 2014;12(9):1562–1569.
608. Hayward CPM, Moffat KA, Plumhoff E, Van Cott EM. Approaches to investigating common bleeding disorders: an evaluation of North American coagulation laboratory practices. *Am. J. Hematol.* 2012;87 Suppl 1:S45-50.
609. Ruoslahti E. Fibronectin and its receptors. *Annu. Rev. Biochem.* 1988;57:375–413.
610. Qiu Y, Mekkat A, Yu H, et al. Collagen Gly missense mutations: Effect of residue identity on collagen structure and integrin binding. *J. Struct. Biol.*

2018;203(3):255–262.

611. Yigit S, Yu H, An B, et al. Mapping the effect of Gly mutations in collagen on  $\alpha 2\beta 1$  integrin binding. *J. Biol. Chem.* 2016;291(36):19196–19207.